Generation of early human neuroepithelial progenitors from primary cells for biomedical applications

Generierung früher humaner neuroepithelialer Vorläufer aus primären Zellen für biomedizinische Anwendungen

Thesis

for the conferral of the degree

"Doctor rerum naturalis" (Dr.rer.nat.)

at the Graduate School of Life Sciences, Section Biomedicine

Julius-Maximilians-Universität Würzburg

submitted by

Katharina Günther

born in Almaty

Würzburg, 2016

Submitted on: ………………………………………………………..……..

Office stamp

Members of the “*Promotionskomitee”*:

Chairperson: Prof. Dr. Christian Janzen

Primary Supervisor: Prof. Dr. Frank Edenhofer

Second Supervisor: Prof. Dr. Albrecht Müller

Third Supervisor: PD Dr. Robert Blum

Date of Public Defense: ……………………...

Date of Receipt of Certificates: ………………………

To my parents

List of Contents

Summary

Patient-specific induced pluripotent stem cells (iPSCs) emerged as a promising cell source for disease modeling and drug screening as well as a virtually unlimited source for restorative therapy. The thesis deals with three major topics to help realizing biomedical applications with neural stem cells. To enable the generation of transgene-free iPSCs, alternatives to retroviral reprogramming were developed. Hence, the adaptation and evaluation of reprogramming using excisable lentiviral constructs, Sendai virus (SeV) and synthetic mRNA-based methods was assessed in the first part of this thesis. hiPSCs exhibit the pluripotency markers OCT4, SSEA-4, TRA1-60 which were confirmed by immunofluorescence and flow cytometry. Besides, the potential to differentiate in cell types of all three germ layers was detected, confirming pluripotent identity of proliferating colonies resulting from various reprogramming strategies. However, major differences such as high efficiency with SeV in contrast to a relatively low efficiency with mRNA in regard to passage number and the phenotype of starting fibroblasts were observed. Furthermore, a prolonged clone- and passage-dependent residual presence of viral RNA genes was identified in SeV-iPSCs for up to 23 passages using RT-PCR underlining the importance of careful monitoring of clone selection. In contrast, viral-free reprogramming by synthetic mRNA represents a fully non-integrative approach but requires further refinement to be efficiently applicable to all fibroblasts.

The second part of this thesis deals with the establishment of a rapid monolayer approach to differentiate neural progenitor cells from iPSCs. To achieve this, a two-step protocol was developed allowing first the formation of a stable, primitive NPC line within 7 days which was expanded for 2-3 passages. In a second step, a subsequent adaptation to conditions yielding neural rosette-like NPCs followed. Both neural lines were demonstrated to be expandable, cryopreservable and negative for the pluripotency marker OCT4. Furthermore, a neural precursor identity including SOX1, SOX2, PAX6, Nestin was confirmed by immunofluorescence and quantitative RT-PCR. Moreover, the differentiation resulted in TUJ1-positive neurons and GFAP-positive astrocytes. Nonetheless, the outcome of glial differentiation from primitive NSCs remained low, whereas FGF/EGF-NPCs were efficiently differentiated into GFAP-positive astrocytes which were implicated in a cellular model of the blood brain barrier.

The third and major objective of this study was to generate human early neural progenitor cells from fetal brain tissue with a wide neural differentiation capacity. Therefore, a defined medium composition including small molecules and growth factors capable of modulation of crucial signaling pathways orchestrating early human development such as SHH and FGF was assessed. Indeed, specific culture conditions containing TGFβ inhibitor SB431542, SHH agonist Purmorphamine, GSK3β inhibitor CHIR99021 and basic FGF, but no EGF enabled robust formation of early neuroepithelial progenitor (eNEP) colonies displaying a homogeneous morphology and a high proliferation rate. Moreover, primary eNEPs exhibit a relatively high clonogenicity of more than 23 % and can be monoclonally expanded for more than 45 passages carrying a normal karyotype. Characterization by immunofluorescence, flow cytometry and quantitative RT-PCR revealed a distinct NPC profile including SOX1, PAX6, Nestin and SOX2 and Prominin. Furthermore, primary eNEPs show NOTCH and HES5 activation in combination with non-polarized morphology, indicative of an early neuroepithelial identity. Microarray analysis unraveled *SOX11*, *BRN2* and other *HES*-genes as characteristic upregulated genes. Interestingly, eNEPs were detected to display ventral midbrain/hindbrain regional identity. The validation of yielded cell types upon differentiation indicates a strong neurogenic potential with more than 90 % of TUJ1-positive neurons. Moreover, astrocytes marked by GFAP and putative myelin structures indicating oligodendrocytes were identified. Electrophysiological recordings revealed functionally active neurons and immunofluorescence indicate GABAergic, glutamatergic, dopaminergic and serotonergic subtypes. Additionally, putative physiological synapse formation was observed by the presence of Synapsin and PSD-95 as well as by ultrastructural examination. Notably, rare neurons stained positive for the peripheral neuronal marker Peripherin suggesting the potential of eNEPS to give rise to cells of neural tube and neural crest origin. By the application of specific differentiation protocols an increase of TH-positive neurons or neural crest-derivatives such as putative A- and C-sensory neurons and mesenchymal cells was identified. Taken together, primary eNEPs might help to elucidate mechanisms of early human neurodevelopment and will serve as a novel source for cell replacement and further biomedical applications.

Zusammenfassung

Patientenspezifische induziert pluripotente Zellen (iPSZ) haben sich als eine vielversprechende Möglichkeit erwiesen Zellen zu gewinnen, die für Krankheitsmodellierung, Arzneimitteltests und Zellersatztherapie in Frage kommen. In dieser Arbeit wurden drei wichtige Fragestellungen adressiert, die für potenzielle biomedizinische Anwendungen von neuralen Stammzellen von großem Interesse sind.

Um die Generierung von transgenfreien iPSZ zu ermöglichen, wurden Alternativen zur retroviralen Reprogrammierung entwickelt. Im ersten Teil dieser Arbeit wurden Reprogrammierungsmethoden, die auf deletierbaren, lentiviralen Konstrukten oder nichtintegrativen Verfahren wie Sendaivirus (SeV)-Transduktion und Transfektion synthetischer mRNA basieren, adaptiert und evaluiert. Die daraus resultierenden iPSZ exprimieren die Pluripotenz-marker OCT4, SSEA-4 und TRA1-60. Weiterhin wurde das Potenzial in Zelltypen aller drei Keimblätter zu differenzieren nachgewiesen. Dadurch konnte die pluripotente Identität der proliferativen Kolonien bestätigt werden. Beim Vergleich der angewandten Methoden fielen, bezüglich der generierten iPSZ-Linien, sowohl qualitative als auch quantitative Unterschiede auf. Bei der Verwendung von SeV-Partikeln wurde eine hohe Reprogrammierungseffizienz festgestellt. Bei der Transfektion von mRNAs hingegen war die Reprogrammierungseffizienz deutlich niedriger. Diese war darüber hinaus abhängig von der Passage und dem Genotyp der Ausgangsfibroblasten. Des Weiteren konnte eine klon- und passagenabhängige Präsenz viraler Gene in SeV-iPSZ bis zu 23 Passagen lang beobachtet werden, während bei der mRNA-Transfektion keine Spuren der genetischen Manipulation zurückblieben. Dies verdeutlicht die Bedeutung einer sorgfältigen Qualitätskontrolle bei der Klonselektion im Falle der SeV-iPSZ. Im Gegensatz dazu stellt die Reprogrammierung durch Transfektion synthetischer mRNAs eine völlig nicht-integrative Strategie dar, erfordert allerdings weitere Verfeinerung um das Verfahren effizient und vor allem für alle Fibroblastenpräparationen anwendbar zu machen.

Der zweite Teil der Arbeit behandelt die Etablierung eines schnellen, adhärenten Protokolls, um neurale Vorläuferpopulation aus iPSZ zu differenzieren. Um dies zu erreichen, wurde ein zweiphasiges Protokoll entwickelt, welches zunächst die Generierung einer primitiven neuralen Vorläuferzellpopulation innerhalb von 7 Tagen erlaubt. In einem zweiten Schritt erfolgte die Adaptierung an Kulturbedingungen, die eine neurale, rosettenähnliche Zellpopulation induzieren. Beide neuralen Zellpopulationen konnten weiter expandiert und eingefroren werden und waren negativ für den Pluripotenz-assoziierten Transkriptionsfaktor OCT4. Darüber hinaus konnte die neurale Vorläuferidentität mittels positiver Expression von SOX1, SOX2, PAX6 und Nestin bestätigt werden. Eine weitere Differenzierung dieser Zellen resultierte in TUJ1-positiven Neuronen und GFAP-positiven Astrozyten, die die Verwendung der Zellpopulation beispielweise in einem zellulären Modell der Blut-Hirn-Schranke erlaubten.

Das Hauptprojekt dieser Dissertation war es, frühe humane neurale Vorläuferzellen aus fetalem Hirngewebe zu isolieren und in Kultur zu stabilisieren. Diese Population sollte eine breite Differenzierungskapazität aufweisen. Zu diesem Zweck wurde eine chemisch definierte Medienzusammensetzung gewählt, die zusätzlich pharmakologisch wirksame Verbindungen und Wachstumsfaktoren beinhaltet. Hierdurch konnten Signaltransduktionswege wie zum Beispiel der Sonic-Hedgehog- (SHH) oder FGF-Signalweg, die bei der frühen neuralen Entwicklung eine bedeutende Rolle spielen, moduliert werden. In der Tat ermöglichten spezifische Kultivierungsbedingungen, die den TGFβ-Inhibitor SB431542, den SHH-Agonisten Purmorphamin, den GSK3β-Inhibitor CHIR99021 und basisches FGF, jedoch kein EGF enthielten, die robuste Bildung einer früheren neuroepithelialen Vorläuferpopulation (eNEP). Die so stabilisierten Kolonien wiesen eine homogene Morphologie und eine hohe Proliferationsrate auf. Außerdem zeigten sie eine hohe Klonogenitätsrate von 23%, die es ermöglichte monoklonale Zelllinien zu isolieren und für mehr als 45 Passagen zu expandieren. Dabei blieb ein normaler Karyotyp erhalten. Die Zellen zeigten ein eindeutiges neurales Profil, gekennzeichnet durch SOX1, PAX6, Nestin, SOX2 und Prominin-Expression. Weiterhin wiesen eNEPs *NOTCH* und *HES5*-Aktivierung in Kombination mit nicht-polarisierter Morphologie auf, was auf eine frühe neuropitheliale Identität hinweist. Eine Microarray-Analyse demonstrierte weiterhin *SOX11*, *BRN2* und einige *HES*-Gene als charakteristisch hochregulierte Gene. Interessanterweise zeigen eNEPs eine regionale Identität, die auf eine Mittelhirn/Hinterhirn-Regionalisierung hinweist. Die Validierung ungerichtet ausdifferenzierter Zelltypen offenbarte mit einem Kulturanteil von 90 % TUJ1-positiven Neuronen ein stark neurogenes Potenzial. Zusätzlich konnten GFAP-positive Astrozyten sowie mögliche Myelinstrukturen, die auf Oligodendrozyten hinweisen, nachgewiesen werden. Elektrophysiologische Aufzeichnungen deuten auf funktionell aktive Neurone hin und Immunofluoreszenzfärbungen zeigten GABAerge, glutamaterge, dopaminerge und serotonerge neuronale Subtypen. Außerdem wurden mittels Immunfluoreszenzanalyse Synapsin- und PSD-95- positive synaptische Strukturen nachgewiesen. Ultrastrukturelle Analysen mittels Transmissionselektronenmikroskopie bestätigten das Ergebnis. Hervorzuheben ist, dass einige Neurone positiv für den peripheren Neuronenmarker Peripherin gefärbt wurden, was darauf hinweist, dass eNEPs das Potenzial besitzen, in Zellen der Neuralleiste zu differenzieren. Durch die Verwendung von spezifischen Differenzierungsprotokollen konnte das Vorkommen TH-positiver und auch möglicher A- und C-sensorischer Fasern, sowie mesenchymaler Zellen nachgewiesen werden. Zusammenfassend lässt sich sagen, dass primäre eNEPs dazu beitragen könnten, die frühe humane Gehirnentwicklung zu verstehen. Darüber hinaus stellen eNEPs eine potentielle zelluläre Quelle für Zellersatztherapien und weitere biomedizinische Anwendungen dar.

List of Abbreviations

A-P	Anterior-posterior
AA	L- Ascorbic acid
AFP	Alpha1-Fetoprotein
BDNF	Brain derived neurotrophic factor
bMG	Basement membrane growth factor reduced Matrigel
BMP	Bone morphogenic protein
BSA	Bovine serum albumine
cAMP	Cyclic adenosinmonophosphate
cDNA	Complementary DNA
CHIR	CHIR99021
CNS	Central nervous system
Cre	Cre recombinase
CRISPR	Clustered regularly interspaced short palindromic repeats
D-V	Dorso-ventral
DAPI	4',6-diamino-2-phenylindole
DAPT	*N*-[(3,5-Difluorophenyl)acetyl]-L-alanyl-2-phenylglycine-1,1-dimethyl esther
dbcAMP	Dibutyryl-cAMP
DMEM	Dulbecco's Modified Eagle Medium
DMSO	Dimethyl sulfoxide
dNTP	Deoxynucleotide triphosphate
EB	Embryoid body
EGF	Epidermal growth factor
eNEP	Early neuroepithelial precursors
ESC	Embryonic stem cell
EtOH	Ethanol
F	forward
FACS	Fluorescence activated cell sorting
FCS	Fetal calf serum
FGF	Fibroblast growth factor
GABA	Gamma amino butyric acid
GAD	Glutamate decarboxylase
GDNF	Glial derived neurotrophic factor
GFAP	Glial fibrillary protein
GSK-3	Glycogen synthase kinase-3

h	hour
hLIF	Human leukemia inducing factor
HSC	Hematopoietic stem cells
iN	Induced neurons
iNPC	Induced neural progenitor cells
iPSC	Induced pluripotent stem cells
KSR	Knockout serum replacement
L	Liter
Ln	Laminin
MEF	Mouse embryonic fibroblast
min	minute
MOI	Multiplicity of infection
mRNA	Messenger ribonucleic acid
NEAA	Non-essential amino acids
NeuN	Neuronal nuclei
NPC	Neural progenitor cells
Oct	Octamer-binding transcription factor
PAX	Paired box
PBS	Phosphate buffer saline
PCR	Polymerase chain reaction
PD	Parkinsons Disease
PFA	Paraformaldehyde
PMA	Purmorphamine
PNS	Peripheral neural system
PO	Polyornithin
R	reverse
RA	Retinoic acid
RG	Radial glia
RI	Rho associated kinase inhibitor
RNA	Ribonucleic acid
rpm	Rounds per minute
RT	Room temperature
SB	SB431542
SeV	Sendai virus
SHH	Sonic hedgehog
SOX	Sex determining region Y-box
SSEA	Stage-specific embryonic antigen

STAT	Signal transducers and activators of transcription
SVZ	Subventricular zone
TALEN	Transcription activator-like effector nuclease
TF	Transcription factor
TGF β	Transforming growth factor beta
TH	Tyrosine hydroxylase
TRA	Tumor recognition antigen
WNT	Wingless-type MMTV integration site family

1. Introduction

1.1 General background of stem cells

Stem cells are undifferentiated cells which possess unique hallmarks defined by self-renewal and potential to give rise to other cell types (Till and McCulloch, 1980; Weissman, 2000). In the late 19th century, Theodor Boveri and others adopted the term *Stammzelle* from the German scientist Ernst Haeckel (Haeckel, 1868) and defined it further in context of studies concerning the field of what we refer nowadays to as primordial germline cells (Ramalho-Santos and Willenbring, 2007). The concept of stem cells and their potential benefit in clinical applications was revived by Till and McCulloch who successfully demonstrated the existence of hematopoietic stem cells (Becker et al., 1963; Siminovitch et al., 1963; Till and McCulloch, 1961). This idea has been previously hypothesized by many researchers since the identification of different white blood lineages but could not be confirmed thus far due to the lack of sufficient experimental techniques (Ramalho-Santos and Willenbring, 2007). One can differentiate between totipotent, pluripotent embryonic and multipotent somatic stem cells which are committed to a specific lineage (Eckfeldt et al., 2005a).

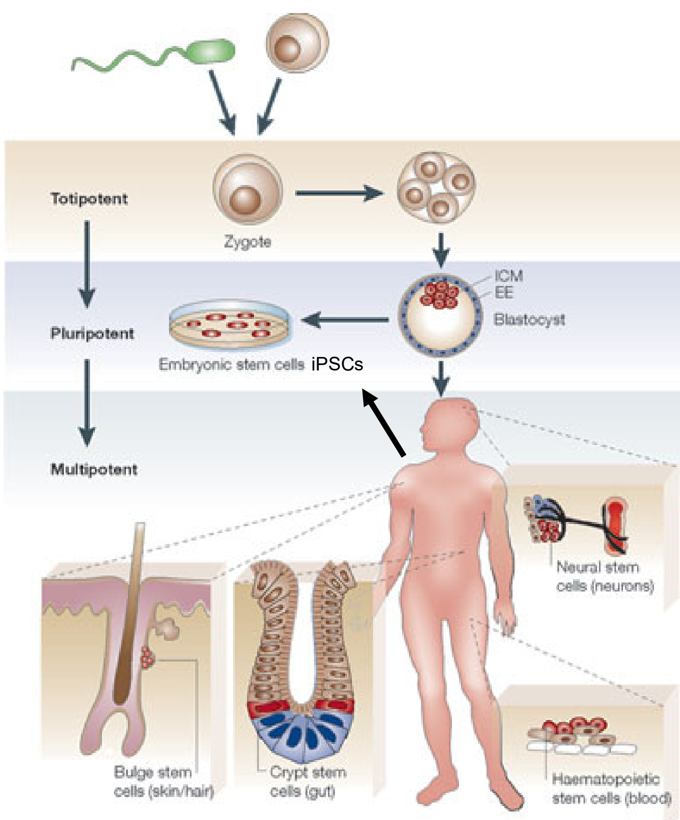

Figure 1.1 Graphical overview of various human stem cells. Stem cells can be subdivided in totipotent, pluripotent and multipotent cells. Pluripotent cells can be derived from the blastocyst or through reprogramming of somatic cells. Multipotent progenitors and their progenies e.g. neural stem cells and neurons can be differentiated from pluripotent cells or isolated from tissue. Modified, (Eckfeldt et al., 2005b).

1.2 Pluripotent stem cells

1.2.1 Embryonic stem cells (ESCs)

Embryonic stem cells can be derived from the inner cell mass of a blastocyst and are pluripotent. As first shown in two separate studies, pluripotent stem cells could be isolated from murine blastocysts and expanded *in vitro* (Evans and Kaufman, 1981; Martin, 1981). The experiments conducted demonstrated their clonogenicity, proliferation *in vitro* and their potential to form teratocarcinoma consisting of cell types of all three germ layers which is considered as a proof of pluripotency. Soon after research succeeded in the establishment of cell lines from other species including sheep (Handyside et al., 1987), rabbit (Giles et al., 1993) as well as bovine (Cherny et al., 1994) and porcine (Gerfen and Wheeler, 1995) ESC lines. Yet, it took more than 15 years until a human pluripotent ESC line could be derived and stably expanded *in vitro* (Thomson et al., 1998). These finding enabled the use of a human line which like their counterparts from other species is self-renewing and can be differentiated in cell types of the three germ layers thus allowed novel potential clinical implications and insight into early human development. First transcriptomic analyses of ESCs revealed the transcription factor OCT4 crucial for self-renewal (Niwa, 2001; Niwa et al., 2000). Furthermore, various studies gave important insights into the transcriptional network of stem cells and thus the molecular signature of “stemness”. For instance, they identified the importance of extrinsic bone morphogenic protein (BMP) and internal Nanog interactions resulting in the activation of signal transducer and activator of transcription 3 (STAT3) (Chambers, 2004; Ivanova et al., 2002; Ramalho-Santos et al., 2002). ESCs can be cultivated under mouse embryonic fibroblast (MEF) feeder conditions, when basic fibroblast growth factor (bFGF) is added or in feeder-free conditions using stem cell media and Matrigel (MG) coating substrate. MG is a protein mixture resembling the extracellular matrix or basement matrix and was shown suitable for ESCs and other cell types (Xu et al., 2001). Pluripotent cells can be identified not only by a typical marker profile of the pluripotency-associated TFs OCT4, SOX2 and NANOG, but also by a surface marker expression. Among others, surface markers such as stage-specific embryonic antigen 3 and 4 (SSEA-3/4) as well as tumor recognition antigens (TRA) 1-60 and TRA1-81 mark human pluripotent cells (Thomson et al., 1998). Various cell types, including cardiac, intestinal and neural cell types have been successfully derived from ESC which makes them a valuable self-renewing cell source and the gold standard for pluripotent cells. On the downside, the sacrifice of pre-implantation embryos for the derivation of ESC lines holds obvious ethical limitations. Therefore, the generation and use of ESCs underlies strict regulations varying upon countries. Notably, the German Embryo Protection Act and the Stem Cell Act prohibit the derivation of ESCs in Germany, but permit the import of ESCs after passing an official approval (Heinemann and Honnefelder, 2002). To circumvent these critical aspects, alternative paths for obtaining pluripotent cells emerged.

1.2.2 Induced pluripotent stem cells (iPSCs)

Reprogramming of fibroblasts and other somatic cells to iPSCs

The pioneer cloning work of the later Nobel laureate Gurdon, who established somatic-cell nuclear transfer in *Xenopus laevis* by continuing preliminary studies conducted 10 years earlier (Briggs and King, 1952; Gurdon, 1962; Gurdon et al., 1958). Applying this technique, the generation of sexually mature adults after the transfer of embryonic and somatic cell nuclei to enucleated unfertilized eggs was demonstrated. Further advances were reported by the landmark study of Wilmut et al. in the sheep. The researchers succeeded to generate a viable offspring applying the same principle by transferring nuclei from cells of different origin to enucleated unfertilized sheep oocytes which were thereafter implanted (Wilmut et al., 1997).

Nevertheless, the first reprogramming of somatic cells into iPSCs followed one decade later by the ground-breaking work of Takahashi and Yamanaka (2006). The induction of pluripotency could be achieved by the overexpression of four transcription factors being OCT4, KLF4, SOX2 and c-MYC using a retroviral system. Previously, those transcription factors have been proposed to play an important role in murine and human ESC. Given the fact, that those cells display the unique properties that have been previously demonstrated in ESCs, they have been also shown to produce viable mice through tetraploid complementation (Zhao et al., 2009). Only one year later, human iPSCs were generated from human foreskin fibroblasts using the same four transcription factors (Yamanaka factors) (Takahashi et al., 2007). Like their murine correlates, they are able to be differentiated into all three germ layers and formed teratoma when injected in immunodeficient mice. Furthermore, in consistency with hESCs they exhibit a characteristic marker profile defined by various TFs and surface molecules. In parallel, other researchers developed alternative combinations of transcriptions factors to induce pluripotency such as OCT4, SOX2, NANOG and LIN28 (Nakagawa et al., 2008; Yu et al., 2007a). However, the reprogramming efficiency remained considerably low.

Many researchers are involved in understanding what processes determine the efficiency and the process of reprogramming. Single cell expression profiles analyzed by Buganim and colleagues identified three phases of reprogramming - an early stochastic phase marked by heterogeneous gene expression, followed by an intermediate rate-limiting phase and a hierarchical phase. The hierarchical phase is initiated by the activation of SOX2 and leads to the activation of further genes and DNA methylation downstream resulting in persisting and stable pluripotency (Buganim et al., 2012; Polo et al., 2012; Tiemann et al., 2011).

In recent years, major progress has been made to demonstrate potential impact on the reprogramming efficiency and alternations in iPSCs-quality depending on the use of alternative cell sources. Thus far, most of the cell types used are represented by dermal fibroblasts but easier accessible alternative cell types have been successfully reprogrammed. Keratinocytes can be obtained by skin biopsies and from plucked hair and reprogrammed more efficient than fibroblasts (Aasen et al., 2008). Further, mesenchymal stem cells from the umbilical cord matrix and amniotic membrane as well as cord blood have been shown to be reprogrammed by using the four classical Yamanaka-factors or less TFs (OCT4 and SOX2) in case of cord blood (Cai et al., 2010; Giorgetti et al., 2009; Haase et al., 2009). To circumvent invasive biopsies and loss of time due to expansion in vitro, peripheral blood was demonstrated as an alternative cell source feasible for the generation of patient-specific iPSCs (Loh et al., 2010; Merling et al., 2013; Staerk et al., 2010). Further cell sources include amniotic fluid-derived cells (Li et al., 2009), adipose tissue-derived cells (Sugii et al., 2010), hepatocytes (Liu et al., 2010) and urine-derived cells (Zhou et al., 2012).

Integration-based and integration-free reprogramming

Soon after the establishment of more robust and efficient reprogramming protocols it became evident that integration-based methods had to be revised to enable future application in biomedical science. The initial use of retroviral vectors bears several disadvantages as only dividing cells are infected and the transgene remains present in the genome. Consequently, it has been replaced by lentiviral vectors which serve as a stronger tool for overexpressing genes in non-dividing cell types (González et al., 2011; Yu et al., 2007b). However, the prolonged presence of viral vectors or reactivation of tumorigenic transcription factors such as c-MYC arose safety concerns (Okita et al., 2007). As an alternative, protocols suggesting to albeit c-MYC were developed, but resulted in low efficiency (Nakagawa et al., 2008; Wernig et al., 2008). Hence, considerable effort has been made to establish alternative systems depending on downstream applications. For instance, as demonstrated by transient expression of relevant transgenes with an adenoviral system (Okita et al., 2008; Stadtfeld et al., 2008; Zhou and Freed, 2009). Others proposed polycistronic single lentiviral vectors (Sommer et al., 2009) which can be induced by the application of Doxycycline and/or excised by Cre recombinase allow to remove transgenes after completed reprogramming (Soldner et al., 2009; Somers et al., 2010; Sommer et al., 2010; Kadari et al., 2014). Moreover, reprogramming using the non-integrating RNA-Sendai virus was shown to be highly efficient for fibroblasts, cord blood and peripheral blood cells (Ban et al., 2011; Fusaki et al., 2009; Merling et al., 2013). Although some of the critical aspects have been solved using excisable or non-integrating viral vector systems it was desirable to omit viral systems which do not satisfy safety requirements needed for therapeutic use.

Therefore, nonviral reprogramming methods emerged. For instance, DNA-based delivery methods include transfection of linear DNA with very low efficiency (Gonzalez et al., 2009) and the use of PiggyBac transposons (Woltjen et al., 2009; Yusa et al., 2009). Moreover, transient overexpression of genes by episomal-based vectors was sufficient to reprogram mouse and human fibroblasts (Yu et al., 2009). Notably, the efficiency could be enhanced when replacing c-Myc by L-Myc and suppressing p53 (Okita et al., 2011). As a novel approach, the use of modified synthetic mRNA was suggested to fully eliminate the use of plasmids or viruses during reprogramming (Warren et al., 2010), but requires daily transfections for a prolonged time. Few studies demonstrated the possibility to use recombinant reprogramming proteins which are fused to peptides mediating their transduction (D. Kim et al., 2009; Zhou et al., 2009; Thier et al., 2012; Bosnali et al., 2009).

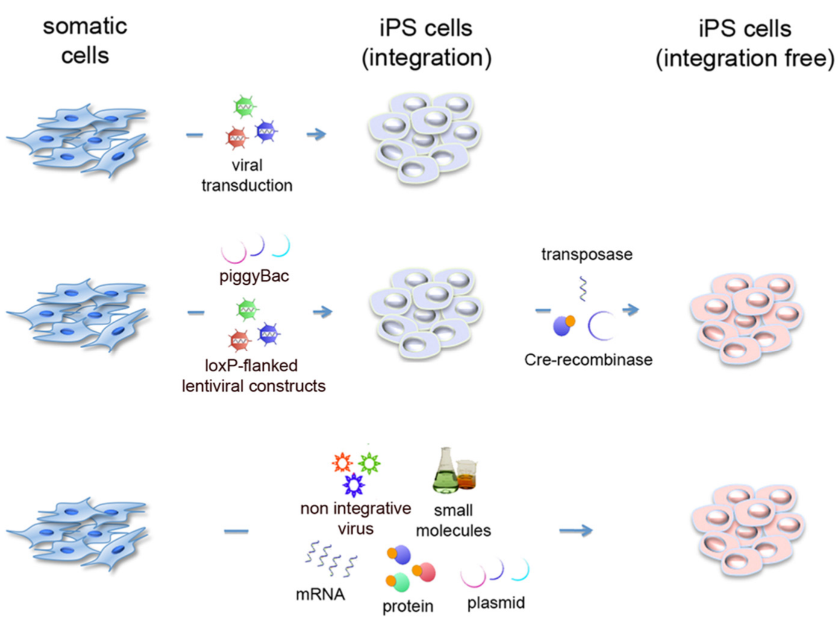

Figure 1.2 Schematic overview of reprogramming methods to yield human iPSCs. Viral transductions result in iPSCs with genome integration, whereas strategies based on piggyBAC/transposase and Cre-excisible lentiviral constructs eliminate transgenes. Other non-integrative methods result in zero-footprint hiPSCs (Wörsdörfer et al., 2013).

A major goal is to achieve not only safe bona-fide hiPSC but also to increase the efficiency when generating hiPSC. The reprogramming efficiency and duration was demonstrated to be enhanced by the use of chemical compounds, often referred to as small molecules, in addition to the classical Yamanaka-factors (Lin et al., 2009; Shi et al., 2008). Zhou and colleagues used valproic acid (VPA), a histone deacetylase inhibitor which facilitates the access of transcription factors to the chromatin in addition to proteins in the media (Zhou et al., 2009). Further examples suggest the supplement with the glycogen synthase kinase-3 beta (GSK3 β)

inhibitor and WNT activator CHIR99021 (CHIR) together with ascorbic acid (AA) that led to iPSCs induction from MEFs as fast as 48 h (Bar-Nur et al., 2014; Esfandiari et al., 2012). Intriguingly, Hou and colleagues addressed this subject by identifying a combination of small molecules which enabled the reprogramming of mouse fibroblasts (Hou et al., 2013). More recently, the induction of iPSCs and NPCs by chemical compounds only was shown using mouse fibroblasts (Biswas and Jiang, 2016). However, thus far a chemical cocktail for reprogramming of human cells has not been established (Lin and Wu, 2015). Knowledge has been gained evaluating various transgene-free reprogramming protocols as done in a comprehensive meta-analysis by Schlaeger and colleagues (2015). Interestingly, major differences could be identified regarding efficiency, time-consumption and aneuploidy suggesting a selecting adjusted to individual research goals. Despite constantly evolving new protocols considerations should include starting cell type, reprogramming method and quality control (González et al., 2011).

Disease-specific iPSCs

Before the hiPSC- technology emerged, modelling of diseases was mostly carried out using model organisms due to restricted accessibility of affected cell types in the human body and ethical concerns. In contrary, reprogramming techniques enable to generate patient-specific iPSCs which can be differentiated in the desired cell type. Thus, enabling to elucidate molecular disease mechanisms and facilitate the discovery of novel biomarkers. Moreover, pharmacological screening, gene editing and correcting as well as cell replacement represent potential applications in biomedical research, as summarized in Fig.1.3 (Stadtfeld and Hochedlinger, 2010; Sterneckert et al., 2014).

Neurodegenerative diseases are of particular interest for researchers since many of them are age-related and affect a growing population group worldwide. Notably, iPSC-type reprogramming contributed to major progress in modeling of various neurological diseases such as Parkinson’s (PD) and Huntington disease (Park et al., 2008; Soldner et al., 2009; Yu et al., 2013). PD-specific hiPSC-derived dopaminergic neurons showed mutation associated effects and were phenotypically close to patients’ neurons. For instance, some of the lines were generated with synuclein dysfunction (Devine et al., 2011), mutations in PINK1-gene (Seibler et al., 2011), LRRK2 mutants (Nguyen et al., 2011) as well as sporadic PD (Sánchez-Danés et al., 2012). Therefore, for instance hiPSCs from patients suffering from Alzheimer Disease helped to elucidate the role of related mutations recapitulating accumulations of amyloid β and phospho-tau in AD-derived neurons (Israel et al., 2012). hiPSCs from patients with neurodevelopmental diseases like Rett-syndrome or Williams syndrome help to elucidate causative effects by accurately representing synaptic defects *in vitro* (Chailangkarn et al., 2016; Marchetto et al., 2010). Even multifactorial psychiatric diseases (Brennand et al., 2012; Wen et al., 2014) can be analyzed and understood using hiPSC-derived cells revealing alterations in synaptic arboration, spine density and soma size connected to candidate genes contributing to various diseases.

Despite fast progressing disease-specific iPSC-models, many of late onset diseases are challenging to be recapitulated *in vitro* since the generated cell types possess properties of "rejuvenated" cells. Thus, their progenies as for instance differentiated neurons, represent early immature cell types comparable to fetal neurons which might fail to develop age-related phenotype needed to elucidate mechanisms of degeneration (Ho et al., 2016). Therefore, concepts of induced aging emerged. Notably, age-related DNA-methylation patterns have been described by Horvath allowing an evaluation of resulting cell phenotypes (Horvath, 2013). For instance, an overexpression of the mutated *LMNA* gene were shown to lead to an age-related phenotype, as reported for the Hutchinson-Gilford progeria syndrome (Liu et al., 2011; Miller et al., 2013). Alternative approaches focus on the downregulation of telomerase leading to telomere shortening of manipulated hiPSCs and age-associated phenotypes of their neuronal progenies (Vera et al., 2016). To achieve transgene-free aging other means such as toxins or reactive oxygen species causing cellular stress have been reviewed (Studer et al., 2015). Furthermore, rapid development of gene editing technologies, especially zinc-finger nucleases (H. J. Kim et al., 2009), transcription activator-like effector nucleases (TALEN) and clustered regularly interspaced palindromic repeats (CRISPR)/Cas9 contribute immensely to progress in understanding of diseases and allows modelling and correction of disease-related phenotypes (Mali et al., 2013; Miller et al., 2011; Ran et al., 2013).

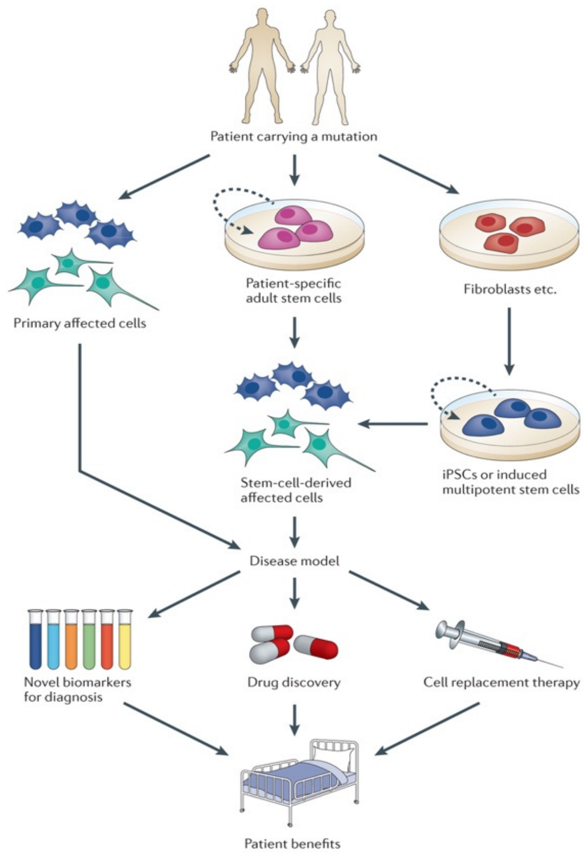

Figure 1.3 Graphical summary of potential applications of stem cell-based disease models. Disease models established using primary and stem cell-derived affected cells which are specific to the patient allow divers applications. Besides diagnostic screening for novel biomarkers, innovative compounds and drugs with less off-target effects can be developed. Moreover, progenies of iPSCs or multipotent stem cells could be used for cell replacement, leading overall to benefits for individuals affected by disease (Sterneckert et al., 2014).

1.3 Multipotent stem cells

In contrary to pluripotent cells which have the unique ability to differentiate into all other cell types and are virtually unlimited in their expansion potential, adult stem cells are multipotent cells. In other words, they are restricted in their lineage potential giving rise to some tissue specific cell types and showing limited proliferation. They can represent either progenies of ESCs or can be found in specific tissues where they are crucial for continual regeneration (Eckfeldt et al., 2005b). Self-renewal and differentiation are dependent on intrinsic signaling pathways as well as complex microenvironmental cues of the so called stem cell niche (Spradling et al., 2001). The best characterized adult stem cells are hematopoietic stem cells (HSCs) which were first described by Till and McCulloch (1961). Their differentiation and proliferation capacity and molecular signature has been extensively studied by many others (Eckfeldt et al., 2005b; Ogawa, 1993). HSCs give rise to hematopoietic precursor cells and their progenies including all myeloid and lymphoid blood lineages which are regenerated throughout the whole lifetime. The maintenance of the HSC pool is supported by the stem cell niche localized in the endosteal marrow (Gong, 1978; Spradling et al., 2001), where growth factors provide a microenvironment which has regulative effects (Calvi et al., 2003). Besides, more adult stem and precursor cells have been reported (see Fig.1.1) such as mesenchymal stem cells in the bone marrow stroma (Gronthos et al., 2003), cardiac progenitor cells (Oh et al., 2003), intestinal epithelial progenitors in the gut crypt (Stappenbeck et al., 2003), bulge cells/epithelial stem cells in the hair follicle (Blanpain et al., 2004; Morris et al., 2004; Tumbar et al., 2004) and neural progenitor cells (NPCs) (Reynolds and Weiss, 1992).

1.3.1 Definition and characteristics of adult neural progenitor cells (NPCs)

Neural stem cells (NSCs) and NPCs are multipotent stem cells which can give rise to the three cell types of the central neural system (CNS) namely neurons, astrocyte and oligodendrocytes. Physiologically, NPCs can be found during neural development as well as in the adult mammalian brain. Nevertheless, until the 1990s it remained under debate if stem cells persist in the adult CNS and thus contribute to neural replacement. Although first evidence of postnatal neurogenesis in rats was shown in 1965 (Altman and Das, 1965), in 1992 Reynolds and Weiss who succeeded to confirm adult neurogenesis (Reynolds and Weiss, 1992). Thereafter, various studies demonstrated and characterized NPCs located in the dentate gyrus of the hippocampus which can give rise to functionally integrated neurons (Gage et al., 1998; Kempermann et al., 1997; van Praag et al., 2002) as well as the subventricular zone (Cameron et al., 1993; Doetsch et al., 1999; Lois and Alvarez-Buylla, 1993) of the adult mammalian brain. Moreover, NPCs were successfully derived from murine adult forebrain (Pollard et al., 2006). The presence of adult neurogenesis in human brains and thus closing the gap between rodent models and human physiology was confirmed in the adult hippocampus (Eriksson et al., 1998; Jessberger and Gage, 2014). However, somatic NPCs are restricted to several neuronal subtype and glial cells with some NPC-types possessing a glial nature themselves (Kriegstein and Alvarez-Buylla, 2009). Due to the restricted access and ethical considerations, it is not challenging to isolate and study adult human NPCs *in vitro* thus indicating the requirement of alternative sources to allow detailed studies.

1.3.2 Regulatory pathways of NPCs

The self-renewal activity and differentiation of NPCs in adult niches are regulated by the microenvironment. Many key players have been identified to sustain the NPC identity. Studies suggest that the stem cell niche in embryonic and adult neural progenitor cells is regulated by endothelial cells in the vascular niche (Shen et al., 2004) as well as by surrounding astrocytes which are able to modulate synapse formation and synaptic transmission (Song et al., 2002). Thus, an interplay between Notch-signaling which regulates NPC maintenance and self-renewal in concert with endothelial growth factor (EGF) receptor signaling which is involved in proliferation and migration (Aguirre et al., 2010) takes place. During neural development, Notch signaling plays a major role in the transition from primitive to full definitive NSC identity and its maintenance. Interestingly, Notch 1-4 signaling and its downstream effector genes are activated by ligands such as Delta-like and Serrate-like (Jagged-1, 2) provided by other cells by direct cell-cell contact. The initiation of the signaling leads to transcriptional activation of the basic helix-loop-helix genes Hairy-Enhancer of Split (HES) and other gene families (Louvi and Artavanis-Tsakonas, 2006). The blocking of the Notch signaling pathway can be effectively achieved by the γ-secretase inhibitor DAPT (Geling et al., 2002).

Sonic hedgehog (SHH) signaling has been described to be important in regulating self-renewal, proliferation and patterning of neural progenitors in the developing brain and the adult SVZ (Lai et al., 2003; Rowitch et al., 1999). In presence of SHH ligand the canonical pathway is activated involving the transmembrane receptor Patched and its co-receptor Smoothened and a subsequent translocation of the Gli-complex into the nucleus where it regulates gene expression of e.g. GLI1 and SOX2. Specific agonistic compounds have been developed, such as Purmorphamine (PMA) which activates Smoothened (Rimkus et al., 2016; Sinha and Chen, 2006). Intriguingly, SOX2 expression plays a major role in self-renewal and differentiation and was further identified as an important regulator of NOTCH1 signaling depending on the developmental stage (Pevny and Nicolis, 2010).

In contrast to previously mentioned factors which promote neural identity and self-renewal, members of the transforming growth factor (TGF)-β family have been implicated to have an opposing effect, promoting differentiation. Prominent representatives are BMP and TGF-β proteins which bind to serine/threonine kinase receptors and therefore induce the activation of SMAD 1/5/8 or SMAD 2/3, respectively. Pharmacological modulation of receptor kinases can be achieved by e.g. Dorsomorphin (BMP inhibitor) or SB431543 (SB) which antagonizes specifically TGF-β activation (Inman et al., 2002; Kandasamy et al., 2011).

1.4 Neurogenesis *in vivo*

The early human development is initiated after fertilization of the oocyte resulting in the zygote containing a diploid set of maternal and paternal chromosomes. By mitotic processes, the zygote is undergoing cell division and forms multicellular stages e.g. blastomer, morula and blastocyst containing the inner cell mass. In the process of gastrulation, the three germ layers form. The endodermal layer gives rise for instance to cells of the gastrointestinal tract and respiratory system, mesoderm is the origin of bones, skeletal muscles and heart tissue and the ectodermal layer is fated to give rise to epidermis and neural tissue.

1.4.1 Neural induction and neurulation

Neural induction in the ectoderm (epiblast) is initiated by molecular signals from an organizer region in the dorsal mesoderm (Spemann and Mangold, 2001). Many signaling molecules such as noggin (Smith and Harland, 1992), follistatin (Hemmati-Brivanlou et al., 1994) and chordin

(Sasai et al., 1994) have been identified to play a role in the specification of the neuroepithelium. Shortly after, BMP in concert with FGF have been suggested as crucial key-players in the complex interactions leading to neural induction (Levine and Brivanlou, 2007). FGF signaling can be activated by 18 ligands binding to transmembrane tyrosine kinase receptors. Downstream, their action is mediated through four effector pathways (RAS-RAF-MAPK, PI3K-AKT, STAT and phospholipase Cγ) (Turner and Grose, 2010). Notably, FGF was reported to regulate the neuroectoderm specification by increasing PAX6 expression (Yoo et al., 2011). Cells of the neuroepithilium are undergoing a morphogenetic process called neurulation consisting of four stages: the formation of the neural plate, shaping and thickening of the neural plate, bending and folding and finally fusion of the neural folds. During this process, the neural tube is formed giving rise to the future CNS. In parallel the dorso-lateral parts of the neuroectoderm, consisting of neural crest precursors are migrating to eventually form cells of the PNS as well as various other cell types (Smith, 1997). Multiple genes and molecular pathways have been reported to be involved in this process and its abnormalities resulting in neural tube defects (Lowery and Sive, 2004). For instance, extracellular signal-regulated kinase 1/2-mediated FGF signaling has been proposed to regulate the expression of PAX6 and thus contributing together with SOX1 to neuroectoderm specification (Suter et al., 2009; Yoo et al., 2011; Zhang et al., 2010).

1.4.2 Patterning of the CNS

During embryogenesis, the neural tube is subjected to morphogen gradients that mediate positional information resulting in the acquirement of specific regional identities (Temple, 2001). Cells are undergoing proliferation and anterior-posterior (A-P) patterning which serves as a base for the formation of several vesicles which later develop into parts of the central nervous system (Lumsden and Krumlauf, 1996). The subdivision in prosencephalon (the future forebrain), mesencephalon (the prospective midbrain), rhombencephalon (which becomes the hindbrain) and spinal cord is regulated by various signal molecules. It is well understood, how this morphogenic process depends on the interaction of WNT proteins in concert with RA and FGF signals as graphically depicted in Fig. 1.4 A (Kudoh et al., 2002; Niehrs, 2004). Increasing WNT and FGF concentrations suppress the expression of anterior genes and activate posterior genes (Kudoh et al., 2002). Regional identity is marked by a distinct set of highly upregulated genes as for instance FOXG1, OTX2 and DACH1 indicating the anterior fate. Expression of EN1 and NKX2.1 is characteristic for cells of the midbrain fate (Elkabetz et al., 2008; Koch et al., 2009). Recently, the influence of WNT signaling has been studied in ESC-derived single cell RNA-seq studies identifying an early segregation of mid/hindbrain primed cells in response to activation of canonical WNT pathway (Yao et al., 2016). WNT ligands origin from paracrine and autocrine secretion and bind to the receptor Frizzled. This leads to the deactivation of the

GSK3-β, followed by a subsequent β-catenin stabilization and translocation to the nucleus activating target genes (Faigle and Song, 2013; Logan and Nusse, 2004). Hindbrain patterning and segmentation strongly depends on RA influencing the expression of HOX genes and other hindbrain specific genes in a concentration-dependent manner (Rhinn and Dollé, 2012).

In parallel, patterning of the neural tube along the dorsal-ventral (D-V) axis occurs (De Robertis and Kuroda, 2004). It is hallmarked by an orchestrated interplay of the dorsalizing activity of BMP and canonical WNT signaling (Lee and Jessell, 1999) which antagonizes ventralizing cues provided by the SHH proteins (Echelard et al., 1993; Le Dréau and Martí, 2012). While, BMP and WNT proteins are secreted by the non-neural ectoderm and roof plate, SHH origins from the notochord and the floor plate (Wurst and Bally-Cuif, 2001). As a result, a specialization of the ventral parts of rostral neural tube into the medial and lateral ganglionic eminence which are structures crucial for subsequent migration of cell and later axons into the cortex (Fig. 1.4 B) (Tao and Zhang, 2016). Further examinations in the spinal cord unraveled a ventral to dorsal gradient of SHH which might be transduced into an intracellular gradient of downstream effectors modulating Gli activity. Resulting from a dose-dependent SHH signaling the expression of various TFs is affected promoting the determination of distinct ventral progenitor domains (Figure 1.4.C). Several marker genes can be assigned to the ventral neural tube, such as NKX2.2, NKX6.1, FOXA2, SPON1, NTN1 (Dessaud et al., 2008; Fasano et al., 2010). In contrast, only a few TF have been described to be involved in roof plate development including PAX3 and LMX1A (Chizhikov and Millen, 2004a; Millonig et al., 2000).

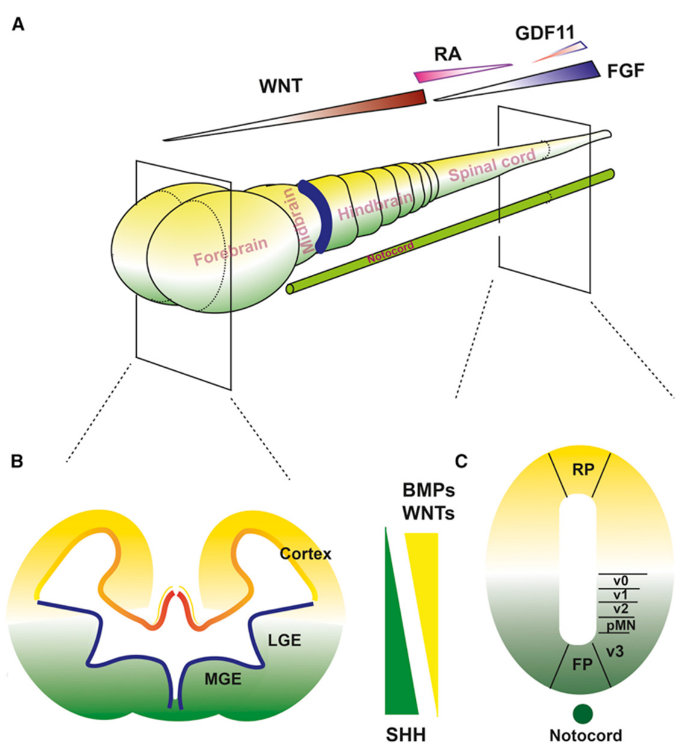

Figure 1.4 Schematic overview of patterning principles in the neural tube. (A) Patterning along the A-P axis is dependent on gradients of morphogenes like WNT, RA and FGF. Similarly, D-V specification is influenced by gradients of SHH, BMPs and WNTs resulting in defined regions of the prospective forebrain (B) and spinal cord (C). MGE: medial ganglionic eminence, LGE: lateral ganglionic eminence, RP: roofplate, FP: floorplate. V0-V3 represent four classes of ventral interneurons, pMN represents motor neurons. Tao and Zhang, 2016.

1.4.3 Neuronal specification and gliogenesis

Subsequent, the specification of various parts of the neural tube into neuronal subtypes as well as glial cells represents a critical step of the neural development. The major part of the progenitors with anterior fate differentiates into cerebral glutamatergic cortical neurons in addition to GABAergic medium spiny neurons, GABA interneurons and basal forebrain cholinergic neurons (Tao and Zhang, 2016). The subtypes are specified along the D-V axis depending on the prepatterning to medial and lateral ganglionic eminence and cortical regions due to aforementioned morphogen gradients (Fig. 1.4 A). Recently, additional key player namely the PRDM family proteins were suggested to influence various subtype specification-related gene networks. Along the neural tube the subdivision in distinct D-V progenitor domains results in different gene expression and subsequently distinct neuronal progenies. In particular, high levels of SHH activate ventral genes such as *NKX2.2*, *NKX6.1* and *OLIG2* from which dopaminergic neurons arise in the midbrain and serotonergic neurons in the hindbrain. Accordingly, cholinergic motor neurons origin from ventral spinal progenitors (Tao and Zhang, 2016; Zannino and Sagerström, 2015). During progressing development, astrocytes origin from the SVZ which harbor radial glia cells. With a pronounced delay, oligodendrocytes origin from some parts of the ventral telencephalon and neural tube, dorsal neural tube and the SVZ (Kriegstein and Alvarez-Buylla, 2009; X Qian et al., 2000).

1.5 Neurogenesis *in vitro*

For deeper understanding of the molecular mechanisms involved in neural induction, patterning and specification of NPCs, *in vitro* correlates emerged to be helpful. By mimicking the major developmental steps of the nervous system, the role of morphogens and signaling pathways corresponding to time frames *in vivo* can be elucidated. Various approaches have been taken to obtain human NPCs such as isolation from fetal material, differentiation from ESCs and iPSCs, respectively and by the application of direct conversion protocols to somatic cells (Mertens et al., 2016; Uchida et al., 2000). However, it is still a subject of debate if this NPC lines accurately represent the *in vivo* status due to potential alterations of genetic and epigenetic profiles (Conti and Cattaneo, 2010). Nevertheless, state-of the art techniques made it possible to enrich otherwise transiently appearing central and peripheral neural cell types by the application of well-established specific differentiation protocols.

1.5.1 NPCs from fetal sources

Early studies show the possibility to isolate fetal neural precursor cells from rats and use them in a variety of transplantation studies (Dunnett and Björklund, 1999; Gage et al., 1995; Uchida et al., 2000). Further, neuroepithelial precursor population from rats of E10.5 which can be differentiated in central and peripheral lineages and are therefore more plastic in their differentiation potential have been generated (Kalyani et al., 1997). However, similar experimental approaches were developed for human fetal brain derived neural precursor cells (NPCs) to obtain a reliable source of human neural tissue for drug screening and grafts. Those isolated NPCs are multipotent cells giving rise to neurons, astrocytes and partly oligodendrocytes and can be expanded in spheres in a serum free media supplemented by basic fibroblast factor (bFGF) and epidermal growth factor (EGF) (Carpenter et al., 1999; Svendsen et al., 1998; Vescovi et al., 1999). In addition, directly isolated cells from human fetal brain tissue using antibodies to cell surface markers such as CD133 and fluorescence-activated cell sorting have been shown to engraft successfully in mice (Tamaki et al., 2002; Uchida et al., 2000). Furthermore, monolayer cultures have been also generated from adult and fetal brains (Walton et al., 2006; Yan et al., 2007). Moreover, a prolonged cultivation could be successfully achieved (Wachs et al., 2003). Further investigations showed the derivation of NPCs which retain their regional identity (Horiguchi et al., 2004). Notably, a tetracycline-controlled immortalized NPC line of midbrain origin has been reported and is nowadays widely used to yield dopaminergic neurons (Lotharius et al., 2002).

Hook et al. reported a broad application of primary human NPCs such as a cell-based assay platform, including scale-up and automation, genetic engineering and functional characterization of differentiated progeny (Hook et al., 2011). Recent studies suggest the use of genetically modified fetal derived human neural progenitor cells for delivery of factors e.g. glial cell line-derived neurotrophic factor (GDNF) after grafting in various animal disease models (Behrstock et al., 2006; Emborg et al., 2008; Gowing et al., 2014; Suzuki et al., 2007). However, the described cell populations are displaying radial glia-like characteristics although physiologically earlier neural stem cell stages with a broader differentiation potential such as rosette stage cells appear (Elkabetz et al., 2008). A more recent protocol using human fetal brains describes the derivation of progenitors which are grown in adherent cultures in the presence of EGF and bFGF and possess a highly neurogenic capacity. Those cells form rosette-like structures and seem to be similar to neuroepithelial rosette-like cells as previously generated from human ES and hiPSCs (Elkabetz et al., 2008; Koch et al., 2009; Tailor et al., 2013). Novel protocols describe the stabilization of a midbrain NPC line which can be used for clinical applications, especially as a cell source for a therapeutic approach to PD (Moon et al., 2016), but are keeping to FGF/EGF conditions.

1.5.2 Differentiation of NPCs from ES cells and iPSCs

The potential of ESCs to differentiate in neural lineages has been confirmed by spontaneous differentiation of ESCs after deprivation of serum or a supportive feeder layer (Tropepe et al.,

2001) and teratoma as well as three germ layer assays. Based on knowledge gained from intensive studies of early neural development *in vivo*, directed neural induction *in vitro* could be established. For Instance, neural induction was shown to be achieved by the application of retinoic acid to spherical embryoid bodies (Bain et al., 1995; Bibel et al., 2004) but were claimed to be restricted to gliogenic properties with prolonged propagation (Brüstle et al., 1999; Glaser and Brüstle, 2005). Notably, Conti and colleagues succeeded to derive and maintain a NPC line from murine ESCs which can be expanded without accompanying differentiation (Conti et al., 2005). When differentiating human ESCs as embryoid bodies in the presence of bFGF the formation of neural tube-like structures was observed by Zhang and colleagues. The researchers successfully isolated, expanded and differentiated the neural rosettes into numerous region-specific neuronal and glial cell types (Zhang et al., 2001). Moreover, early rosette stage cells with a broad differentiation capacity in CNS and PNS fates were established from ESC cells (Elkabetz et al., 2008). Beforehand, neural crest cells (NCS) which can generate cells of the PNS as well as mesenchymal cells were shown to be differentiated from ESCs (Lee et al., 2007). Specific protocols were developed which allowed the differentiation of neural crest cells from pluripotent cells harboring potential use in regenerative biology (Lee et al., 2007; Menendez et al., 2013).

Early development of the CNS and PNS is regulated by WNT and BMP signaling (Patthey et al., 2009, 2008). Hence, the inhibition of differentiating cues to mesodermal or endodermal lineages must be blocked by the modulation of relevant signaling. The establishment of a highly efficient neural induction of ESCs and iPSCs which is marked by dual SMAD signaling inhibition achieved by the use of the chemical compounds Noggin, a BMP-signaling inhibitor, and TGFβ inhibitor SB431542 (Chambers et al., 2009). Interestingly, the derivation of a rosette-type, self-renewing human FGF- and EGF-dependent NPCs being highly responsive to extrinsic fate induction while maintaining a long term proliferation potential could be achieved (Koch et al., 2009). Notably, hLIF-dependent primitive neuroepithelial NPCs have been rapidly inducted from ESCs and iPSCs by defined media conditions consisting of CHIR and SB (Li et al., 2011). Besides, relevant signaling pathways were modulated to enable the derivation of small molecule NPCs by applying a media composed of CHIR, SB and PMA (Reinhardt et al., 2013). Notably, these smNPCs are responsive to patterning cues and acquire various phenotypes of central and peripheral lines.

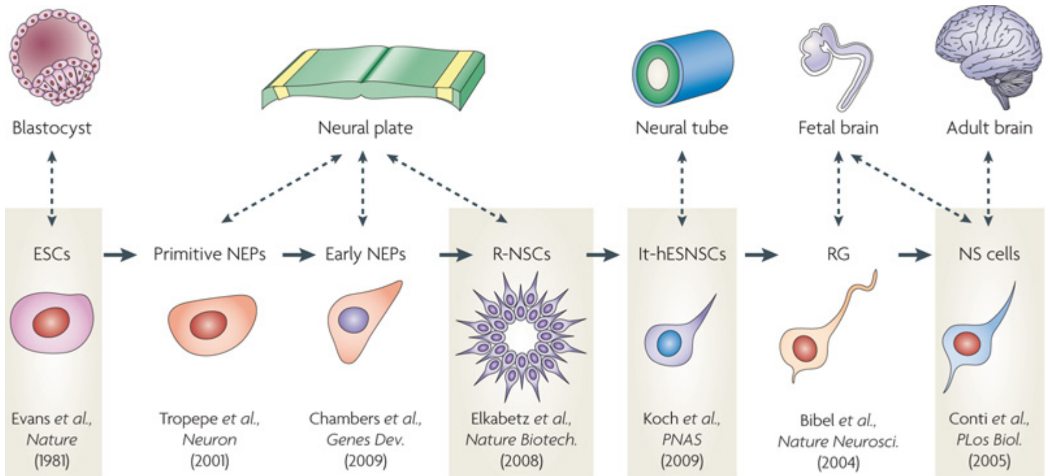

Figure 1.5 Schematic presentation of ESC-derived neural lines and their *in vivo* correlates. Cell populations which appear transient *in vivo* can be differentiated and enriched from pluripotent cells such as ESCs. Primitive and early NEPs as well as R- NSCs possess similar characteristics like cells of the neural plate. More restricted progenies such as lt-hESNSCs, radial glia (RG) and NS cells resemble cells from the neural tube, fetal brain and the adult brain, respectively (Conti and Cattaneo,

However, there are considerable arguments which limit the use of iPSC-derived NPCs. On the one hand, through passing the pluripotent state there is a remaining risk of requiring of pluripotent and thus eventual tumorigenic effects (Miura et al., 2009). On the other hand, the derivation of NPCs is a laborious procedure. It was shown that transient overexpression of lineage-specific factors could induce directly converted multipotent stem cells or terminally differentiated cells. Therefore, direct conversion protocols of somatic cells to induced NPCs (iNPCs) or induced neurons (iN) bypassing the pluripotent state emerged as an alternative (Mertens et al., 2016).

1.5.3 Direct conversion of fibroblasts to NPCs

The concept of direct conversion, also known as transdifferentiation, proposes a transition from one cell type into another progenitor or somatic cell type. In the first attempt to convert an adult cell type into another rodent fibroblasts were successfully converted into myoblasts overexpressing one single gene MyoD (Davis et al., 1987). The landmark study of the Wernig group provided evidence for successful conversion of mouse embryonic fibroblasts (MEFs) into postmitotic neurons. The protocol is based on ectopic overexpression of only three lineage specific TFs, namely Ascl1, Brn2 and Myt1 (Vierbuchen et al., 2010). A different approach suggests a transient overexpression of Yamanaka-factors which lead to the generation of neural progenitor cells giving rise to neuronal and glial cells (Kim et al., 2011). Our group demonstrated that time-dependent overexpression of Oct4 together with a chemically defined neural induction media is able to convert MEFs to iNPCs (Thier et al., 2012). Compelling data proposed that SOX2 is a crucial key factor in neural induction directly regulating SHH signaling

(Favaro et al., 2009). Thus, it was reported that conversion into NPCs can be achieved by the overexpression of SOX2 alone (Ring et al., 2012) or in a combination with other factors. Promising protocols emerged which proposed the acquisition of iNPC-phenotype in a short and efficient manner replacing OCT4 by Brn4, another Pou-family member (Kim et al., 2014). Others suggested the use of Yamanaka factors in combination with defined neuroinductive culture conditions implementing chemical compounds which are able to modulate relevant signaling pathways (Cairns et al., 2016; Lu et al., 2013; Meyer et al., 2015).

However, it has been shown that the transition of protocols to human cells may require some modifications in the expression system, additional transcription factors or chemical enhancers. Exemplary, the overexpression of the three TF used initially to directly convert neurons from murine fibroblasts resulted only in immature neurons from human fibroblasts. Thus, an additional transcription factor (NeuroD1) was needed to obtain mature neurons (Pang et al., 2011). In contrary, embryonic fibroblasts acquired neuronal phenotype and could be even specifically converted in dopaminergic neurons upon addition of two subtype-specific factors (Pfisterer et al., 2011). Other factor combinations for generation of dopaminergic neurons from MEFs, fetal and adult fibroblasts were implicated (Caiazzo et al., 2011). Moreover, the addition of small molecules facilitates direct conversion and was demonstrated to result in higher efficiency (Ladewig et al., 2012). To overcome the lack of age-associated phenotypes artificial induced aging can be achieved resulting in directly converted neurons which show age related properties (Mertens et al., 2015). On the downside, it is still under debate if there might be a transient pluripotent stage as suggested by Bar-Nur and colleagues reviewing current protocols (Bar-Nur et al., 2015). Although direct conversion represent a time-saving straight-forward method to obtain specific cell types many mechanisms underlying lineage transition remain to be fully disclosed (Vierbuchen and Wernig, 2011).

1.5.4 Neuronal differentiation of NPCs *in vitro*

Many disease-associated molecular phenotypes can be analyzed at the level of terminally differentiated cells. Default neuronal differentiation in vitro can be achieved by omitting relevant NPC self-renewal growth factors resulting in neurons, astrocytes and oligodendrocytes. Furthermore, unspecific differentiation can be promoted by pharmacologically inhibiting Notch signaling using DAPT and neurotrophic factors such as glial cell line-derived neurotrophic factor (GDNF) and brain-derived neurotrophic factor (BDNF) (Geling et al., 2002). Based on detailed knowledge that has been gained on patterning and specification cues acquisition of specific phenotypes can be directed. Resulting postmitotic neurons can be validated by transmitter phenotype, marker gene expression as well as functional properties such as synaptic activity and electrophysiological studies (Prè et al., 2014). Thus, enabling the understanding of disease affected neurons as well as serving as healthy control neurons and drug screening platforms. A prominent neurotransmitter is GABA which is synthesized from the amino acid Glutamate catalyzed by the enzyme glutamate decarboxylase (GAD 65/67) by GABAergic neurons. GABA has distinct roles in neural development and the adult brain exhibiting excitatory effects first and serving mostly as excitatory inhibitory transmitter in the mature nervous system (Ben-Ari, 2002; Szabadics et al., 2006). Specific receptors termed GABA-B (metabotropic) and GABA-A (ionotropic) are localized on many neurons to promote GABA-mediated signaling. Interestingly, the default neuronal differentiation tends to yield predominantly GABAergic neurons (Jain et al., 2003). Therefore, specific protocols to force the acquisition of other subtypes are required. Nevertheless, it must be taken into account that neuronal differentiation *in vivo* to yield mature postmitotic neurons is a time-consuming process. To assess maturation status electrophysiological firing pattern and the presence of synaptic marker proteins like Synapsin and PSD95 can be evaluated (Tao and Zhang, 2016).

Targeted dopaminergic differentiation

Based on detailed understanding of underlying processes for midbrain development, Perrier and colleagues were the first to establish directed differentiation in midbrain dopaminergic neurons from ESCs *in vitro.* In detail, they achieved neural induction using stromal cells, followed by patterning towards ventral midbrain/hindbrain fate by SHH and FGF8 and a subsequent maturation step (Perrier et al., 2004). More recent, optimized protocols which implicate small molecules activating SHH and canonical WNT signaling showed efficient engrafting in PD animal models either in a rosette-based (Kriks et al., 2011) or in a floorplate precursor approach (Kirkeby et al., 2012). Similarly, patterning with PMA and FGF8, followed by a maturation period with medium including BDNF, GDNF, TGFb3, AA and dbcAMP was used to successfully induce dopaminergic neurons from stable NPCs (Reinhardt et al., 2013). Notably, these protocols result in functionally integrating neurons demonstrated in a rat model of PD (Grealish et al., 2014).

Differentiation of peripheral neurons

The vast majority of NPCs has a limited capacity to give rise to peripheral lineages including sensory neurons and nociceptors. However, a number of syndromes affecting peripheral neurons such as Hirschsprung disease, familial dysautonomia or chronic pain require an accurate human model (Lee et al., 2012; Nat, 2016). Early studies postulated the existence of a common progenitor of CNS and PNS lineages (Mujtaba et al., 1999). Specific protocols allow the differentiation of such cell types from pluripotent cells by either establishing neural crest cells and their subsequent differentiation or direct differentiation of nociceptors (Chambers et al., 2012; Lee et al., 2007; Menendez et al., 2013; Young et al., 2014). Further advances demonstrated that iPSC and ESC-derived as well as directly converted NPCs can be differentiated into central as well as neural crest related cell types (Elkabetz et al., 2008; Lee et al., 2015; Reinhardt et al., 2013). To achieve this, a dose-dependent exposure to WNT and BMP proteins in combination with trophic factor activation by e.g. BDNF or nerve growth factor is inevitable. Markers associated with peripheral sensory neurons are Peripherin, BRN3a, as well as subtype specific expression of Calcium and Natrium voltage or transient receptor potential channel proteins (Nat, 2016; Reinhardt et al., 2013).

1.6 Biomedical application of stem cells

A variety of biomedical applications in cardiovascular, diabetic, and neurological research and regenerative therapy can be addressed with the help of stem cells. Besides, modelling diseases by recapitulating specific phenotypes and thus unraveling molecular mechanisms, cell replacement, tissue engineering and drug testing are potential targets.

Most notably, cell replacement in cardiovascular (e.g. myocardial infarct), metabolic (e.g. diabetes) and neurological diseases (e.g. PD, Huntington, Amyotrophic lateral sclerosis, spinal cord injury) are of central focus for emerging restorative cell therapy strategies (Stadtfeld and Hochedlinger, 2010). Due to the unrestricted self-renewal capacity of pluripotent stem cells, a virtually unlimited number of cells can be generated in 2D or 3D. Hence, fulfilling the needs of upscaling processes for the generation of sufficient number of cells required for cell replacement (Zweigerdt et al., 2011). Despite first attempts to apply iPSC-derived retinal pigment epithelium in treatment of macular degeneration, obstacles have to be overcome such as the reduction of risk of dedifferentiation into tumorigenic cells (Steinbeck and Studer, 2015). As proofed by clinical trials on PD patients, thus far fetal derived NPCs are the gold standard source of dopaminergic neurons (Abbott, 2014; Barker et al., 2013). Although, the initial evaluation was of poor outcome, most likely due to unequal preparation procedures of grafted cells, improved and standardized protocols help address this issue (Brundin et al., 2010). Nevertheless, promising grafting outcomes of specifically differentiated dopaminergic progenitors in preclinical animal models of PD could demonstrate an amelioration comparable to fetal neurons (Grealish et al., 2014). Therefore, efficient and specific differentiation protocols for midbrain dopaminergic neurons as well as a high level of quality control and trial design are crucial for safe and successful future cell therapy trials (Barker et al., 2015; Kriks et al., 2011). Moreover, high purity and xeno-free differentiation, as reported recently (Kirkeby et al., 2016), represent important steps towards feasible progenies of clinical grade.

High throughput standardized screening libraries for drugs or small molecules are a versatile tool to predict (neuro)toxic and therapeutic effects. With a virtually unlimited number of cells stem cells could contribute enormously to the development of pharmacological substances with less off-target effects (Heilker et al., 2014). Notably, some effort has been taken to establish iPSC-based platforms of NPCs and neurons for substance screening (Nierode et al., 2016; Zhang et al., 2013). However, reproducible and highly efficient differentiation protocols remain the critical aspects to assure an adequate *in vitro* recapitulation of human neural cells. Recent advances of regenerative biology allow to establish organoid models to assess complex organ-specific interactions (Lancaster et al., 2013). Complex physiological systems incorporating stem cells or stem cell-derived lines together with other somatic cells can be established using bioprinting, forced self-organization as shown for instance in liverbud-like tissue, or co-culture systems such as the stem cell-based model of the blood brain barrier (Lippmann et al., 2012). Hence, opening novel doors towards patient-specific precision medicine and gene engineering e.g. using CRISPR/Cas9 (Ran et al., 2013) based on the unique properties of pluripotent and multipotent stem cells.

1.7 Aim of the thesis

The aim of this thesis was to explore strategies to generate human neural progenitor cells from two primary sources: skin-derived fibroblasts and fetal brain tissue. The main objectives of this work can be divided into three parts.

The first part describes the establishment and optimization of three different transgene-free reprogramming methods utilizing control and patient-specific dermal fibroblasts. The central goal was to compare the feasibility of the protocols regarding reprogramming efficiency, quality of the iPSCs as well as time consumption and robustness of the procedure. Those iPSCs provide a source for derivation of NPCs as elaborated in the second part.

The experiments conducted in the second part pursue to optimize a previously published monolayer differentiation protocol for the derivation of primitive NPCs from pluripotent cells. Moreover, it was investigated whether it is possible to subsequently adapt the primitive NPCs to a chemically defined medium containing FGF/EGF. This strategy was examined to obtain rosette-like FGF/EGF-dependent NPCs suitable for the differentiation into glial progeny.

The third and major part of this thesis intents to examine strategies to generate a primary primitive or neuroepithelial cell line from human fetal brain tissue. iPSC-derived NPCs can be generated directly from patients and represent a theoretically unlimited cell source for biomedical applications. However, it remains to be proven if they represent physiologically relevant cells. In contrast, primary neural progenitor cells have been already used in clinical settings and represent the gold standard. However, a vast majority of these cells has been reported to have either neural rosette-like (Tailor et al., 2013) or radial glia-like properties and thus are restricted in differentiation capacity to central lineages and a limited number of neuronal subtypes. Therefore, a protocol for the derivation of a primitive neuroepithelial cell line would be of great interest. The main challenge is to develop a chemically defined medium enabling to enrich and stabilize such NPCs, otherwise transiently appearing during development. This task was addressed by combining growth factors and small molecules which are capable to modulate crucial signaling pathways orchestrating early human development. Subsequently, it should be determined if such an early proliferative candidate cell line displays higher plasticity and unrestricted differentiation capacity compared to previously established primary lines. Thus, a primary primitive neuroepithelial cell line would allow deeper insights into mechanisms of early neural development and might serve as a potential reference line for novel reprogramming and differentiation protocols. Furthermore, such an early, self-renewing and cryopreservable cell population might be feasible for biomedical applications such as cell replacement and compound screening.

2. Material and Methods

2.1 Material

2.1.1 Laboratory equipment

Autoclaves	
DX-23	Systec, Wettenberg, Germany
Hiclave HG-133	HMC Europe, Tüßling, Germany
Varioklav Classic 400E	HP Medizintechnik, Oberschleißheim, Germany
Centrifuges	
Heraeus Multifuge X1R	Thermo Fisher Scientific, Waltham, USA
Heraeus Pico 17	Thermo Fisher Scientific, Waltham, USA
J2-21	Beckman Coulter, Brea, USA
Rotanta	Hettich, Tuttlingen, Germany
Sorvall Evolution RC	Thermo Fisher Scientific, Waltham, USA
Sorvall SLA-1500 Rotor	Thermo Fisher Scientific, Waltham, USA
Sorvall SS-34 Rotor	Thermo Fisher Scientific, Waltham, USA
Microcentrifuge IR	Carl Roth, Karlsruhe, Germany
Centrifuge 5430	Eppendorf, Hamburg, Germany
Microspin FV2400	Biosan, Riga, Latvia
Cryostorage	
ARP 110	Air Liquide, Paris, France
Cryo 1°C freezing container	Nalgene, Roskilde, Denmark
Electrophoresis chamber	
PerfectBlue™ Mini L	Peqlab, Erlangen, Germany
Flow cytometer	
BD FACSCanto™ II	BD Biosciences, San Jose, USA
Heaters	
TDB-100	Biosan, Riga, Latvia
WiseStir MSH-20A	Witeg, Wertheim, Germany
Ice machine	
AF-100	Scotsman, Vernon Hills, USA
Incubators	
C150	Binder, Tuttlingen, Germany
Heraeus Heracell 240	Thermo Fisher Scientific, Waltham, USA
MCO-19AIC(UV)	Panasonic, Gunma, Japan

Laminar flow hoods	
Airstream	Esco Micro, Singapore
Aura 2000 M.A.C.	EuroClone Bioair Pero, Italy
Microscopes	
Ai Confocal	Nikon, Chiyoda, Japan
Axiovert 40 CFL	Carl Zeiss Microscopy GmbH, Jena, Germany
Axiovert 135 TV	Carl Zeiss Microscopy GmbH, Jena, Germany
Biorevo BZ-9000	Keyence, Neu-Isenburg, Germany
DMIL LED	Leica Microsystems GmbH, Wetzlar, Germany
ZEISS LEO912AB	Zeiss NTS, Oberkochen, Germany
Microtome	
Ultracut E Microtome	Reichert-Jung, current Leica Microsystems GmbH, Wetzlar, Germany
Diatome	Reichert-Labtec, Wolfratshausen, Germany
pH meter	
inoLab pH 720	WTW GmbH, Weilheim, Germany
Pipettes	
accu-jet pro	Brand, Wertheim, Germany
Research plus	Eppendorf, Hamburg, Germany
Transferpette S	Brand, Wertheim, Germany
Research pro	Eppendorf, Hamburg, Germany
Peqpette	Peqlab, Erlangen, Germany
Power supply	
PowerPac Basic	BioRad, Hercules, USA
Rocker	
Multi MR-12	Biosan, Riga, Latvia
Stirrer	
WiseStir MS-20A	Witeg Wertheim, Germany
Scale	
EG 2200-2NM	Kern & Sohn GmbH, Balingen, Germany
PLJ 2100-2M	Kern & Sohn GmbH, Balingen, Germany
AB104	Mettler Toledo, Gießen, Germany
Spectrophotometer	
NanoDrop 2000c	Thermo Fisher Scientific, Waltham, USA
Thermocycler	
Veriti	Life Technologies, Darmstadt, Germany
CFX384TM RT-System C1000TM	Bio-Rad, Hercules, USA
UV transilluminator	

Quantum-ST4	Vilber Lourmat, Eberhardzell, Germany
Vortex	
Vortex-2 Genie	Scientific Industries, New York, USA
Analog Vortex Mixer	VWR, Radnor, USA
Water baths	
W12	Labortechnik Medingen, Arnsdorf, Germany
WNB14	Memmert, Schwabach, Germany

2.1.2 Disposables

Table 1.1 List of disposable materials.

Item	Manufacturer
384-well PCR plate	Brand, Wertheim, Germany
Biosphere filter tips (20, 100, 200, 1000 µL)	Sarstedt, Nümbrecht, Germany
Cell culture dishes (3.5, 6, 10 cm)	Greiner Bio-One, Kremsmünster, Austria
Cryovials (1.8 mL)	Sarstedt, Nümbrecht, Germany
FACS tubes	Sarstedt, Nümbrecht, Germany
Falcon tubes (15 mL)	Greiner Bio-One, Kremsmünster, Austria
Falcon tubes (15, 50 mL)	Sarstedt, Nümbrecht, Germany
Glass cover slips (15 mm)	Hecht/Assistent, Sondheim/Rhön, Germany
Glass slides	Marienfeld, Lauda-Königshofen, Germany
Hemocytometer Neubauer improved	Brand, Wertheim, Germany
Kimtech wipes	Kimberley-Clark, Dallas, USA
Microseal B-seal	BioRad, Hercules, USA
Microtube strips	Brand, Wertheim, Germany
Needles	B.Braun, Melsungen, Germany
Nickel grids	Plano, Wetzlar, Germany
Nitrile gloves	Hartmann, Wiener Neudorf, Austria
PARAFILM® „M“	Bemis Company, Neenah, USA
Pasteur pipets	Kimble Chase, Rockwood, USA
Pipet tips (10, 100, 1000 µL)	Sarstedt, Nümbrecht, Germany
Pipet tips with filter (10,100, 200, 1000 µL)	Greiner Bio-One, Kremsmünster, Austria
Reaction tubes (0.5, 1.5, 2.0 mL)	Sarstedt, Nümbrecht, Germany
RNAse, DNAse-free tubes (1.5 mL)	Eppendorf, Hamburg, Germany
Serological pipettes (5, 10, 25, 50 mL)	Greiner Bio-One, Kremsmünster, Austria
Surgical disposable scalpels	B.Braun, Melsungen, Germany
Syringe filters (0.2 µm)	Pall GmbH, Dreieich, Germany
Syringes	BD, East Rutherford, USA
Tissue culture flasks (T25, T75, T175)	Greiner Bio-One, Kremsmünster, Austria

Tissue culture plates (6-, 12-, 48-, 96-wells)	Greiner Bio-One, Kremsmünster, Austria
Tissue pads	MaiMed®, Neuenkirchen, Germany

2.1.3 Cells

Commercially purchased cell lines

BJ fibroblasts	ATCC, Manassas, USA
HEK293T cells	Clontech, Mountain View, USA
IMR-90 iPSCs	Wi-Cell, Madison, USA
MEF feeder cells	Thermo Fisher Scientific, Waltham, USA
NHDF fibroblasts	Promocell, Heidelberg, Germany
Plat-E cells	Cell Biolabs Inc., San Diego, USA

Primary and generated cell lines

All primary samples were obtained after receiving informed consent from patients and healthy controls as well as ethical approval by the by the Ethics Committee of the Medical Faculty Würzburg, Germany (No. 96/11) and University Clinic of Erlangen, Germany (No. 4120). Research on fetal-derived tissue was approved by the Ethics Committee of the Medical Faculty Würzburg (No. 151/14). Cells were either isolated from biopsies or were received in culture or cryopreserved from collaborators.

Table 1.2 Primary cell lines used in this study.

ID	Name	Cell type	Source	Disease	Collaborative partner
UKERf1JF-X-1	Ctrl. 1 FB	fibroblast	Skin punch biopsy	healthy	Department of Neurology, Erlangen, Germany
UKERf33Q-X-1	Ctrl. 2 FB	fibroblast	Skin punch biopsy	healthy	Department of Neurology, Erlangen, Germany
UKERfO3H-X-1	Ctrl. 3 FB	fibroblast	Skin punch biopsy	healthy	Department of Neurology, Erlangen, Germany
UKERfAY6-X-1	Pat. 1 FB	fibroblasts	Skin punch biopsy	PD	Department of Neurology, Erlangen, Germany
UKERfVK2-X-1	Pat. 2 FB	fibroblasts	Skin punch biopsy	PD	Department of Neurology, Erlangen, Germany
UKERfPX7-X-1	Pat. 3 FB	fibroblasts	Skin punch biopsy	PD	Department of Neurology, Erlangen, Germany
PEN1	Pat. 4 FB	fibroblast	Skin punch biopsy	Episodic ataxia	Department of Neurology, Würzburg, Germany
FD1	Pat. 5 FB	fibroblast	Skin punch biopsy	Fabry Disease	Department of Neurology, Würzburg, Germany
FD2	Pat. 6 FB	fibroblast	Skin punch biopsy	Fabry Disease	Department of Neurology, Würzburg, Germany
HP1	Ctrl. 4 FB	fibroblast	Skin punch biopsy	healthy	Department of Psychiatry, Würzburg, Germany
HP2	Ctrl. 5 FB	fibroblast	Skin punch biopsy	healthy	Department of Psychiatry, Würzburg, Germany

FT1	CSPFL KA, K3	NEPs	Fetal brain tissue	healthy	TERM Würzburg, Germany
FT2	CSPFL K2	NEPs	Fetal brain tissue	healthy	TERM Würzburg, Germany

2.1.4 Chemicals, small molecules and growth factors

Table 1.3 Chemicals, compounds, commercial media and supplements as well as proteins used in this thesis.

Component	Manufacturer
2,4,6-Tris(dimethylaminomethyl)phenol	SERVA Electrophoresis GmbH, Heidelberg, Germany
7-Amino-Actinomycin D (7-AAD)	BD, East Rutherford, USA
Advanced DMEM/F12	Thermo Fisher Scientific, Waltham, USA
ALK5 inhibitor	Enzo Life Sciences, Lörrach, Germany
Ascorbic acid (AA)	Sigma-Aldrich, St. Louis, USA
B18R	Affymetrix, Santa Clara, USA
B27 supplement (50X)	Gibco™, Karlsruhe, Germany
B27 supplement without Vitamin A (50X)	Gibco™, Karlsruhe, Germany
BDNF	PeproTech, Rocky Hill, USA
bFGF recombinant human protein	Invitrogen, Carlsbad, USA
BMP4 (recombinant human)	PeproTech, Rocky Hill, USA
Bovine serum albumin (BSA)	Sigma-Aldrich, St. Louis, USA
Cacodylic acid	Merck Millipore, Darmstadt, Germany
cAMP	Sigma-Aldrich, St. Louis, USA
CHIR99021 (CHIR)	Axon Medchem, Groningen, Netherlands
Collagenase	SERVA Electrophoresis GmbH, Heidelberg, Germany
D-Glucose	Carl Roth, Karlsruhe, Germany
DABCO	Carl Roth, Karlsruhe, Germany
DAPT	Promocell, Heidelberg, Germany
dbcAMP	Sigma-Aldrich, St. Louis, USA
Dimethyl sulfoxide (DMSO)	Carl Roth, Karlsruhe, Germany
Dispase II	PAN-Biotech, Aidenach, Germany
DMEM	Gibco™, Karlsruhe, Germany
DMEM/F12	Gibco™, Karlsruhe, Germany
Dodecenylsuccinic anhydride	SERVA Electrophoresis GmbH, Heidelberg, Germany

Dulbecco's PBS without Ca2+ and Mg2+ (DPBS)	Sigma-Aldrich, St. Louis, USA
EGF	PeproTech, Rocky Hill, USA
EtOH	Applichem, Darmstadt, Germany
FCS	Biochrom, Berlin, Germany
FGF8	PeproTech, Rocky Hill, USA
Formvar	Merck Millipore, Darmstadt, Germany
GDNF	PeproTech, Rocky Hill, USA
Gelatin	Sigma-Aldrich, St. Louis, USA
Glutaraldehyde 25 %	Carl Roth, Karlsruhe, Germany
Glycidyl ether 100 (Epon)	SERVA Electrophoresis GmbH, Heidelberg, Germany
Horizon Fixable Viability Stain 450	BD, East Rutherford, USA
Isopropanol	Carl Roth, Karlsruhe, Germany
KaryoMAX® Colcemid™ Solution	Thermo Fisher Scientific, Waltham, USA
KCl	Applichem, Darmstadt, Germany
Knockout DMEM	Gibco™, Karlsruhe, Germany
KnockOut™Serum Replacement (KSR)	Gibco™, Karlsruhe, Germany
L-Glutamine 200mM	Gibco™, Karlsruhe, Germany
Laminin (recombinant human)	Sigma-Aldrich, St. Louis, USA
Lead citrate	Agar Scientific, Stansted, UK
Leukemia inhibitory factor, human (hLIF)	Miltenyi Biotec, Bergisch Gladbach, Germany
Matrigel® Basement Membrane Matrix Growth Factor reduced (bMG)	Corning, Corning, USA
Methanol	Carl Roth, Karlsruhe, Germany
Methylnadic anhydride	SERVA Electrophoresis GmbH, Heidelberg, Germany
Midori Green Advance	Nippon Genetics Europe GmbH, Düren, Germany
Mowiol	Sigma-Aldrich, St. Louis, USA
mTeSR™1	STEMCELL Technologies, Vancouver, Canada
N2 supplement (100X)	Gibco™, Karlsruhe, Germany
Na-Pyruvate	Gibco™, Karlsruhe, Germany
Neural induction supplement	Thermo Fisher Scientific, Waltham, USA
Neurobasal medium	Gibco™, Karlsruhe, Germany
Non-essential amino acids (NEAA; 100X)	Gibco™, Karlsruhe, Germany
Osmium tetroxide	Electron Microscopy Sciences, Hatfield, USA
Paraformaldehyde (PFA)	Applichem, Darmstadt, Germany
PBS	Sigma-Aldrich, St. Louis, USA
Poly-D-Lysine	Sigma-Aldrich, St. Louis, USA

Poly-L-Ornithine	Sigma-Aldrich, St. Louis, USA
Polybrene	Sigma-Aldrich, St. Louis, USA
PSC neural induction medium supplement	Thermo Fisher Scientific, Waltham, USA
Purmorphamine (PMA)	Miltenyi Biotec, Bergisch Gladbach, Germany
SB431542 (SB)	Miltenyi Biotec, Bergisch Gladbach, Germany
StemMACS™ iPS-Brew XF	Miltenyi Biotec, Bergisch Gladbach, Germany
StemMACS™ Repro-Brew XF	Miltenyi Biotec, Bergisch Gladbach, Germany
StemPro® Accutase®	Gibco™, Karlsruhe, Germany
Tannic acid	Carl Roth, Karlsruhe, Germany
TGFβ3	PeproTech, Rocky Hill, USA
Triton™ X-100	Sigma-Aldrich, St. Louis, USA
Trypsin/EDTA	Biochrom, Berlin, Germany
Uranyl acetate	SERVA Electrophoresis GmbH, Heidelberg, Germany
Y27632 Rock Inhibitor (RI)	Miltenyi Biotec, Bergisch Gladbach, Germany
β-Mercaptoethanol (50 mM)	Gibco™, Karlsruhe, Germany

2.1.5 Buffers

For buffer preparation, double desalted H_2O (ddH_2O) water has been used.

PBS

1.5 mM	KH_2PO_4
2.7 mM	KCl
8.1 mM	Na_2HPO_4
137 mM	NaCl

50x TAE (Tris acetate/EDTA) buffer

242.2 g/L	Tris free base
18.61 g/L	Disodium EDTA
57.1 mL/L	Glacial acetic acid

2 x HBS Buffer

100 mM	Hepes
280 mM	NaCl
1.5 mM	Na_2HPO_4

Dissolve in ddH_2O and adjust pH to three different values (6.95, 7.00, 7.05) and test which leads to best efficiency.

2.1.6 Cell culture media and solutions

All material and liquids used in cell culture experiments were purchased sterile or have been decontaminated by autoclaving. Preparation of solutions was handled using sterile filtered or autoclaved solvents.

Freezing medium

Freezing medium was prepared freshly before use and varied in composition depending on culturing conditions using FCS for fibroblasts and HEK293T cells or SR for NPCs and hiPSCs:

90 %	FCS or KO Serum Replacement
10 %	DMSO

MEF-medium

88 %	DMEM
10 %	FCS
1 %	100x NEAA
2 mM	L-Glutamine
0.1 mM	β-Mercaptoethanol

2 % Adv. MEF-medium

97 %	Advanced DMEM
2 %	FCS
2 mM	L-Glutamine

5 % Adv. MEF-medium

94 %	Advanced DMEM
5 %	FCS
2 mM	L-Glutamine

Reprogramming medium (Kadari et al., 2014)

79 %	KO DMEM/F12
20 %	KO SR
2 mM	L-Glutamine
1 %	NEAA
100 µM	β-Mercaptoethanol
10 ng/mL	bFGF

200 µM	AA

Neural induction medium (Yan et al., 2013)

98 %	Neurobasal® medium
2 %	Neural Induction Supplement

NPC expansion medium (Yan et al., 2013)

49 %	Neurobasal® medium
49 %	Advanced DMEM/F-12
2 %	Neural Induction Supplement

FGF/EGF medium (modified from Koch et al., 2009, Günther et al., 2016)

DMEM/F-12 +

0.1 %	B27® Supplement
1 %	N2 Supplement
2 mM	L-Glutamine
1.6 mg/mL	D-Glucose
10 ng/mL	human bFGF
10 ng/mL	EGF
0.8 µM	CHIR

CS –medium (modified from Li et al., 2011)

49 %	Advanced DMEM/F12-medium
49 %	Neurobasal medium
1x	100x N2-supplement
1x	50x B27-supplement (without Vitamin A)
2 mM	L-Glutamine
5 µg/mL	BSA
4 µM	CHIR
3 µM	SB
10 ng/mL	hLif

CSPFL-medium (Günther et al., in preparation)

49 %	Advanced DMEM/F12-medium
49 %	Neurobasal medium
1x	100x N2-supplement
1x	50x B27-supplement (without Vitamin A)

2 mM	L-Glutamine
5 µg/mL	BSA
4 µM	CHIR
3 µM	SB
0.5 µM	PMA
10 ng/mL	hLif
10 ng/mL	bFGF

CAP-medium (Günther et al., in preparation)

49 %	DMEM/F12-medium
49 %	Neurobasal medium
1x	100x N2-supplement
1x	50x B27-supplement without Vit A
2 mM	L-Glutamine
5 µg/mL	BSA
4 µM	CHIR
3 µM	ALK5
0.5 µM	PMA
200 µM	AA

Differentiation medium for undirected differentiation

48 %	DMEM/F12-medium
48 %	Neurobasal medium
1 %	100x N2-supplement
2 %	50x B27-supplement
2 mM	L-Glutamine

Neuronal differentiation medium

48 %	DMEM/F12-medium
48 %	Neurobasal medium
1 %	100x N2-supplement
2 %	50x B27-supplement
2 mM	L-Glutamine
20 ng/mL	BDNF
20 ng/mL	GDNF
300 ng/mL	cAMP
200 µM	AA

2 µM	DAPT (addition for two initial weeks of differentiation)

Dopaminergic differentiation medium I (Reinhardt et al., 2013)

49 %	DMEM/F12 medium
49 %	Neurobasal medium
0.5 %	100x N2-supplement
1 %	50x B27-supplement (without Vitamin A)
2 mM	L-Glutamine
100 ng/mL	FGF8
1 µM	PMA
200 µM	AA

Dopaminergic differentiation medium II (Reinhardt et al., 2013)

49 %	DMEM/F12 medium
49 %	Neurobasal medium
0.5 %	100x N2-supplement
1%	50x B27-supplement (without Vitamin A)
2 mM	L-Glutamine
10 ng/mL	BDNF
10 ng/mL	GDNF
1 ng/mL	TGF-β3
200 µM	AA
500 µM	dbcAMP
0.5 µM	PMA

Maturation medium (Reinhardt et al., 2013)

49 %	DMEM/F12 medium
49 %	Neurobasal medium
0.5 %	100x N2-supplement
1 %	50x B27-supplement (without Vitamin A)
2 mM	L-Glutamine
10 ng/mL	BDNF
10 ng/mL	GDNF
1 ng/ mL	TGF-β3
200 µM	AA
500 µM	dbcAMP

Peripheral neuron differentiation medium I (Reinhardt et al., 2013)

49 %	DMEM/F12 medium
49 %	Neurobasal medium
0.5 %	100x N2-supplement
1 %	50x B27-supplement (without Vitamin A)
2 mM	L-Glutamine
3 µM	CHIR

Peripheral neuron differentiation medium II (Reinhardt et al., 2013)

49 %	DMEM/F12 medium
49 %	Neurobasal medium
0.5 %	100x N2-supplement
1 %	50x B2-supplement (without Vitamin A)
2 mM	L-Glutamine
3 µM	CHIR
10 ng/mL	BMP4

Mesenchymal differentiation medium

44 %	DMEM/F12 medium
44 %	Neurobasal medium
10 %	FCS
0.5 %	100x N2-supplement
1 %	50x B27-supplement (without Vitamin A)
2 mM	L-Glutamine
10 ng/mL	BDNF
10 ng/mL	GDNF
1 ng/mL	TGF-ß3
200 µM	AA
500 µM	dbcAMP

2.1.7 Immunocytochemistry

PFA solution

4 %	PFA
96 %	PBS

Blocking and staining solution

95 %	PBS
5 %	FCS
0.1 %	Triton-X

If cells needed to be permeabilized for nuclear and intracellular staining, 0.1% Triton-X was added to blocking and staining solution.

Mowiol solution

2.4 g	Mowiol 4-88
6.0 g	Glycerol
6.0 ml	ddH$_2$O
12.0 ml	0.2 M Tris-HCl (pH 8.5)
25 mg/mL	DABCO

Mix all components, except Tris-HCl, for 2 h at RT, then add Tris-HCl and continue mixing for further 2 h at 50 °C. Add DABCO and blend at RT over night before aliquoting and storing at -20°C.

2.1.8 Electron microscopy

Cacodylate buffer (CB), 0.2 M stock solution

4.28 g	Cacodylic acid sodium salt trihydrate

Fill up to 100 mL with ddH$_2$O, and adjust to pH 7.5 using 1 N HCl solution

Fixing buffer

2.5 %	Glutaraldehyde 25 %
0.8 %	Tannic acid
in 0.1 M	CB, pH 7.5

Epon embedding mixture

26 g	Glycidyl ether 100
10 g	Dodecenylsuccinic anhydride
15 g	Methylnadic anhydride
0.25 g	2,4,6-Tris(dimethylaminomethyl)phenol

Mix all components slowly until dissolved and degas using vacuum to remove remaining air bubbles.

2.1.9 Antibodies

Antibodies for immunocytochemistry

Table 1.4 List of primary antibodies.

Antigen	Species	Working dilution	Manufacturer
AFP	Rabbit, polyclonal	1:400	Dako, Glostrup, Denmark
Brn-2	Goat, polyclonal IgG	1:50-1:200	Santa Cruz, Dallas, USA
DCX	Goat, polyclonal IgG	1:50-1:200	Santa Cruz, Dallas, USA
GABA	Rabbit, IgG	1.200 -1:500	Sigma-Aldrich, St. Louis, USA
GAD65/67	Rabbit, polyclonal	1:500	EMD Milipore, Darmstadt, Germany
GFAP	Rabbit, polyclonal	1:1000	Dako, Glostrup, Denmark
Ki67	Rabbit	1:200	Thermo Fisher Scientific, Waltham, USA
$NA_V1.7$	Mouse, monoclonal IgG1	1:200	Abcam, Cambridge, UK
Nestin	Mouse monoclonal igG1	1:100	R&D, Minneapolis, USA
NeuN	Mouse, IgG	1:50	EMD Milipore, Darmstadt, Germany
NF200	Chicken polyclonal	1:200	Aves LABS, Tigard, USA
Oct3/4	Mouse, monoclonal IgG	1:50	Santa Cruz, Dallas, USA
Pax6	Rabbit, polyclonal	1:100	BioLegend, San Diego, USA
Peripherin	Rabbit, polyclonal IgG	1:500	EMD Milipore, Darmstadt, Germany
PSD-95	Mouse, monoclonal	1:1000	Affinity Bioreagents, Golden USA
S100β	Rabbit, Ig	1:1000	Dako, Glostrup, Denmark
SMA	Mouse, monoclonal IgG2a	1:200	Abcam, Cambridge, UK
SOX1	Goat IgG, polyclonal IgG	1:50	R&D, Minneapolis, USA
SOX2	Mouse, monoclonal IgG2A	1:500	R&D, Minneapolis, USA

SSEA-4	Mouse, monoclonal IgG3	1:50	DSHB, Iowa City, USA
Synapsin 1	Mouse, monoclonal IgG1	1:500	Synaptic Systems, Göttingen, Germany
Synapsin 1/2	Rabbit, polyclonal IgG	1:20000	Synaptic Systems, Göttingen, Germany
TH	Rabbit, polyclonal	1:100	Abcam, Cambridge, UK
TPH2	Rabbit, polyclonal IgG	1:500	Thermo Fisher Scientific, Waltham, USA
TRA1-60	Mouse, monoclonal IgM	1:50	EMD Milipore, Darmstadt, Germany
TUJ1	Mouse, monoclonal IgG21	1:1000	BioLegend, San Diego, USA
VGlut1	Rabbit, polyclonal IgG	1:500	Synaptic Systems, Göttingen, Germany

Table 1.5 List of secondary antibodies.

Antigen	Species	Working dilution	Manufacturer
anti-goat Cy™3	Donkey	1:800	Jackson ImmunoResearch Laboratories, West Grove, USA
anti-mouse Cy™2	Goat	1:400	Jackson ImmunoResearch Laboratories, West Grove, USA
anti-rabbit Cy™3	Goat	1:800	Jackson ImmunoResearch Laboratories, West Grove, USA
anti-mouse Cy™5	Goat	1:400	Jackson ImmunoResearch Laboratories, West Grove, USA

Antibodies for flow cytometry

Table 1.6 List of antibodies used for flow cytometry.

Antigen	Species	Working dilution	Manufacturer
CD133/1 (AC133)	Mouse IgG1	1:11	Miltenyi Biotec, Bergisch Gladbach, Germany
SSEA-4	Recombinant human IgG1, APC-conjugated	1:11	Miltenyi Biotec, Bergisch Gladbach, Germany

TRA-1-60	Recombinant human IgG1, PE-conjugated	1:11	Miltenyi Biotec, Bergisch Gladbach, Germany

2.1.10 Oligonucleotides

Human specific primer oligonucleotides were synthesized by Invitrogen (Carlsbad, USA) or Eurofins Genomics (Ebersberg, Germany) and dissolved in appropriate volume of ddH$_2$O yielding a stock concentration of 100 µM.

Table 1.7 Primer sequences used for RT-PCR and qRT-PCR. F is indicating forward primer (5'-3'), while R marks reverse primers (5'-3'). Primers marked with asterisk contain SeV genome sequences to specifically detect transgenes introduced by SeV vectors.

Target gene	Primer sequences
C-MYC	F: TAA CTG ACT AGC AGG CTT GTC G* R: TCC ACA TAC AGT CCT GGA TGA TGA TG
DACH1	F: GGG GCT TGC ATA CGG TCT AC R: CGA ACT TGT TCC ACA TTG CAC A
DCX	F: TTC AAG GGG ATT GTG TAC GCT R: GTC AGA CAG AGA TCG CGT CAG
EEF1A1	F: AGG TGA TTA TCC TGA ACC ATC C R: AAA GGT GGA TAG TCT GAG AAG C
EN1	F: CGC AGC AGC CTC TCG TAT G R: CCT GGA ACT CCG CCT TGA G
GAPDH	F: GCA CAG TCA AGG CCG AGA AT R: GCC TTC TCC ATG GTG GTG AA
HOXA2	F: CCC CTG TCG CTG ATA CAT TTC R: TGG TCT GCT CAA AAG GAG GAG
KLF4	F: TTC CTG CAT GCC AGA GGA GCC C R: AAT GTA TCG AAG GTG CTC AA*
KOS	F: ATG CAC CGC TAC GAC GTG AGC GC R: ACC TTG ACA ATC CTG ATG TGG
NESTIN (for 3.3)	F: CTG CTA CCC TTG AGA CAC CTG R: GGG CTC TGA TCT CTG CAT CTA C
NESTIN (for 3.2)	F: GAG GGA AGT CTT GGA GCC AC R: AAG ATG TCC CTC AGC CTG G
PAX6 (for 3.3)	F: AAC GAT AAC ATA CCA AGC GTG T R: GGT CTG CCC GTT CAA CAT C
PAX6 (for 3.2)	F: TCC GTT GGA ACT GAT GGA GT R: GTT GGT ATC CGG GGA CTT C

POU5F1	F: GGT TCT CGA TAC TGG TTC GC R: GTG GAG GAA GCT GAC AAC AA
PROM1	F: AGT CGG AAA CTG GCA GAT AGC R: GGT AGT GTT GTA CTG GGC CAA T
RPL6	F: ATT CCC GAT CTG CCA TGT ATT C R: TAC CGC CGT TCT TGT CAC C
SeV	F: GGA TCA CTA GGT GAT ATC GAG C* R: ACC AGA CAA GAG TTT AAG AGA TAT GTA TC*
SOX1 (for 3.2)	F: ATT ATT TTG CCC GTT TTC CC R: TCA AGG AAA CAC AAT CGC TG
SOX1 (for 3.3)	F: GCC AAG CAC CGA ATT CAC AG R: CAG CAG TGT CGC TCC AAT TCA
SOX2 (for 3.2)	F: GCT TAG CCT CGT CGA TGA AC R: AAC CCC AAG ATG CAC AAC TC
SOX2 (for 3.3)	F: GCC GAG TGG AAA CTT TTG TCG R: GGC AGC GTG TAC TTA TCC TTC T

2.1.11 Plasmids

Plasmids used in this study were taken from common laboratory stock (purified from transformed bacterial culture using standard DNA-isolation technique).

hSTEMCCA	Sommer et al., 2009
psPAX2	Addgene, Cambrige, USA
pMD2.G	Addgene, Cambrige, USA

2.1.12 Kits

Table 1.8 Commercially available kits used in this thesis.

100 bp DNA ladder	Thermo Fisher Scientific, Waltham, USA
CytoTune™-iPS 2.0 Sendai Reprogramming Kit	Thermo Fisher Scientific, Waltham, USA
GoScript Reverse Transcriptase	Promega, Mannheim, Germany
Hs_UBC_1_SG QuantiTect Primer Assay	Qiagen, Hilden, Germany
Lenti-X GoStix	Clontech, Mountain View, USA
NucleoBond® Xtra Maxi Kit	Macherey-Nagel, Düren, Germany
RNeasy Mini Kit	Qiagen, Hilden, Germany

StemMACS^{TM} mRNA Reprogramming Kit	Miltenyi Biotec, Bergisch Gladbach, Germany
SuperScript II Reverse Transcriptase	Thermo Fisher Scientific, Waltham, USA
SYBR Select Master Mix for CFX	Thermo Fisher Scientific, Waltham, USA

2.2 Methods

2.2.1 Cell Culture

All cells were cultured at 37 °C, 5% CO_2 with saturating humidity and handled in sterile environment under a laminar sterile hood. Testing for mycoplasma contamination was performed on a regular basis.

Coatings of cell culture dishes

Matrigel coating

Growth factor reduced basement membrane matrix Matrigel (bMG) or human ESC-qualified Matrigel (hESC-MG) was used for coating of tissue culture plates or sterile glass coverslips in tissue culture plates. Stock aliquots of bMG were diluted in a ratio of 1:20 - 1:25, whereas hESC-MG was diluted 1:25 up to 1:30 in cold DMEM/F12 and dispenseded quickly to prevent gelation into plates using 1 mL per well of a 6-Well-plate, 0.5 mL/well of a 12-Well-plate and 0.2 mL/well of a 48-well plate. Cell culture dishes were coated in advance and stored for up to two weeks at 4°C or used directly after at least one overnight incubation at 4°C, or 2 h at RT, or for 30 min at 37°C.

Gelatin coating

Gelatin was diluted 0.1% in PBS and autoclaved. For coating tissue cultures plates were filled with the solution and incubated 10-30 min at 37°C in the incubator.

MEF-feeder layer

Irradiated MEF-feeders should be seeded one day prior cell plating on 0.1 % gelatin coated plates using MEF-medium. Frozen, commercially acquired aliquots of 2 x 10^6 cells were thawed as described further and plated using MEF-medium.

Poly-L-ornithine/Laminin (PO/Ln) coating

First, PO was diluted to a final concentration of 15 µg/mL in sterile PBS and dispensed in TC-plate wells. After incubating for at least 2 h or ON at 37°C, plates were washed three time with PBS. Ln-stock was diluted to a final concentration of 1 µg/mL in sterile PBS and applied to the PO-precoated plates. Before proceeding with cell culture, plates were incubated for 2 h or overnight at 37°C.

<u>Poly-D-Lysine-coating (PDL)</u>

PDL-stock was diluted to a final concentration of 1 µg/mL in sterile PBS and dispensed into 100 mm TC dishes. Following an incubation of 2 h at 37°C, plated were rinsed three times with PBS and utilized further.

Thawing of cells

Cells were stored in liquid nitrogen and thawed in 37°C water bath until only small piece of ice was left. Relocating into a falcon tube and filling up to 10 mL using DMEM/F12 or DMEM-Medium followed. After centrifuging at appropriate speed the pellet was resuspended for counting or direct seeding into cell culture dishes.

Isolation of primary cells

Informed consent was received for all patients donating samples used in this study prior to the donation using a written form and protocol (compare Tab. 1.2).

<u>Isolation of human dermal fibroblasts from punch biopsy</u>

Punch biopsies are a minimal invasive approach to isolate adult human dermal fibroblasts (AHDF) from healthy controls and patients. All preparations were approved by the ethical committee. Biopsies were obtained from collaborators, namely Prof. Dr. Üceyler, Thomas Klein and Dr. Lorenz Müller from the Department of Neurology, Würzburg. Other primary firbroblasts were provided after isolation as indicated in Table 1.2 by Dr. Sarah Kittel-Schneider from the Department of Psychiatry, Psychosomatic Medicine and Psychotherapy, Frankfurt and the and the Department of Molecular Neurology, Erlangen within the ForIPS-consortium.

Briefly, punch biopsies were obtained from an area of skin near the ankle after local anesthesia using 1 % Scandicain solution. Biopsies could be stored for up to 36 hours in sterile DPBS without Ca and Mg at 4°C or processed immediately. After transferring into a 35 mm dish, the lipid layer next to the dermis was removed with a scalpel. The biopsy was rinsed twice with sterile DPBS before aspirating the entire liquid and adding 4 mL of Dispase solution with a concentration of 2.4 U/mL. Next, the biopsy was incubated for 16-18 h at 4°C (in the fridge) and removed. The prolonged incubation allows a gentle removal of the epidermis from the biopsy after washing twice with PBS. Having rinsed for another time, the biopsy is covered with collagenase solution and transferred to a 15 mL tube and media was added up to 5 mL. The tube was incubated for 45 min in a 37°C-prewarmed water bath and centrifuged at 1200 rpm for 5 min. The supernatant was aspirated carefully and the pelleted biopsy was resuspended in 10 mL of MEF-medium with P/S prior to a second centrifugation at 1200 rpm for 5 min. Sedimented biopsy pieces were resuspended in 1.5 mL of MEF medium with P/S and transferred to a T25 tissue culture flask and further cultured in the incubators. After 2-3 days, the outgrowth of fibroblasts could be observed and media was changed, followed by changes every 2-3 days until fibroblasts reached confluence in the biopsy surrounding area. From then on fibroblasts were split using regular protocol, and expanded without addition of antibiotics from passage 2 on. Since primary fibroblasts should not reach a high passage number for reprogramming, cells were grown from passage 2 onwards in T75 TC flasks and cryopreserved in early passages.

Isolation of neural cells from fetal preparations

The fetal brain tissue was obtained following abortive interventions at 8-12 weeks of pregnancy at the Department of Gynecology and Obstetrics, Würzburg in collaboration with Dr. Tanja Stüber and Dr. Antje Appelt-Menzel from the Department of Tissue Engineering and Regenerative Medicine, Würzburg (compare Tab. 1.2). Following the interruptions, the tissue was kept at 4 °C for up to 2 h and processed further at the Department of Pathology. The samples were rinsed with cold PBS and brain tissue was isolated manually under stereoscopic visual control. All remaining tissue was further analyzed by the Department of Pathology while the isolated tissue specimens were transferred in cold DMEM/F12 medium to either to the Department of Tissue Engineering and Regenerative Medicine, Würzburg or the Institute of Anatomy and Cell Biology, Würzburg. The next steps were carried out under sterile cell culture settings. The material was cut repeatedly into small pieces using a scalpel and a 10 mm TC dish. Beforehand, the tissue was rinsed briefly with cold PBS to remove residual blood. Tissue pieces were treated enzymatically with Accutase for 15 min by adding 10 mL of enzymatic solution to a tube and incubating in a water bath at 37°C. Next, the sample was centrifuged at 300x g for 5 min at 4°C and the supernatant was aspirated. Pelleted cells were resuspended in 1 mL of CSPFL or other selected medium, counted and plated as single cells at a density of 2.6×10^4 - 3.5×10^4 cells/cm^2 on bMG-coated plates in the presence of 10 µM RI.

Cultivation of cells

Human fibroblasts

Primary adult dermal fibroblasts and commercially purchased foreskin-derived fibroblasts (NHDF and BJ fibroblasts) were cultured in FCS-containing MEF-medium without coating. For splitting cells were rinsed once with PBS, covered with Trypsin/EDTA solution and subjected to incubation at 37°C. Having incubated approximately 5 min or until visual inspection showed detachment of cells, the trypsinization was terminated by adding MEF-medium. Cell were collected and pelleted at 300x g for 3 min at 4°C and reseeded in culture vessels as required.

HEK293T cells

For lentivirus production, HEK293T cells were utilized. For routine culturing and expanding cells were grown on 0.1 % gelatin-coated T75 cell culture flasks using 12 mL MEF-medium until a confluence of 80 %. We subcultured the cells by rinsing once with sterile DPBS and adding 3 mL of trypsin solution afterwards. After 3-5 min, detachment of cells was visually checked under a microscope and the flask was tapped to detach remaining cells. The reaction was stopped using MEF-medium and cell suspension was collected into a tube and centrifuged at 300x g for 3 min. Thereafter, the cell pellet was resuspended and cells were reseeded in the desired splitting ratio into a new flask containing 12 mL of fresh MEF-medium. Medium was continuously changed every other day.

Induced pluripotent stem cells (iPSCs)

iPSCs cultivation was performed in feeder-free conditions using hESC-MG tissue culture dishes and daily change of mTeSR™1 or StemMACS™ iPS-Brew XF (MACS-Brew) medium. Passaging of cells was done at about 80 % confluence or every 4-5 days by using Accutase for 3-5 min at 37°C, harvesting cells by the addition of DMEM/F-12 and centrifuging at 300x g for 3 min at 4°C. Cells were seeded in a ratio of 1:6 on freshly coated tissue cultured plates in a single cell suspension and 10 µM Rho associated kinase inhibitor Y27632 (RI) was added for the first day.

Culturing of early neuroepithelial precursors (eNEPs)

For the cultivation of early neuroepithelial precursors (eNEPs) a chemically defined medium called CSPFL is used. Passaging of cells was performed at a confluency of 80 % enzymatically using Accutase for 3-5 min at 37°C and seeded as a single cell suspension onto bMG-coated plates in a ratio of 1:20-1:30. Directly after splitting, RI was used to improve survival of freshly split cells on the first day while it was omitted later. Medium change was performed every other day. For differentiation experiments, cells were seeded on bMG-coated glass coverslips whereas differentiation conditions varied according to the specific protocol.

For the cultivation of eNEPs on mitomycin C-treated MEF-feeders a chemically defined medium called CAP was used. Passaging of cells was performed at a confluency of 80 % enzymatically using Accutase for 3-5 min at 37°C and seeded in a single cell suspension on a MEF-feeder layer in a ratio of 1:20 to 1:30. Directly after splitting, RI Y27632 was used to improve survival of freshly split cells while it was omitted later. Medium change was performed every other day.

Cryopreservation of cells

For cryopreservation of cells, the cells were harvested and pelleted by centrifugation. Thereafter, the pelleted cells from one 80 % confluent well of a 6-well plate were resuspended in 1 mL of the appropriate freezing medium and dispensed into labeled cryovials. The composition of freezing medium varied upon the cell type, either containing FCS for fibroblasts and HEK cells or being free of serum for hiPSCs and all NPC lines (compare 2.1.6). To reduce the number of dead cells, controlled freezing of 1°C per min to -80°C using a freezing container filled with isopropanol was performed and cells were shifted to liquid nitrogen for long-term storage.

Cell counting

Cell numbers were determined manually using a Neubauer- hemocytometer. Harvested cells were pelleted and diluted in at least 1 mL or more depending on the size of the pellet and triturated to achieve a single cell suspension. 10 µL of the suspension were transferred to a counting chamber and the cell number was determined using an inverted microscope and a manual cell counter.

Every counting included 4 squares and resulting cell number was calculated as following:

Average cell number per square x 10^5 *= cells/mL*
Cells/mL x volume in mL = total cells

2.2.2 Generation of STEMCCA lentivirus using HEK293T-cells

For virus production, 5 x 10^6 293T cells were seeded on PDL-coated dishes (with a diameter of 100 mm) one day prior to transfection. On transfection day, medium was replaced by 9 mL of fresh, prewarmed 2% Adv.-MEF medium 1-2 h before cells were transfected. Transfection mix components were mixed in the following order: sterile ddH_2O, lentiviral construct STEMCCA, packaging plasmid psPAX2, envelope-plasmid pMD2.G encoding VSV.G and $CaCl_2$. STEMCCA, psPAX2 and pMD2.G were used in a ratio of 2:1:1. At last, 600 µL of 2 x HBS buffer was added and mixed vigorously with other components before incubating at RT for 15 min.

Transfection mix (for a 100 mm dish):

9 mL	2 % Adv. MEF-medium
18.5 µg	STEMCCA-DNA
9.25 µg	psPAX2-DNA
9.25 µg	pMD2.G

61.5 µL 2.5 M $CaCl_2$
fill up with ddH_2O to 600 µL and add 600 µL 2 x HBS Buffer.

During the incubation, chloroquine was added to HEK293T cells to a final concentration of 25 µM. Transfection mix was then gently pipetted up and down and added dropwise to cells. Dishes were shaken gently to distribute transfection mixture before being carefully transferred to the incubator. Medium was replaced by 13 mL of 5 % Adv. MEF-medium 5-6 h after transfection. Approximately 24 h after transfection, medium was changed to 13 mL of 5 % Adv. MEF-medium for viral production. About 30 h later first harvest of viral particles was conducted by collecting virus-containing supernatant in 50 mL reaction tubes and adding fresh 13 mL of 5 % Adv. MEF-medium to 10 cm dishes. The supernatant was filtered using 0.45 µm sterile filter units to remove debris and stored at 4°C until next harvest. The second harvest was done about 24 h later and thereafter producing cells were discarded. Viral harvest was filtered as well and merged with first yield. The presence of lentiviral particles in the supernatant was tested using the Lenti-X™ GoStix™. As a final step, virus-containing medium was either used freshly to infect fibroblasts in the presence of 7 µg/mL of polybrene or aliquoted and stored in -80°C freezer for later use.

2.2.3 Reprogramming of human fibroblasts

Lentiviral reprogramming

FSiPS cells were generated from normal human dermal fibroblasts (NHDF) by reprogramming using hSTEMCCA-lentiviral construct as described by Somers and colleagues with minor changes (Somers *et al.*, 2010). Briefly, 1×10^5 cells were plated on a well of a 6-well plate pre-coated with 0.1 % gelatin in MEF-medium. One day after plating, freshly produced, unconcentrated hSTEMCCA-lentivirus was added to the cells in fresh medium in the presence of 7 µg/mL polybrene. Medium was changed one day later and from then on daily to reprogramming medium. On day 6, cells were dissociated with Accutase and replated on a 100 mm tissue culture dish with gamma-irradiated MEFs as a feeder layer on gelatin in reprogramming medium supplemented with 10 µM RI. Medium change was continued daily. Putative hiPSC colonies started appearing on day 12 after transduction and were isolated manually by colony picking on day 28. From here on, putative hiPSC colonies were expanded under feeder-free conditions using mTeSR or MACS-Brew and hES-MG.

Reprogramming using Sendai virus (SeV)

SeV reprogramming technique results in transgene-free hiPSCs in a rapid and efficient procedure (Fusaki et al., 2009). We adapted this protocol using the commercially available CytoTune Kit 2.0. In detail, 7 x 10^5 cells/well were plated on a 12-well TC plate one day prior to infection. It is recommended by the manufacturer to use an MOI of 5 for KOS, MOI of 5 for c-Myc and an MOI of 3 for Klf4. As the concentration of viral particles fluctuates between different lot-numbers, concentration for every kit needs to be recalculated after accessing this information from the homepage. A volume of viral supernatant needed for the infection two 6-wells is indicated which we divided by four. For infection of cells, medium volume was reduced to 300 µL per well and virus with according MOI was applied dropwise to cells and spread homogeneously. Next, medium was changed after 24 h to fresh MEF-medium and changed daily until day 7 post infection. On day 8, cells were replated to a 6-Well of MEF-feeder cells adding 10 µM of RI. Medium change continued daily using reprogramming medium until colonies appear around day 12. Colonies were picked manually when reaching appropriate size while fresh MEF-feeder were plated every 7 days on top.

mRNA-based reprogramming

To omit the use of viral vectors during transgene-free reprogramming Warren and colleagues established a protocol consisting of daily transfections of synthetic mRNAs of relevant reprogramming factors (Warren et al., 2010). A kit following the adapted version of this protocol can be purchased from Miltenyi Biotec utilizing mRNAs of the Yamanaka-factors in combination with Lin28, Nanog and eGFP for transfection efficiency control. Before the first transfection cells were plated on hES-MG-coated 24-wells in different cell densities and allowed to adapt to StemMACS™ Repro-Brew XF (Repro-Brew) medium for 72 hours. Thereafter, cells were transfected daily for the next 12 days at intervals of 24 h. In detail, medium was replaced by 475 µL of fresh prewarmed Repro-Brew including 0.2 µg/mL B18R-protein. mRNA cocktail and transfection reagent were combined according to manufacturer's instructions and incubated for 20 min at RT. Thereafter, transfection mix was added to cells and distributed evenly. Cells were incubated for another 4 h at 37°C before media and transfection mix were aspirated and replaced by Repro-Brew and B18R. After 12 consecutive transfections, cells were allowed to remain in the same tissue culture conditions up to day 16 with daily medium change. We observed that some cell lines did not show appearance of colonies as suggested by manufacturer's instructions. Hence, we modified the protocol by replating transfected fibroblasts to MEF-feeder-coated tissue culture 6-well plate in a ratio of one 24-well to one 6-well. We observed colony formation approximately one week after replating and switched to iPSC-medium MACS-Brew. When colonies had appropriate size, they were manually isolated and further characterized and expanded.

2.2.4 Isolation of candidate hiPSC colonies

For picking, an inverted microscope was placed inside of a laminar hood and decontaminated exposure to UV-light and wiping with 70 % EtOH. Colonies were selected by morphology and circled and detached using a syringe needle. Floating colony was collected by aspirating with a pipette and transferred to a coated well of 48-well plate. Prior, bMG was removed and every well was filled with fresh media, supplemented with 10 µM RI. Having resuspended in prepared media, cells were allowed to attach and media was changed every other day until 80% of confluence was reached. Expansion continued by increasing the format from one well of a 48-well plate to one well of a 12-well plate and with the next split to one well of a 6-well plating resulting in an approximate splitting ratio of 1:2.5. With further expansion, splitting ratio was increased up to 1:6 till 1:12 and monoclones started to be characterized from passage 5 on.

2.2.5 Default differentiation of hiPSCs in three germ layers

To assess spontaneous differentiation capacity of hiPSCs *in vitro,* a spontaneous differentiation paradigm resulting in the formation of cell types of the three germ layers was carried out. First, hiPSCs were harvested by standard method and centrifuged at 300x g to obtain a pellet. Having aspirated the supernatant, the pellet was resuspended gently in 13 mL of hiPSCs medium resulting in a single cell suspension. Following, it was transferred into a 100 mm non-TC-treated Petri dish (bacterial dish). Medium change was conducted daily for 2-4 days until aggregates have formed. When reaching a size of 200-400 µm, medium was replaced by serum-containing MEF-medium which induces spontaneous differentiation and replaced by fresh medium every other day for 7-8 days. Next, aggregates were placed into TC plates containing gelatin-coated glass coverslips and covered with MEF-medium. Incubation for 2 days followed to minimize agitation allowing aggregates to attach to the gelatin-coated plate. Thereafter, medium was changed every 2 to 3 days. After 21-28 days of culture in differentiation medium, cells were either fixed in 4% PFA for analyzing germ layer differentiation potential by assessing TUJ1, AFP and SMA by immunofluorescence. Alternatively, cells were further cultured to continue differentiation and maturation for a prolonged period.

2.2.6 Differentiation of NPCs from hiPSCs

smNPC-derivation

For comparison of isolated or newly derived NPCs established protocols were reproduced following Reinhardt and colleagues with minor changes starting with FS STEMCCA iPS (Reinhardt et al., 2013).

Two-step monolayer induction protocol

hiPS-NPCs differentiation from hiPSC line ARiPS (Kadari et al., 2014) and IMR90-IPS was performed as previously described by Yan et al. with slight modifications (Yan et al., 2013). Briefly, hiPSCs were seeded at a density of 2 - 2.5 x 10^4 cells/cm^2 on hESC-MG coated 6-well

TC plates. After approximately 24 hours (day 0 of neural induction), reaching 15 - 20 % confluence, medium was changed to PSC Neural Induction Medium. Medium exchange was performed every other day until day 4 of neural induction. From day 4 to day 7, medium was changed daily due to higher confluency. Primitive NPCs were passaged enzymatically using Accutase at day 7 of neural induction. Cells were seeded in a density of 0.5 - 1 x 10^5 cells/cm^2 on bMG coated 6-well plates and treated for 5 days with NPC expansion medium. After seeding, hiPS-NPCs were treated with 10 µM RI overnight to prevent cell death. Neural expansion medium was changed every other day until day 5. To achieve a later stage rosette-like NPC-population, cells in passage 5 were adapted to FGF/EGF conditions as described in the following (Günther et al., 2016). Cells were cultured in NPC medium on PO/Ln coating. Cells were cryo-preserved in freezing medium for serum-free cells.

2.2.7 Clonogenicity assay

To investigate the clonogenic potential of cells to give rise to clonal lines *in vitro*, cells were harvested, counted using a hemocytometer (see 2.2.1) and diluted one cell per 100 µL of culturing media. After dilution, cell counting was repeated to assure proper dilution and 10 µM RI was added to prevent cell death after seeding. Thereafter, 100 µL of the cell suspension was dispensed in every well of a bMG-coated 96-well plate. Presence of single cells was checked visually using an inverted microscope one day after plating. Wells with either no cells or more than one were excluded from analysis. Visual inspection and imaging continued for up to 14 days. Thereafter, number of monoclones were determined and normalized to total number of wells with initially one cell seeded.

$$\frac{number\ of\ wells\ with\ monoclones}{total\ number\ of\ wells\ with\ single\ cells} \times 100 = clonogenicity\ rate\ in\ \%$$

Monoclonal lines were established from polyclonal cell lines by either performing the clonogenicity assay and further expansion of monoclonal lines. Alternatively, a highly diluted cell suspension including 10 µM RI was plated on a coated 60 mm-dish and visually checked if single cells attached on the next day. Single cells were allowed to give rise to colonies until those reached appropriate size for manual picking.

2.2.8 Growth curve experiments

To examine the proliferation of eNEPs, a useful approach is to obtain growth curves based on cell numbers harvested during a defined period. Briefly, 5 x 10^5 cells/well were seeded on a fresh 6-well plate. During consecutive 6 days, cells were collected from single wells and cell number was determined by manual counting. Based on these numbers, an exponential growth curve could be generated and the doubling time was extrapolated. Experiments were conducted on four biological samples.

2.2.9 Differentiation of NPCs

Default differentiation of NPCs

Spontaneous differentiation of eNEPs was initiated by the deprivation of small molecules and growth factors and by changing medium conditions to undirected differentiation medium two days after seeding. Density varied according to the purpose of differentiated cells between 2 x 10^4 and 5 x 10^4 cells/well of a 12-well TC plate containing coated glass coverslip.

Neuronal differentiation

For neuronal differentiation NPCs were plated on MG-coated glass coverslips at a density of 0.8 – 1.3 x 10^4 cells/cm^2 and 10 µM RI was added for better survival. Two days after seeding the medium was changed to neuronal differentiation medium containing 2 µM DAPT which was omitted after two weeks of differentiation. Cells were differentiated for 4-8 weeks in total while medium was replaced with fresh, prewarmed medium every 2-3 days in either full or half volume change.

Dopaminergic neuron differentiation

To increase the fraction of midbrain dopaminergic neurons, a previously published directed differentiation protocol was applied (Reinhardt et al., 2013). Two days after plating eNEPs as single cells in expansion medium, cells were exposed to dopaminergic differentiation medium I for the following 8 days, changing every other day, thus patterning the cells to midbrain identity. After 8 days, a subsequent change to dopaminergic media II is made. After 2 days, maturation medium is applied and cells were kept in this condition for at least 2 days. Maturation phase takes at least two weeks and can be prolonged.

Peripheral neuron and mesenchymal cell differentiation

To increase the yield of peripheral neurons, differentiation can be forced into cells of neural crest fate by the switch to peripheral differentiation medium I for two days after plating and expanding in growth medium and 10 µM RI. Further, cells can be subsequently differentiated into either peripheral neurons or mesenchymal cells. To achieve peripheral neurons, peripheral neuron differentiation medium II is used for the following 8 days and thereafter continued using maturation medium up to a desired time point of maturation. The same procedure can be followed differentiating to mesenchymal cells when using mesenchymal cell differentiation medium. Medium was replaced by prewarmed fresh media every other day.

2.2.10 FGF-dependence experiment

To assess the influence of bFGF and EGF signaling, we blocked FGF signaling by the commonly used chemical compound PD173074 (here referred to as FGFi) which specifically inhibits bFGF receptor signaling (Skaper et al., 2002). Additionally, we inhibited the EGF-signaling by the use of the chemical compound PD153035 (referred here as EGFi) which has been reported to specifically block EGF receptor tyrosine kinase in a highly efficient manner (Fry et al., 1994).

Having seeded a defined cell number using expanding medium (CSPFL) and 10 µM RI, we initiated the addition of the inhibitors one day later (time point -24 h). Treatment was conducted for up to 120 h, quantifying the number of cells every 24 h. Cells underwent treatment of vehicle (DMSO and medium), 100 nM FGFi and EGFi, respectively, or a combination of both at the same time. Cells were harvested and counted at indicated time points and normalized to starting cell numbers.

2.2.11 Immunocytochemistry

Cells were fixed using appropriate fixing solution for 15 minutes at room temperature and washed three times for 5 min each using PBS without Ca and Mg. For blocking and permeabilizing, cells were incubated for one hour at room temperature. Next, incubation with respective antibody (Table 1.5) diluted in blocking solution overnight at 4°C was performed. Cells were washed carefully three times using PBS and incubated with species-specific fluorochrome-conjugated secondary antibodies (Table 1.6) diluted in PBS for one hour at room temperature and protected from light. After rinsing three times with PBS, 1:5000 DAPI (4',6-diamidino-2-phenylindole) solution was applied for 15 minutes at room temperature to counterstain nuclei. Before coverslips were mounted with Mowiol®4-88 + DABCO® on glass slides, three additional washing steps were carried out.

2.2.12 Flow cytometry

For each sample, 0.5 to 1 × 10^6 cells were harvested enzymatically using Accutase and centrifuged at 1200 rpm for 5 min at 4°C to yield a cell pellet. To assure the lack of nonspecific binding and background fluorescence, isotype and unstained controls were included as controls. Staining procedure varied upon utilized antibodies as indicated in the following. Data was acquired using BD FACSCanto™ II flow cytometer, capturing $3x10^4$-$5x10^4$ events per sample. For analysis, FlowJo 10.0.7 software was used.

For conjugated antibodies directed against surface pluripotency markers we applied the following protocol. After excluding dead cells from the analysis using BD Horizon Fixable

Viability Stain 450, cell pellets were resuspended in staining buffer containing 5 % FCS in DPBS. Thereby unspecific binding sites were blocked during an incubation for 10 min on ice and cells were pelleted by centrifugation at 300 ×*g* for 5 min at 4 °C. Cells were stained for 10 min at 4°C using TRA-1-60-PE and SSEA-4-APC antibody diluted in staining buffer. Next, centrifugation and washing with DPBS was carried out before cells were carefully singularized in DPBS for analysis.

Staining procedure using CD133-antigen recognizing antibody includes blocking of unspecific binding sites by resuspending and incubating the cells in 5% FCS in PBS for 15 min on ice. Next, cells were centrifuged cells at 300 ×*g* for 5 min at 4 °C. Incubation with primary antibody diluted in blocking buffer or control conditions was carried out for 10 min on ice. Cells were pelleted and rinsed twice with 2 mL of DPBS by centrifuging and resuspended in fresh DPBS. Cy5-conjugated secondary antibody diluted in DPBS was applied for 10 min on ice. Thereafter, washing of cells was repeated twice. For viability staining, 5 µL of 7AAD was added to every specimen, previously resuspended in 500 µL of DPBS and allowed to incubate 10 min on ice. Finally, stained samples were transferred into tubes, using cell strainer to ensure singularity.

2.2.13 Transmission electron microscopy (TEM)

Preparation of samples was carried out as previously described by Yadav et al. (2016). In detail, neurons after 7 weeks of differentiation (see chapter 2.2.9) on glass coverslips were fixed using electron microscopy fixing solution for 5 min at 37°C after rinsing once with DMEM/F12 medium. The incubation was carried out for 90 min at room temperature. All following procedures were performed at room temperature. Cells were washed three times, 5 min each with CB and covered with 1% osmium tetroxide in CB for 1 h. in order to dehydrate the cells, specimens were treated with ascending concentrations of EtOH including en-bloc contrasting using 0.5 % uranyl acetate (30 and 50 % EtOH for 5 minutes, 0.5 % uranyl acetate in 70 % EtOH for 30 min, followed by 90, 96 % EtOH for 5 min in each case, and finally 2 times 100 % EtOH for 10 min each). At last, cells were embedded in a mixture of one part Epon embedding mixture and one part EtOH, for 30 min. Finally, pure Epon mixture was applied and changed after 2 h to a thin layer of fresh Epon which was allowed to polymerize for 48 h at 60°C on empty Epon blocks. For imaging, ultrathin sections of 80 nm were prepared from resin blocks and transferred to Formvar-coated nickel grids. Sections were post stained with 2% uranyl acetate and 0.2 % lead citrate and observed using a transmission electron microscope. Capture of TEM images was performed in collaboration with the TEM imaging unit at the Institute of Anatomy and Cell Biology, University of Würzburg.

2.2.14 Electrophysiology

Before conducting electrophysiological analysis, eNEPs were differentiated into neurons using directed neuronal differentiation protocol for 8 weeks on glass coverslips (see chapter 2.2.9). Electrophysiological recordings were conducted by Prof. Dr. Erhard Wischmeyer from the Department of Physiology, University of Würzburg as depicted for instance in Koilert et al., (2015).

2.2.15 Molecular biology

Extraction of RNA

RNA extraction was performed according to the manufacturer’s manual. Briefly, cells were harvested from one 6-Well by standard method and centrifuged to yield a pellet. After aspirating the supernatant, pellet was dissolved using RLT Plus buffer, previously mixed with 10 µL β -Mercaptoethanol per 1 mL of buffer. Dissolving the pellet was enhanced by vortexing for 30 s. To eliminate genomic DNA, mixture was added to a gDNA elimination column and centrifuged at 8000x g for 30 s collecting to the flow through. Next, the column was discarded and 350 µL of 70% EtOH solution was added to flow through before transferring the mixture into a new RNeasy spin column. Having centrifuged at 8000x g for 15 s, flow through was discarded and 700 µL RW1 buffer were applied to the column and the centrifugation was repeated. The step was repeated using 500 µL of RPE buffer. As following, column was washed again with 500 µL of RPE buffer by centrifuging at 8000x g for 2 min. The elution of the RNA was accomplished using 30 µL of RNase free water applied directly to column membrane and collected into RNase-free tubes while centrifuging at 8000x g for 1 min. RNA concentration was measured using Nanodrop and stored thereafter at -20°C.

Reverse transcription of RNA into complementary DNA (cDNA)

For each reverse transcription, 200 ng - 1000 ng of RNA was used and conducted according to manufacturer’s instructions. As individually required, control transcriptions including water only or RNA without RT were carried out to exclude water contaminations or genomic DNA in RNA-preparations. Yielded cDNA was used immediately for RT- or qRT-PCR analysis or stored at -20 °C.

When using GoScript Reverse Transcriptase (for RT-PCR), 1000 ng RNA was mixed with 1.25 µL Oligo (dT) primers and adjusted with sterile ddH$_2$O to 5 µL. Next, the mixture was incubated for 4 min at 70°C and chilled for 5 min on ice. Transcription reaction mixture was prepared as following and RNA-mixture was added.

7.5 µL sterile ddH$_2$O

4 µL	GoScript reaction buffer
2 µL	25 mM $MgCl_2$
1 µL	10 mM dNTPs
5 µL	RNA-dT Oligo primer mix
1 µL	Reverse transcriptase
5 µL	RNA-Oligo (dT) primer mixture

Following steps were carried out in the thermocycler:

25 °C	5 min
42 °C	60 min
70 °C	15 min
4 °C	∞

For qRT-PCR experiments, SuperScript II Reverse Transcriptase was used for cDNA transcription. For each reaction, 200 ng RNA was mixed with 1 µL Oligo (dT) primers, 1 µL dNTP mix and filled up to 12 µL using sterile ddH_2O. Thereafter, reaction mixture was incubated at 65 °C for 5 min and cooled down on ice. Next, the transcription mixture was prepared adding following components and gently pipetting up and down. Before adding SuperScript II RT, components were incubated at 42 °C for 2 min.

12 µL	RNA-mixture
4 µL	5x First-stranded buffer
2 µL	DTT
1 µL	SuperScript II RT

Following steps were carried out in the thermocycler:

42 °C	50 min
70 °C	15 min
4 °C	∞

Agarose gel electrophoresis

2 % w/v agarose was diluted in 1 x TAE-buffer and heated up until boiling to dissolve all solid particles. After cooling down to approximately 50-60 °C 5 µL of the DNA-intercalating chemical Midori Green Advanced was added per 100 mL agarose solution and mixed gently by rotating. Thereafter, a gel of appropriate size and well number (defined by selection of comb) was

prepared and allowed to polymerize at room temperature. Samples were loaded and electrophoresis was performed in TAE buffer at 80 V for 10 min followed by an increase of voltage to 120-140 V for additional 50 – 60 min.

Reverse transcriptase- polymerase chain reaction (RT-PCR)

RT-PCR was used to analyze the presence of residual SeV gene fragments. For every sample PCR-mixture was prepared as following. For better handling of larger number of samples, master mixes containing all ingredients besides cDNA was prepared.

17.375 µL	Sterile ddH_2O
2.5 µL	5x GoGreen Taq Flexi Buffer
1 µL	25 mM $MgCl_2$
0.125 µL	GoTaq Flexi DNA Polymerase
1.5 µL	mixture of F and R primers (5 µM each)
2.5 µL	cDNA

Samples were briefly centrifuged and RT-PCR was carried out in the thermocycler with parameters below repeated for 35 cycles. Resulting PCR product was analyzed using agarose gel electrophoresis.

95 °C	30 s
55 °C	30 s
72 °C	30 s

Quantitative RT-PCR (qRT-PCR)

To quantify and compare gene expression of different cell lines we used qRT-PCR and the fluorochrome SYBR green. After RNA extraction and transcription of 200 ng into cDNA using SuperScript II Kit, the cDNA was further diluted in a 1:5 ratio using RNAse, DNAse-free water. Further, for each gene a mix of forward and reverse primers with a dilution ratio of 1:20 each, resulting in a final concentration of 0.5 µM, was prepared. Beside genes of interest, two housekeeping genes namely GAPDH and UBC were quantified to allow a normalization of gene expression. Moreover, negative control samples including a H_2O- sample and a sample without reverse transcription were tested. For every gene, a mixture of 1 µL of primermix and 5 µL SYBR per reaction was prepared and increased in volume according to the number of assessed specimens (plus 20 % excess for pipetting errors). A second mixture containing 1 µL prediluted cDNA and 3 µL H2O and a surplus of 20 % per reaction was prepared. Next, 6 µL of mixture containing primers and SYBR was dispensed in a well of a 384-well plate. 4 µL of cDNA-mixture was added per well. Each combination of cDNA and primer appeared as 3 technical replicates. After sealing the plate, a short centrifugation step followed to remove potential air bubbles. Thereafter, the plate was placed in the fridge overnight and the PCR was started next morning. qRT-PCR was run as following:

1	50 °C	2 min
2	95 °C	2 min
3	95 °C	15 s
4	60°C	1 min
5	repetition of steps 3 and 4 for 45 cycles	
6	95 °C	10 s
7	Melt curve 65°C - 95°C, increment of 0.5°C for 5 s	

Data were collected and analyzed by the ΔΔCt method using Bio-Rad CFX Manager 3.0. LinReg PCR was used to determine qRT-PCR efficiency.

2.2.16 Microarray

For microarray analysis cells were harvested and centrifuged to yield a pellet that was stored at -80°C and transferred for further analysis to our collaboration partner Dr. Marc-Christian Thier (HI-STEM, DKFZ Heidelberg, Germany). Samples were examined using the Illumina HumanHT.12 v4 ExpressionChip. The expression raw data were subjected to quantile normalization with respect to pluripotent stem cells samples using Chipster. The differentially expressed genes between two groups were computed using T-test with Benjamini Hochberg-method for the correction of the raw p-values. Downstream analysis for selected genes in Fig. 3.20 B, was done using Chipster and R/Bioconductor packages by Thileepan Sekaran (currently at the Max-Planck Institute of Biomedical Research, Münster). Further gene set specific visualization of fold changes was done using Microsoft® Office 365.

2.2.17 Karyotype analysis

There is convincing evidence that prolonged cultivation of cells *in vitro* might result in chromosomal aberrations. Thus, it is highly important to assess this in karyograms by analyzing G-banding pattern. First, cells were seeded in a coated T25-flask and allowed to reach a confluency of 70 % but still undergoing cell division. Some cell types e.g. pluripotent stem cells or NPCs are rather challenging because of unclear banding of the chromosomes. Therefore, we optimized the duration and concentration of chemicals according to cell types. Colcemid solution was added to a final concentration of 100 ng/mL for 3 h in case of hiPSCs and 20 ng/mL for 45 min for eNEPs. This results in synchronization of the cells in the metaphase when incubated for the indicated time at 37°C. Thereafter, cells were harvested using classical splitting protocol, pelleted at 1400 rpm for 8 min at 4°C and resuspended in 1 mL of pre-warmed 75 mM KCl. Next, 14 mL of pre-warmed 75 mM KCl buffer being a hypo-osmolar solution which facilitates cell swelling and disruption of cell membrane was added to each reaction tube and incubated for 16 min at 37°C. Next, cells were centrifuged for 8 min at 1400 rpm and resuspended in an ice-cold 1:3 mixture of acetic acid and methanol to fix chromosomes at least over night at -20°C. If necessary, storage for a longer period was carried out. Thereafter, fixed and disrupted cells were centrifuged for 8 min at 1400 rpm and supernatant was removed by aspiration. Resulting pellet was resuspended in 500-1000 µL of fixing buffer and applied dropwise to a glass slide. Previously, the slides were cleaned thoroughly by 3 washing steps in hot water and dried. Presence of metaphases was controlled visually and dropping of chromosomes suspension was repeated if needed. Aging and staining using Giemsa stain solution resulted in visible banding pattern which can be used for analysis. Chromosome spreading and following procedures were carried out in collaboration with Julia Flunkert and Anna Maierhofer (Department of Human Genetics, University of Würzburg).

2.2.18 Software

Bio-Rad CFX Manager 3.0	Bio-Rad Laboratories, Hercules, USA
FIJI	Schindelin et al., 2012
Leica LAS X Core	Leica Microsystems, Wetzlar, Germany
Linreg PCR 11.1	Ruijter et al., 2009
NIS Elements AR.4.10.04	Nikon, Chiyoda, Japan
Office 365	Microsoft, Redmond, USA

3. Results

3.1 Adaptation of reprogramming techniques

Different reprogramming protocols were examined to obtain transgene-free hiPSCs. In addition to the classical lenti-virus based protocol using Cre-excisible STEMCCA–viral (Sommer et al., 2009), pluripotency was induced with the single RNA-Sendai Virus (SeV) (Ban et al., 2011). In addition, virus free-approach hallmarked by daily mRNA-transfections was analyzed (Warren et al., 2010). To adapt the transgene-free methods, we utilized commercially available foreskin fibroblasts (NHDF and BJ-lines) as well as control and patient-derived adult dermal fibroblasts.

3.1.1 Reprogramming of foreskin-derived control fibroblasts

First, all three methods of reprogramming were assessed on commercially available foreskin-derived fibroblasts (compare 2.1.3), which can be regarded as control fibroblasts as (referred to as NHDFs or BJs) (Fig. 3.1 and Fig. 3.2, respectively). Colonies appeared in all three reprogramming approaches, although there were differences in time points and overall procedure. Using the two viral approaches for the reprogramming of NHDFs, reseeding on a MEF feeder layer 7 days after infection was crucial as well as the use of a reprogramming medium containing bFGF and AA. Using the lentiviral protocol, colonies started to appear at day 12 post infection and 8 colonies per line were isolated manually after additional 3-4 weeks (representative colony in Fig. 3.1, first panel, middle image). We continued culturing the isolated clones under feeder-free conditions using hES-MG and selected after two passages 3 most promising clones per line hallmarked by sharply edged and homogeneous morphology (Fig. 3.1, first panel, right image). In comparison, colonies appeared rapidly following SeV infection around day 12 (Fig. 3.1, lower panel, middle) and could be picked manually when reaching appropriate size on MG coating and expanded thereafter (Fig.3.1, lower panel, right image).

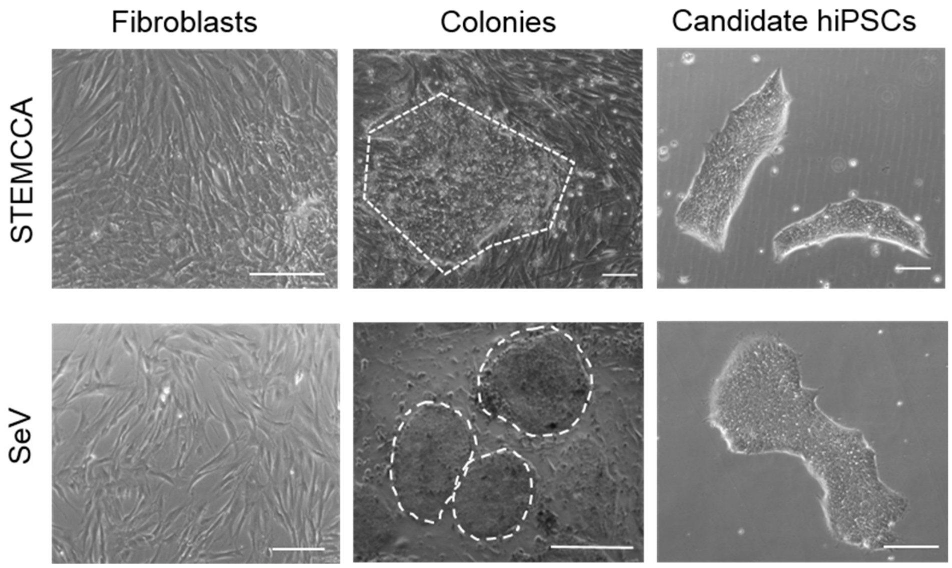

Figure 3.1 Phase contrast images of defined stages of reprogramming. Upper panel shows NHDF fibroblasts before reprogramming at the very left (scale bar = 200 µm), colony formation on day 16 (circled) in the middle and candidate hiPSCs after manual picking and culturing on hES-MG for 2 passages on the very right (each scale bar = 100µm). Lower panel demonstrates the same workflow as shown upper panel after reprogramming of NHDFs with SeV. Scale bars in left image: 200 µm, middle: 500 µm and 100 µm in the right image.

Notably, a different approach was followed reprogramming the second control line, named BJ fibroblasts, with synthetic mRNA including daily transfections for 12 consecutive days. B18R, a recombinant protein inhibiting interferon antiviral response and thus enhancing reprogramming efficiency was added to the culture medium. First established by Warren and colleagues (2010), this technique is now commercially available and allows a transient overexpression of reprogramming proteins in combination with a chemical reprogramming medium (Repro-Brew) which composition is undisclosed. Following manufacturer's instruction which includes an adaptation of fibroblasts for to Repro-Brew and initiating reprogramming with cells at different densities (identifying 20000 per single 24-well as the best, representative picture in Fig. 3.2 A) resulted in high transfection rates determined by nuclear GFP expression (>90 %, representative image in Fig. 3.2 B). However, colony formation on day 14 was not observed and cells were kept under previous conditions, but no colonies appeared. As a consequence, the proposed protocol was changed and therefore cells were reseeded the cells on a MEF feeder layer on day 16 continuing previous media conditions. Approximately one week later colonies appeared and medium conditions were changed to MACS-Brew media, the medium routinely used for iPSC-culture (compare Fig. 3.2 C). Around 2-3 weeks later, when appropriate in size (500 µm – 1000 µm) colonies were manually isolated and expanded in feeder free culture conditions (Fig. 3.2 D). In other words, despite successful reprogramming outcome, this method turned out to be more laborious compared to the viral approaches as an additional replating was required and colony formation was observed in average one week later than using other protocols. Therefore, it took a longer period of time before isolation and expansion of lines was possible. However, all three methods were able to induce colony formation and allowed the isolation of candidate iPSCs-lines in healthy foreskin- derived fibroblasts.

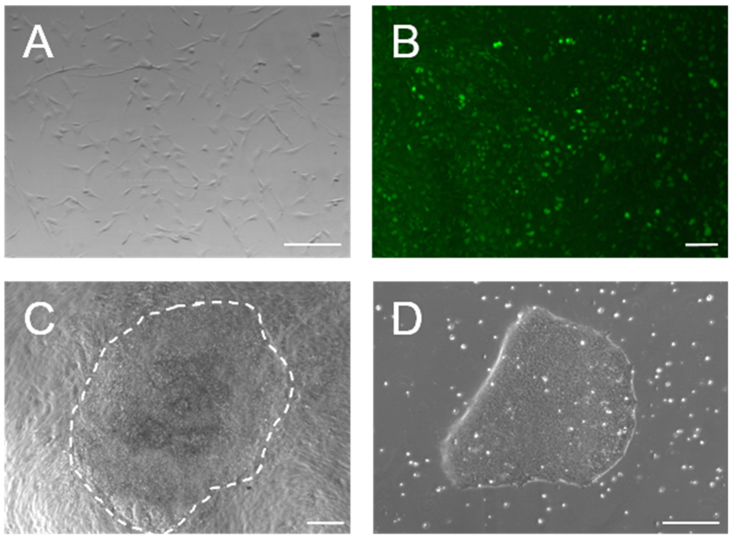

Figure 3.2 Overview of reprogramming stages of BJ fibroblasts using synthetic mRNA. (A) BJ fibroblasts before infection exhibit characteristic morphological features. (B) The transfection efficiency can be monitored using eGFP-mRNA and exhibits constantly >90% GFP-positive cells. (C) Colonies are formed after splitting on feeders. (D) Isolated and feeder-free expanded candidate hiPSCs. Scale bar = 200 µm in A, D; 100 µm in B; 250 µm in C.

3.1.2 Characterization of reprogrammed hiPSCs from foreskin fibroblasts

To confirm pluripotency, we examined the expression of the surface proteins SSEA4 or TRA-1-60 as well as the nuclear TF OCT4 by immunofluorescent stainings. hiPSCs obtained from three different strategies displayed a homogeneous staining pattern of the surface proteins as indicated in the first column (Fig. 3.3). Moreover, the OCT4 staining unravels a positive signal in all three hiPSCs lines (Fig. 3.3, right column).

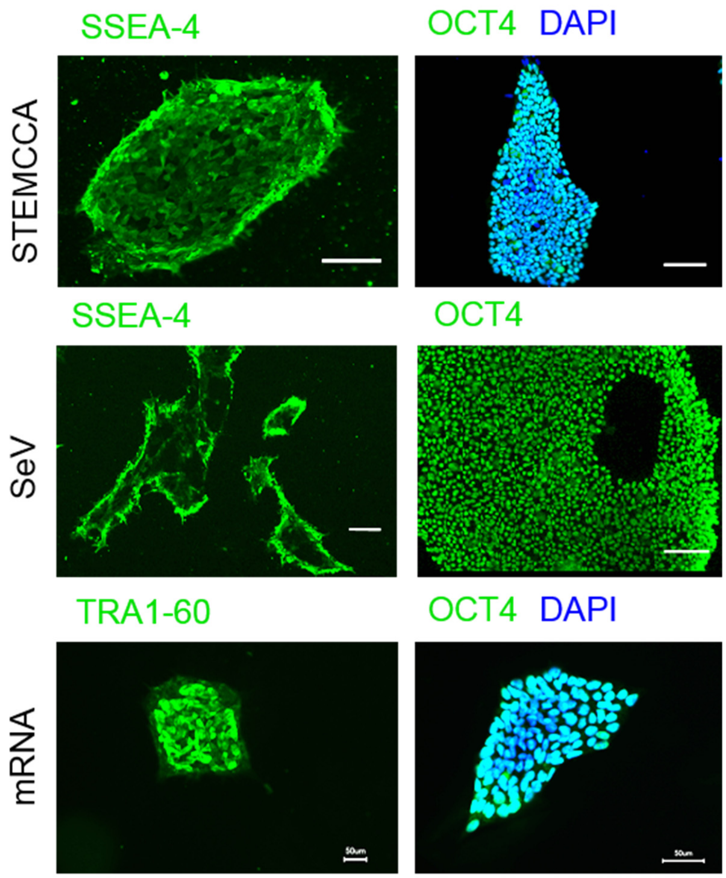

Figure 3.3 Characterization of hiPSCs by immunofluorescent staining. Three hiPSCs lines reprogrammed by different techniques were stained for marker proteins. NHDF STEMCCA iPS were positive for the surface protein SSEA-4 and the nuclear protein OCT4 (upper panel). Middle panel verifies NHDF SeV IPS being positive for the same markers but shown in a different magnification. Moreover, mRNA-BJ IPS colonies demonstrated the presence of TRA1-60 proteins on the surface and were homogeneously positive for OCT4. DAPI was used to counterstain nuclei in some images. Scale bars = 100 µm in two upper panels, 50 µm in lower panel.

Next, the cells were subjected to flow cytometric analyses of the surface markers TRA1-60 (orange) and SSEA-4 (red) (Fig. 3.4.). Whereas the unstained (grey) and isotype controls (light blue) remained negative in all measurements depicted as overlapping graphs, 98.2 % of NHDF STEMCCA iPS cells positive for TRA1-60 and 99.6 % positive for SSEA-4 (first panel) were identified. In case of NHDF SeV iPS, 99.1 % stained positive for TRA1-60 and 97.6 % for SSEA-4. When analyzing those markers in mRNA BJ iPS, 99.4 % TRA1-60 positive and 99.7 % SSEA-4 positive cells were found. These findings correlate with previous results from the immunostainings.

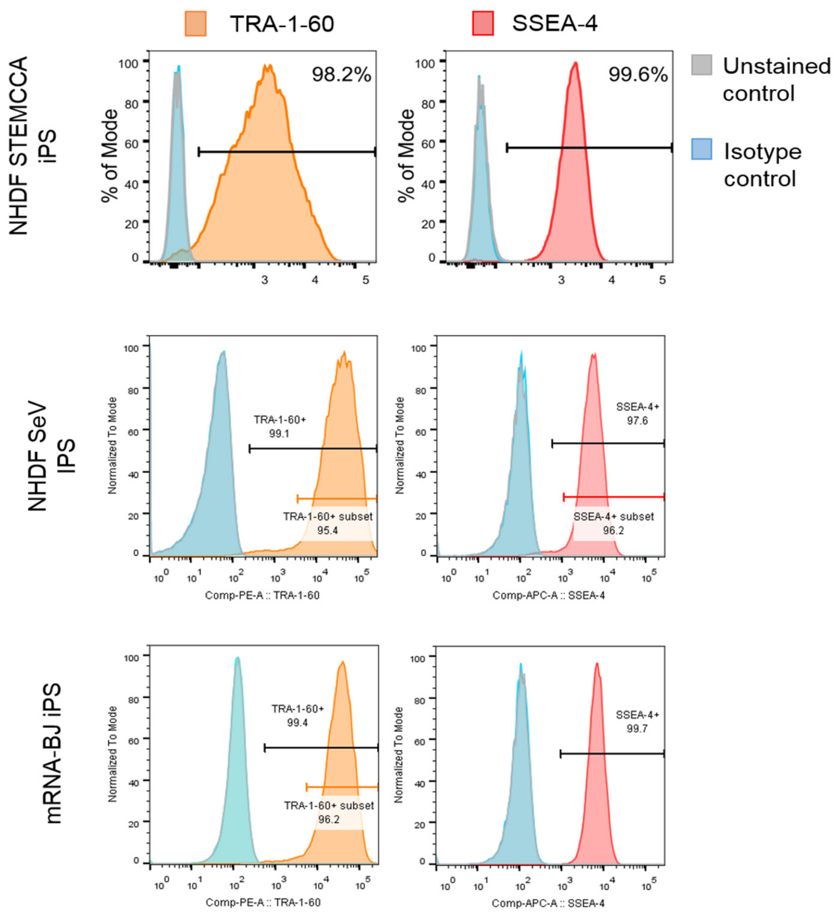

Figure 3.4 Flow cytometry analysis of hiPSC lines. Cells were stained for pluripotency surface markers including TRA1-60 (orange) and SSEA-4 (red). As negative controls, we included unstained samples and isotype controls. First panel shows NHDF STEMCCA iPS which are 98.2 % positive for TRA1-60 and 99.6 % for SSEA-4. In the second panel NHDF SeV iPS are presented, being 99.1 % TRA1-60 and 97.6 % SSEA-4-positive. In the lower panel (mRNA BJ iPS), high percentage of cells are positive for TRA1-60 (99.4 %) and SSEA-4 (99.7%). Negative controls show no shift in all measurements. (Experiments and analysis conducted together with Chee Keong Kwok.)

One of the hallmarks of hiPSCs is their capacity to subsequently differentiate in cell types of all three germ layers. To confirm this potential of the newly generated cell lines, an assay assessing the presence of germ layer associated marker proteins in differentiated hiPSCs was performed. Differentiated hiPSCs derived from NHDF using the lentivirus STEMCCA gave rise to TUJ1-positive cells, representing the ectodermal layer, SMA-positive cells (mesodermal lineage) and AFP-positive cells (endodermal layer). As a representative image, are shown (Fig. 3.5) confirming the presence of TUJ1-, SMA- and AFP- positive cells. The germ layer assay was applied to the other lines, but turned out to be technically challenging as discussed later in 4.1.

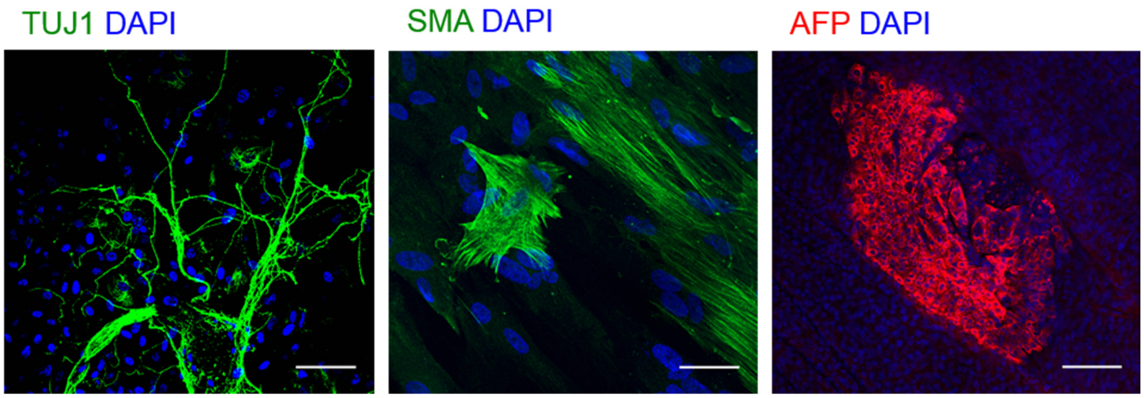

Figure 3.5 Three germlayer differentiation assay using FS STEMCCA hiPSC. After default differentiation of hiPSCs various cell types of distinct germ layer origin can be found. Among these, we could identify TUJ-1 positive cells (left) which resemble neuronal cell types, representative for the ectodermal layer. Additionally, we can demonstrate the presence of SMA positive (middle), indicating mesodermal germ layer cells. Finally, AFP positive cells (right) can be found which suggest the presence endodermal cell types. DAPI is used to counterstain nuclei in all images. Scale bar = 100 µm in left and right image. Scale bar = 60 µm in the middle image.

It has been reported that reprogramming and prolonged passaging of cells may cause abnormal karyotype and further chromosomal aberrations (Schlaeger et al., 2015). Therefore, a G-banding staining was conducted to assess the karyotype of the lentiviral reprogrammed control line. Having examined 10 metaphases, the presence of numeric or chromosomal aberrations (as shown in Figure 3.6 as a representative result) could not be detected. Moreover, a normal human male karyotype consisting of 22 chromosome pairs and X and Y chromosome each was identified.

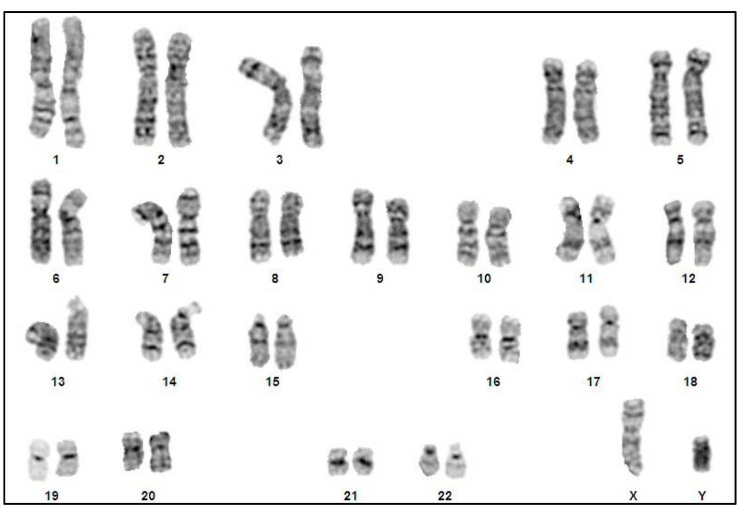

Figure 3.6 Karyogram of control hiPSCs reprogrammed using STEMCCA lentivirus. Analyzing of 10 metaphases after G-banding revealed normal human male karyotype consisting of 22 chromosome pairs, as well as one X- and Y-chromosome. No numeric or chromosomal aberrations were identified suggesting a genomic stable hiPSCs line.

Our reprogramming efforts using foreskin-derived fibroblasts were successful in all three approaches and resulted in the generation of three healthy hiPSC lines showing self-renewal and pluripotency. However, it is claimed that patient derived adult fibroblasts result in lower reprogramming efficiency and need further adjustments or longer periods until being fully reprogrammed. Thus, the reprogramming of non-foreskin derived fibroblasts was examined.

3.1.3 Reprogramming of adult dermal fibroblasts from healthy controls and patients

Lentiviral delivery of Yamanaka-factors represents a stable method for patient-derived cells as shown previously by our group (Kadari et al., 2014). On the downside, the excision of the stably integrated reprogramming cassette using DNA recombinase Cre is required to finally obtain trans-gene free hiPSCs. Thus, we used SeV and mRNA to reprogram primary healthy and disease-related adult fibroblasts in a non-integrative manner.

The fibroblasts were obtained from punch biopsies or collaborating groups as indicated in Tab. 1.3. Intriguingly, the SeV protocol represented the more efficient method, whereas it was challenging to obtain positive reprogramming outcomes using the mRNA-approach. Besides massive cell death caused by consecutive daily transfections as well as increasing starting cell numbers and reseeding on MEF-feeders, we could not succeed applying the mRNA protocol in all patient-derived cells (compare Tab. 3.1). In contrast, SeV reprogramming was characterized by rapid colony appearance starting from day 11 post infection. In Fig. 3.7 A, data from the reprogramming procedure of a PD patient-derived fibroblast line using SeV is exemplarily shown.

Table 3.1 Overview of reprogrammed lines generated within the thesis. Number of clones established for more than 5 passages varied from 2 to 5 per line, not indicated in the table. Compare fibroblasts to Tab. 1.2. NT = not tested; +++ very efficient (>50 colonies/well of a 6-well plate), ++ efficient (10-50 colonies/well of a 6-well plate), + low efficiency (<10 colonies/well of a 6-well plate), - not successful. Asterisk indicates transgene-free lines, hash points to putative transgene-free lines (passaging or excision required). Reprogramming of FD1, FD2 was carried out by Thomas Klein (Department of Neurology, Würzburg).

Cell line	Fibroblasts name	Healthy/disease?	SeV (#)	mRNA (*)	STEMCCA (#)
BJ IPS	BJ	healthy	+++	+	NT
NHDF iPS	NHDF	healthy	+++	++	+++
Ctrl. 1 iPS	UKERfJF-X-1	healthy	+++	-	NT
Ctrl. 2 iPS	UKERf33Q-X-1	healthy	+++	-	NT
Ctrl. 3 iPS	UKERfO3H-X-1	healthy	+++	-	NT
Pat. 1 iPS	UKERfAY6-X-1	PD	++	-	NT
Pat. 2 iPS	UKERfVK2-X-1	PD	+	-	NT
Pat. 3 iPS	UKERfPX7-X-1	PD	++	-	NT
Pat. 4 iPS	PEN1	Episodic ataxia	+++	NT	NT

Pat. 5 iPS	FD1	Fabry disease	NT	+++	NT
Pat. 6 iPS	FD2	Fabry disease	NT	+++	NT
Ctrl. 4 iPS	HP1	healthy	++	NT	+++
Ctrl. 5 iPS	HP2	healthy	+++	NT	+++

An important aspect in regard of safety is the confirmation of virus free cell lines. Therefore, cell lines from passage 10 on were examined for remaining SeV RNA-sequences by using oligonucleotides containing SeV genome sequences. Having isolated RNA, we analyzed the presence of remaining viral RNA at the cDNA level using RT-PCR (Fig. 3.7 D). NHDF STEMCCA IPS (referred in Fig 3.7 D as LeV IPS) were used as negative control because sells were not generated using SeV. RNA from freshly infected 293T HEK cells were used as a positive control for the presence of all tested viral RNA sequences. Whereas KOS and Klf RNA could not detected after a few passages in all lines, testing in some passages was omitted. As a result, no bands representing of the vectors containing KOS and Klf were identified in analyzed lines as depicted in Fig. 3.7 D. In contrast, we could still detect the presence of c-Myc and SeV. Continued testing at different passages led to the observation of cell lines with no positive bands around passage 15 on, suggesting that some hiPSCs had lost the viral RNA encoding the transgenes. In other lines, residual SeV sequences were still detectable (Fig. 37 D). It has been reported that the exposure to a temperature shift helps to eliminate remaining SeV particles (Ban et al., 2011; Lu et al., 2013) and is recommended by the manufacturer. Therefore, these lines were exposed to 5 days of culture at 39°C which should result in the elimination of remaining transgenes. However, the detection of SeV gene fragments was still possible in some lines e.g. the hiPSCs from Pat. 1-5 depicted the presence of SeV and c-Myc in passage 23 and 27 even after thermic shift, suggesting that these clones cannot be considered transgene-free. In contrast, in some clones (e.g. iPSCs from Ctrl. 1-6) no persistence of SeV-related genes was observed as early as P 15 and 16, whereas another clone 7 of the Ctrl. 1-7 shows the presence of viral genes. Thus, suggesting a clone-dependent effect which should be taken into account for subsequent studies.

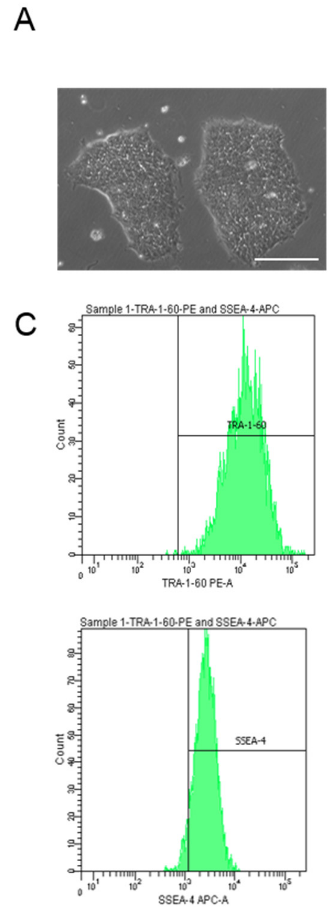

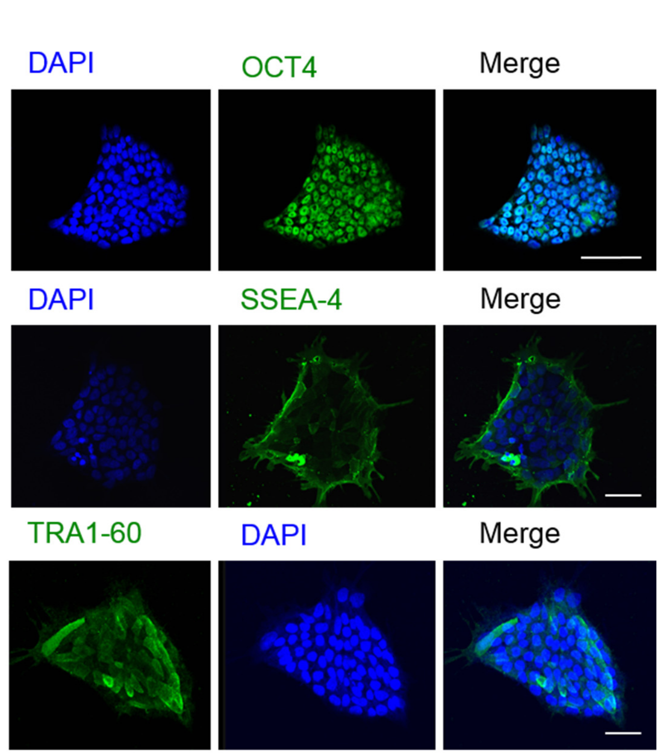

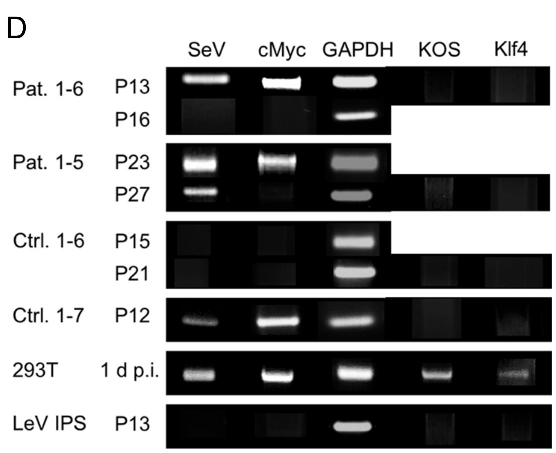

Fig. 3.7 Characterization of PD patient-specific iPSCs, obtained by SeV reprogramming. Exemplary, Pat. 1-3 iPSC are shown including (A) Phase contrast, (B) Immunofluorescence staining of pluripotency-associated markers OCT4, SSEA-4 and TRA1-60. (C) Flow cytometry of TRA1-60 and SSEA-4 confirms pluripotent cells. (D) RT-PCR results show residual SeV, cMyc, KOS and Klf4 virus RNA. Various clones at different stages were subjected analyses (compare table 3.1), but KOS and Klf4 was not analyzed in every sample. Freshly infected 293T cells and NHDF STEMCCA IPS (here shown as LeV) are used as positive and negative controls, respectively. Scale bars in A and upper row = 100 µm, in B = 50 µm

In conclusion, various approaches for the generation of hiPSCs were assessed. Three different protocols were successfully applied to reprogram foreskin fibroblasts. The validation confirmed pluripotency by stainings and flow cytometry analysis. However, the goal was to adapt reprogramming protocols using SeV and synthetic mRNA to punch biopsy-derived adult dermal fibroblasts from patients and healthy controls. Whereas the approach was successful in many lines using SeV, challenges were faced using the mRNA protocol on some primary lines. Thus, a modification of the protocol was applied and resulted in a higher reprogramming efficiency in some patient-specific lines proposing a high dependence on the starting population. Although SeV reprogramming represents an efficient method, persisting SeV genes up to approximately 15 passages were identified limiting their usage.

3.2 Differentiation of NPCs from iPSCs in a monolayer approach

hiPSCs emerged as a promising cell source with unique qualities allowing expansion and differentiation in progenitors and cell types of all three germ layers. Many protocols are aiming to provide a rapidly generated NPC line which can be used for subsequent differentiation into desired neural cell types including neurons or glia. In this part, it was investigated whether it is possible to establish a two-step protocol, which allows the generation of an early primitive NPCs line which is more neurogenic in the first step and an adaption to a widely used FGF/EGF-media condition which allows to establish a gliogenic cell line in a second step (Fig. 3.8). Thus, providing the opportunity to use one iPSC line for the differentiation of two cell populations being feasible for different needs. To achieve this, a previously published protocol was used which was applied to two iPSCs-lines (Yan et al., 2013) after validating their quality.

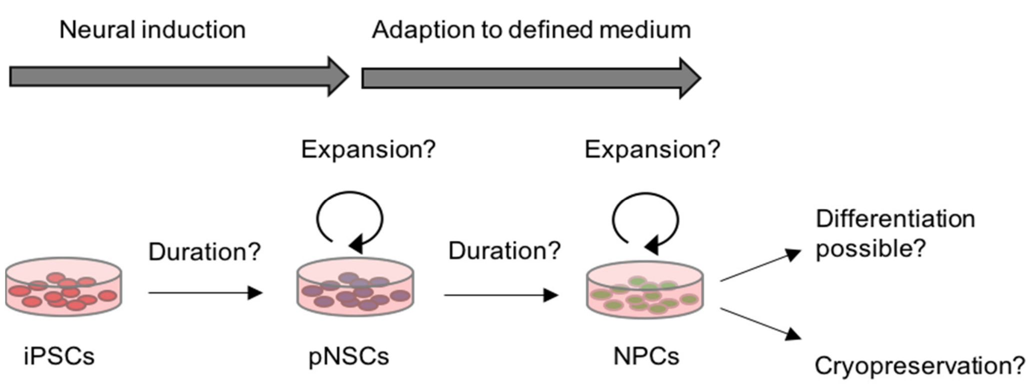

Figure 3.8 Graphic depiction of a projected two-step protocol yielding NPCs from hiPSCs. To assess whether it is possible to derive a NPC line step-wise in a monolayer approach, iPSCs should be subjected neural induction yielding in an early stage NSC type. It has to be elucidated how long the induction should take and whether an expandable neural cell type can be stabilized. If the first part can be accomplished, a differentiation into a second late stage NPC line using defined media conditions could be attempted. Thus, potentially yielding a NPC line which should be tested for proliferation and differentiation potential. (pNSCs = primitive NSCs)

3.2.1 Initial validation of iPSCs

Two human IPSC lines, a commercially available line derived from IMR90-fibroblasts and a previously published line from our lab reprogrammed from human adult dermal fibroblasts were analyzed (Kadari et al., 2014). First, morphological features were investigated by phase contrast microscopy. Typically formed iPSCs-colonies which were of homogeneous and of compact shape were identified (Fig. 3.9 A). In order to assess the expression of pluripotency-associated markers immunofluorescence analyses of OCT4, SOX2 and SSEA-4 were done (Fig. 3.9 B). A homogeneous staining for all proteins suggesting a homogenously pluripotent cell population was observed. Additionally, pluripotent fraction was quantified by flow cytometry analysis using a specific antibody recognizing the surface protein TRA-1-60. According to this analysis more than 98 % of iPSCs carried the pluripotency-associated marker TRA-1-60 (Fig. 3.9 C), hence confirming the immunofluorescent stainings.

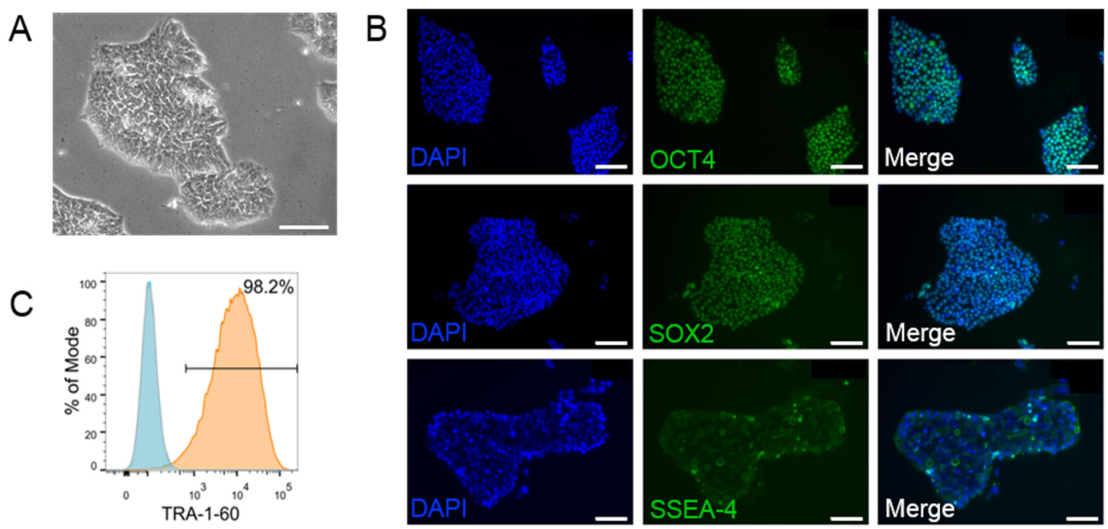

Figure 3.9 Validation of AF-iPSCs before neural induction. Before starting neural induction, the quality of hiPSCs was ensured by phase contrast (A) and immunofluorescent staining (B). Positive staining for the nuclear proteins OCT4 and SOX2 were detected. Further, the presence of the surface marker protein SSEA-4 was confirmed. Moreover, it could be demonstrated that more than 98 % of the cells express the pluripotency protein TRA-1-60 on the pluripotency (C). Scale bar = 100 µm.

3.2.2 Neural induction of hiPSCs

First, iPSCs were exposed to the monolayer neural induction media to as described in detail in 2.1.6 and 2.2.6. After the application of neural induction medium cells initially continued to form dense, roundly-shaped colonies. Intriguingly, their morphology changed on day 4 marked by unclearly defined edges of the colonies and a heterogeneous morphology (Fig. 3.10 A, upper panel). Increasing heterogeneity along with strongly proliferating cells during the first days of monolayer induction was observed. Cells were passaged at day 7 and replated on MG-coated culture dishes. Thereafter, cells changed their morphology drastically decreasing in heterogeneity of partly compact colony-growth and loosely dispersed larger cells to relatively homogeneous cultures consisting of highly proliferating cells exhibiting a neuroepithelial-like morphology (Fig. 3.10 A, lower panel). Cells were grown until full confluence before passaging and further expanded until passage 5. To characterize differentiated cells at this stage, the expression of several markers was investigated the by immunostaining. According to this analyses cells lost the expression of pluripotency marker OCT4 but remained in a strongly proliferative status as indicated by a high percentage of Ki67-positive cells (Fig. 3.10 B). Moreover, the differentiated cells homogeneously express NPC markers such as the cytoskeletal protein Nestin and transcription factors PAX6, SOX1 and SOX2 (Fig. 3.10 C and D). These data indicate that the IPSCs lost their pluripotency properties and adapted a multipotent, highly proliferative NPC status.

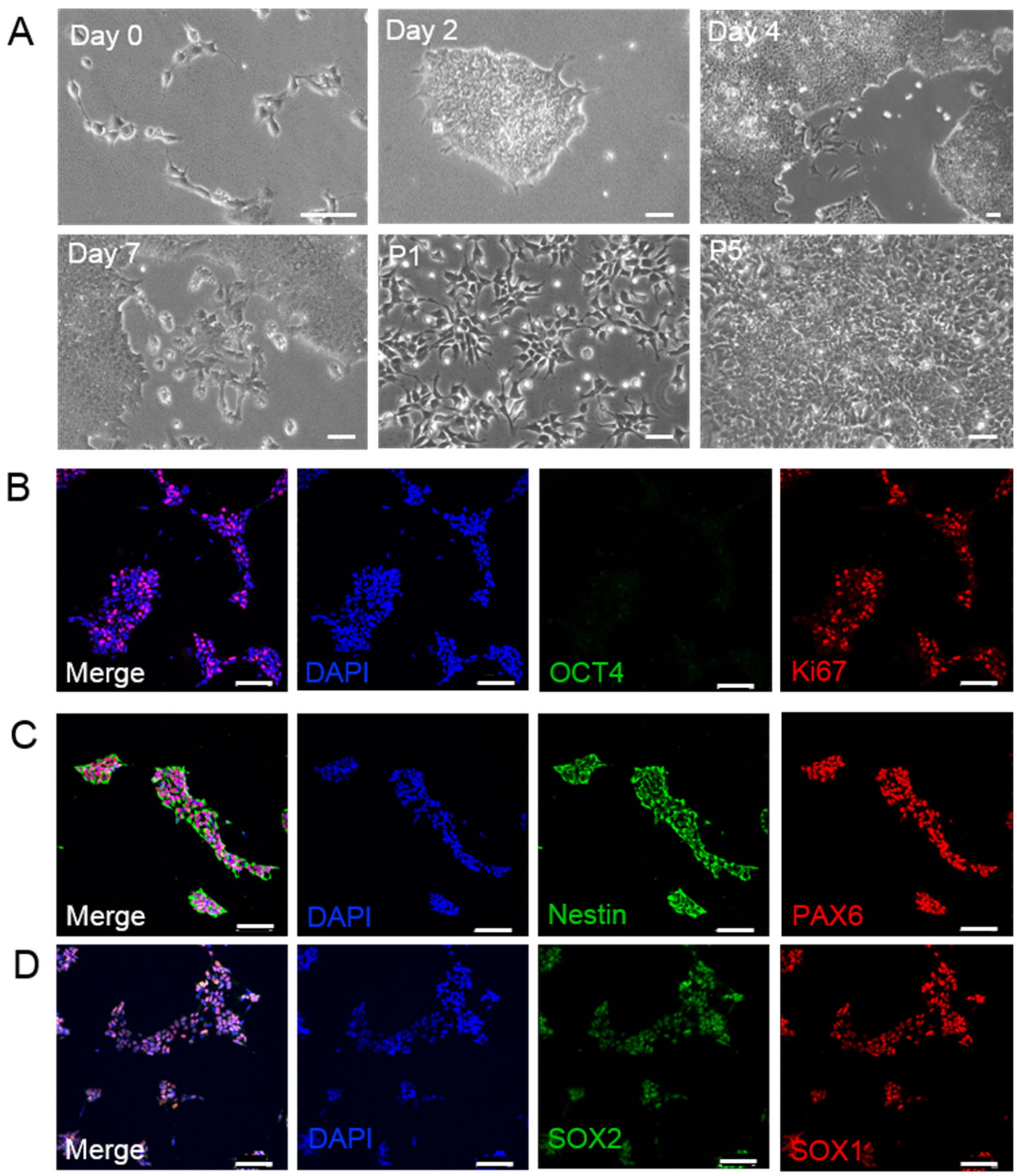

Figure 3.10 Morphological changes and characterization after neural induction from iPSCs. (A) Phase contrast images at different time points of differentiation of IPSCs to primitive NPCs including day 0, 2, 4, 7 as well as passage 1 and 5 during expansion. (B) Immunostainings confirm the loss of the pluripotency protein OCT4 after differentiation. In contrast, no change in proliferation, indicated by positive nuclear Ki67 staining, was observed. Further, NPC markers can be found in (C) and (D) represented by homogeneous distribution of Nestin and PAX6 (C) as well as SOX2 and SOX1 (D). DAPI is used as nuclear staining. Scale bars are indicating 50 µm.

To confirm the NPC identity, the differentiation potential was assessed by applying unbiased differentiation towards glial and neuronal lineages. High proportions of GFAP-positive cells as well as TUJ1-positive neurons in the differentiated cultures were found (Fig. 3.11 A and B, respectively). In conclusion, a stably proliferating NPCs from iPSCs within 7 days of monolayer culture that can be differentiated into neurons and astrocytes *in vitro* was derived. Since those NPCs are being maintained in commercially available media with partially undisclosed composition (Yan et al., 2013), their adaption to a more defined media conditions that are commonly used in the community was examined.

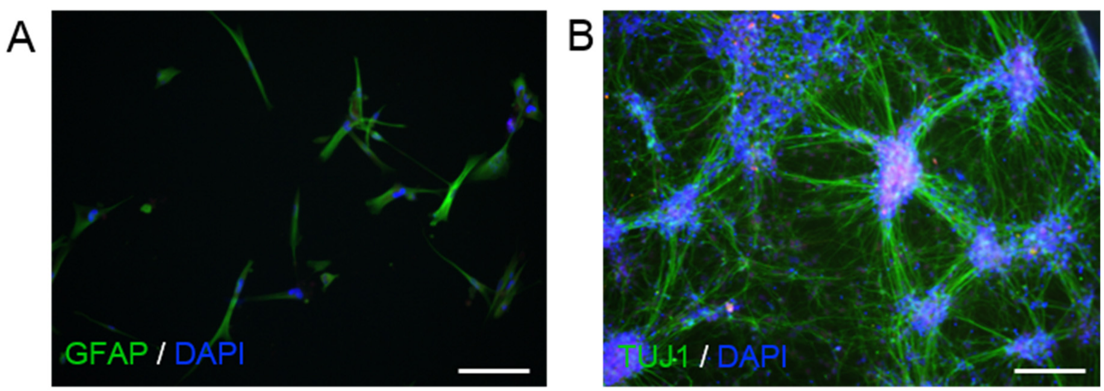

Figure 3.11 Differentiation of NPCs in neural cell types. Having differentiated in a default approach, staining for the marker protein GFAP was done (A) to demonstrate the differentiation of primitive NPCs in astrocytes. Moreover, the presence of TUJ1-positive neurons (B) can be demonstrated. DAPI is used in all fluorescent images as nuclear staining. Scale bars are indicating 50 µm.

3.2.3 Adaptation of monolayer NPCs to FGF/EGF medium conditions

Koch et al. reported a pure population of long-term self-renewing rosette-type NPCs, that are dependent on FGF and EGF, exhibit a NSCs marker profile and allow stable differentiation (Koch et al., 2009). These NPC-type has been successfully used in numerous studies since then and can be derived from human pluripotent stem cells by neural induction and laborious manual isolation of neural rosettes. Thus, it is of interest whether or not one can adapt the monolayer-NPCs to this commonly used, more defined FGF/EGF-state which might be more suitable to yield glial cells. For that, a FGF/EGF-supplemented media described by Koch et al. (2009) was applied to our monolayer derived pNPCs (Figure 3.8).

The initially observed heterogeneity of the FGF/EGF-adapted cells (data not shown) was counteracted by additional supplementing with low concentrations of CHIR (0.8 µM). CHIR has been reported to induce sustained self-renewal of human NPCs and particularly low concentrations appear to enhance homogeneity of neural progenitor populations (Moya et al., 2014). Using this media, a prominent change in morphology from unstructured neuroepithelial islands to rosette-like clusters being radially centered was observed (Fig. 3.12 A). Those FGF/EGF-NPCs showed continuous proliferation and could be successfully expanded until passage 30 thus far while keeping their morphological features. Moreover, the cells kept their proliferation potential after cryopreservation.

Gene expression analysis of relevant genes was conducted at different time points of differentiation by quantitative real-time PCR (Fig. 3.12 B and Table 1). Among the samples, samples from undifferentiated iPSCs, monolayer-derived primitive NPCs (passage 1 and 5) and FGF/EGF-NPCs derived thereof were included. As expected the pluripotency marker gene *POU5F1* is expressed only in IPSCs cells, whereas *SOX2* mRNA as detected in iPSCs is slightly downregulated in pNPCs of passage 1 and 5 (0.35 and 0.54-fold, respectively), but shows almost equal expression in FGF/EGF-NPCs. Interestingly, *Nestin* mRNA is found only at a basal level in early-passage primitive NPCs but strongly increased in NPCs from passage 5 (2.18-fold) and FGF/EGF-NPCs (7.32-fold). Even stronger upregulation was observed for the neural marker genes *SOX1* and *PAX6*. A major gain of *SOX1*-expression revealed during the differentiation of iPSCs to primitive NPCs (177.43-fold in passage 1 and 412.01-fold in passage 5) and expression remains high in FGF/EGF-NPCs (380.39-fold). Moreover, strong augmentation in *PAX6* gene-expression is observed during FGF-EGF-NPC derivation compared to iPSCs (893.42-fold in P1 and 3494.55-fold in P5 of primitive NPCs, 3344.13-fold in FGF/EGF-NPCs). These data indicate that rapid change of morphology during both steps of differentiation is correlating with the upregulation of neural markers at molecular level. Moreover, it suggests, that expansion of primitive NPCs up to 5 passages before changing the media conditions seems to be beneficial since there are differences in gene expressions between earlier and later passages.

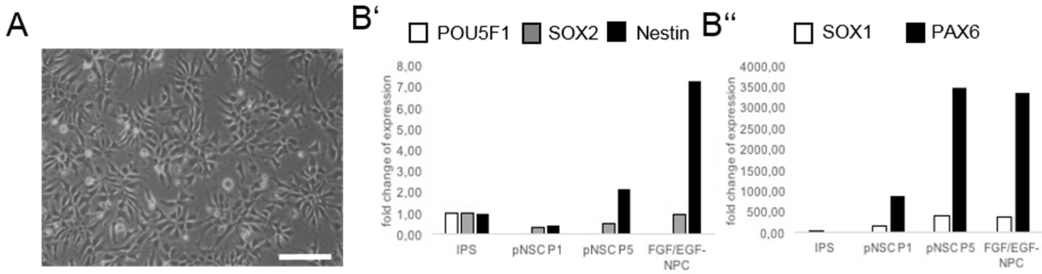

Figure 3.12 FGF/EGF-dependent NPCs exhibit a distinct morphology and show an upregulation of NPC genes. (A) Rosette-like morphology can be found in representative phase contrast image of FGF/EGF-NPCs. (B') Gene expression analysis reveals downregulation of the pluripotency gene *POU5F1* (white) during the differentiation and the expression of *SOX2* (grey). Enhanced expression of *Nestin* (black) can be observed during differentiation being the highest in FGF/EGF-NPCs. (B'') The NPC marker genes *SOX1* (white) and *PAX6* (black) are strongly upregulated upon differentiation in primitive NPCs, showing even stronger increase after expanding for 5 passages and adapting to FGF/EGF-medium. Scale bar indicating 100 µm.

Table 3.2 Relative fold changes of gene expression at selected NPC stages.

	POU5F1	*SOX2*	*Nestin*	*SOX1*	*PAX6*
iPSCs	1	1.0	1.0	1.0	1.0
pNPCs P1	0	0.4	0.4	177.4	893.4
pNPCs P5	0	0.5	2.2	412	3494.6
FGF/EGF NPCs	0	1.0	7.3	380.3	3344.1

3.2.4 Characterization of established FGF/EGF-NPCs

To further characterize the obtained FGF/EGF-NPCs immunocytochemical analysis was carried employing antibodies directed against various NPC marker proteins (in cooperation with Antje Appelt-Menzel, Appelt-Menzel et al., in revision, Günther et al., 2016). According to this analysis FGF/EGF-NPCs turned out to be positive for Nestin, PAX6, SOX1 and SOX2 confirming the NPC-profile of the cells (Fig. 3.13 A-C). Next, the differentiation potential of FGF/EGF-NPCs was assessed by applying established directed differentiation protocols towards neurons and astrocytes. Neuronal differentiation resulted in a very high percentage of elongated cells with characteristic protrusions staining positive for the neuronal protein TUJ1 (Fig. 3.13 D). Moreover, efficient differentiation into astrocytes as judged by typical morphology as well as staining for glial cytoskeletal proteins such as GFAP and S100ß was observed (Fig. 3.13 E and F, respectively). Taken together, these data demonstrate that FGF/EGF-dependent NPCs yielded in neuronal cells and a high proportion of astrocytes after differentiation.

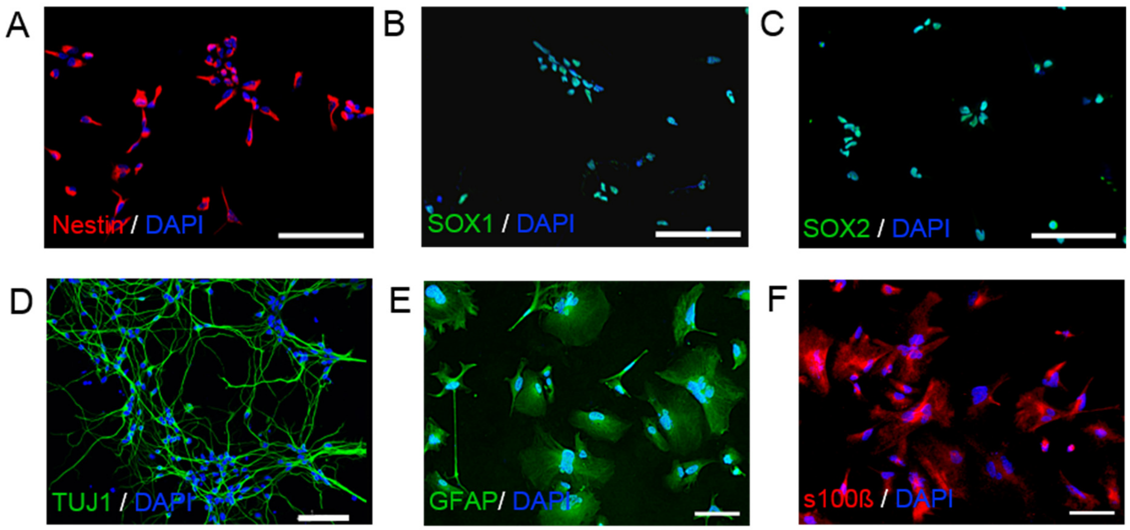

Figure 3.13 Characterization and differentiation of FGF/EGF-NPCs. (A – C) Immunocytochemical analysis confirms the presence of NPCs marker proteins in FGF/EGF-NPCs. Cells can be stained for the intermediate filament protein Nestin (A) as well as the nuclear proteins SOX1 (B) and SOX2 (C) Differentiation of FGF/EGF-NPCs yields TUJ1-positive neurons (D) as well as GFAP and S100β-positive astrocytes (E and F, respectively). DAPI is used in all fluorescent stainings to counterstain nuclei. Scale bars are indicating 100 µm.

Taken together, the second part of this thesis provided evidence for a monolayer induction within 7 days yielding primitive NSCs. This cell line can be expanded and cryopreserved, but also subsequently adapted to FGF/EGF medium conditions resulting in expandable NPCs. Both cell lines can be cryopreserved and differentiated in neurons and astrocytes, although the astrocyte yield is increased using FGF/EGF-NPCs.

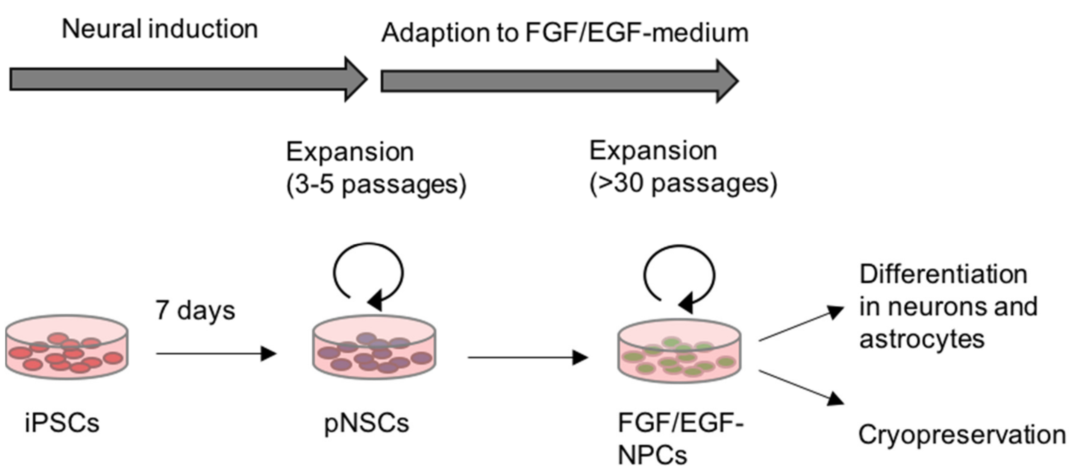

Figure 3.14 Schematic overview of the 2-step monolayer protocol for NPC derivation. Having validated pluripotency of the iPSCs, a previously published protocol which allows a monolayer neural induction from hiPSCs within 7 days was adapted (Yan et al., 2013). Resulting primitive NSCs can be expanded and cryopreserved, but are dependent on media conditions which are not disclosed. Thus, this cell population was expanded for 3 to 5 passages before adapting to more common FGF/EGF conditions capturing a later NPC state. Moreover, expansion for more than 30 passages, cryopreservation and differentiation could be demonstrated. pNSC = primitive NSCs.

3.3 Isolation and monoclonal expansion of NPCs from human fetal brain tissue

Various cell programming approaches have been explored resulting in a variety of developmentally early and late NPC cell lines, among these primitive NPCs (Li et al., 2011) and neuropithelial precursors (Reinhardt et al., 2013) as well as rosette-like cells (Koch et al., 2009) (Fig. 3.15). It remains to be demonstrated whether or not these cell populations represent physiological relevant cells. Thus far, highly proliferative primary human neural cells were isolated and expanded *in vitro* as stable primary reference NPCs. However, they were reported to have either rosette-like (Tailor et al., 2013) or radial glia like properties and being dependent on bFGF and EGF (Moon et al., 2016; Tailor et al., 2013). Following indications that it is possible to derive a murine eNEP line independent from EGF- and/or FGF-signaling (Günther et al., in preparation) it was aimed to isolate a human correlate. Previous studies suggested that medium conditions modulating crucial early neurodevelopmental pathways instead of FGF/EGF-containing media are able to contribute to the stable derivation of a primitive, long term self-renewing NPCs population dependent on hLif-signaling (Li et al., 2011). Thus, isolated cells from the fetal brain tissue obtained from abortive interventions during the 8-12 week of pregnancy (compare Tab. 1.2 and 2.2.1) were isolated and exposed to highly selective medium conditions based on published findings and unpublished successful application on murine primary cells.

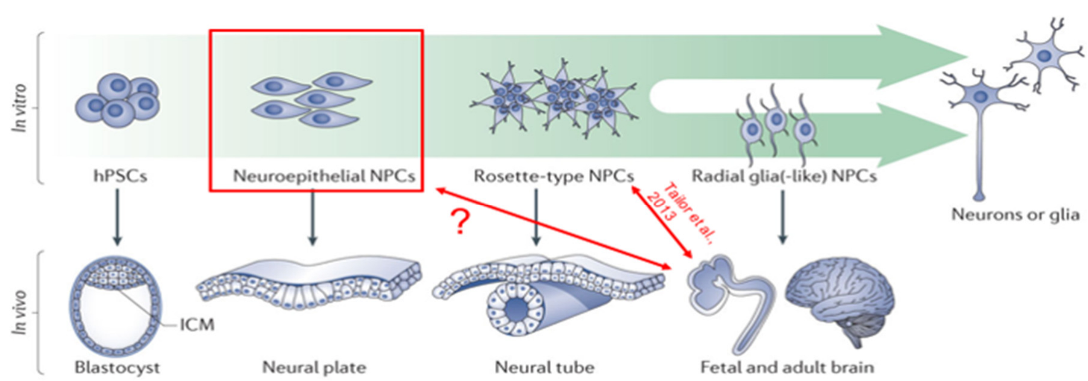

Figure 3.15 Schematic overview of correlating *in vivo* and *in vitro* cells types. Various cell types have been stabilized *in vitro* representing different developmental stages *in vivo*. Previously published protocols suggest the derivation of rosette-type NPCs (Tailor et al., 2013) or later stages. We hypothesize that it could be possible to capture an early neuroepithelial NPC line from fetal tissue (red arrow with question mark) applying alternative media conditions. Modified from Mertens et al., 2016.

During the first days after isolation, a heterogeneous cell population was observed which was subjected to various media compositions including CS-medium which contains hLif and the chemical compounds CHIR and SB based on the conditions established by Li and colleagues (Li et al., 2011). The supplemented compounds are promoting WNT signaling by the use of CHIR along with blocking of TGF-beta signaling by SB and as a consequence inhibiting differentiation. Further, FGF/EGF-supplemented medium as proposed by Tailor and colleagues was investigated (Tailor et al., 2013). Consequently, to capture an early FGF-dependent, but EGF-independent cell line, we used a third medium condition based on CS-medium, but additionally supplemented with bFGF which is promoting proliferation and self-renewal as well as the potent SHH-agonist PMA (from here on referred to as CSPFL, compare to 2.1.6).

Having dissociated the primary tissue, $2.6 \times 10^4 – 3.5 \times 10^4$ cells/well of a 6-well plate were seeded in different media conditions and supplemented with RI (see 2.2.1). When culturing on bMG-coated plates, we observed differences in morphology and proliferation from passage 0 on (Figure 3.16). The application of CS-Medium resulted in a heterogeneous morphology resembling differentiating neural cells and reduced proliferation (Fig. 3.16, first panel, left side). When applying FGF/EGF conditions (Fig. 3.16, first panel, right side) the cells acquired a polarized, spindle-like morphology similar as reported by Tailor et al. (2013). The application of CSPFL medium led to a distinct morphological appearence (Fig. 3.16, lower panel). Although less cells survived, surviving cells were highly proliferative cells and a tended to form densely packed colonies. The observed colonies morphology resembled of the iPSC-derived NPC line reported by Reinhardt et al. (2013). Continued subculture the cells resulted in a highly proliferative and increasingly homogeneous cell layer. From here on, efforts were focused on the most homogeneous and proliferative cell lines cultured in CSPFL-conditions. As an additional condition, CAP/MEF medium was applied to some clones at later passages, although not assessed from the beginning on due to limited access to primary material. Adaptation from CSPFL to CAP/MEF conditions was conducted for at least 5 passages resulting in similar morphology as CSPFL cells.

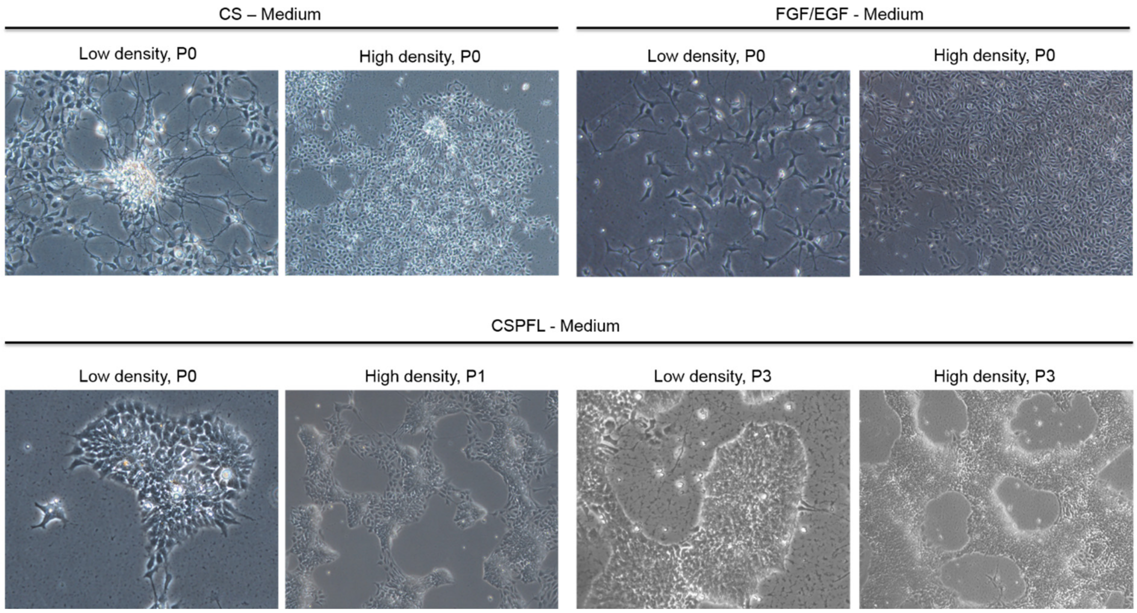

Figure 3.16 Phase contrast images of early passages of preparations of fetal brain tissue in diverse media. Left images in the upper panel show passage 0 cells in CS-medium in a low density or high density, hallmarked by a heterogeneous cell morphology. Right images in the upper panel demonstrate low and high density cells in FGF/EGF conditions which show a homogeneous, but polarized spindle-like morphology. Images in the lower panel indicate the forming of tightly clustering cells upon the cultivation in CSPFL medium. They can be observed from passage 0 on and further expanded resulting in a homogeneous polyclonal cell layer (lower panel, right side).

The polyclonal cell population can be expanded under CSPFL conditions giving rise to a homogeneous culture with compact round shaped colonies. Further, it was of interest to addressed whether this polyclonal population could yield clonal cell lines. Therefore, having subcultured the polyclonal line for 5 passages we seeded single cells using a limited dilution approach and observed colonies arising from single cells (Fig. 3.17). In approximately 23% of seeded single cells proliferating progeny were observed up to day 13 (exemplary for clone 3: Fig. 3.17, upper panel) until they formed large colonies. These colonies were manually isolated and further expanded as monoclonal lines in CSPFL. Intriguingly, splitting in high dilutions was possible (up to ratios of 1:50) but standard passaging occurred in 1:20 ratio supplemented with RI for better cell survival. We observed clustering of cells from day 3 after seeding and proceeded splitting every 6-7 days. Directly after seeding and during the next two days, cells display a spindle-like morphology (Fig. 3.17, lower panel). Remarkably, cell morphology and proliferation behavior did not change with higher passages (representative image of clone 3 at passage 30: Fig. 3.17, lower panel, right side). In order to assess the potential of the cells to generate monoclonal lines arising from single cells, a clonogenicity assay was conducted (as described in 2.2.7) revealing a clonogenicty rate of 23%.

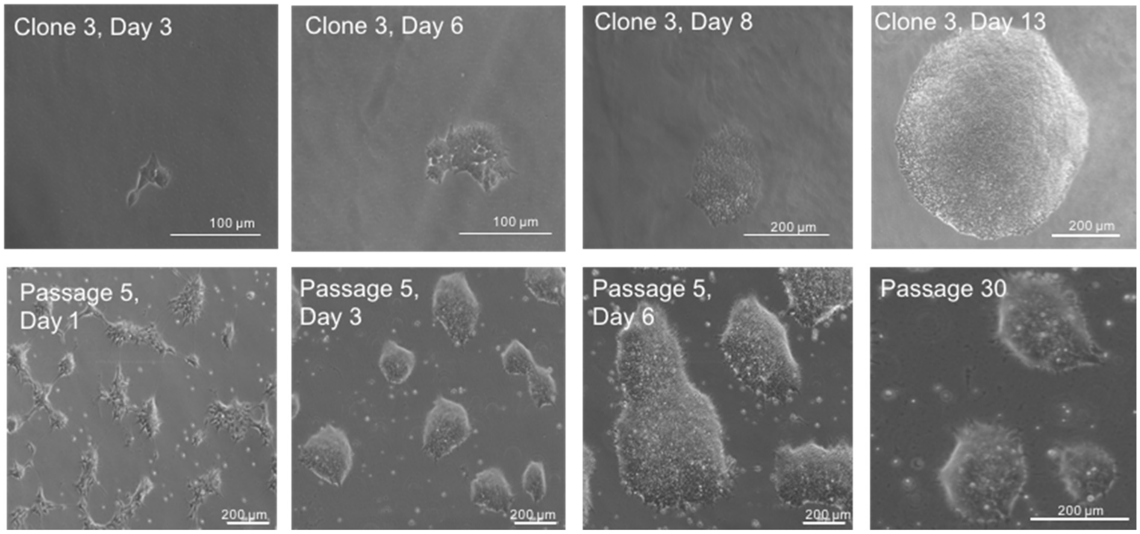

Figure 3.17 Morphological examination of monoclonal line eNEP, clone 3 rising from single cells and in later passages. Phase contrast images of monoclonal expansion procedure. Representative pictures of a single clone in expansion on days 3, 6, 8, 13 (upper panel). First three images in lower panel show densities one day after seeding, clustering of cells at day 3 and large colonies on days 6 of clone 3 in passage 5. Cells are appearing loose on day 1 after splitting, but continue to form densely packed colonies on day 3 and 6 after splitting before splitting the cells on day 6. Very right image in lower panel shows colony morphology in passage 30 after monoclonal

The next aim was to investigate whether monoclonal lines proliferate throughout prolonged cultivation. As a marker of proliferation, we used Ki67, a protein present in active cell cycle phases (G1, S, M, G2), but not in the resting G0 phase (Scholzen and Gerdes, 2000). The proliferation potential of eNEP clones was confirmed by Ki67 positive staining outcome (Figure 3.18 A). Moreover, the growth of different clones by quantifying cells every 24 h over a period of 120 h was examined. By that identifying a doubling time of about 33 h for CSPFL K3 (n = 4), which is shown representatively in passage numbers of 21 – 24 (Figure 3.18 B, C; Table).

A

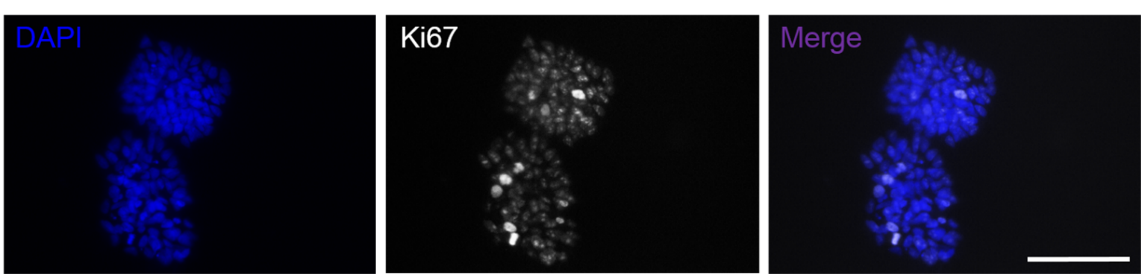

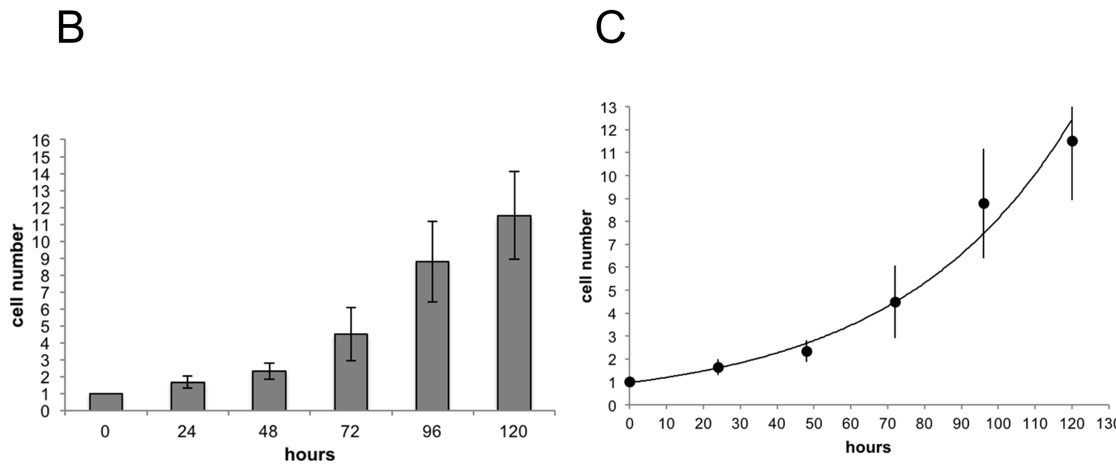

Figure 3.18 Immunofluorescence stainings and growth curve of clone 3. (A) Ki67-staining confirms proliferative cells within colonies. Nuclei are counterstained using DAPI. Scale bar = 100 µm. (B) Graphic shows number of cells assessed every 24 h after seeding up to 120 h. (C) Nearly exponential growth could be identified and extrapolated, resulting in a doubling time as 33.07 h (n = 4 biological samples).

hours	mean cell number	SD
0	1.00	0,0
24	1.65	0.4
48	2.33	0.5
72	4.49	1.6
96	8.78	2.4
120	11.52	2.6

Table 3.3 Cell numbers harvested at different time points. Cells were collected every 24 h until 120 h after seeding and normalized to starting cell number at seeding time point. Data from 4 independent experiments.

Taken together, these data provide evidence that a media composition was identified yielding highly proliferative monoclonal cell lines. Furthermore, sustained proliferation was observed for 2 clones until passage 40 with no apparent changes in morphology and growth properties.

3.3.1 Investigation of NPC-marker protein expression in clonal eNEP cells

Having identified the cells as highly proliferative and expandable, the neural identity of the cell population was confirmed by investigating the expression of characteristic markers using immunofluorescence analyses. Homogeneously stained colonies for the intermediate filament protein Nestin as well as the TF PAX6 (Fig. 3.19 A) were observed. Moreover, the early neural TFs SOX1 and SOX2 were detected (Fig. 3.19 A). Furthermore, a staining for BRN2, (Fig. 3.19 C) which has been described as an important regulator of neural induction was carried out. In addition, flow cytometry analysis for the surface stem cell marker CD133/Prominin 1 could demonstrate that more than 90 % of the cells stained positive (n= 3), while the appropriate control cells, namely PlatE-cells, showed no surface expression (D). We tested different stem cell lines regarding the expression of CD133 and detected positive signals on previously published iNPCs and iPSCs (data not shown).

In conclusion, these data indicate that a primary clonogenic cell population which can be expanded and possesses distinct morphology features as well a positive NPC marker profile was isolated.

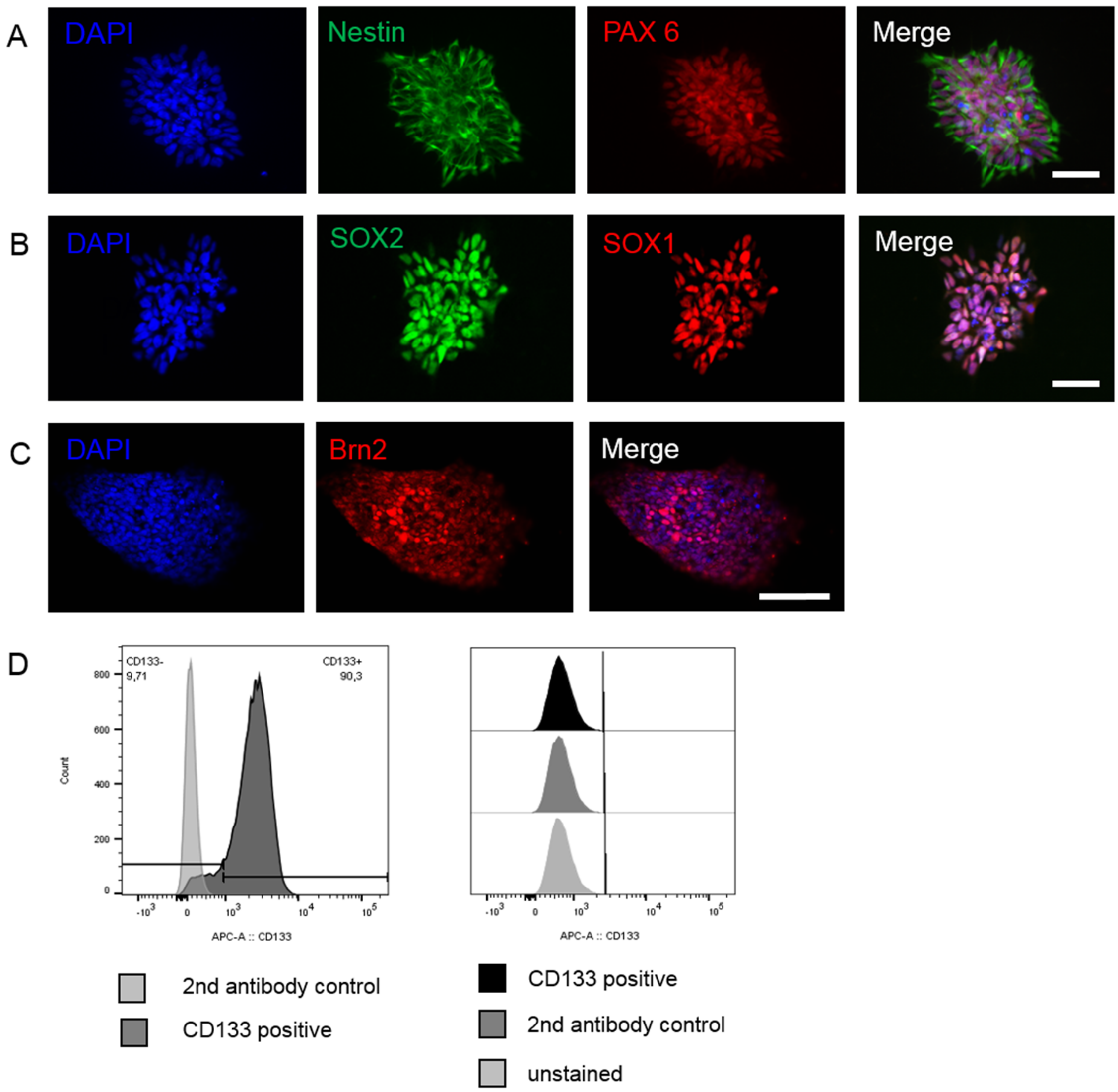

Figure 3.19 Marker protein expression of eNEP clone 3. The presence of NPC marker proteins was addressed by immunofluorescent stainings. Indeed, evidence of Nestin (green) and PAX6 (red) positive cells as demonstrated in (A) was provided. Moreover, SOX1 (red) and SOX2 (green) double positive cells were found which provide further evidence for neural profile of the stabilized cell line (B). Additionally, the colonies stained homogeneously for the protein Brn2 (C). Moreover, more than 90 % of viable cells were identified positive for the surface marker CD133/Prominin 1 (D, dark grey peak in left graphic) in flow cytometry analysis (n = 3). As a negative control PlatE cells remained negative after CD133 staining (D, right graphic). Nuclei were counterstained using DAPI. Scale bar = 50 µm in A, B and 100 µm in C.

3.3.2 Expression of NPC-related genes

After confirming the NPC-identity of eNEPs on protein level, the verification of this results was planned by analyzing the mRNAs of selected genes (Fig. 3.20). Hence, a comparison of three biological samples of one eNEP clone in passage 24 (P24, P24.2) and passage 25 to gene expression of the same clone in passage 5 was conducted. Moreover, the gene expression in smNPCs derived from FS STEMCCA iPSCs was evaluated (Reinhardt et al., 2013). The gene expression was normalized to the housekeeping genes *GAPDH* and *UBC*. The results confirmed the transcription of the *PROM1*-gene as well as the genes *DCX*, *NESTIN*, *PAX6* and *SOX1* being expressed similarly among different clones and passages, also in comparison to the expression of smNPCs. In contrast, an upregulation of *SOX2* in the biological replicates of eNEPs in late passages was observed. The expression was markedly reduced in passage 5 eNEPs as well as in smNPCs. All in all, qRT-PCR analyis confirmed the NPC marker identity on mRNA level and identified comparable gene expression in relation to low passage samples and smNPCs.

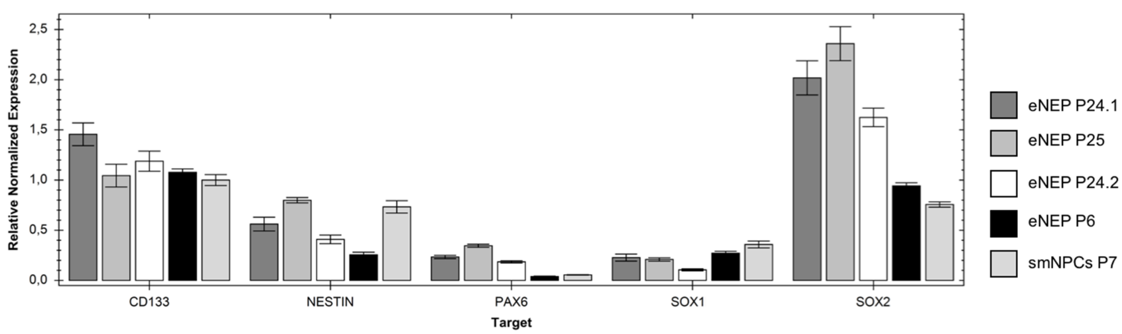

Figure 3.20 qRT-PCR analysis of NPC-related genes in eNEP clone 3. Gene expression of *CD133/PROM1*, *NESTIN*, *PAX6*, *SOX1* and *SOX2* was analyzed in 3 samples of primary eNEPs in P24 and P25, as well as an eNEP line in P6. smNPCs derived following Reinhardt et al., (2013) were used for comparison. All genes were normalized to *GAPDH* and *UBC*.

Moreover, the gene expression of three clonal lines from two preparations relative to the microarray data of three pluripotent cell lines (hiPSCs and two hESCs) was assessed to identify further gene expression changes (in collaboration with Dr. Marc-Christian Their, HI-STEM, DKFZ, Heidelberg). Microarray analysis for examining fold change of mRNA expression between pluripotent and established eNEP lines in CAP/MEF conditions and CSPFL medium conditions was used (compare 2.2.16) (Figure 3.21 A). A distinct gene expression profile clearly distinguishing between pluripotent and neural cell lines could be identified. Further, cells were subjected to different media conditions (CAP/MEF vs. CSPFL, compare 3.3) resulting in a minimal change of gene expression between neural lines. Moreover, the heat map reveals differences between clones cultured despite same media conditions. Differences are evident in particular between clone 2 (referred to in Fig 3.21 A as

K2) and clones A and 3 (referred to in Fig 3.21 A as KA and K3, respectively) which originate from different preparations. To analyze the gene expression of CSPFL clones in detail, analysis was focused on fold changes of the 3 clones in relation to 3 pluripotent cell lines (Fig. 3.21 B). We considered fold changes of more than 1.5 as significant. However, due to interclonal differences the p-value exceeded 0.05. An upregulation of neural genes with the greatest fold change in the neural gene *HES5* (4.608) and other *HES*-genes e.g. *HES4* (2.570) and *HES6* was identified. Further, a 2.782-fold higher expression of the gene *POU3F2* coding for the protein BRN2 and *PAX6* (1.845-fold) was observed which were also detected by immunofluorescence analysis. Moreover, an upregulation of *DCX* (1.348-fold) and *PROM1* (1.291-fold) was registered as previously identified in qRT-PCR analysis. Interestingly, *ASCL1* (1.249-fold) and *NEUROG2* (2.072-fold) which are known to be involved in direct conversion to neural cells are upregulated endorsing the neural identity of eNEPs. Additionally, *CDH2* encoding the cell-cell adhesion protein N-cadherin was 1.454-fold upregulated in neural lines relative to pluripotent cells. Moreover, the expression of *SOX11* which is known to be involved in the regulation of neurogenesis is 1.785-fold increased. These differences in the gene expression in comparison to pluripotent cells suggest a distinct cell line with a neural gene profile.

A

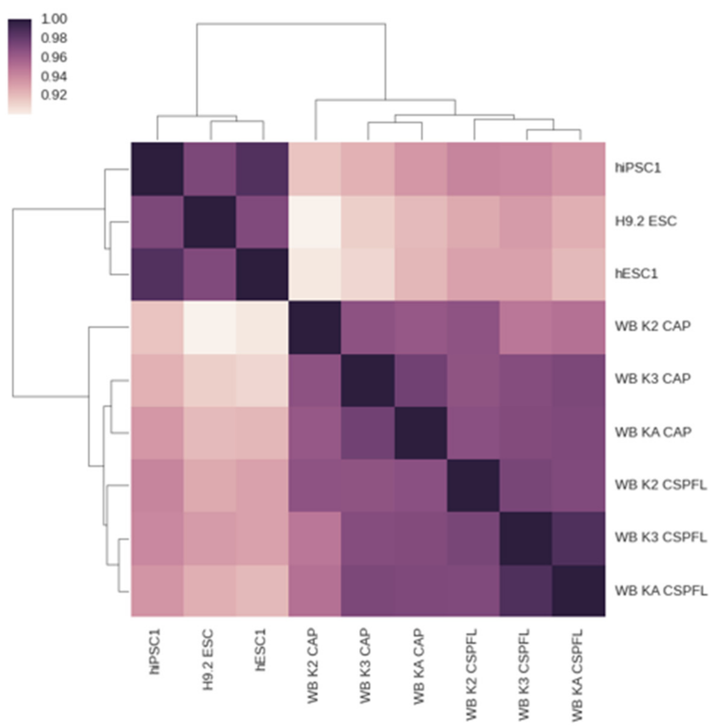

B

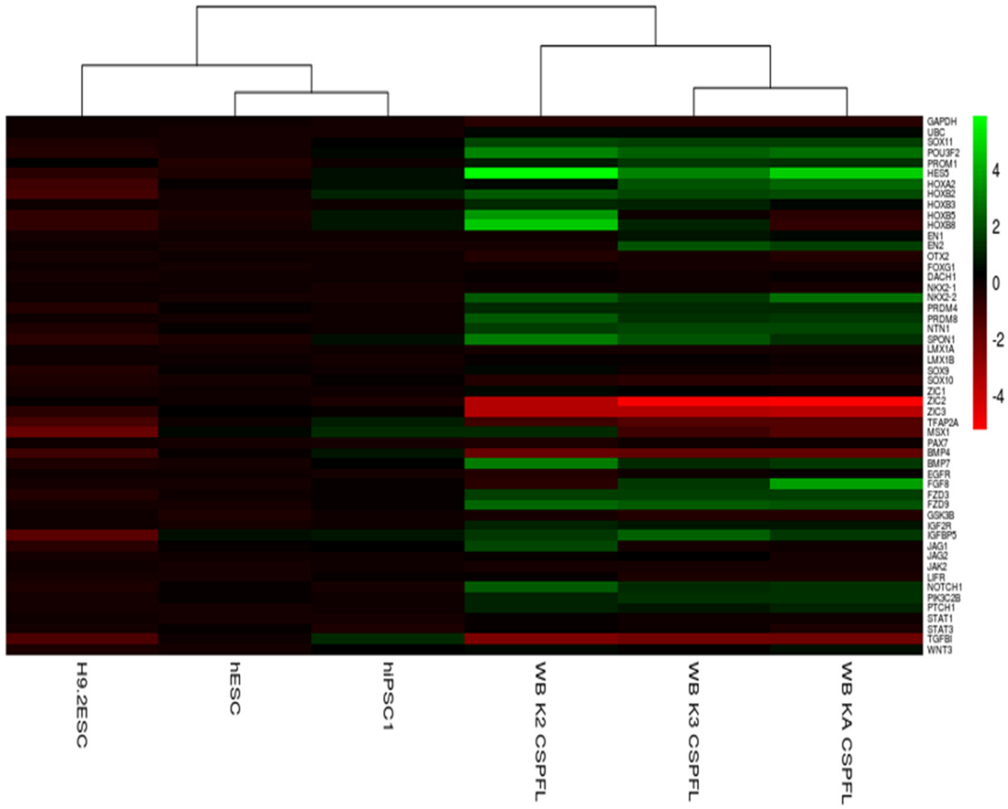

C

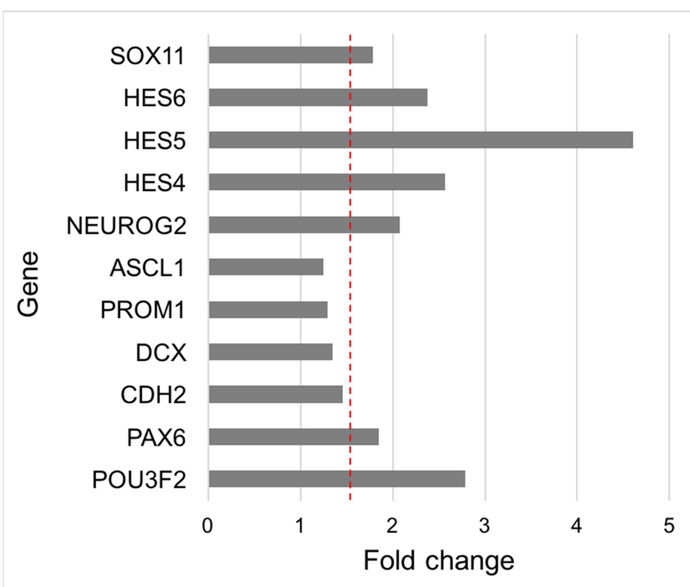

Gene	Fold change	P-value
POU3F2	2.782	0.06
PAX6	1.845	0.13
CDH2	1.454	0.40
DCX	1.348	0.17
PROM1	1.291	0.13
ASCL1	1.249	0.62
NEUROG2	2.072	0.21
HES4	2.570	0.16
HES5	4.608	0.11
HES6	2.378	0.19
SOX11	1.785	0.06

Figure 3.21 Global gene expression assessed by microarray analyses. (A) Correlation map of global gene expression of 3 pluripotent cell lines (hiPSC1, H9ESC, hESC1), 3 primary eNEP clones in CAP/MEF conditions (K2, K3, KA) and the same 3 eNEP clones cultured under CSPFL conditions (K2, K3, KA). (B) Heatmap of selected gene sets from 3 pluripotent lines as well as 3 eNEP lines in CSPFL conditions as explained in A. (C) Fold change of gene expression of selected NPC-related genes of 3 eNEP clones in CSPFL compared to 3 pluripotent cell lines and correlating table.

3.3.3 Assessment of the regional identity of eNEPs

In order to determine a putative regional identity of eNEPs, the expression of genes specifically found within distinct brain regions was investigated. As reviewed in 1.4.2, exposure to some growth factors can have patterning effects affecting the regional fate along the A-P and D-V axes. Since the CSPFL cultivation medium contains SHH and WNT agonists, mimicking patterning cues, it is intriguing to investigate their potential effect on regional fate.

Patterning along the anterior-posterior axis

Many evidence from the literature suggest that early NPC lines represent different cell fates typically found along the A-P axis. Consistent with neural development, early NPCs show forebrain identity and acquire posterior fate when stabilized in a later stage. Thus, the expression of three prominent genes, namely *DACH1* for forebrain, *EN1* for midbrain as well as *HOXA2* for hindbrain was assessed in eNEPs by qRT-PCR experiments. Three biological samples of eNEPs in passage 24 and 25 to the same line in passage 5 and smNPCs (same samples as in Fig. 3.20) were compared. Gene expressions were normalized for *GAPDH* and *UBC*. We could detect a low expression level of the forebrain-marker gene *DACH1* in all lines (Fig. 3.22 A), whereas the midbrain-related gene *EN1* was upregulated in late (passages 24, 25) and early passage eNEPs higher expressed in passage 6. eNEPs in low and high passages expressed the hindbrain marker gene *HOXA2*.

As a second approach, we analyzed A-P related genes of three eNEP clones relative to three pluripotent lines (Fig. 3.22 B). We examined the forebrain marker genes *OTX2*, *FOXG1* and *DACH1* (marked yellow in table) which were not upregulated in comparison to pluripotent cells. Apart from that, the midbrain genes *EN1* and *EN2* were increased in expression (blue set). Notably, we found a higher expression of hindbrain marker genes, especially *HOXA2, HOXB2, HOXB8 and IRX3* (green set). These data strongly endorsed our outcome from qRT-PCR and suggests a mixed midbrain-hindbrain identity or a mid-hindbrain border profile of eNEPs.

A

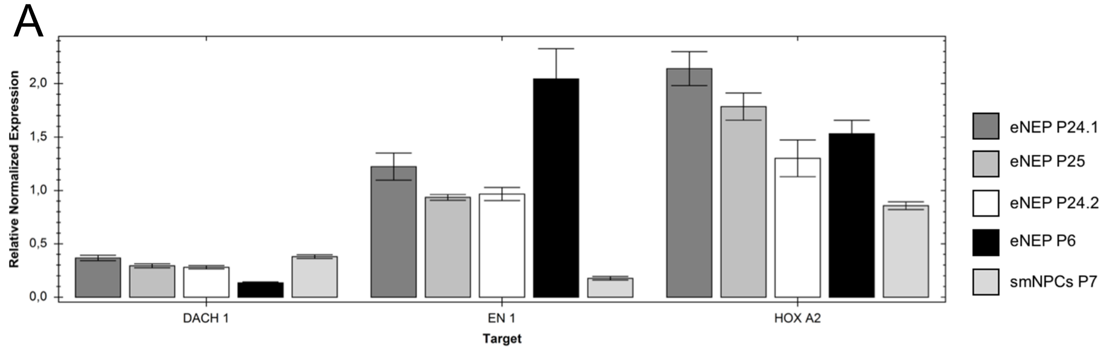

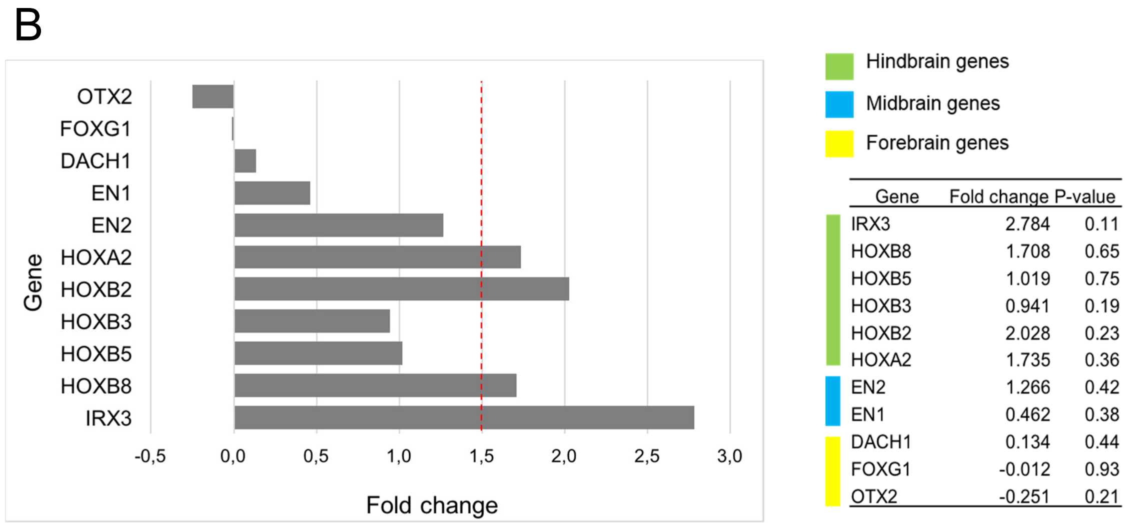

Gene	Fold change	P-value
IRX3	2.784	0.11
HOXB8	1.708	0.65
HOXB5	1.019	0.75
HOXB3	0.941	0.19
HOXB2	2.028	0.23
HOXA2	1.735	0.36
EN2	1.266	0.42
EN1	0.462	0.38
DACH1	0.134	0.44
FOXG1	-0.012	0.93
OTX2	-0.251	0.21

Figure 3.22 Expression of A-P genes. (A) Gene expression of *DACH1*, *EN1* and *HOXA2* was analyzed in 3 samples of primary eNEPs in P24 and P25, as well as an eNEP line in P6. smNPCs derived following Reinhardt et al. were used for comparison. All genes were normalized to *GAPDH* and *UBC*. (B) Genes of interested e.g. forebrain, midbrain and hindbrain-related genes were selected from microarray analysis and depicted as a fold change between 3 primary eNEP lines, in regard to 3 pluripotent lines.

Patterning along the dorsal-ventral axis

Next, the microarray data was analyzed to define the gene expression profile of eNEPs along the D-V axis (Fig.3.23). No change of expression levels of roof plate-related genes *LMX1A*, *LMX1B* (Chizhikov and Millen, 2004b) and *PAX3* in eNEPs was registered as compared to pluripotent cells (blue set in Fig. 3.23). In contrast, floor plate genes were highly increased in expression. Most prominent, *NKX2.2* was upregulated 2.161-fold but not the related homeodomain gene *NKX2.1*. Moreover, two genes of the *PRDM* family, namely *PRDM4* (1.270-fold) and *PRDM8* (1.755-fold) which are known to be involved in ventral patterning are upregulated (Zannino and Sagerström, 2015). Moreover, genes coding for the proteins Netrin1 (*NTN1*) and F-Spondin (*SPON1*) typically found in the floorplate (Fasano et al., 2010) were higher expressed in eNEPs (1.741 and 2.214-fold, respectively). However, it has to be considered that the p-values were not significant (except *NTN1*, p=0.04) indicating that the fold changes represent a tendency of gene upregulation and need further validation. Taken together, compelling evidence of increased gene expression of floor plate related genes was found which proposes a ventral neural tube patterning of eNEPs.

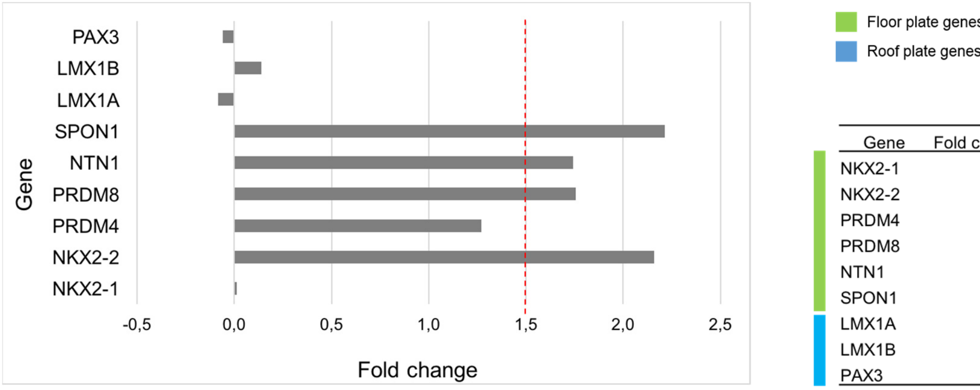

Gene	Fold change	P-value
NKX2-1	0.013	0.90
NKX2-2	2.161	0.09
PRDM4	1.270	0.08
PRDM8	1.755	0.08
NTN1	1.741	0.04
SPON1	2.214	0.18
LMX1A	-0.084	0.62
LMX1B	0.141	0.44
PAX3	-0.060	0.85

Figure 3.23 Expression of D-V related genes. Fold genes of gene expression of eNEPs in CSPFL conditions compared to pluripotent lines assessed by microarray analysis. A strong upregulation of floorplate related genes, especially *NKX2-2*, *PRDM8*, *NTN1* and *SPON1* could be identified, whereas the expression of dorsal genes remained unchanged. Table shows fold changes and distinguish between floor plate/ventral genes (green) and roof plate/ dorsal genes (blue).

3.3.4 Expression of neural plate border (NPB) and neural crest related genes

Next, the expression of genes related to the neural plate border (Fig. 3.24, green panel in table) or the neural crest (marked blue in table) was. The analysis revealed the unchanged (e.g. *ZIC1*, *PAX7*) or downregulated expression (e.g. *ZIC2*, *ZIC3*, *TFAP2A*) of all NPB-related genes compared to pluripotent cells. This applied also to neural crest genes including *SOX9*, *SOX10* and *SNAI1*. This data unravels the identity of eNEPs as non NPB or neural crest without excluding potential acquisition of this phenotype upon responding to external cues.

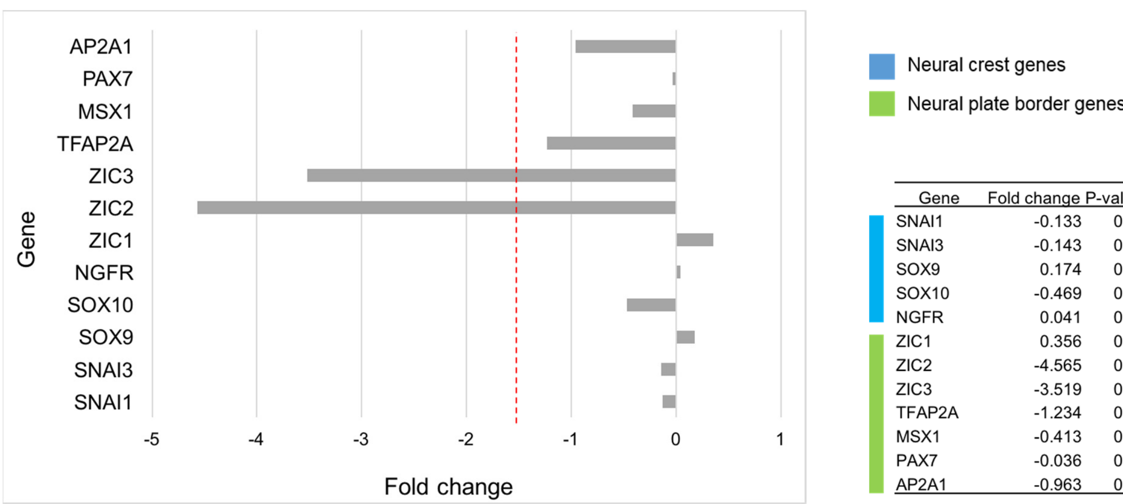

Gene	Fold change	P-value
SNAI1	-0.133	0.24
SNAI3	-0.143	0.53
SOX9	0.174	0.76
SOX10	-0.469	0.18
NGFR	0.041	0.96
ZIC1	0.356	0.21
ZIC2	-4.565	0.06
ZIC3	-3.519	0.04
TFAP2A	-1.234	0.39
MSX1	-0.413	0.90
PAX7	-0.036	0.85
AP2A1	-0.963	0.12

Figure 3.24 Expression of neural plate border and crest genes. Fold genes of gene expression of eNEPs in CSPFL conditions compared to pluripotent lines assessed by microarray analysis. No upregulation of neural crest related genes can be identified suggesting a non-crest identity of eNEPs. Further, examination of neural plate border genes reveals a downregulation of ZIC2 and 3 but no further changes in gene expression compared to pluripotent cells.

3.3.5 Karyotype analysis

In order to assess whether, the isolated cells are of normal karyotype, G-banding of chromosomes during synchronized metaphases was performed. A normal human male chromosome set marked by 23 chromosome pairs including XY chromosomes was identified, showing no aberrations (representative image in Fig. 3.25).

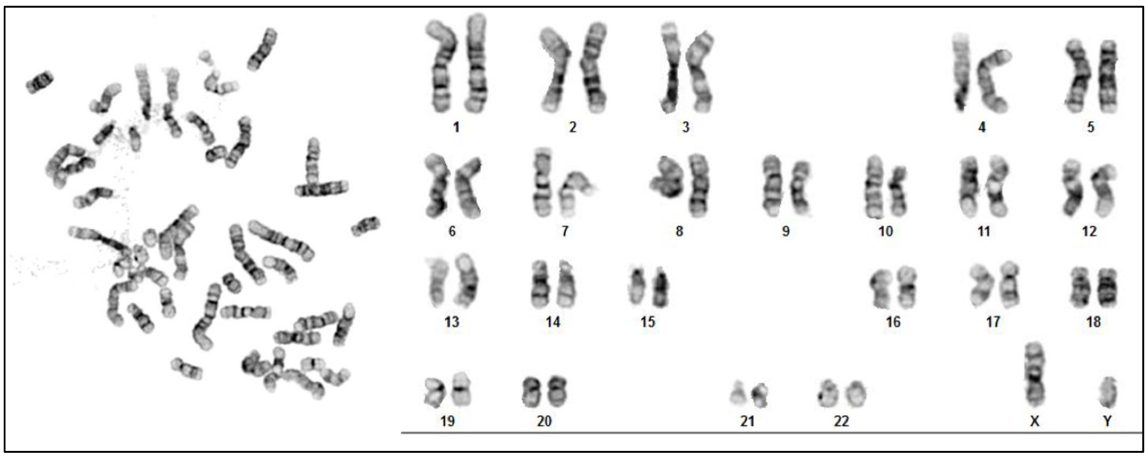

Figure 3.25 Representative karyogram from eNEPs. Karyotype analysis of eNEP clone 3 after monoclonal expansion at passage 27. On the left-hand side, chromosomes synchronized in the metaphase can be identified after Giemsa staining. On the right-hand side, human male karyotype off 22 chromosome pairs and XY-chromosomes can be identified. No aberrations can be identified.

3.3.6 Investigation of differentiation potential in central neural lineages

Early neuroepithelial cells are characterized by their broad differentiation potential into central and peripheral lineages in contrast to more committed rosette-like or radial glia cells which are restricted to central lineages and have been reported to possess gliogenic characteristics. We examined the potential of eNEPs to differentiate into neuronal subtypes and glial cells when undergoing default differentiation for 6-8 weeks on bMG-coated glass (compare 2.2.9) (Fig. 3.26). Initially, the morphologically dense colonies lose their compact shape and result in loose colonies and differentiating cells. Indeed, a high number of TUJ1-positive neurons indicative of a high neurogenic potential was observed (Fig. 3.26 B). Besides, GFAP positive astrocytes were found as well (Fig. 3.26).

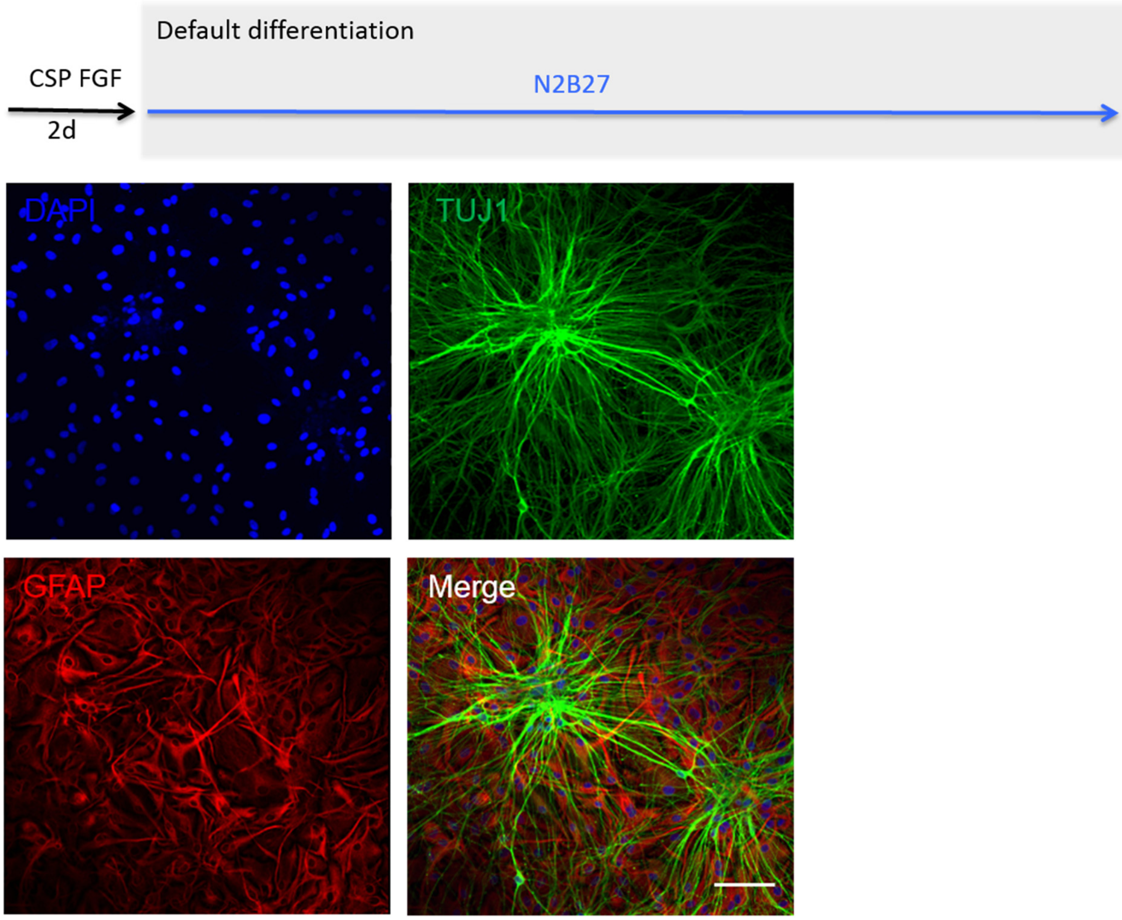

Figure 3.26 Default differentiation of eNEP clone 3 results in neurons and astrocytes. After the deprivation of small molecules and growth factors, cells differentiate in an undirected manner, nuclei were counterstained with DAPI (A) As a result, TUJ1-positive cells indicating neurons can be found (B). Furthermore, astrocytes can be identified using GFAP staining. Scale bar = 100 µm.

Obstacles were faced when adapting terminal oligodendrocyte differentiation protocols to confirm trilineage potential of eNEPs by immunostainings. The differentiation mostly resulted in a highly neuronal culture and staining using an O4-specific antibody were not successful. Thus, ultra-structural analyses were employed to study fine structures such as neuronal synapses, cell organelles and filaments (as reported in 3.3.9). Intriguingly, we found compelling signs of *in vitro* myelination (Fig. 3.27), hallmarked by structures that are termed “myelin swirls” and have been described *in vitro*, consisting of sheets of myelin being wrapped in one another. Notably, unlike *in vivo* myelination which is found surrounding a neuron, it has been reported that oligodendrocytes, but not Schwann cells can contribute to myelin sheets without centrally located neurons (Lauder, 2013). The identification of those putative myelin structures, suggests that oligodendrocytes which are the myelin producing cells of the CNS, are present after 7 weeks of differentiation. In conclusion, putative myelination proposing the potential of eNEPs to be differentiated not only in neurons and astrocytes, but also in a third cell type, namely oligodendrocytes, was observed. This would confirm the tripotent identity of human eNEPs.

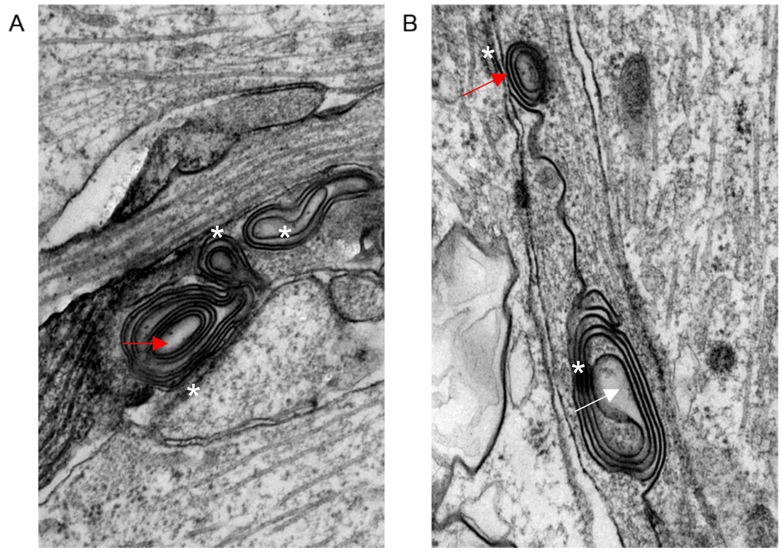

Figure 3.27 Ultra-structural images of putative myelin sheets after 7 weeks of neuronal differentiation. TEM reveals ultra-structures that represent putative myelin structures (white asterisks) in a cross-section view. Such "myelin swirls" can be found repeatedly sur-rounding a putative neuron (indicated by cross-sections of neuro-filaments, indicated by a red arrow) or no neuronal structure (indicated in B by a white arrow).

Characterization of neurons after forced neuronal differentiation

To demonstrate the differentiation ability into diverse neuronal subtypes eNEP-derived neuron-like cells were stained for subtype specific markers after 6 - 8 weeks of neuronal differentiation. In contrast to default differentiation where growth factors and small molecules are deprived, a neuronal differentiation medium (NDM) containing BDNF, GDNF and cAMP was used. As a result, a culture of neurons was obtained (Fig. 3.28 A - C). By adding the Notch signaling inhibitor DAPT during the first two weeks of differentiation neuronal differentiation was promoted as previously described (Borghese et al., 2010). Thereafter, DAPT was omitted and neurons were allowed to mature for a longer period in NDM medium only. This neuronal differentiation results in more than 90% of TUJ1-positive neurons (Fig. 3.28 D) as well as NeuN-positive neurons (Fig. 3.28 E).

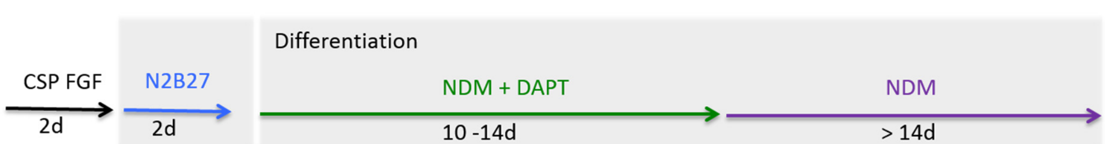

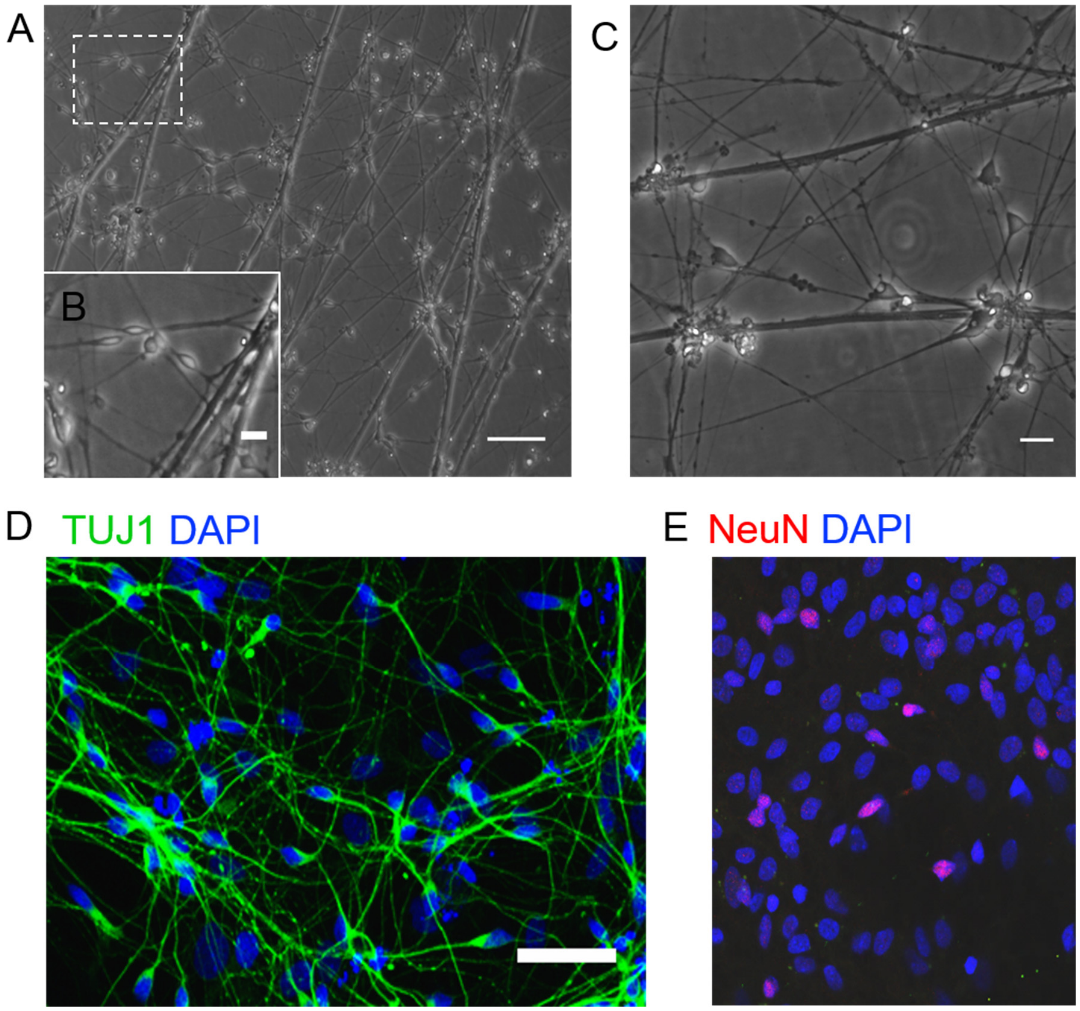

Figure 3.28 Specific neuronal differentiation of eNEP clone 3 leads to a homogeneous neuronal culture. (A) Phase contrast image of specifically differentiated putative neurons on bMG-coated glass slides after 6 weeks shows a pure neuronal network. This is marked by neurites which occur alone or among others in structures reminiscent of neurite bundles. In a higher magnification, (B) soma of putative neurons can be identified. (C) Differentiated neurons in a higher magnification than (A) and lower density facilitate to identify different neuronal outgrowing structures. (D) When stained for the neuronal protein TUJ1, a major proportion of cells appear positive. (E) A proportion of differentiated cells can be confirmed as positive for the neuronal nuclei specific protein (NeuN) which marks maturing neurons. Scale bar in A and D = 100 µm, scale bar in B and C 20 µm.

Identification of neuronal subtypes upon neuronal differentiation

Having confirmed specific neuronal differentiation, it was of interest to assess whether it was possible to distinguish among neuronal subtypes marked by used neurotransmitter characteristics and resulting functional properties. By immunofluorescence stainings of subtype-specific proteins, various neuronal subtypes among TUJ1-positive neurons after 7 weeks of differentiation were identified (Fig. 3.29). To confirm the presence of GABA receptors a specific antibody which recognizes the subtype GABA-A receptor alpha 2 was used (Hevers and Lüddens, 1998) (Fig. 3.29, upper panel). Moreover, GAD 65/67 was used as a marker protein for GABAergic cells as seen in the second panel of Fig. 3.29. Thus, providing evidence for GABA-receptor carrying as well as GABA-producing neurons. Moreover, glutamatergic neurons can be found, marked by positive staining for the vesicular glutamate transporter 1 (vGLUT1, Fig. 3.29, third panel) which is associated with synaptic vesicles and glutamate transport. Furthermore, we can demonstrate the presence of neurons which can be stained for the rate-limiting enzyme in serotonin synthesis namely tryptophan hydroxylase (TPH2, Fig. 3.29, lowest panel). Taken together, we provide evidence that neurons acquire different phenotypes upon differentiation from eNEPs including GABAergic, glutamatergic and serotonergic neurons.

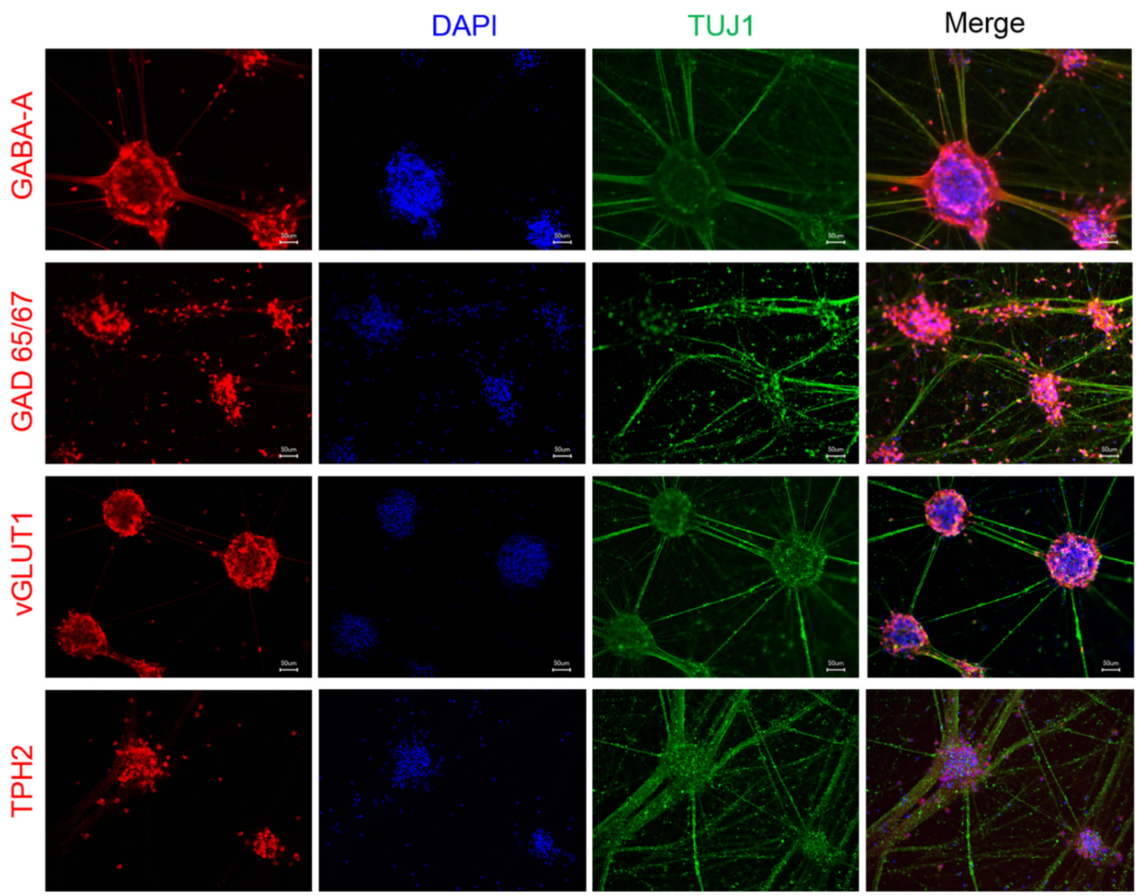

Figure 3.29 Directed neuronal differentiation of eNEPs results in various neuronal subtypes. The identification of neuronal subtypes was addressed by immunofluorescent double stainings using the specific neuronal protein TUJ1 in combination with a subtype-specific marker protein after 7 weeks of differentiation. Among TUJ1 positive fibers, evidence for neurons carrying GABA-A receptors (first panel) as well as GABAergic neurons staining positive for GAD 65/67 (second panel) was found. Additionally, glutamatergic neurons marked by vGLUT1 (third panel) and serotonergic neurons indicated by TPH2-positive neurons can be found. Nuclei are counterstained using DAPI. Scale bars represent 50 µm.

Application of specific differentiation protocols

After demonstrating that eNEPs can be differentiated into various central neuronal subtypes, further efforts were focused on selected subtypes to present a proof of principle result for the generation of specific subtypes. Since the qRT-PCR data suggest a midbrain identity, it can be hypothesized that the differentiation results in some TH positive midbrain neurons. This number might be increased by the application of a directed dopamine neuron differentiation protocol (Fig. 3.30, upper scheme). This protocol promotes more specific midbrain floorplate patterning using PMA and FGF8 and a second step promoting the maturation of neurons, modified from Reinhardt et al. (2013). Indeed, single TH-positive neurons were observed following undirected neuronal differentiation, but a higher number of TH-positive cells following the specialized protocol (Fig. 3.30 B) was found (Fig. 3.30 A). Therefore, proposing the potential of eNEPs to differentiate into TH-positive neurons and respond to patterning clues resulting in an augmented differentiation of TH-positive cells.

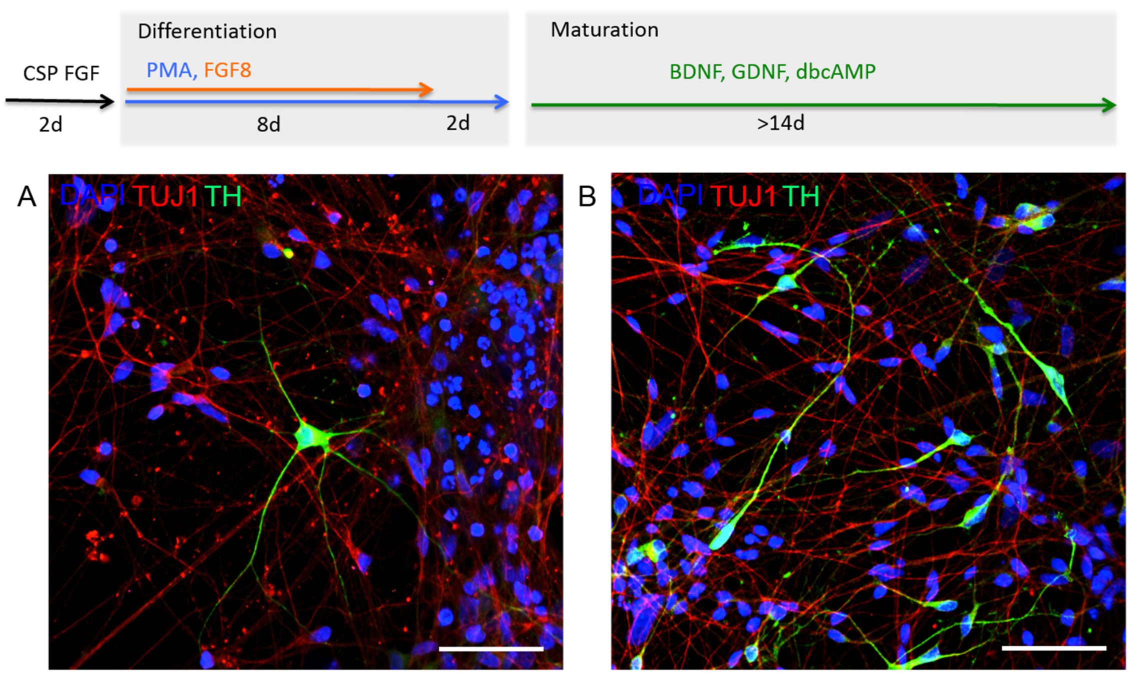

Figure 3.30 Directed ventral midbrain neuronal differentiation of eNEPs yields increased number of TH-positive cells. Neuronal differentiation was compared to directed midbrain dopaminergic differentiation. For the specific protocol, cells were plated and cultured in regular medium for two days until switching to a differentiation medium containing PMA and FGF8 resulting in midbrain patterning of eNEPs. Thereafter, medium conditions were changed to maturation medium and cells were differentiated for at least 14 days. Among TUJ1 positive neurons which we found after neuronal differentiation rare TH positive neurons can be identified (A). When applying a specific protocol, the number of TH-positive cells increased (B). DAPI was used to counterstain

3.3.7 Evaluation of the differentiation capacity into peripheral cell types

Intriguingly, screening for various neuronal markers following default differentiation revealed rare Peripherin-positive cells among TUJ1-positive neurons reaching out from differentiated colonies (Fig. 3.31). Hence, this indicates the presence of neurons in addition to central subtypes and suggests an early origin of eNEPs hallmarked by unrestricted differentiation to peripheral and central lineages. However, it is of high interest whether this is an intrinsic property of eNEPs by showing that one can increase the yield of peripheral neurons can be ameliorated using after optimized differentiation conditions towards neural crest derived cell types. Moreover, further investigation should address whether other neural crest-derived cell types can be generated.

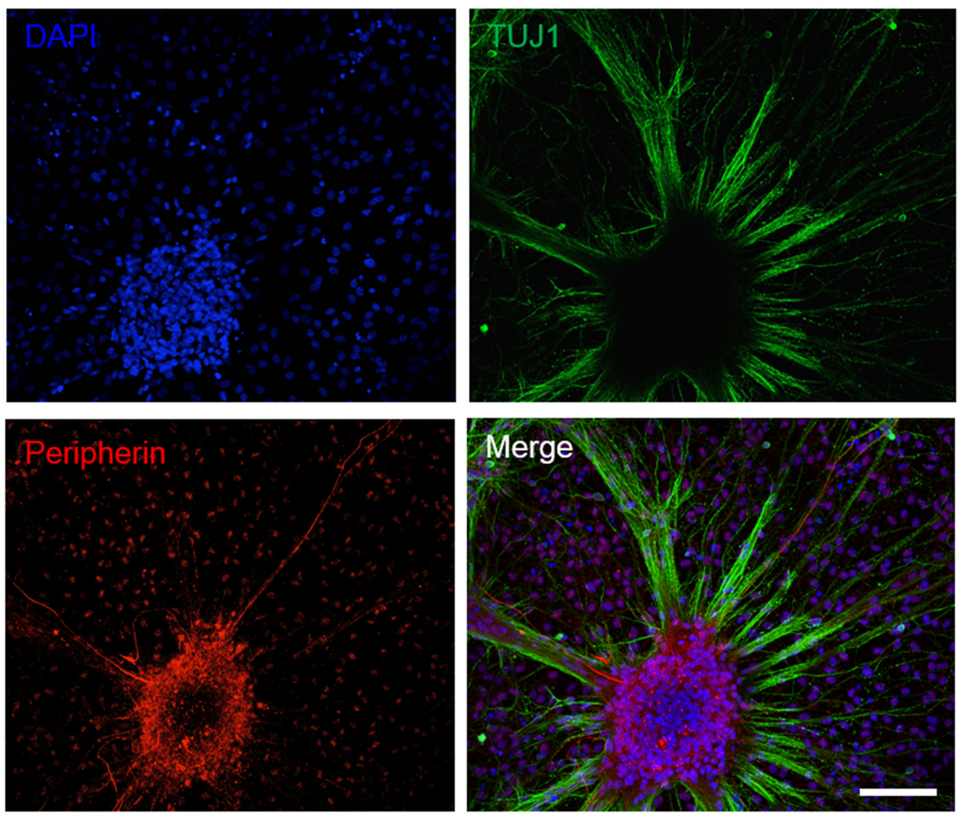

Figure 3.31 Peripheral neurons can be identified after neuronal differentiation. Among TUJ1 positive neurons rare Peripherin-positive outgrowing fibers can be found after neuronal differentiation. Hence, suggesting the potential of eNEPs to give rise to central as well as peripheral neurons. DAPI is used to counterstain nuclei. Scale bar = 100 µm.

Next, it was investigated whether it might be possible to enhance the presence of peripheral cell types by inducing a neural crest cell fate by shortly activating the canonical WNT-pathway using CHIR and subsequent activation of BMP4-signalling for 8 days (Reinhardt et al., 2013). Thereafter, a maturation period of at least 14 days followed. Indeed, the appearance of Peripherin-positive neurons after applying that protocol was increased (Fig. 3.32 A, B). Those neurons possess long and extended neurites. Moreover, their identity was futher investigated by addressing sensory neuron specific proteins using immunostainings. The presence of the voltage-gated Na-channel NAV1.7 (Fig. 3.32 C) as well as the expression of NF-200 (Fig. 3.32 D) marking sensory neurons could be identified. Taken together, these findings suggest that it might be possible to increase the proportion of peripheral neurons by a forced specification protocol. Moreover, resulting neurons were identified as putative sensory neurons.

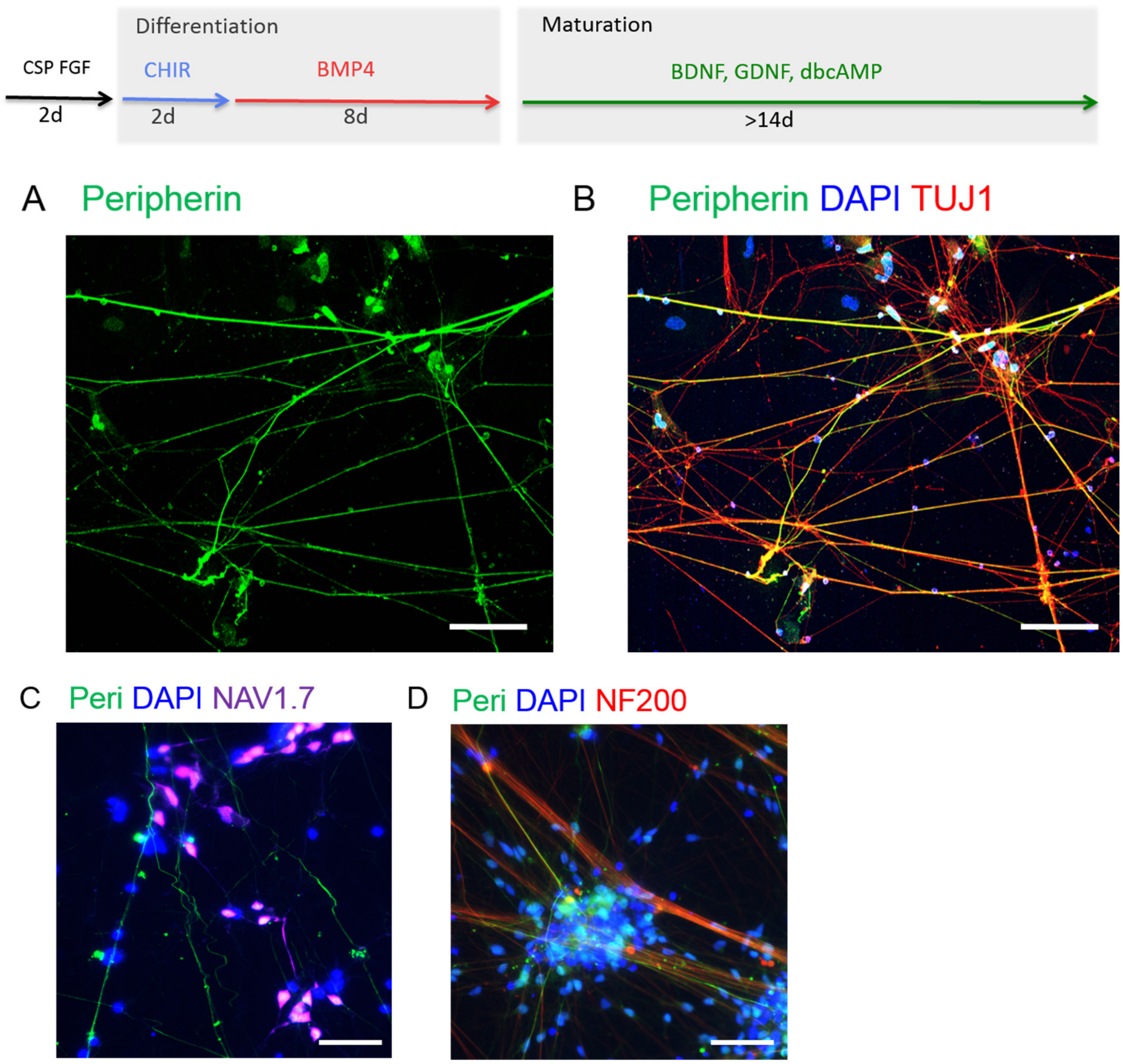

Figure 3.32 Directed peripheral neuron differentiation of eNEPs results in increased differentiation of Peripherin positive cells. Specific differentiation protocol as described in the text leads to an increased number of Peripherin-positive neurons (A). In (B) it can be demonstrated that not all TUJ1- positive fibers are double positive for Peripherin, the number seems higher than indicated in Fig 3.31 after neuronal differentiation. Moreover, NAV1.7 (C) and NF200 (D) positive cells can be determined proposing that sensory neurons occur. DAPI is used to counterstain nuclei. Scale bar in A, B= 100 µm, in C, D = 50 µm.

In order to confirm broad neural crest potential, eNEPs were differentiated in mesenchymal cell types after two days of treatment with CHIR and further differentiation with 10 % FCS containing medium (Fig. 3.33, upper graphic). Following this protocol, a morphological change after a short differentiation time was observed (Fig. 3.33 from A to B). When staining for proteins, we could demonstrate morphologically distinct SMA positive cells indicating the presence of mesenchymal cells among S100β positive glial cells (Fig. 3.33 C).

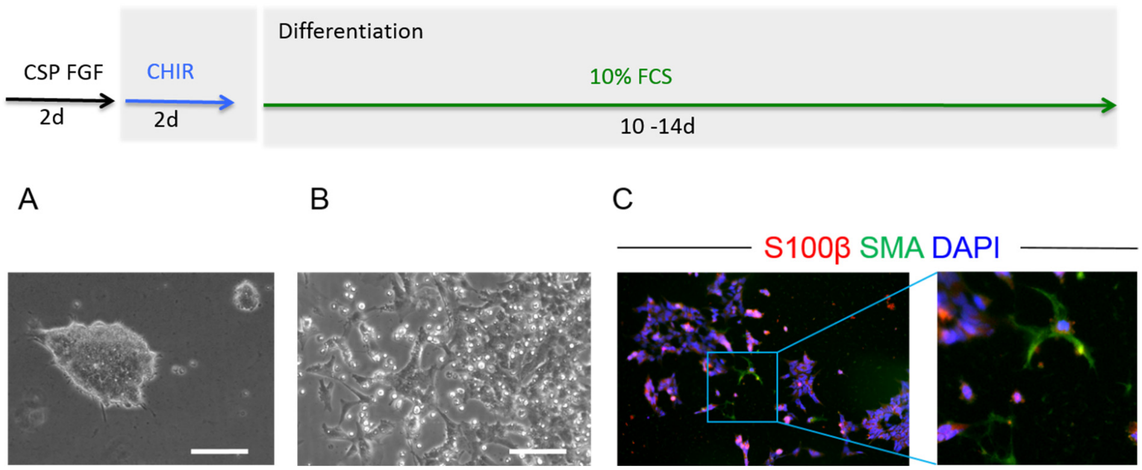

Figure 3.33 Specific differentiation of eNEPs in mesenchymal cells. (A) eNEPs after two days of CHIR-containing medium keeping colony morphology. (B) After applying FCS-containing medium conditions which induce the differentiation of mesenchymal cells, we observed a morphological change hallmarked by losing the densely packed morphology and acquiring a differentiated shape. Scale bar = 100 µm. (C) By immunofluorescent double stainings we identified the presence of SMA-positive cells (green) along with S100β positive glial cells (red). DAPI is used to counterstain nuclei.

Taken together, it was possible to demonstrate that human eNEPs have the potential to give rise to cells of the peripheral lineage including peripheral neurons which can be identified as putative sensory neurons as well as mesenchymal cells. These cell types can be obtained by specific differentiation protocols as proposed by previously published literature. These findings suggest a broad differentiation potential.

3.3.8 Functional characterization of differentiated neurons

Some evidence was provided for the wide differentiation potential of human eNEPs. Next, it was of interest if the resulting neurons were functionally active. Therefore, the homogeneous neurogenic culture of eNEPs after 7 weeks of differentiation as described in 2.2.9 was stained for the pre-synaptic protein Synapsin (Fig. 3.34, A). As a result, a typical punctuate staining pattern could be identified suggesting the presence of the synaptic proteins potentially pointing to functionally active synapses. To verify this, a double immunofluorescence labeling was applied of differentiation which allows to reveal sub-synaptic compartments. Thus, visualizing protein pairs of active zone (Synapsin 1) and the postsynaptic density (PSD-95) and allowing to measure the synaptic cleft (Di Biase et al., 2009). This experimental approach, carried out by Marta Suarez Cubero, confirmed the presence of Synapsin, in close vicinity with PSD-95 after 5 weeks of differentiation (Fig. 34, B) indicative of a functional synapse formation. Following this observation, electrophysiological analysis was conducted in order to assess physiological function of neuron candidate cells after 7 weeks of differentiation (Fig. 3.34, C) in collaboration with Prof. Dr. E. Wischmeyer, Department of Physiology, Würzburg. Voltage patch clamp measurements of single neurons showed inwards and outward currents and the presence of potassium-channels which could be blocked by the selective blocker tetraethylammonium (Fig. 3.34, TEA, middle image)). In addition, spontaneous spiking of neurons could be observed (Fig. 3.34, right image).

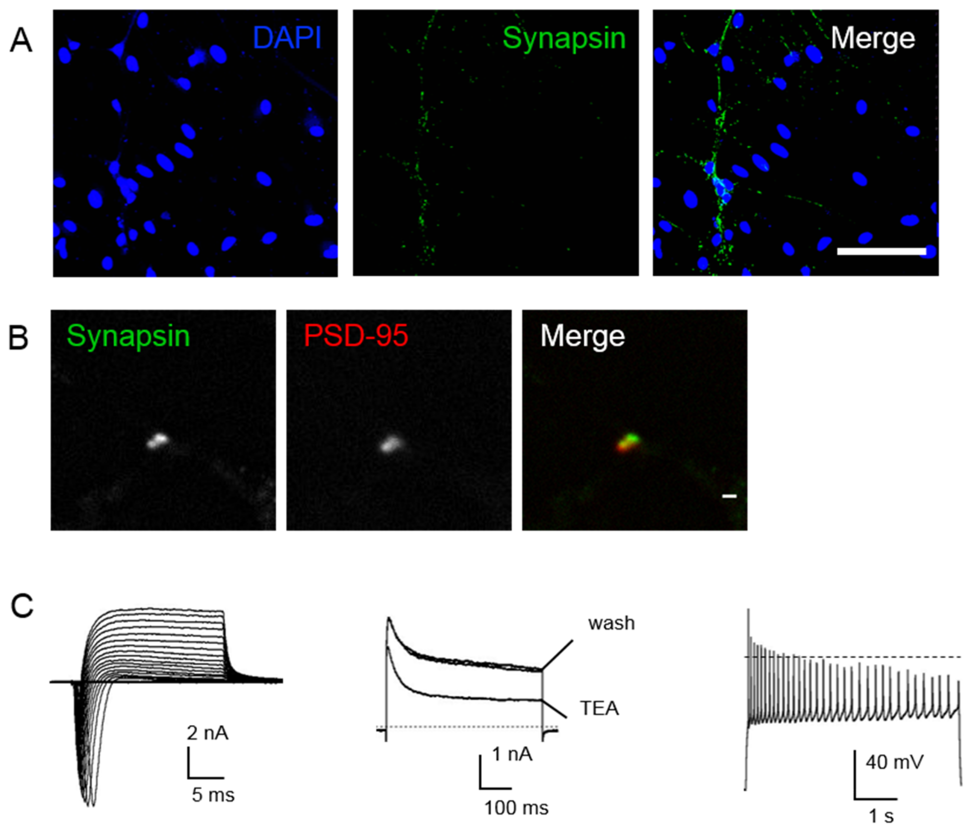

Figure 3.34 Assessment of synapse formation in eNEP-derived neurons. (A) eNEP, clone 3-derived candidate neurons after 7 weeks of differentiation are immunoreactive for the presynaptic protein Synapsin. DAPI is used to counterstain nuclei. Scale bar = 100 µm. (B) High magnification microscopy following 5 weeks of differentiation reveals pre- and postsynaptic proteins indicated by Synapsin and PSD95-staining, respectively, in close vicinity. Scale bar = 1 µm. (C) Voltage patch clamp measurements of differentiated indicate that action potentials can be evoked as visualized by inward and outward currents (left). Further, Potassium-channels which can be blocked specifically by the chemical TEA are present in neurons (middle). Spontaneous firing of neurons hallmarked by spikes was identified using current clamp (right).

To confirm formation of synaptic contacts, the ultrastructures of differentiated neurons were subjected to TEM analysis after 7 weeks of differentiation. Multiple neuronal hallmarks such as neurofilaments and microtubules indicating the presence of neuritis were found. The presence of synapse-like structures has been observed widely (Fig. 3.35). As an indication, contacts between neurites including synaptic densities, synaptic cleft and vesicles were identified. Such synaptic connections are observed between axons as well as between axons and soma. The presence of these structures suggests putative synapses which are developing. Interestingly, in addition to post synaptic densities (PSD), presynaptic electron-dense regions are very prominent, even exceeding the number of PSDs.

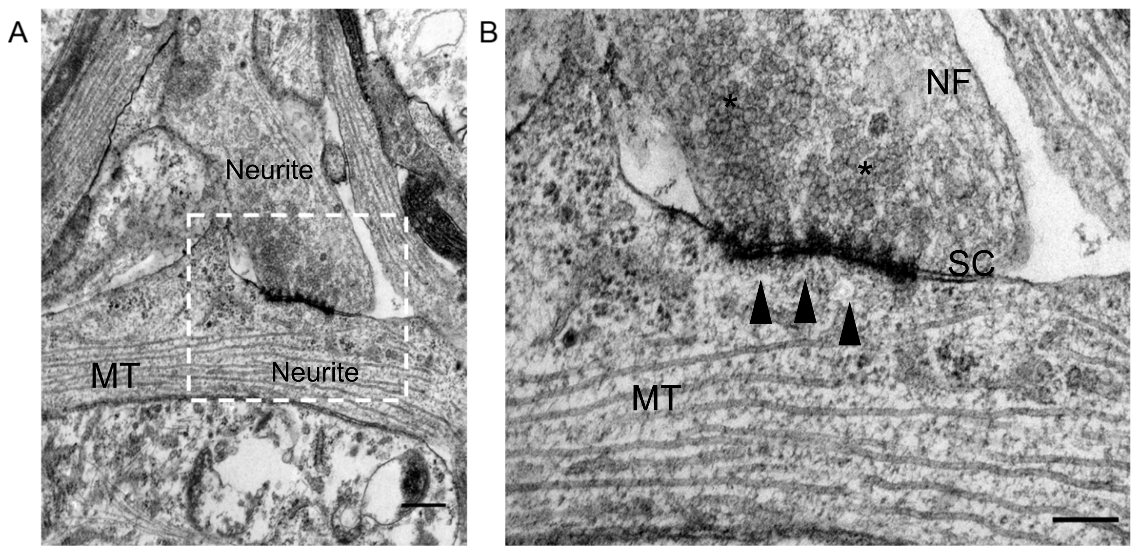

Figure 3.35 TEM images of *in vitro* differentiated neurons reveal the presence synaptic contacts. (A) eNEPs were differentiated for 7 weeks and processed as described in 2.2.13. Neurites can be defined by the presence of microtubule (MT) and putative neuron spine. Neurite-neurite contact can be identified and shows prominent structures. (B) Enlarged view illustrates putative synaptic connections including synaptic cleft (SC) and synaptic density (triangles) which would allow a synaptic transmission. Moreover, synaptic vesicles can be found (marked by asterisks). Scale bar in A = 500 nm, in B = 250 nm.

Overall, the characterization of generated neurons by immunofluorescence stainings of synaptic proteins, electrophysiological and ultrastructural analyses reveals compelling evidence endorsing their functional integrity after differentiation *in vitro*.

3.3.9 Deciphering the signaling network involved in stabilization of eNEPs

We hypothesized that the modulation of relevant pathways would allow us to stabilize a less committed early NPC line which is not dependent on EGF signaling. Since the media is supplemented with a number of growth factors and chemical compounds which specifically act as agonists or antagonists. Pathway-related genes encoding either receptors or downstream signaling factors in comparison with pluripotent cells were analyzed (Fig. 3.36).

As a first approach, two genes coding for FGF-downstream signaling proteins (purple set in table), namely *AKT1* (encoding serine-threonine protein kinase AKT1) and *PIK3C2B* (encoding a phosphoinositide-3-kinase) were analyzed. An upregulation of both genes, suggesting an activation of FGF-signaling was identified. Further, the expression of *NOTCH* was increased (1.623-fold). WNT-signaling (yellow set in Fig. 3.36) is activated by the addition of the GSK3 beta-inhibitor. Hence, just a minimal upregulation of the *WNT3* gene and a minimal downregulation of *GSK3B* gene was seen. However, a higher expression of *FZD3* and *FZD9*, which code for WNT-receptors was observed. As hypothesized before that SHH-signaling is crucial to stabilize eNEPs, it was interesting to find of an increased expression of *PTCH1* encoding for a subunit of the SHH receptor Patched. This might be an indication for active SHH-signaling. LIF/STAT-signaling has been reported to play a role in primitive NPCs but not in human ES-cells. Nevertheless, no differences in gene-expression of LIF-signaling related genes (blue set in 3.36) were seen. Moreover, no upregulation of the *EGFR* gene was detected, supporting our theory of an EGF-independent cell line, equally to pluripotent cells. Having observed cells patterned for ventral midbrain regional identity, the fold-change in the expression of *FGF8*, *FGF9* and *BMP7* (grey set in Fig. 3.36) was analyzed. Indeed, all three genes were higher expressed in eNEPs. In contrary, the BMP4 gene expression was noteworthy decreased in eNEPs. Further, *IGFBP5* and *IGF2R*, encoding protein involved in Insulin-signaling were higher expressed than in pluripotent cells (red set in Fig. 3.36). As expected because of specific inhibition by SB, *TGFB1* gene was decreased in expression.

In conclusion, the microarray analysis of genes involved in FGF and NOTCH signaling showed an increased expression in eNEPs. We could observe no changes in WNT and hLIF/STAT3 signaling relative to pluripotent cells. On the one hand, genes playing a role in insulin signaling were increased in expression, whereas *EGFR* and *BMP4* were decreased. On the other hand, ventral midbrain signaling related genes were increased opposed by an immensely downregulated *TGFB1*. To fully investigate the signaling network, further experiments elucidating the activation of key proteins of FGF, Notch, LIF, WNT and SHH- signaling are necessary

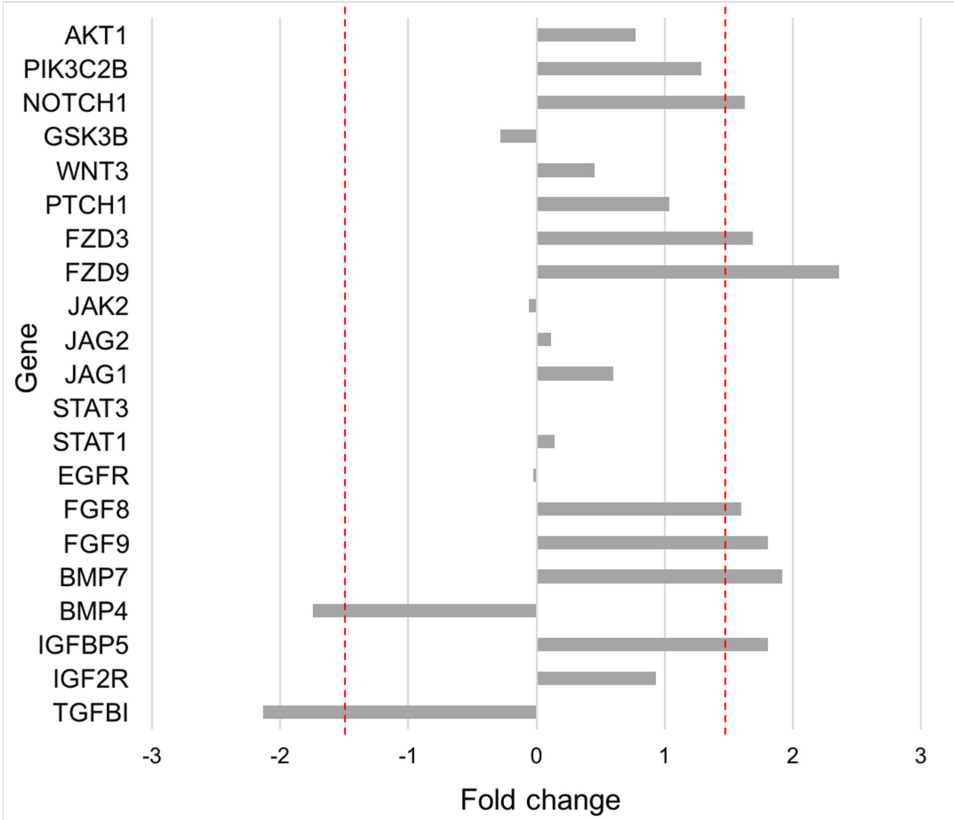

Gene	Fold change	P-value
TGFBI	-2.132	0.26
IGF2R	0.933	0.08
IGFBP5	1.805	0.37
BMP4	-1.743	0.21
BMP7	1.915	0.21
FGF9	1.804	0.18
FGF8	1.600	0.58
EGFR	-0.026	0.95
STAT1	0.144	0.37
STAT3	0.010	0.98
JAK2	-0.059	0.45
JAG1	0.596	0.70
JAG2	0.117	0.70
FZD9	2.361	0.03
FZD3	1.692	0.05
PTCH1	1.035	0.04
WNT3	0.457	0.39
GSK3B	-0.282	0.45
NOTCH1	1.623	0.13
PIK3C2B	1.288	0.05
AKT1	0.770	0.10

Insulin related
Ventral midbrain related
LIF signaling related
SHH related
WNT signaling related
FGF signaling related

Figure 3.36 Gene expression profile of eNEPs under proliferating conditions in CSPFL. Data taken form microarray analysis shows the fold change of gene expression in primary eNEPs in comparison to pluripotent lines. Selected gene cluster being related to specific signaling pathways were highlighted as

3.3.10 Examination of bFGF- and EGF- dependence on the growth of eNEPs

It was sought to investigate the influence of some of the aforementioned signaling pathways involved in the stable proliferation of eNEPs. In the initial steps, two additional growth conditions were examined (see 3.3). Omitting basic FGF on MG (CS medium) it let to loss of cells and reduced proliferation. In contrary, in absence of bFGF but cultured on MEF-feeder which are known to secret bFGF and other factors, we observed high proliferation and colony formation ability. Thus, I hypothesized that bFGF was important to establish a proliferative colony-forming cell population. It was of interest whether it was possible to verify this using specific chemical inhibitors.

The addition of inhibitors was started one day after seeding a defined cell number (time point -24 h) and treatment of cells continued for up to 120 h quantifying the number of cell every 24 h. Cells underwent treatment of solvent, 100 nM FGFi or EGFi, respectively or both at the same time (Fig. 3.37). Interestingly, reduced cell numbers were identified upon treatment with FGFi alone or FGFi/EGFi but no differences using EGFi or DMSO alone. Higher density was observed in culture using phase contrast light microscopy (Fig. 3.37 A) and could be verified by cell number assessment (Fig. 3.37 B). Further, the blocking of FGF-signaling resulted in morphological distinct colonies exhibiting pronounced differentiation hallmarks as observed from 72 h on. In contrast, EGFi-alone treated cells did not show any effect resulting in morphological changes. Distinct morphologies became even more evident after 120 h. While control and EGFi-treated cells continued forming compact, roundly shaped colonies, FGFi-treated colonies were of flat, loosened morphology and included spindle-like cells which remind of beginning differentiation. This preliminary data endorses our findings from the microarray analysis (3.3.10) that eNEPs represent a non-EGF, but bFGF-signaling dependent cell line.

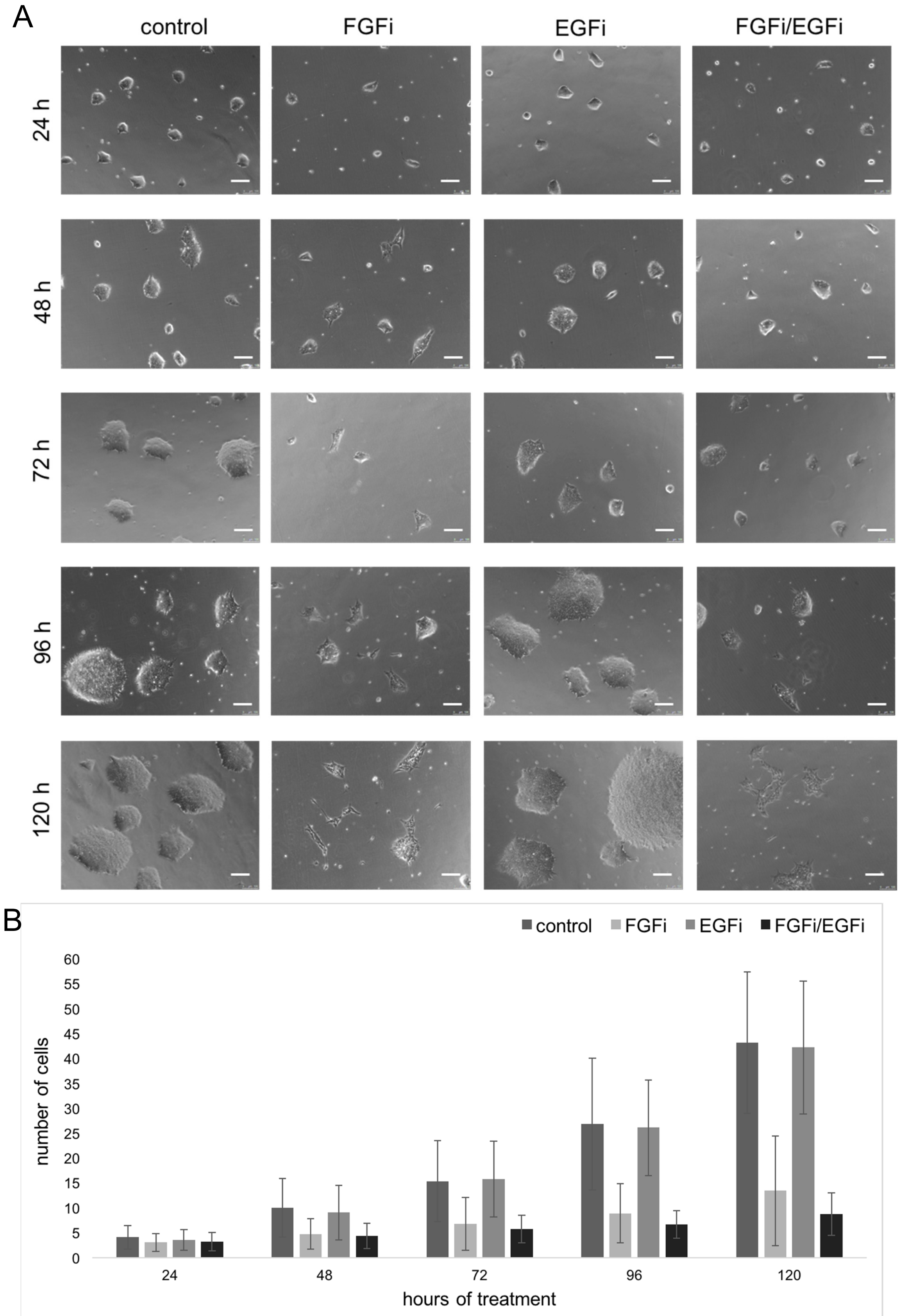
A
control
FGFi
EGFi
FGFi/EGFi
24 h
48 h
72 h
96 h
120 h
B
control
FGFi
EGFi
FGFi/EGFi
number of cells
0
5
10
15
20
25
30
35
40
45
50
55
60
24
48
72
96
120
hours of treatment

Figure 3.37 Morphological analysis of eNEPs after chemical inhibition of FGF and EGF signaling. (A) Phase contrast images of eNEPs cultured at different time points of treatment, including 24, 48, 72, 96 and 120 hours. Cell underwent either vehicle treatment (control) or treatment with 100 nM FGFi or EGFi, as well as both at the same time. Inhibitors were added every 24 h freshly with new media. Scale bars indicate 100 µm. (B) Cell numbers (normalized to starting cell number) at different time points showing control, FGFi- EGFi, and FGFi/EGFi-treated cells (n = 2).

4. Discussion

4.1 mRNA-based reprogramming is preferable to generate transgene-free hiPSCs

To enable the application of either hiPSCs, or progenies such as precursors or differentiated cells in replacement therapy it is indispensable to use integration-free reprogramming. Although many protocols emerged, as reviewed in 1.2.2 and by Schlaeger and colleagues (2015), there is no clear gold standard and in general the ideal method of choice should ve selected carefully based on the individual requirements. Therefore, the adaptation of three different IPS generation protocols was of major interest to provide a broad basis of suitable protocols to reprogram primary adult human dermal fibroblasts into iPSCs in a transgene-free manner. Among these, SeV and modified synthetic mRNA-based delivery which have emerged as promising, DNA-free approaches were used (Bernal, 2013). All three protocols yielded in hiPSCs displaying a pluripotent stem cell marker profile, which was confirmed on protein level using immunofluorescence and flow cytometry. Moreover, the differentiation into cell types of all three germ layers was demonstrated indicating the typical developmental potential of pluripotent cells.

The integration of transgenes remains critical after virus-based reprogramming

The STEMCCA lentivirus has been previously used by our group and establishing a robust protocol for cardiac differentiation from such reprogrammed adult fibroblasts was established (Kadari et al., 2014). During this thesis, a stable healthy control line using foreskin-derived fibroblasts was generated. This line is utilized for different so far unpublished studies and has been stably expanded in 2D adherent and 3D suspension culture (Kwok et al., in revision). Moreover, efficient differentiation into cardiovascular and neural lineages could be demonstrated (Kwok et al., in revision, Nose et al., in preparation). However, lentiviral reprogramming highly depends on the quality of the lentivirus production, which varies form batch to batch and ideally needs to be carefully evaluated for every experiment. Although, the reprogramming procedure is robustly reproducibe, a laborious additional cre-excision using either transducible cre-protein or transfected synthetic mRNA and a clonal validation step is required in order to obtain transgene-free hiPSCs.

A second virus-based protocol implicates the use of SeV, which is commercially available and can be used in a highly reproducible manner. The SeV reprogramming method could be successfully adapted to control fibroblast from foreskin samples and human dermal fibroblasts from healthy and diseased donors. The protocol could be robustly applied with first colonies emerging as early as day 12 yielding in bona fide hiPSCs. However, remaining SeV and c-Myc viral RNA was observed up to passage 25 which we were not able to completely eliminate in every cell line using suggested strategies which include a temperature shift to 39 °C (Ban et al., 2011). This outcome limits the value of SeV-reprogrammed lines for some applications and creates a need for a close monitoring of remaining viral RNA sequences representing a time-intensive and laborious procedure.

Virus-free reprogramming is feasible for the generation of zero-footprint-iPSCs, but needs further refinement

Due to aforementioned hurdles, a non-viral gene delivery strategy was explored. It is based on 12 consecutive daily transfections of a synthetic mRNA mixture, which includes the four Yamanaka factors as well as Nanog, Lin28 and eGFP. Initial trials demonstrated that the plating density and the addition of B18R plays a major role (Warren et al., 2010). Moreover, a changed morphology and decreased proliferation during the adaptation for at least one passage to Repro-Brew medium was observed. The application of the protocol provided by the manufacturer seems to be not fully suitable in our hands and needed to be optimized resulting in the introduction of several changes to the protocol. First, a relatively high seeding density (20,000 per 24-well) was beneficial even using control foreskin-derived fibroblasts. Second, colony formation did not occur as noted on day 14, but required passaging of cells and replating on a MEF-feeder layer. However, even if the slightly modified protocol was applied to patient-derived cells and despite a high transfection efficiency, difficulties to induce pluripotency was apparent. This was particularly the case in sporadic PD patient-derived cells as well as adult fibroblasts of passage number higher than 7, which were showed declined proliferation and considerable signs of senescence. In contrast, the reprograming of these cells using SeV robustly resulted in iPSCs. This indicates that mRNA-based gene delivery highly depends on the quality, proliferative capacity and passage number of the starting fibroblast preparation and needs to be adjusted for every line individually (Hausburg et al., 2015). Due to daily transfection over a longer period, cells are subjected to cellular stress responses, which leads to increased cell death following multiple transfections. As a consequence, modified protocols which would reduce the hands-on time of transfection or enhance reprogramming outcome e.g. the additional delivery of microRNAs (Lee et al., 2016) have to be examined to improve the robustness of the method. As analyzed by Schlaeger and colleagues, the combination of mRNAs and miRNAs led to a higher reprogramming success than mRNA alone, but needs a prolonged hands-on time than other methods (Schlaeger et al., 2015).

The resulting lines could be utilized as reference lines in further studies. For instance, our group used the cell line reprogrammed by STEMCCA to demonstrate how hiPSCs can be efficiently expanded using stirred suspension culture (Kwok et al, unpublished). Interestingly, it was found that mRNA-IPS failed in our hands thus far to stably maintain proliferating aggregates in suspension resulting in fallen apart cell debris. Similar difficulties were faced when conducting the three-germ layer assay. Hence, indicating some limitations to the use of the reprogrammed lines due to reasons that have to be clarified. However, reprogramming using the mRNA technique allows a GMP-compliant and xeno-free derivation of patient-specific hiPSCs (Durruthy and Sebastiano, 2015). Furthermore, it could facilitate disease modeling using subsequent gene editing via Cas9 and guiding mRNA (Kehler et al., 2016). Therefore, we suggest to use the mRNA-reprogrammed lines for further experiments as the definitely lack integration of transgenes and viral components. Hence, representing the safer reprogramming method tested. In other words, the observations made during this thesis indicate that mRNA-based reprogramming needs further refinement, but represents a promising gene-delivery method to induce pluripotency and is highly feasible for applications that require GMP settings or high safety levels.

Although further investigations involving more IPS cell lines need to be carried out, the findings of this thesis enable an experimental basis to allow the selection an appropriate integration-free and efficient reprogramming method for patient-derived fibroblasts. The resulting hiPSCs from diseased adult fibroblasts can be used to analyze their progenies such as NPCs and neurons in comparison to healthy controls. Consistent with a recent comparative meta-study (Schlaeger et al., 2015), comparably lower success rates using the mRNA-based technique were identified while the success rate using SeV and STEMCCA virus was very high and robustly yielded hiPSCs. Further analyses revealed a slightly increased aneuploidy rate when using SeV and lentiviral constructs suggesting that mRNA-reprogramming is preferable in this regard (Schlaeger et al., 2015). Thus far, chromosomal numeric aberrations only in lentivirus-derived iPSC-lines were addressed in our group. Therefore, more detailed analyses concerning chromosomal stability as well as copy number variations of the generated cell lines is in progress with cooperation partners. This will allow a comprehensive comparison of the reprogramming methods with regards to genomic stability and epigenetic marker profiles.

Further adjustments of the reprogramming protocols elaborated in this study should move into the direction of feeder-free reprograming and cultivation. Hence, the effects of omitting MEF-feeders were tested and resulted in successful reprogramming. However, a rapid and more efficient reprogramming with replating on MEF-feeders was observed. In order to increase the efficiency without the use of feeder cells, the supplementation of reprogramming media conditions with additional chemical enhancers besides AA represents a promising approach. Based on previous reports (Esteban et al., 2010), the composition of the reprogramming media was modified by the addition of the Vitamin C derivate AA which serves as an antioxidant and allows a more efficient reprogramming. Further modifications to increase the efficiency could include supplementing the reprogramming media with chemical compounds facilitating the access to chromatin by TFs. For instance, the use of the histone deacetylase inhibitors valproic acid and sodium butyrate (Cantone and Fisher, 2013) or more recently reported Gadd45a, which helps to relax the chromatin structure (Chen et al., 2016) could help to enhance the efficiency. However, unwanted side effects of small molecules need to be carefully evaluated as these might influence the quality of iPSCs with regard to genomic stability and epigenetic signatures. Alternatively, the use of hypoxic culture conditions (<5 %) instead of atmospheric oxygen concentration enhances reprogramming efficiency (Yoshida et al., 2009). Changing culture conditions accordingly might improve reprogramming efficiency. and in parallel suppress the induction of differentiation without avoiding the use of additional chemical compounds.

4.2 The establishment of a rapid monolayer protocol allows to derive FGF/EGF-dependent NPCs from hiPSCs in two steps

The use of hiPSC progenies contributes immensely to the discovery of novel therapeutic compounds for the treatment of neurological, neurodegenerative and psychiatric diseases (Mertens et al., 2016). However, the scale of high throughput approaches requires robust neural induction and differentiation protocols free of cost-intense ingredients or cumbersome manual picking and selection steps. In recent times, various novel NPC differentiation protocols emerged, however many are time intensive and may not be suitable for biomedical applications. Interestingly, it has been suggested that monolayer protocols and suspension protocols passing the EB stage lead to regionally distinct neural progenitors (Chi et al., 2016b). Therefore it might be beneficial for some purposes to give preference to a rapid monolayer protocol instead of more time consuming and less straight forward EB based protocols which often depend on careful manual rosette picking and selection (Chambers et al., 2009; Koch et al., 2009). Interestingly, major differences upon protocol selection has been also reported between rosette and floorplate based protocols as demonstrated in a recent study analyzing midbrain dopaminergic neurons from different protocols (Chung et al., 2016). Thus, suggesting that protocol selection is a crucial step. For instance, if you aim to yield glial cells, early primitive precursors may not be the best choice since later stages such as rosette or radial glia-like cells have been demonstrated to be more gliogenic (X Qian et al., 2000).

Based on this assumption, a rapid, straight forward monolayer differentiation protocol using hiPSCs which requires two steps was established in this thesis. During the first step, an adherent neural induction protocol is applied as reported by Yan and colleagues (2013) resulting in SOX1, SOX2, Nestin and PAX6-positive primitive NPCs. A stably proliferating and homogeneous cell line can be obtained after 3-5 rounds of passaging. From this point on, it is possible to preserve the cells by cryoconservation and subsequently differentiate in neuronal or glial cell types. On the downside however, the media composition of the induction medium remains undisclosed, which does not allow to modify and optimize culture conditions. Furthermore, although pNPCs are feasible for efficient neuronal differentiation, the outcome of glial differentiation was not fully convincing represented by a low percentage of GFAP-positive astrocytes (data not shown). In order to overcome these hurdles, the pNPC-line was subjected to well defined, commonly used FGF/EGF conditions as described e.g. by Koch and colleagues (2009). As a consequence, a transformed morphology displaying rosette-like cell clusters, which were distinct from pNPCs was detected. Moreover, these cells remained proliferating on PO/Ln, cryo-preservable and showed a reasonable NPC marker profile (Günther et al., 2016). In contrast to pNPCs enhanced differentiation towards astrocytes was identified. This suggests, that the second stabilized FGF/EGF state holds a higher gliogenic potential (Li et al., 2011; Xueming Qian et al., 2000). By yielding two subsequently differentiated NPCs lines from the same hiPSCs line a time-saving approach allowing to generate two self-renewing neural precursor populations from the same parental line according to the desired differentiation outcome can be proposed. While the pNPCs can be utilized for high yield neurogenic differentiation, FGF/EGF-dependent rosette-like cells might be useful to obtain astrocytes as demonstrated in a model of the blood brain barrier (Appelt-Menzel et al., in revision).

Since only basic analyses of the FGF/EGF line was carried out, it would be important to examine gene expression of this cell population in more detail and adapt further specific protocols for terminal differentiation to fully determine their developmental capacity. In order to generate oligodendrocytes, a cell type which is affected in diseases like Multiple Sclerosis, the adaptation of a recent published protocol (Gorris et al., 2015) which implicates a glial precursor step would be of interest. Furthermore, it would be desirable to adapt our protocol to GMP conditions as it could serve as a rapid, straight forward protocol which is easily adapted and could be used for many biomedical applications. Overall, evidence for a rapid strategy to obtain rosette-like NPCs using a monolayer differentiation protocol was provided. This was achieved by the application of a previously published protocol to obtain pNPCs and a subsequent adaptation to defined media conditions containing bFGF, EGF and CHIR. The presented protocol enables the rapid derivation of highly proliferative FGF/EGF-dependent NPCs useful in particularly for glial differentiation.

4.3 The generation of NPCs-line from primary tissue with a monoclonal expansion and wide differentiation potential

In the third and major part of this thesis, the derivation of a stably proliferating human neuroepithelial cell line from primary brain tissue is presented. The main aim was to assess whether it is possible generate an early human NPCs line from fetal brain tissue by selective media conditions. Indeed, a highly proliferative neural precursor line which we could expand monoclonally and characterize regarding marker expression, differentiation potential, regional identity and gene regulatory network was isolated and will be discussed in the following.

As reviewed in the introduction part 1.5.1, the generation of primary non-immortalized neural lines either as adherent monolayer or suspension neurosphere culture has been established using cell culture media supplemented with bFGF and EGF. More recent, also rosette like NPCs could be derived from fetal material of younger origin (Tailor et al., 2013) being of hindbrain identity. Recently, a report describes a stably midbrain patterned NPC line which can be compared with the immortalized Lund human mesencephalic line (Lotharius et al., 2002; Moon et al., 2016). However, culturing conditions have not been further modified in contrast to constantly evolving novel iPSC-based protocols. Here, the isolation and stabilization of primary neural progenitors using a media composition that has not been reported before was shown. Importantly, the cell line shows high and sustained proliferative activity tough it does not require immortalization. Moreover, an additional main difference in comparison to previously published primary NPCs becomes obvious upon the investigation of the differentiation potential to central and peripheral lineages. Moreover, the cellular and colony morphology is distinct from previously published adherent primary lines. However, the derived cell line exhibits pronounced similarities in relation to primitive and NEPs derived from pluripotent lines as described in several well established and reproducible protocols (Li et al., 2011, Reinhardt et al., 2013). The doubling time of approximately 33 h suggests a fast-growing cell line, which can be expanded for more than 40 passages retaining its proliferative state. This doubling time is slightly longer compared to previously published NPC-lines (Reinhardt et al., 2013) which is reported to divide once a day. Further, it was identified that the cells can be passaged using high splitting ratios of more than 1:30. Besides the splitting ratio, the resulting compact, sharply edged colonies resemble the mentioned smNPCs line derived from pluripotent cells (Reinhardt et al., 2013) as well as the primitive NPCs line obtained by direct conversion of fibroblasts by Miura and colleagues (Miura et al., 2015).

By analyzing the global gene expression profile using microarray analysis a clearly distinct gene expression profile compared to pluripotent stem cells could be identified. Intriguingly, also differences in gene expression upon the cultivation in either CAP medium or the more comprehensively analyzed medium CSPFL were identified, which points to specific medium composition dependent alterations. It would be of great future interest to examine in detail which genes are targeted upon distinct culturing. However, our further interpretation in this thesis focused on clones cultivated only CSPFL conditions on MG. Notably, comparing the gene profile of the three different CSPFL clones from two preparations reveals interclonal differences which might propose that resulting preparations can maintain features related to primary material despite chemical manipulation. In this regard, it remains to be elucidated how strong the patterning effects of CSPFL are.

The monoclonally isolated and CSPFL-conditioned population was positive for commonly used neural markers such as PAX6, Nestin, BRN2 and CD133. Notably, a strong signal of SOX1 and SOX2 on mRNA and protein level, as previously found in many NPC lines, could be demonstrated. Intriguingly, an upregulation of SOX11 mRNA in NPC clones compared to pluripotent cells using microarray were identified. SOX11 has been reported to be involved in neural lineage development and can be found as a marker in recent iNPCs protocols (Cairns et al., 2016). It has been described to interact with the BAF-PAX6 complex and result in a severe developmental disorder termed Coffin-Siris syndrome when mutated (Tsurusaki et al., 2014). Furthermore, we found an augmented HES5 expression in comparison to pluripotent cells which confirms the neural identity of the primary line (Elkabetz et al., 2008). Moreover, it has been suggested that ESC-derived, HES5-positive neural precursors ontogeny can be analyzed isolating consecutively Notch signaling active cell lines following neural induction. The presented observations point out differences in marker expression and signaling allowing to distinguish between neuroepithelial, early, mid as well as late radial glia and long-term NPCs. Intriguingly, Edri and colleagues exposed a stage-specific co-expression of SOX1, PAX6 along with Nestin and SOX2 found in non-polarized HES5-positive progenies. This transient stage could be identified early after neural induction by SHH and FGF8 possibly marking establishment of the earliest neuroepithelial cells (Edri et al., 2015). Accordingly, the primary NPC line presented in this study shows expression of aforementioned marker proteins, NOTCH and HES5 activation in combination with non-polarized morphology, endorsing the assumption of an neuroepithelial cell line. Hence, the cell line is referred to as human eNEPs.

The effect of different growth conditions has been described, but it remains yet to be shown how the coating of tissue culture vessels can contribute to the stabilization of cell populations. bMG can be utilized as a coating substrate providing a protein matrix resembling the extracellular matrix. On the downside, protein concentrations may underlie batch to batch variations and cannot be regarded as GMP-conform. As a consequence, an alternative coating substrate like fibronectin or recombinant laminin 111 (Kirkeby et al., 2016) would be a more cost intensive, but potential appropriate coating whose feasibility should be testified in our system. Additionally, it must be elucidated to which extent commercial supplements can be omitted in order to achieve a defined media composition, which is not depending on N2 or B27 supplement. Both additives were shown to be used in concentrations reduced by 50 % (Reinhardt et al., 2013) and B27 has been omitted in some protocols (Kirkeby et al., 2016) as some of the ingredients are redundantly included.

4.3.1 eNEPs show ventral midbrain-hindbrain identity and can be patterned to neural tube and neural crest derivatives upon exposure to regional-specific cues

Since stem cells are exposed to media conditions which modulate signaling pathways and provide patterning cues it is important to examine the cellular identity corresponding to disitinct regions of the developing brain. Using microarray analysis and qRT-PCR, an upregulation of the midbrain genes *EN2* as well as a strong upregulation of hindbrain-related *HOX*-genes was found. Intriguingly, the expression of *HOXA2* by late passage eNEPs was higher than *EN1*-expression, whereas early passage eNEPs showed a higher expression of *EN1* than *HOXA2*. These findings suggest that eNEPs are either a mixed population of midbrain and hindbrain patterned cells or represent a cell population on the border of mid- and hindbrain. Furthermore, *IRX3* expression was increased which confers the ability to express *EN2* and *NKX6.1* in response to FGF8 and SHH, respectively (Fasano et al., 2010; Kobayashi et al., 2002). To fully understand which genomic cell profile is expressed, it is crucial to deepen the understanding of single cell gene profiles during self-renewal and after specification into distinct cell types. For instance, a recent study carried out fate mapping with human ESC-derived neural progenies on single cell level and identified crucial events resulting in lineage bifurcation (Yao et al., 2016). Recent reports suggest that SOX2 serves as a key regulator for a stem cell pool at the midbrain-hindbrain boundary in chick neural development (Peretz et al., 2016). Further evidence points to differences regarding the differentiation of dopaminergic neurons influenced by the rostral or caudal midbrain fate and correlating distinct gene-expression profiles of the starting precursors identified by RNA-sequencing of 30 NPC batches. As a consequence, progenitors of caudal midbrain fate could be identified as the population yielding in high dopaminergic integration upon transplantation (Kirkeby et al., 2016). Thus, the assumption of midbrain-hindbrain origin or a mixed population of midbrain and hindbrain patterned identity of primary eNEPs could point to a cell line with a high differentiation capacity into dopaminergic and serotonergic neurons. Further marker protein assessment of resulting neurons after default neuronal and directed dopaminergic as well as analysis of transplantation outcomes could help to elucidate if the differentiation potential could be confirmed in *vivo*. Moreover, previously published studies reported that some pluripotent-derived NPC lines might undergo a regional shift with increasing passage number (Koch et al., 2009). This has been as well implicated for primary lines, but nevertheless, regionally stable primary lines have been proposed. Those lines exhibit and retain either mesencephalic or hindbrain identity (Moon et al., 2016; Tailor et al., 2013). In this study, a decrease of *EN1* and an increase of *HOXA2* expression with passage number was observed possibly indicating a shift towards the hindbrain identity with growing passages. However, it should be determined whether we can exclude more pronounced caudalization effects along with increasing passage number.

Interestingly, it was detected that floor plate marker genes were redundantly expressed by primary eNEPs including *SPON1*, *NETRIN1*, *PRDM8* and *NKX2.2*. It is known that SHH and Netrin1 signaling is involved in the regulation of the floor plate organization. Therefore, since PMA is applied in order to induce SHH signaling it is somewhat expected that floor plate development is enhanced because SHH is known to repress dorsal genes and is used for directed floor plate induction (Chi et al., 2016a; Fasano et al., 2010; Kutejova et al., 2016). Some additional genes that were upregulated in primary eNEPs were proposed to regulate the floorplate fate. Moreover, an increased gene expression of *PRDM8*, which has been proposed to play a significant role in concerted process of the dorso-ventral patterning was identified (Zannino and Sagerström, 2015).

In contrast to many previously published evidence, no augmented expression of the marker genes *LMX1A* and *B* in undifferentiated primary eNEPs was identified. These genes have essential functions in the development of floor and roof plate and are in particular important for the differentiation of midbrain dopaminergic neurons (Yan et al., 2011). Instead, an increased expression of *ASCL1* (also referred to as MASH1) in comparison with pluripotent cells was unraveled. Notably, MASH1 secreted from the floor plate has been proposed to suppress the expression of LMX1B in chick caudal roof plate (Chizhikov and Millen, 2004b). However, it is crucial to further investigate if the LMX1A and B will be upregulated with beginning targeted dopaminergic differentiation. Moreover, the efficiency might be enhanced by the addition of BMP7, Pramipexol and other growth factors as recently reported using forebrain derived NPCs (Yang et al., 2016).

As a next step, the potential of primary eNEPs to differentiate into cells of PNS or mesenchymal origin was investigated. Although any upregulation of neural plate border or neural crest related genes could not be detected in the undifferentiated cell line, primary eNEPs have the ability to differentiate into peripheral neurons and mesenchymal cells. Therefore, one can assume that besides yielding neural tube derivate, eNEPs response to patterning cues towards the neural crest lineage after providing appropriate molecular cues which include the activation of BMP4 and WNT signaling (Patthey et al., 2008). Intriguingly, a downregulation of ZIC2 and 3 was revealed. Besides, neural crest border functions, these genes have been additionally suggested to be involved in the pluripotency regulation and posing inhibitory action on WNT signaling. Therefore, the downregulation in eNEPs is consistent with the absence of pluripotency and active WNT signaling. To exclude the possibility that the wide differentiation capacity was caused by having a mixed population of cells committed to either neural tube or neural crest lineages, we isolated several monoclonal lines. Taken together, a number of efficient protocols emerged to derive neural crest cells from ESCs and iPSCs without stabilizing a precursor state (Lee et al., 2007; Menendez et al., 2013). However, some of the NPCs obtained through direct conversion and from differentiation from pluripotent cells are able to give rise to central and peripheral lineages upon forced differentiation demonstrating a strong fate plasticity (Cairns et al., 2016; Elkabetz et al., 2008; Lee et al., 2015; Reinhardt et al., 2013). Similarly, we suggest a highly plastic primary neural progenitor line capable of PNS and CNS differentiation.

4.3.2 eNEPs possess neuro- and gliogenic potential and can be differentiated specifically into functional central and peripheral lineages

Having demonstrated the potential of eNEPs to differentiate in central and peripheral neurons the capacity to yield glial lineages was confirmed. In accordance to evidence from the literature, resulting neurons were TUJ1 and NeuN positive and were of heterogeneous subtype identity marked by specific protein expression. The presence of TUJ1 positive neuronal outgrowths was found as early as on day 7 (data not shown), but the differentiation was routinely continued for 4 to 8 weeks to allow further maturation.

Moreover, primary eNEPs are suggested to respond to patterning cues allowing a directed differentiation into specific subtypes. For dopaminergic neuronal differentiation FGF8 has been reported indispensable and is used in the protocol of targeted differentiation of eNEPs (Lim et al., 2015). However, recent findings unravel that current protocols may not exclusively yield midbrain dopaminergic neurons but in parallel subthalamic neurons (Kee et al., 2016). Accordingly, a novel specific protocol has been published that yields non-diencephalic, midbrain dopaminergic neurons of high purity achieved by a time dependent exposure to FGF8b (Kirkeby et al., 2016). It has been implicated that reduced oxygen (3 %), representing the physiological concentration, resulted in augmented dopaminergic differentiation of fetal NPCs in comparison to atmospheric oxygen levels of 20 % (Krabbe et al., 2014). This recent finding could contribute to further improvement of differentiation efficiency.

Given the heterogeneity of neuronal subtypes that can be found in the physiological brain it is of major interest to further investigate which subtypes can be differentiated specifically from primary eNEPs *in vitro*. Some indication has been found that eNEPs might be able to respond to patterning cues and subsequently differentiate to specific subtypes. Hence, the potential to specifically differentiate in medium spiny neurons, motoneurons or serotonergic neurons, which would be of great biomedical interest, has to be disclosed. This can be achieved by the adaptation of recently published protocols although those were developed for the differentiation from pluripotent cells. For motoneuron differentiation, SHH and RA patterning is widely used to achieve HB9 and ISL1 positive subtypes (Shimojo et al., 2015). In case of for serotonergic neurons which can be found physiologically in the raphe nuclei and play a significant role in many psychiatric diseases, a protocol which involves a patterning step to midbrain-hindbrain organizer fate could be pursued. For this purpose, increased concentrations of FGF8 and SHH proteins in combination with WNT-activation can be applied followed by the differentiation to TPH2 positive neurons (Lu et al., 2016; Vadodaria et al., 2016).

It is however, important not only to focus on diverse differentiation capacities but also to obtain functional neurons. Although initial electrophysiological analyses in this study provided some evidence for functionally active neurons which can generate action potentials, fire spontaneously and display K^+-currents, further analyses of neuronal activity are desirable. This can be achieved by more detailed electrophysiological examination using a panel of inhibitors or Calcium-imaging. Furthermore, the neuronal circuit connectivity can be testified using multi-electrode array (Spira and Hai, 2013). Since ultrastructural evidence for synapse formation was found, it would be highly interesting to elucidate synaptic connectivity within differentiated networks and to trace putative changes with growing maturation. Furthermore, it is crucial to demonstrate the differentiation potential *in vivo* to ensure an integration of neuronal subtypes and glial cells into functionally active brain structures. As aforementioned, the reduction of oxygen level to 3 % in regular culturing procedure was demonstrated as beneficial for the survival of transplanted NPCs (Stacpoole et al., 2013). It is currently examined if intracerebrally transplanted primary eNEPs can survive and contribute to functional circuits in rodent models. To investigate which cell types are generated *in vivo* it is important to subject the animals to prolonged survival and analyze the presence of neuronal and glial progenies at various time points.

Intriguingly, hardly any GFAP-positive cells could be identified after short differentiation. By the application of unspecific differentiation protocols prolonged differentiation without the addition of DAPT it was possible to increase the GFAP-positive fraction. However, the differentiation of oligodendrocytes remains critical. It has been reported that the differentiation of oligodendrocytes from early NPCs is challenging and can take more than 6 months (Bian et al., 2016) because they are of a highly neurogenic fate. As a result, further differentiation in a late-type NPC line is necessary marked by differential signaling network. This stage can give rise to astrocyte and oligodendrocyte precursors as suggested by Wiese and colleagues (Wiese et al., 2012). Obstacles were faced adapting existing protocols for the differentiation of oligodendrocytic progenitors for pluripotent cells (Gorris et al., 2015). This might be due to the early neurogenic fate of primary eNEPs (Wiese et al., 2012) which is distinct from glial precursors as well as the highly active SHH signaling. It has been demonstrated in EAE mouse models that the inhibition of the SHH downstream protein Gli1 resulted in mobilization of myelinating cells (Samanta et al., 2015). Nevertheless, some remarkable structures resembling myelin swirls were found examining ultrastructures after 7 weeks of differentiation. Whether oligodendrocytes can be differentiated from primary eNEPs can be best evaluated *in vivo* after transplantation in rodent models. Thereafter, glial cells can be identified by the co-expression of human nuclei protein expression together with specific marker proteins such as myelin basic protein or O4.

4.3.3 The stabilization of eNEPs depends of a concerted signaling network of Notch, SHH, WNT and bFGF

In order to stabilize a defined, homogenous cell population presented in this thesis, a medium composition consisting of a N2/B27 supplemented basal medium, the growth factors bFGF and hLIF and chemical compounds that are synergistically modulating signaling pathways were used. Among these, TGFbeta signaling is blocked by SB, SHH activation is achieved by PMA and the canonical WNT pathway is activated by specific GSK3ß inhibition via CHIR. In the following, it is discussed how the aforementioned signaling pathways can contribute to the robust stabilization of primary eNEPs.

The vast majority of thus far reported, non-immortalized cell lines are cultured adherent or in suspension while adding bFGF and EGF. It has been suggested that these condition might be necessary for the stable cultivation of primary precursors (Carpenter et al., 1999; Hook et al., 2011; Moon et al., 2016). However, FGF/EGF-media conditions are known to force differentiation of neural precursor to a more gliogenic phenotype implicating the loss of a wide repertoire in terms of generating neuronal subtypes. Consistent with findings from rat-derived neuroepithelial cells (Kalyani et al., 1997) and hiPSCs-derived primitive NPCs or neuroepithelial precursors, EGF can be omitted under the supplementation with bFGF and chemical compounds which were identified to be beneficial by others and us (Li et al., 2011; Reinhardt et al., 2013). Preliminary results suggested that primary eNEPs might be dependent on FGF-signaling resulting in impaired proliferation as well as promoted differentiation upon blockage using specific inhibitors. Consistent results from recent publications indicated that bFGF has a developmental stage-specific role in NPCs and inhibition of the bFGF signaling leads to premature neurogenesis and reduced cell proliferation (Grabiec et al., 2016). To gain further insights in the role of bFGF-signaling in eNEPs downstream effectors should be analyzed in follow up studies.

Many succesful protocols for the derivation of NPCs use the dual SMAD inhibition approach, established by Chambers and colleagues (2009). Besides, the use of Noggin, a BMP4 inhibitor, the chemical compound SB is used to inhibit TGFβ signaling and thus ensure neural induction. Upon addition of SB to culture media it was found to inhibit differentiation and ensure self-renewal. As an alternative, the use of more specific inhibitor of the TGFβ type I receptor such as ALK5 and A83-01, along with other inhibitors was proposed and could be utilized as an alternative medium composition. Moreover, insulin signaling activation was detected by the upregulation of *IGFBP5* and *IGF2R* which have been implicated to be important in NPC homeostasis (Ziegler et al., 2015). Although insulin was not specifically added to the media, Insulin signaling is activated by the supplementation with B27 and N2 since both are containing insulin.

In accordance to findings in the literature, where Notch signaling and the upregulation of HES genes has been suggested as crucial for cells of neuroectodermal origin, eNEPs exhibit an activation of NOTCH1 and HES5. Furthermore, cells positive for Notch, HES5, PAX6 and SOX1 have been suggested of early neuropithelial with a wide plasticity (Edri et al., 2015). It is under debate to which extent hLIF signaling is contributing to the self-renewal of early neural precursors. In human pluripotent cells, which are not LIF-dependent and are referred to as primed, it has been proposed to be dispensable. However, it has been suggested to play a role in early, primitive NPCs. Hence, hLIF is one of the components in the media used, based on findings from ESC-derived primitive NPCs (Li et al., 2011). Interestingly, within this study no detection of an up- or down-regulation of hLIF/STAT signaling related genes in comparison to pluripotent cells was possible. As human pluripotent cells grow LIF independent, this might indicate LIF-independence of eNEPs as well being opposed to our initial hypothesis. To draw further conclusions, validation using qRT-PCR and immunoblot needs to be carried out.

Table 4.1 Comparison of eNEPs to other NPC lines from primary and pluripotent sources. Data taken from references as indicated. NT = not tested

Characteristic		**Cell type**					
	Markers						
Origin	-	fetal	fetal	fetal	fetal	ESCs	iPSCs

Reference	-	(Carpenter et al., 1999)	(Tailor et al., 2013)	(Moon et al., 2016)	(Günther et al., in preparation)	(Li et al., 2011)	(Reinhardt et al., 2013)
Self-renewal	-	Yes	Yes	Yes	Yes	Yes	Yes
Clonogenicity	-	NT	NT	NT	Yes	NT	Yes
2D or 3D	-	3D	2D	2D	2D	2D	2D
hLIF dependent?		Yes/No	No	No	Yes/No	Yes	No
EGF dependent?		Yes/No	Yes	Yes	No	No	No
Small molecules?		No	No	No	Yes	Yes	Yes
Neural progenitors	SOX1	NT	Yes	NT	Yes	NT	Yes
	PAX6	NT	Yes	Yes	Yes	Yes	Yes
	SOX2	NT	Yes	Yes	Yes	Yes	Yes
	Nestin	Yes	Yes	NT	Yes	Yes	Yes
	CD133	NT	NT	Yes	Yes	Yes	NT
Regionalization		Not tested	Hindbrain	Midbrain	Midbrain/ hindbrain	Midbrain	Midbrain/ plastic
Neurons	TUJ1/MAP2	Yes	Yes	Yes	Yes	Yes	Yes
	subtypes	TH, GABA		TH, 1-2% other	TH, vGlut1, GABA-A, TPH2	TH	TH, MN
Synapses		NT	Synapto-physin	Not tested	Synapsin, PSD-95, TEM	NT	NT
Astrocytes	GFAP	Yes	Yes	Yes	Yes	Yes	Yes
	S100β	NT	S100β	NT	Yes	NT	S100β
Oligodendrocytes		GalC	O4	O4	TEM	No	Yes
Peripheral neurons		NT	NT	NT	Yes	No	Yes
Mesenchymal cells	SMA	NT	NT	NT	Yes	NT	Yes

4.3.4 Primary eNEPs bear a great potential in application as a reference cell line as well as in cell replacement and transplantation strategies

Despite emerging protocols describing various strategies to obtain NPCs with different characteristics it remains to be shown how physiological the resulting cell lines are. Thus far, it has not been elucidated if the differentiated or converted cell lines are *in vitro* artifacts of cell culture and genetic manipulation or can be considered and used as a captured state of otherwise transient developmental time frames. However, it becomes evident that hiPSC-derived or direct conversion protocols aiming to result in a developmental early NPC stage are of major importance. Therefore, a physiological reference line which correlates with early-stage primitive and neuroepithelial precursors is inevitable. Unlike FGF/EGF-dependent cell lines, primary eNEPs could represent such a proliferative, long-term stable cell line which has unrestricted potential to yield central and peripheral cell types. Hence, it could be used as a physiological bona fide control line to validate novel NPCs obtained by programming techniques (Fig. 4.1).

Due to the finding that eNEPs have a vast expansion and self-renewal capacity, a prospective potential in generating a physiological healthy platform of NPCs or neurons might be suggested. Using standardized protocols a high grade of reproducibility can be achieved and serve as a high throughput platform for toxicity testing for instance on a microarray chip platform as recently published (Nierode et al., 2016). Moreover, gene expression profiles and functional properties can be compared to patient-derived *in vitro* differentiated neurons. On the other hand, gene editing of healthy neurons can contribute significantly to understand and model genetically defined disorders using TALEN or more efficient, CRISPR/Cas9 technique (Fig. 4.1). Emerging recent studies confirm the great impact of CRISPR/Cas9 in disease modelling allowing to generate isogenic diseased and corrected lines or implicate the gene editing in programming strategies (Black et al., 2016; Kehler et al., 2016).

Tissue engineering applications require an enormous number of cells that can be provided by self-renewing stem cells. Thus, it might be possible to engage primary NPCs or NPC-derived cells in tissue structures generated by cell printing or seeding on engineered substrates. Recently, ESCs derived neural tube-like 3D structures have been reconstructed *in vitro* (Meinhardt et al., 2014) and were further improved by adding ECM-like matrices (Ranga et al., 2016). Similar experiments could be also conducted with the primary eNEP line described in this thesis. Moreover, physiological cerebral or cerebellar organoids could be established from primary eNEPs alone or combined with other stem cells. Previously, this has been shown using pluripotent cell lines (Keiko et al., 2015; Lancaster et al., 2013) in order to gain further insights into early neurodevelopmental processes and model disturbed neural development e.g. in microcephaly. As a further refinement, novel hydrogels such as gelatin methacryloyl could represent a promising substrate for organoid, cell incorporating approaches and could serve as a less cost-intensive, defined alternative to MG while providing the appropriate stiffness (Loessner et al., 2016).

This study demonstrates the *in vitro* differentiation potential of eNEPs into neurons and astrocytes and finds compelling signs of myelination pointing to the presence of oligodendrocytes. However, to investigate whether primary eNEPs are feasible for transplantations it is crucial to test this *in vivo*. The *in vivo* differentiation capacity can been investigated in chick and rodent models and is useful to obtain preclinical data (Glaser et al., 2007). Importantly, in contrast to iPSCs-derived NPCs, there is no risk of dedifferentiation resulting in tumor formation, as reported previously (Gao et al., 2016). Emerging constantly improving protocols for high quality cell preparations and specific differentiation contribute immensely to promising and standardized cell replacement strategies rapidly moving towards clinics. For instance, in case of PD recent progress on evaluation and prediction of transplantation has been reported by the introduction of a an expanded, comprehensive marker panel (Kirkeby et al., 2016) and might be potentially applied to eNEPs. The novel protocol implicates a chemically defined, GMP suitable procedure with a timed delivery of FGF8b, which could be useful to establish a more defined and comparable patterning procedure in comparison to previously freshly isolated fetal preparations. Despite comparable preclinical benefits and efficiency of ESC-derived dopaminergic neurons, fetal derived grafts represent thus far the most comprehensively analyzed cell source (Grealish et al., 2014). Follow-up studies on post-mortem samples of 24 years post grafting could confirm positive clinical outcome and elucidate crucial points for future trials (Li et al., 2016). Starting more than 30 years ago and continuing in recent times, cell restorative therapy using cells of fetal origin was reintroduced into clinical trials representing still the gold standard (Abbott, 2014; Barker et al., 2013; Brundin et al., 2010). Nevertheless, midbrain dopaminergic progenitors and neurons from ESCs and autologous hiPSCs are paving the road to future cell replacement strategies (Barker et al., 2015). In parallel, improved protocols for novel primary progenitor lines are constantly introduced (Moon et al., 2016). Besides the engagement of primary cells in cell replacement studies of PD, it has been proposed to use genetically engineered human NPCs to specifically deliver inducible GDNF after transplantation and thus ameliorating the survival of degenerating neurons (Behrstock et al., 2006; Gowing et al., 2014). However, the utilized preparation method of the NPCs has not been changed since more than twenty years resulting in some limitations including restrictions of the differentiation capacity (Svendsen et al., 1998). Moreover, it has been reported that BDNF-overexpressing ESC-derived neural progenitors could contribute to recovering in Huntington Disease mouse models representing a promising result (Zimmermann et al., 2016). Further application of NPCs has been shown to beneficially contribute to recovery after spinal cord injury (Kadoya et al., 2016).

On the other hand, the application of pluripotent cell-derived counterparts brings obstacles such as ethical limitations and potential tumorigenic risk upon spontaneous dedifferentiation. Although, strategies e.g. the pretreatment with DAPT has been proposed to address this issue, (Okubo et al., 2016) this question has not been fully solved. Thus, the use of a novel physiological primary neural cell line which can be differentiated in a variety of central and peripheral cell type could serve as a delivery strategy of cells and factors which integrates more easily and does not bear the risk of dedifferentiation. Obstacles which might reduce the usability of eNEPs include for instance ethical considerations. The derivation of and research involving ESCs is highly controversial and therefore strictly regulated by the law. Likewise, fetal-derived cells still represent a controversially discussed research field defined by law regulations and ethical committee decisions as well. Thus, all experimental work has to fulfill ethical requirements and poses borders to potential application areas, especially commercial applications like biological cell banking or screening platforms as well as novel protocols which involve intellectual property applications. Therefore, iPSCs represent an alternative approach enabling to bypass embryonic stem cell legal regulations. However, due to the major self-renewal and differentiation capacity stable primary NPCs can help to minimize the use of experimental animal research allowing to elucidate effects *in vitro*. Exemplarily, major accomplishments were made using stem cells including the generation of organoid structures, 3D microarray assays or the establishment of a blood brain barrier which can be used for toxicity and pharmacological testing (Lancaster et al., 2013; Lippmann et al., 2013; Nierode et al., 2016). But it has to be taken into account, that primary eNEPs may not be feasible as a screening platform or model for degenerated and diseased neurons as yielded primary neurons have still relatively young, immature identity. Despite maturation periods *in vitro*, cells might be subject of *in vitro* artifacts and selection resulting from prolonged cultivation in cell culture. More straightforward strategies to model degenerative neurological diseases, especially age-related syndromes might need a modification of neuronal phenotypes by introducing molecular aging by aforementioned means.

Taken together, the major aim to generate a proliferative, cryo-preservable and monoclonally expandable early neural cell line from primary tissue could be fulfilled. Thus, resulting in a novel, highly plastic and EGF-independent physiological eNEP line of ventral midbrain/hindbrain fate. Of note, the generated cell population might possess a strong neural fate plasticity. In other words, it exhibits a broad differentiation capacity to a variety of cell types of the central and peripheral lineage upon exposure to patterning cues. Consequently, a variety of neuronal subtypes identities can be acquired. Notably, functional neurons and apparently developing synapses can be found. Therefore, primary eNEPs and differentiated progenies therof could be suitable as a physiological reference cell line enabling the validation of novel cell lines resulting from programming studies. In addition, a variety of state-of-the-art techniques of biomedical research and translational medicine could be applied (Fig. 4.1). Among these, gene editing and disease modelling, cell replacement, drug and toxicity screening and organoid model as well as engineered tissue are of major interest. Consequently, primary eNEPs could potentially contribute to advances in regenerative and personalized medicine.

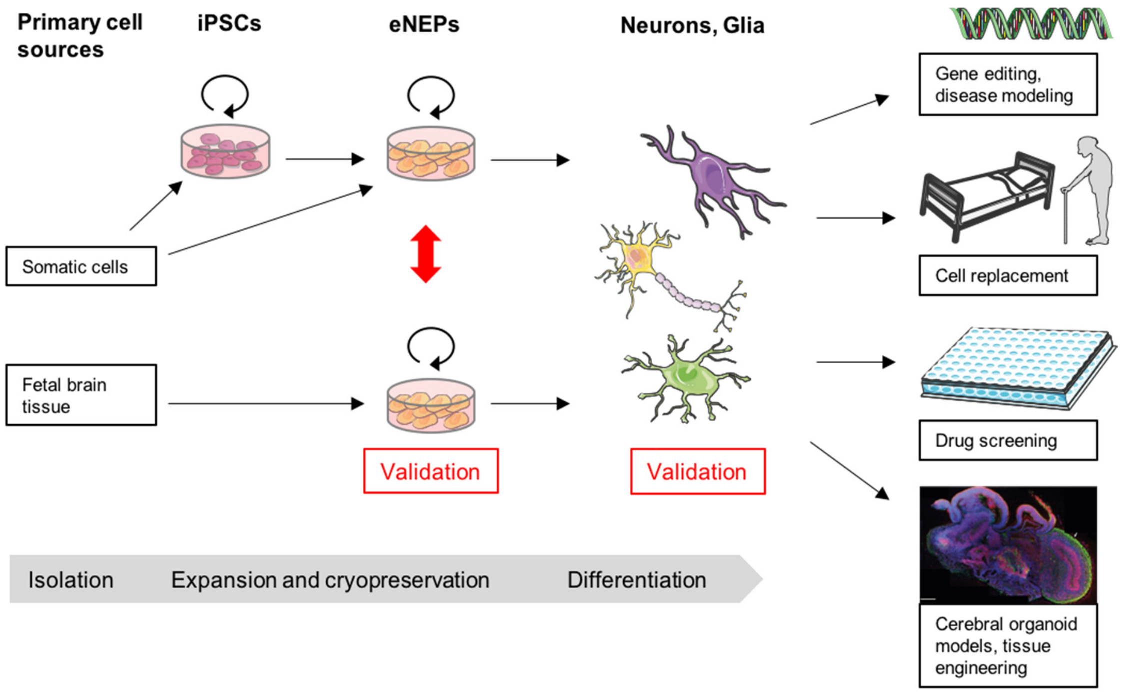

Figure 4.1 Graphical summary of key features and potential biomedical applications of primary eNEPs. Following isolation from fetal brain tissue eNEPs can be stabilized, expanded and preserved. At this stage, they could be useful to validate iPSC-derived eNEPs from different protocols. After terminal differentiation into neurons and glia, patient-derived progenies can be subjected to validation using primary eNEP-derived cells. Yielded cells might be feasible for biomedical applications such as gene editing and disease modeling as well as cell replacement. Moreover, drug and toxicity screening would contribute to beneficial therapeutic applications. Cerebral organoid models and engineering of neural tissue represent additional strategies for the usage of eNEPs. Graphic elements were partly taken and modified from Servier Medical Art, cerebral organoid image adapted from Lancaster et al., 2013.

5. References

Aasen, T., Raya, A., Barrero, M.J., Garreta, E., Consiglio, A., Gonzalez, F., Vassena, R., Bilić, J., Pekarik, V., Tiscornia, G., Edel, M., Boué, S., Izpisúa Belmonte, J.C., 2008. Efficient and rapid generation of induced pluripotent stem cells from human keratinocytes. Nat. Biotechnol. 26, 1276–84. doi:10.1038/nbt.1503

Abbott, A., 2014. Fetal-cell revival for Parkinson's. Nature 510, 195–6. doi:10.1038/510195a

Aguirre, A., Rubio, M.E., Gallo, V., 2010. Notch and EGFR pathway interaction regulates neural stem cell number and self-renewal. Nature 467, 323–7. doi:10.1038/nature09347

Altman, J., Das, G.D., 1965. Autoradiographic and histological evidence of postnatal hippocampal neurogenesis in rats. J. Comp. Neurol. 124, 319–335. doi:10.1002/cne.901240303

Bain, G., Kitchens, D., Yao, M., Huettner, J.E., Gottlieb, D.I., 1995. Embryonic stem cells express neuronal properties in vitro. Dev. Biol. 168, 342–57. doi:10.1006/dbio.1995.1085

Ban, H., Nishishita, N., Fusaki, N., Tabata, T., Saeki, K., Shikamura, M., Takada, N., Inoue, M., Hasegawa, M., Kawamata, S., Nishikawa, S.-I., 2011. Efficient generation of transgene-free human induced pluripotent stem cells (iPSCs) by temperature-sensitive Sendai virus vectors. Proc. Natl. Acad. Sci. U. S. A. 108, 14234–14239. doi:10.1073/pnas.1103509108

Bar-Nur, O., Brumbaugh, J., Verheul, C., Apostolou, E., Pruteanu-Malinici, I., Walsh, R.M., Ramaswamy, S., Hochedlinger, K., 2014. Small molecules facilitate rapid and synchronous iPSC generation. Nat. Methods 11, 1170–6. doi:10.1038/nmeth.3142

Bar-Nur, O., Verheul, C., Sommer, A.G., Brumbaugh, J., Schwarz, B.A., Lipchina, I., Huebner, A.J., Mostoslavsky, G., Hochedlinger, K., 2015. Lineage conversion induced by pluripotency factors involves transient passage through an iPSC stage. Nat. Biotechnol. 33, 761–8. doi:10.1038/nbt.3247

Barker, R.A., Barrett, J., Mason, S.L., Björklund, A., 2013. Fetal dopaminergic transplantation trials and the future of neural grafting in Parkinson's disease. Lancet. Neurol. 12, 84–91. doi:10.1016/S1474-4422(12)70295-8

Barker, R.A., Studer, L., Cattaneo, E., Takahashi, J., 2015. G-Force PD: a global initiative in coordinating stem cell-based dopamine treatments for Parkinson's disease. npj Park. Dis. 1, 15017. doi:10.1038/npjparkd.2015.17

BECKER, A.J., McCULLOCH, E.A., TILL, J.E., 1963. Cytological demonstration of the clonal nature of spleen colonies derived from transplanted mouse marrow cells. Nature 197, 452–4.

Behrstock, S., Ebert, a, McHugh, J., Vosberg, S., Moore, J., Schneider, B., Capowski, E., Hei, D., Kordower, J., Aebischer, P., Svendsen, C.N., 2006. Human neural progenitors deliver glial cell line-derived neurotrophic factor to parkinsonian rodents and aged primates. Gene Ther. 13, 379–388. doi:10.1038/sj.gt.3302679

Ben-Ari, Y., 2002. Excitatory actions of gaba during development: the nature of the nurture. Nat. Rev. Neurosci. 3, 728–39. doi:10.1038/nrn920

Bernal, J.A., 2013. RNA-based tools for nuclear reprogramming and lineage-conversion: towards clinical applications. J. Cardiovasc. Transl. Res. 6, 956–68. doi:10.1007/s12265-013-9494-8

Bian, J., Zheng, J., Li, S., Luo, L., Ding, F., 2016. Sequential Differentiation of Embryonic Stem Cells into Neural Epithelial-Like Stem Cells and Oligodendrocyte Progenitor Cells. PLoS One 11, e0155227. doi:10.1371/journal.pone.0155227

Bibel, M., Richter, J., Schrenk, K., Tucker, K.L., Staiger, V., Korte, M., Goetz, M., Barde, Y.-A., 2004. Differentiation of mouse embryonic stem cells into a defined neuronal lineage. Nat. Neurosci. 7, 1003–9. doi:10.1038/nn1301

Biswas, D., Jiang, P., 2016. Chemically Induced Reprogramming of Somatic Cells to Pluripotent Stem Cells and Neural Cells. Int. J. Mol. Sci. 17, 226. doi:10.3390/ijms17020226

Black, J.B., Adler, A.F., Wang, H.-G., D'Ippolito, A.M., Hutchinson, H.A., Reddy, T.E., Pitt, G.S., Leong, K.W., Gersbach, C.A., 2016. Targeted Epigenetic Remodeling of Endogenous Loci by CRISPR/Cas9-Based Transcriptional Activators Directly Converts Fibroblasts to Neuronal Cells. Cell Stem Cell 19, 406–14. doi:10.1016/j.stem.2016.07.001

Blanpain, C., Lowry, W.E., Geoghegan, A., Polak, L., Fuchs, E., 2004. Self-renewal, multipotency, and the existence of two cell populations within an epithelial stem cell niche. Cell 118, 635–48. doi:10.1016/j.cell.2004.08.012

Borghese, L., Dolezalova, D., Opitz, T., Haupt, S., Leinhaas, A., Steinfarz, B., Koch, P., Edenhofer, F., Hampl, A., Brüstle, O., 2010. Inhibition of notch signaling in human embryonic stem cell-derived neural stem cells delays G1/S phase transition and accelerates neuronal differentiation in vitro and in vivo. Stem Cells 28, 955–64. doi:10.1002/stem.408

Brennand, K.J., Simone, A., Tran, N., Gage, F.H., 2012. Modeling psychiatric disorders at the cellular

and network levels. Mol. Psychiatry 17, 1239–53. doi:10.1038/mp.2012.20
Briggs, R., King, T.J., 1952. Transplantation of Living Nuclei From Blastula Cells into Enucleated Frogs' Eggs. Proc. Natl. Acad. Sci. U. S. A. 38, 455–63.
Brundin, P., Barker, R.A., Parmar, M., 2010. Neural grafting in Parkinson's disease Problems and possibilities. Prog. Brain Res. 184, 265–94. doi:10.1016/S0079-6123(10)84014-2
Brüstle, O., Jones, K.N., Learish, R.D., Karram, K., Choudhary, K., Wiestler, O.D., Duncan, I.D., McKay, R.D., 1999. Embryonic stem cell-derived glial precursors: a source of myelinating transplants. Science 285, 754–6.
Buganim, Y., Faddah, D.A., Cheng, A.W., Itskovich, E., Markoulaki, S., Ganz, K., Klemm, S.L., Van Oudenaarden, A., Jaenisch, R., 2012. Single-cell expression analyses during cellular reprogramming reveal an early stochastic and a late hierarchic phase. Cell 150, 1209–1222. doi:10.1016/j.cell.2012.08.023
Cai, J., Li, W., Su, H., Qin, D., Yang, J., Zhu, F., Xu, J., He, W., Guo, X., Labuda, K., Peterbauer, A., Wolbank, S., Zhong, M., Li, Z., Wu, W., So, K.-F., Redl, H., Zeng, L., Esteban, M.A., Pei, D., 2010. Generation of human induced pluripotent stem cells from umbilical cord matrix and amniotic membrane mesenchymal cells. J. Biol. Chem. 285, 11227–34. doi:10.1074/jbc.M109.086389
Caiazzo, M., Dell'Anno, M.T., Dvoretskova, E., Lazarevic, D., Taverna, S., Leo, D., Sotnikova, T.D., Menegon, A., Roncaglia, P., Colciago, G., Russo, G., Carninci, P., Pezzoli, G., Gainetdinov, R.R., Gustincich, S., Dityatev, A., Broccoli, V., 2011. Direct generation of functional dopaminergic neurons from mouse and human fibroblasts. Nature 476, 224–7. doi:10.1038/nature10284
Cairns, D.M., Chwalek, K., Moore, Y.E., Kelley, M.R., Abbott, R.D., Moss, S., Kaplan, D.L., 2016. Expandable and Rapidly Differentiating Human Induced Neural Stem Cell Lines for Multiple Tissue Engineering Applications. Stem cell reports. doi:10.1016/j.stemcr.2016.07.017
Calvi, L.M., Adams, G.B., Weibrecht, K.W., Weber, J.M., Olson, D.P., Knight, M.C., Martin, R.P., Schipani, E., Divieti, P., Bringhurst, F.R., Milner, L.A., Kronenberg, H.M., Scadden, D.T., 2003. Osteoblastic cells regulate the haematopoietic stem cell niche. Nature 425, 841–6. doi:10.1038/nature02040
Cameron, H.A., Woolley, C.S., McEwen, B.S., Gould, E., 1993. Differentiation of newly born neurons and glia in the dentate gyrus of the adult rat. Neuroscience 56, 337–44.
Cantone, I., Fisher, A.G., 2013. Epigenetic programming and reprogramming during development. Nat. Struct. Mol. Biol. 20, 282–9. doi:10.1038/nsmb.2489
Carpenter, M.K., Cui, X., Hu, Z.Y., Jackson, J., Sherman, S., Seiger, A., Wahlberg, L.U., 1999. In vitro expansion of a multipotent population of human neural progenitor cells. Exp Neurol 158, 265–278. doi:10.1006/exnr.1999.7098
Chailangkarn, T., Trujillo, C.A., Freitas, B.C., Hrvoj-Mihic, B., Herai, R.H., Yu, D.X., Brown, T.T., Marchetto, M.C., Bardy, C., McHenry, L., Stefanacci, L., Järvinen, A., Searcy, Y.M., DeWitt, M., Wong, W., Lai, P., Ard, M.C., Hanson, K.L., Romero, S., Jacobs, B., Dale, A.M., Dai, L., Korenberg, J.R., Gage, F.H., Bellugi, U., Halgren, E., Semendeferi, K., Muotri, A.R., 2016. A human neurodevelopmental model for Williams syndrome. Nature 536, 338–43. doi:10.1038/nature19067
Chambers, I., 2004. The molecular basis of pluripotency in mouse embryonic stem cells. Cloning Stem Cells 6, 386–91. doi:10.1089/clo.2004.6.386
Chambers, S.M., Fasano, C.A., Papapetrou, E.P., Tomishima, M., Sadelain, M., Studer, L., 2009. Highly efficient neural conversion of human ES and iPS cells by dual inhibition of SMAD signaling. Nat. Biotechnol. 27, 275–80. doi:10.1038/nbt.1529
Chambers, S.M., Qi, Y., Mica, Y., Lee, G., Zhang, X.-J., Niu, L., Bilsland, J., Cao, L., Stevens, E., Whiting, P., Shi, S.-H., Studer, L., 2012. Combined small-molecule inhibition accelerates developmental timing and converts human pluripotent stem cells into nociceptors. Nat. Biotechnol. 30, 715–20. doi:10.1038/nbt.2249
Chen, K., Long, Q., Wang, T., Zhao, D., Zhou, Y., Qi, J., Wu, Y., Li, S., Chen, C., Zeng, X., Yang, J., Zhou, Z., Qin, W., Liu, X., Li, Y., Li, Y., Huang, X., Qin, D., Chen, J., Pan, G., Schöler, H.R., Xu, G., Liu, X., Pei, D., 2016. Gadd45a is a heterochromatin relaxer that enhances iPS cell generation. EMBO Rep. doi:10.15252/embr.201642402
Cherny, R.A., Stokes, T.M., Merei, J., Lom, L., Brandon, M.R., Williams, R.L., 1994. Strategies for the isolation and characterization of bovine embryonic stem cells. Reprod. Fertil. Dev. 6, 569–75.
Chi, L., Fan, B., Feng, D., Chen, Z., Liu, Z., Hui, Y., Xu, X., Ma, L., Fang, Y., Zhang, Q., Jin, G., Liu, L., Guan, F., Zhang, X., 2016a. The Dorsoventral Patterning of Human Forebrain Follows an Activation/Transformation Model. Cereb. Cortex. doi:10.1093/cercor/bhw152
Chi, L., Fan, B., Zhang, K., Du, Y., Liu, Z., Fang, Y., Chen, Z., Ren, X., Xu, X., Jiang, C., Li, S., Ma, L., Gao, L., Liu, L., Zhang, X., 2016b. Targeted Differentiation of Regional Ventral Neuroprogenitors and Related Neuronal Subtypes from Human Pluripotent Stem Cells. Stem cell reports. doi:10.1016/j.stemcr.2016.09.003
Chizhikov, V. V, Millen, K.J., 2004a. Mechanisms of roof plate formation in the vertebrate CNS. Nat.

Rev. Neurosci. 5, 808–12. doi:10.1038/nrn1520
Chizhikov, V. V, Millen, K.J., 2004b. Control of roof plate development and signaling by Lmx1b in the caudal vertebrate CNS. J. Neurosci. 24, 5694–703. doi:10.1523/JNEUROSCI.0758-04.2004
Chung, S.Y., Kishinevsky, S., Mazzulli, J.R., Graziotto, J., Mrejeru, A., Mosharov, E. V, Puspita, L., Valiulahi, P., Sulzer, D., Milner, T.A., Taldone, T., Krainc, D., Studer, L., Shim, J.-W., 2016. Parkin and PINK1 Patient iPSC-Derived Midbrain Dopamine Neurons Exhibit Mitochondrial Dysfunction and α-Synuclein Accumulation. Stem cell reports 7, 664–677. doi:10.1016/j.stemcr.2016.08.012
Conti, L., Cattaneo, E., 2010. Neural stem cell systems: physiological players or in vitro entities? Nat. Rev. Neurosci. 11, 176–87. doi:10.1038/nrn2761
Conti, L., Pollard, S.M., Gorba, T., Reitano, E., Toselli, M., Biella, G., Sun, Y., Sanzone, S., Ying, Q.L., Cattaneo, E., Smith, A., 2005. Niche-independent symmetrical self-renewal of a mammalian tissue stem cell. PLoS Biol. 3, 1594–1606. doi:10.1371/journal.pbio.0030283
Davis, R.L., Weintraub, H., Lassar, A.B., 1987. Expression of a single transfected cDNA converts fibroblasts to myoblasts. Cell 51, 987–1000.
De Robertis, E.M., Kuroda, H., 2004. Dorsal-ventral patterning and neural induction in Xenopus embryos. Annu. Rev. Cell Dev. Biol. 20, 285–308. doi:10.1146/annurev.cellbio.20.011403.154124
Dessaud, E., McMahon, A.P., Briscoe, J., 2008. Pattern formation in the vertebrate neural tube: a sonic hedgehog morphogen-regulated transcriptional network. Development 135, 2489–503. doi:10.1242/dev.009324
Devine, M.J., Ryten, M., Vodicka, P., Thomson, A.J., Burdon, T., Houlden, H., Cavaleri, F., Nagano, M., Drummond, N.J., Taanman, J.-W., Schapira, A.H., Gwinn, K., Hardy, J., Lewis, P.A., Kunath, T., 2011. Parkinson’s disease induced pluripotent stem cells with triplication of the α-synuclein locus. Nat. Commun. 2, 440. doi:10.1038/ncomms1453
Di Biase, V., Flucher, B.E., Obermair, G.J., 2009. Resolving sub-synaptic compartments with double immunofluorescence labeling in hippocampal neurons. J. Neurosci. Methods 176, 78–84. doi:10.1016/j.jneumeth.2008.08.025
Doetsch, F., Caillé, I., Lim, D.A., García-Verdugo, J.M., Alvarez-Buylla, A., 1999. Subventricular zone astrocytes are neural stem cells in the adult mammalian brain. Cell 97, 703–16.
Dunnett, S.B., Björklund, A., 1999. Prospects for new restorative and neuroprotective treatments in Parkinson’s disease. Nature 399, A32-9.
Durruthy, J.D., Sebastiano, V., 2015. Derivation of GMP-compliant integration-free hiPSCs using modified mRNAs. Methods Mol. Biol. 1283, 31–42. doi:10.1007/7651_2014_124
Echelard, Y., Epstein, D.J., St-Jacques, B., Shen, L., Mohler, J., McMahon, J.A., McMahon, A.P., 1993. Sonic hedgehog, a member of a family of putative signaling molecules, is implicated in the regulation of CNS polarity. Cell 75, 1417–30.
Eckfeldt, C.E., Mendenhall, E.M., Verfaillie, C.M., 2005a. The molecular repertoire of the “almighty” stem cell. Nat. Rev. Mol. Cell Biol. 6, 726–37. doi:10.1038/nrm1713
Eckfeldt, C.E., Mendenhall, E.M., Verfaillie, C.M., 2005b. The molecular repertoire of the “almighty” stem cell. Nat. Rev. Mol. Cell Biol. 6, 726–737. doi:10.1038/nrm1713
Edri, R., Yaffe, Y., Ziller, M.J., Mutukula, N., Volkman, R., David, E., Jacob-Hirsch, J., Malcov, H., Levy, C., Rechavi, G., Gat-Viks, I., Meissner, A., Elkabetz, Y., 2015. Analysing human neural stem cell ontogeny by consecutive isolation of Notch active neural progenitors. Nat. Commun. 6, 6500. doi:10.1038/ncomms7500
Elkabetz, Y., Panagiotakos, G., Al Shamy, G., Socci, N.D., Tabar, V., Studer, L., 2008. Human ES cell-derived neural rosettes reveal a functionally distinct early neural stem cell stage. Genes Dev. 22, 152–165. doi:10.1101/gad.1616208
Emborg, M.E., Ebert, A.D., Moirano, J., Peng, S., Suzuki, M., Capowski, E., Joers, V., Roitberg, B.Z., Aebischer, P., Svendsen, C.N., 2008. GDNF-secreting human neural progenitor cells increase tyrosine hydroxylase and VMAT2 expression in MPTP-treated cynomolgus monkeys. Cell Transplant. 17, 383–95.
Eriksson, P.S., Perfilieva, E., Björk-Eriksson, T., Alborn, A.M., Nordborg, C., Peterson, D.A., Gage, F.H., 1998. Neurogenesis in the adult human hippocampus. Nat. Med. 4, 1313–7. doi:10.1038/3305
Esfandiari, F., Fathi, A., Gourabi, H., Kiani, S., Nemati, S., Baharvand, H., 2012. Glycogen synthase kinase-3 inhibition promotes proliferation and neuronal differentiation of human-induced pluripotent stem cell-derived neural progenitors. Stem Cells Dev. 21, 3233–43. doi:10.1089/scd.2011.0678
Esteban, M.A., Wang, T., Qin, B., Yang, J., Qin, D., Cai, J., Li, W., Weng, Z., Chen, J., Ni, S., Chen, K., Li, Y., Liu, X., Xu, J., Zhang, S., Li, F., He, W., Labuda, K., Song, Y., Peterbauer, A., Wolbank, S., Redl, H., Zhong, M., Cai, D., Zeng, L., Pei, D., 2010. Vitamin C enhances the generation of mouse and human induced pluripotent stem cells. Cell Stem Cell 6, 71–9. doi:10.1016/j.stem.2009.12.001
Evans, M.J., Kaufman, M.H., 1981. Establishment in culture of pluripotential cells from mouse embryos. Nature 292, 154–6.

Faigle, R., Song, H., 2013. Signaling mechanisms regulating adult neural stem cells and neurogenesis. Biochim. Biophys. Acta 1830, 2435–48. doi:10.1016/j.bbagen.2012.09.002

Fasano, C.A., Chambers, S.M., Lee, G., Tomishima, M.J., Studer, L., 2010. Efficient derivation of functional floor plate tissue from human embryonic stem cells. Cell Stem Cell 6, 336–47. doi:10.1016/j.stem.2010.03.001

Favaro, R., Valotta, M., Ferri, A.L.M., Latorre, E., Mariani, J., Giachino, C., Lancini, C., Tosetti, V., Ottolenghi, S., Taylor, V., Nicolis, S.K., 2009. Hippocampal development and neural stem cell maintenance require Sox2-dependent regulation of Shh. Nat. Neurosci. 12, 1248–56. doi:10.1038/nn.2397

Fry, D.W., Kraker, A.J., McMichael, A., Ambroso, L.A., Nelson, J.M., Leopold, W.R., Connors, R.W., Bridges, A.J., 1994. A specific inhibitor of the epidermal growth factor receptor tyrosine kinase. Science 265, 1093–5.

Fusaki, N., Ban, H., Nishiyama, A., Saeki, K., Hasegawa, M., 2009. Efficient induction of transgene-free human pluripotent stem cells using a vector based on Sendai virus, an RNA virus that does not integrate into the host genome. Proc. Jpn. Acad. Ser. B. Phys. Biol. Sci. 85, 348–62.

Gage, F.H., Kempermann, G., Palmer, T.D., Peterson, D.A., Ray, J., 1998. Multipotent progenitor cells in the adult dentate gyrus. J. Neurobiol. 36, 249–66.

Gage, F.H., Ray, J., Fisher, L.J., 1995. Isolation, characterization, and use of stem cells from the CNS. Annu. Rev. Neurosci. 18, 159–92. doi:10.1146/annurev.ne.18.030195.001111

Gao, M., Yao, H., Dong, Q., Zhang, H., Yang, Z., Yang, Y., Zhu, J., Xu, M., Xu, R., 2016. Tumourigenicity and Immunogenicity of Induced Neural Stem Cell Grafts Versus Induced Pluripotent Stem Cell Grafts in Syngeneic Mouse Brain. Sci. Rep. 6, 29955. doi:10.1038/srep29955

Geling, A., Steiner, H., Willem, M., Bally-Cuif, L., Haass, C., 2002. A gamma-secretase inhibitor blocks Notch signaling in vivo and causes a severe neurogenic phenotype in zebrafish. EMBO Rep. 3, 688–94. doi:10.1093/embo-reports/kvf124

Gerfen, R.W., Wheeler, M.B., 1995. Isolation of embryonic cell-lines from porcine blastocysts. Anim. Biotechnol. 6, 1–14. doi:10.1080/10495399509525828

Giles, J.R., Yang, X., Mark, W., Foote, R.H., 1993. Pluripotency of cultured rabbit inner cell mass cells detected by isozyme analysis and eye pigmentation of fetuses following injection into blastocysts or morulae. Mol. Reprod. Dev. 36, 130–8. doi:10.1002/mrd.1080360203

Giorgetti, A., Montserrat, N., Aasen, T., Gonzalez, F., Rodríguez-Pizà, I., Vassena, R., Raya, A., Boué, S., Barrero, M.J., Corbella, B.A., Torrabadella, M., Veiga, A., Izpisua Belmonte, J.C., 2009. Generation of induced pluripotent stem cells from human cord blood using OCT4 and SOX2. Cell Stem Cell 5, 353–7. doi:10.1016/j.stem.2009.09.008

Glaser, T., Brüstle, O., 2005. Retinoic acid induction of ES-cell-derived neurons: the radial glia connection. Trends Neurosci. 28, 397–400. doi:10.1016/j.tins.2005.05.008

Glaser, T., Pollard, S.M., Smith, A., Brüstle, O., 2007. Tripotential differentiation of adherently expandable Neural Stem (NS) cells. PLoS One 2, 2–5. doi:10.1371/journal.pone.0000298

Gong, J.K., 1978. Endosteal marrow: a rich source of hematopoietic stem cells. Science 199, 1443–5.

Gonzalez, F., Barragan Monasterio, M., Tiscornia, G., Montserrat Pulido, N., Vassena, R., Batlle Morera, L., Rodriguez Piza, I., Izpisua Belmonte, J.C., 2009. Generation of mouse-induced pluripotent stem cells by transient expression of a single nonviral polycistronic vector. Proc. Natl. Acad. Sci. U. S. A. 106, 8918–22. doi:10.1073/pnas.0901471106

González, F., Boué, S., Izpisúa Belmonte, J.C., 2011. Methods for making induced pluripotent stem cells: reprogramming à la carte. Nat. Rev. Genet. 12, 231–42. doi:10.1038/nrg2937

Gorris, R., Fischer, J., Erwes, K.L., Kesavan, J., Peterson, D.A., Alexander, M., Nöthen, M.M., Peitz, M., Quandel, T., Karus, M., Brüstle, O., 2015. Pluripotent stem cell-derived radial glia-like cells as stable intermediate for efficient generation of human oligodendrocytes. Glia 63, 2152–2167. doi:10.1002/glia.22882

Gowing, G., Shelley, B., Staggenborg, K., Hurley, A., Avalos, P., Victoroff, J., Latter, J., Garcia, L., Svendsen, C.N., 2014. Glial cell line-derived neurotrophic factor-secreting human neural progenitors show long-term survival, maturation into astrocytes, and no tumor formation following transplantation into the spinal cord of immunocompromised rats. Neuroreport 25, 367–72. doi:10.1097/WNR.0000000000000092

Grabiec, M., Hříbková, H., Vařecha, M., Střítecká, D., Hampl, A., Dvořák, P., Sun, Y.-M., 2016. Stage-specific roles of FGF2 signaling in human neural development. Stem Cell Res. 17, 330–341. doi:10.1016/j.scr.2016.08.012

Grealish, S., Diguet, E., Kirkeby, A., Mattsson, B., Heuer, A., Bramoulle, Y., Van Camp, N., Perrier, A.L., Hantraye, P., Björklund, A., Parmar, M., 2014. Human ESC-derived dopamine neurons show similar preclinical efficacy and potency to fetal neurons when grafted in a rat model of Parkinson’s disease. Cell Stem Cell 15, 653–65. doi:10.1016/j.stem.2014.09.017

Gronthos, S., Zannettino, A.C.W., Hay, S.J., Shi, S., Graves, S.E., Kortesidis, A., Simmons, P.J., 2003.

Molecular and cellular characterisation of highly purified stromal stem cells derived from human bone marrow. J. Cell Sci. 116, 1827–35.
Günther, K., Appelt-Menzel, A., Kwok, C.K., Walles, H., Metzger, M., Edenhofer, F., 2016. Rapid Monolayer Neural Induction of induced Pluripotent Stem Cells Yields Stably Proliferating Neural Stem Cells. J. Stem Cell Res. Ther. 6. doi:10.4172/2157-7633.1000341
Gurdon, J.B., 1962. The Developmental Capacity of Nuclei taken from Intestinal Epithelium Cells of Feeding Tadpoles. J Embryol Exp Morphol 10, 622–640.
GURDON, J.B., ELSDALE, T.R., FISCHBERG, M., 1958. Sexually Mature Individuals of Xenopus laevis from the Transplantation of Single Somatic Nuclei. Nature 182, 64–65. doi:10.1038/182064a0
Haase, A., Olmer, R., Schwanke, K., Wunderlich, S., Merkert, S., Hess, C., Zweigerdt, R., Gruh, I., Meyer, J., Wagner, S., Maier, L.S., Han, D.W., Glage, S., Miller, K., Fischer, P., Schöler, H.R., Martin, U., 2009. Generation of induced pluripotent stem cells from human cord blood. Cell Stem Cell 5, 434–41. doi:10.1016/j.stem.2009.08.021
Haeckel, E., 1868. Natürliche Schöpfungsgeschichte. Georg Reimer, Berlin.
Handyside, A., Hooper, M.L., Kaufman, M.H., Wilmut, I., 1987. Towards the isolation of embryonal stem cell lines from the sheep. Roux's Arch. Dev. Biol. 196, 185–190. doi:10.1007/BF00376313
Hausburg, F., Na, S., Voronina, N., Skorska, A., Müller, P., Steinhoff, G., David, R., 2015. Defining optimized properties of modified mRNA to enhance virus- and DNA- independent protein expression in adult stem cells and fibroblasts. Cell. Physiol. Biochem. 35, 1360–71. doi:10.1159/000373957
Heilker, R., Traub, S., Reinhardt, P., Schöler, H.R., Sterneckert, J., 2014. iPS cell derived neuronal cells for drug discovery. Trends Pharmacol. Sci. 35, 510–9. doi:10.1016/j.tips.2014.07.003
Heinemann, T., Honnefelder, L., 2002. Principles of Ethical Decision Making Regarding Embrionic Stem Cell Research in Germany. Bioethics 16, 530–543. doi:10.1111/1467-8519.00309
Hemmati-Brivanlou, A., Kelly, O.G., Melton, D.A., 1994. Follistatin, an antagonist of activin, is expressed in the Spemann organizer and displays direct neuralizing activity. Cell 77, 283–95.
Hevers, W., Lüddens, H., 1998. The diversity of GABAA receptors. Pharmacological and electrophysiological properties of GABAA channel subtypes. Mol. Neurobiol. 18, 35–86. doi:10.1007/BF02741459
Ho, R., Sances, S., Gowing, G., Amoroso, M.W., O'Rourke, J.G., Sahabian, A., Wichterle, H., Baloh, R.H., Sareen, D., Svendsen, C.N., 2016. ALS disrupts spinal motor neuron maturation and aging pathways within gene co-expression networks. Nat. Neurosci. 19, 1256–67. doi:10.1038/nn.4345
Hook, L., Vives, J., Fulton, N., Leveridge, M., Lingard, S., Bootman, M.D., Falk, A., Pollard, S.M., Allsopp, T.E., Dalma-Weiszhausz, D., Tsukamoto, A., Uchida, N., Gorba, T., 2011. Non-immortalized human neural stem (NS) cells as a scalable platform for cellular assays. Neurochem. Int. 59, 432–444. doi:10.1016/j.neuint.2011.06.024
Horiguchi, S., Takahashi, J., Kishi, Y., Morizane, A., Okamoto, Y., Koyanagi, M., Tsuji, M., Tashiro, K., Honjo, T., Fujii, S., Hashimoto, N., 2004. Neural precursor cells derived from human embryonic brain retain regional specificity. J. Neurosci. Res. 75, 817–824. doi:10.1002/jnr.20046
Horvath, S., 2013. DNA methylation age of human tissues and cell types. Genome Biol. 14, R115. doi:10.1186/gb-2013-14-10-r115
Hou, P., Li, Y., Zhang, X., Liu, C., Guan, J., Li, H., Zhao, T., Ye, J., Yang, W., Liu, K., Ge, J., Xu, J., Zhang, Q., Zhao, Y., Deng, H., 2013. Pluripotent stem cells induced from mouse somatic cells by small-molecule compounds. Science 341, 651–4. doi:10.1126/science.1239278
Inman, G.J., Nicolás, F.J., Callahan, J.F., Harling, J.D., Gaster, L.M., Reith, A.D., Laping, N.J., Hill, C.S., 2002. SB-431542 is a potent and specific inhibitor of transforming growth factor-beta superfamily type I activin receptor-like kinase (ALK) receptors ALK4, ALK5, and ALK7. Mol. Pharmacol. 62, 65–74.
Israel, M.A., Yuan, S.H., Bardy, C., Reyna, S.M., Mu, Y., Herrera, C., Hefferan, M.P., Van Gorp, S., Nazor, K.L., Boscolo, F.S., Carson, C.T., Laurent, L.C., Marsala, M., Gage, F.H., Remes, A.M., Koo, E.H., Goldstein, L.S.B., 2012. Probing sporadic and familial Alzheimer's disease using induced pluripotent stem cells. Nature 482, 216–20. doi:10.1038/nature10821
Ivanova, N.B., Dimos, J.T., Schaniel, C., Hackney, J.A., Moore, K.A., Lemischka, I.R., 2002. A stem cell molecular signature. Science 298, 601–4. doi:10.1126/science.1073823
Jain, M., Armstrong, R.J.E., Tyers, P., Barker, R.A., Rosser, A.E., 2003. GABAergic immunoreactivity is predominant in neurons derived from expanded human neural precursor cells in vitro. Exp. Neurol. 182, 113–23.
Jessberger, S., Gage, F.H., 2014. Adult neurogenesis: bridging the gap between mice and humans. Trends Cell Biol. 24, 558–63. doi:10.1016/j.tcb.2014.07.003
Kadari, A., Lu, M., Li, M., Sekaran, T., Thummer, R.P., Guyette, N., Chu, V., Edenhofer, F., 2014. Excision of viral reprogramming cassettes by Cre protein transduction enables rapid, robust and efficient derivation of transgene-free human induced pluripotent stem cells. Stem Cell Res. Ther.

5, 47. doi:10.1186/scrt435

Kadoya, K., Lu, P., Nguyen, K., Lee-Kubli, C., Kumamaru, H., Yao, L., Knackert, J., Poplawski, G., Dulin, J.N., Strobl, H., Takashima, Y., Biane, J., Conner, J., Zhang, S.-C., Tuszynski, M.H., 2016. Spinal cord reconstitution with homologous neural grafts enables robust corticospinal regeneration. Nat. Med. 22, 479–487. doi:10.1038/nm.4066

Kalyani, A., Hobson, K., Rao, M.S., 1997. Neuroepithelial stem cells from the embryonic spinal cord: isolation, characterization, and clonal analysis. Dev. Biol. 186, 202–23. doi:10.1006/dbio.1997.8592

Kandasamy, M., Reilmann, R., Winkler, J., Bogdahn, U., Aigner, L., 2011. Transforming Growth Factor-Beta Signaling in the Neural Stem Cell Niche: A Therapeutic Target for Huntington's Disease. Neurol. Res. Int. 2011, 124256. doi:10.1155/2011/124256

Kee, N., Volakakis, N., Kirkeby, A., Dahl, L., Storvall, H., Nolbrant, S., Lahti, L., Björklund, Å.K., Gillberg, L., Joodmardi, E., Sandberg, R., Parmar, M., Perlmann, T., 2016. Single-Cell Analysis Reveals a Close Relationship between Differentiating Dopamine and Subthalamic Nucleus Neuronal Lineages. Cell Stem Cell. doi:10.1016/j.stem.2016.10.003

Kehler, J., Greco, M., Martino, V., Pachiappan, M., Yokoe, H., Chen, A., Yang, M., Jessee, J., Gotte, M., Milanesi, L., Albertini, A., Bellipanni, G., Zucchi, I., Reinbold, R.A., Giordano, A., 2016. RNA-Generated and Gene-Edited Induced Pluripotent Stem Cells for Disease Modeling and Therapy. J. Cell. Physiol. doi:10.1002/jcp.25597

Keiko, M., Ayaka, N., Hideshi, K., Kouichi, H., Sasai, Y., Muguruma, K., Nishiyama, A., Kawakami, H., Hashimoto, K., Sasai, Y., 2015. Self-organization of polarized cerebellar tissue in 3D culture of human pluripotent stem cells. Cell Rep. 10, 537–550. doi:10.1016/j.celrep.2014.12.051

Kempermann, G., Kuhn, H.G., Gage, F.H., 1997. More hippocampal neurons in adult mice living in an enriched environment. Nature 386, 493–5. doi:10.1038/386493a0

Kim, D., Kim, C.-H., Moon, J.-I., Chung, Y.-G., Chang, M.-Y., Han, B.-S., Ko, S., Yang, E., Cha, K.Y., Lanza, R., Kim, K.-S., 2009. Generation of human induced pluripotent stem cells by direct delivery of reprogramming proteins. Cell Stem Cell 4, 472–6. doi:10.1016/j.stem.2009.05.005

Kim, H.J., Lee, H.J., Kim, H., Cho, S.W., Kim, J.-S., 2009. Targeted genome editing in human cells with zinc finger nucleases constructed via modular assembly. Genome Res. 19, 1279–88. doi:10.1101/gr.089417.108

Kim, J., Efe, J.A., Zhu, S., Talantova, M., Yuan, X., Wang, S., Lipton, S.A., Zhang, K., Ding, S., 2011. Direct reprogramming of mouse fibroblasts to neural progenitors. Proc. Natl. Acad. Sci. U. S. A. 108, 7838–43. doi:10.1073/pnas.1103113108

Kim, S.M., Flaßkamp, H., Hermann, A., Araúzo-Bravo, M.J., Lee, S.C., Lee, S.H., Seo, E.H., Lee, S.H., Storch, A., Lee, H.T., Schöler, H.R., Tapia, N., Han, D.W., 2014. Direct conversion of mouse fibroblasts into induced neural stem cells. Nat. Protoc. 9, 871–81. doi:10.1038/nprot.2014.056

Kirkeby, A., Grealish, S., Wolf, D.A., Nelander, J., Wood, J., Lundblad, M., Lindvall, O., Parmar, M., 2012. Generation of regionally specified neural progenitors and functional neurons from human embryonic stem cells under defined conditions. Cell Rep. 1, 703–14. doi:10.1016/j.celrep.2012.04.009

Kirkeby, A., Nolbrant, S., Tiklova, K., Heuer, A., Kee, N., Cardoso, T., Ottosson, D.R., Lelos, M.J., Rifes, P., Dunnett, S.B., Grealish, S., Perlmann, T., Parmar, M., 2016. Predictive Markers Guide Differentiation to Improve Graft Outcome in Clinical Translation of hESC-Based Therapy for Parkinson's Disease. Cell Stem Cell. doi:10.1016/j.stem.2016.09.004

Kobayashi, D., Kobayashi, M., Matsumoto, K., Ogura, T., Nakafuku, M., Shimamura, K., 2002. Early subdivisions in the neural plate define distinct competence for inductive signals. Development 129, 83–93.

Koch, P., Opitz, T., Steinbeck, J.A., Ladewig, J., Brüstle, O., 2009. A rosette-type, self-renewing human ES cell-derived neural stem cell with potential for in vitro instruction and synaptic integration. Proc. Natl. Acad. Sci. U. S. A. 106, 3225–30. doi:10.1073/pnas.0808387106

Krabbe, C., Bak, S.T., Jensen, P., von Linstow, C., Martínez Serrano, A., Hansen, C., Meyer, M., 2014. Influence of oxygen tension on dopaminergic differentiation of human fetal stem cells of midbrain and forebrain origin. PLoS One 9, e96465. doi:10.1371/journal.pone.0096465

Kriegstein, A., Alvarez-Buylla, A., 2009. The glial nature of embryonic and adult neural stem cells. Annu. Rev. Neurosci. 32, 149–84. doi:10.1146/annurev.neuro.051508.135600

Kriks, S., Shim, J.-W., Piao, J., Ganat, Y.M., Wakeman, D.R., Xie, Z., Carrillo-Reid, L., Auyeung, G., Antonacci, C., Buch, A., Yang, L., Beal, M.F., Surmeier, D.J., Kordower, J.H., Tabar, V., Studer, L., 2011. Dopamine neurons derived from human ES cells efficiently engraft in animal models of Parkinson's disease. Nature 480, 547–51. doi:10.1038/nature10648

Kudoh, T., Wilson, S.W., Dawid, I.B., 2002. Distinct roles for Fgf, Wnt and retinoic acid in posteriorizing the neural ectoderm. Development 129, 4335–46.

Kutejova, E., Sasai, N., Shah, A., Gouti, M., Briscoe, J., 2016. Neural Progenitors Adopt Specific

Identities by Directly Repressing All Alternative Progenitor Transcriptional Programs. Dev. Cell 36, 639–53. doi:10.1016/j.devcel.2016.02.013

Ladewig, J., Mertens, J., Kesavan, J., Doerr, J., Poppe, D., Glaue, F., Herms, S., Wernet, P., Kögler, G., Müller, F.-J., Koch, P., Brüstle, O., 2012. Small molecules enable highly efficient neuronal conversion of human fibroblasts. Nat. Methods 9, 575–8. doi:10.1038/nmeth.1972

Lai, K., Kaspar, B.K., Gage, F.H., Schaffer, D. V, 2003. Sonic hedgehog regulates adult neural progenitor proliferation in vitro and in vivo. Nat. Neurosci. 6, 21–7. doi:10.1038/nn983

Lancaster, M.A., Renner, M., Martin, C.-A., Wenzel, D., Bicknell, L.S., Hurles, M.E., Homfray, T., Penninger, J.M., Jackson, A.P., Knoblich, J.A., 2013. Cerebral organoids model human brain development and microcephaly. Nature 501, 373–9. doi:10.1038/nature12517

Lauder, J., 2013. Molecular Aspects of Development and Aging of the Nervous System. Springer Science & Business Media.

Le Dréau, G., Martí, E., 2012. Dorsal-ventral patterning of the neural tube: a tale of three signals. Dev. Neurobiol. 72, 1471–81. doi:10.1002/dneu.22015

Lee, G., Kim, H., Elkabetz, Y., Al Shamy, G., Panagiotakos, G., Barberi, T., Tabar, V., Studer, L., 2007. Isolation and directed differentiation of neural crest stem cells derived from human embryonic stem cells (Supplemental Info). Nat. Biotechnol. 25, 1468–1475. doi:10.1038/nbt1365

Lee, J.-H., Mitchell, R.R., McNicol, J.D., Shapovalova, Z., Laronde, S., Tanasijevic, B., Milsom, C., Casado, F., Fiebig-Comyn, A., Collins, T.J., Singh, K.K., Bhatia, M., 2015. Single Transcription Factor Conversion of Human Blood Fate to NPCs with CNS and PNS Developmental Capacity. Cell Rep. 11, 1367–76. doi:10.1016/j.celrep.2015.04.056

Lee, K.-I., Lee, S.-Y., Hwang, D.-Y., 2016. Extracellular Matrix-Dependent Generation of Integration- and Xeno-Free iPS Cells Using a Modified mRNA Transfection Method. Stem Cells Int. 2016, 6853081. doi:10.1155/2016/6853081

Lee, K.J., Jessell, T.M., 1999. The specification of dorsal cell fates in the vertebrate central nervous system. Annu. Rev. Neurosci. 22, 261–94. doi:10.1146/annurev.neuro.22.1.261

Lee, K.S., Zhou, W., Scott-McKean, J.J., Emmerling, K.L., Cai, G., Krah, D.L., Costa, A.C., Freed, C.R., Levin, M.J., 2012. Human sensory neurons derived from induced pluripotent stem cells support varicella-zoster virus infection. PLoS One 7, e53010. doi:10.1371/journal.pone.0053010

Levine, A.J., Brivanlou, A.H., 2007. Proposal of a model of mammalian neural induction. Dev. Biol. 308, 247–56. doi:10.1016/j.ydbio.2007.05.036

Li, C., Zhou, J., Shi, G., Ma, Y., Yang, Y., Gu, J., Yu, H., Jin, S., Wei, Z., Chen, F., Jin, Y., 2009. Pluripotency can be rapidly and efficiently induced in human amniotic fluid-derived cells. Hum. Mol. Genet. 18, 4340–9. doi:10.1093/hmg/ddp386

Li, W., Englund, E., Widner, H., Mattsson, B., van Westen, D., Lätt, J., Rehncrona, S., Brundin, P., Björklund, A., Lindvall, O., Li, J.-Y., 2016. Extensive graft-derived dopaminergic innervation is maintained 24 years after transplantation in the degenerating parkinsonian brain. Proc. Natl. Acad. Sci. U. S. A. doi:10.1073/pnas.1605245113

Li, W., Sun, W., Zhang, Y., Wei, W., Ambasudhan, R., Xia, P., Talantova, M., Lin, T., Kim, J., Wang, X., Kim, W.R., Lipton, S.A., Zhang, K., Ding, S., 2011. Rapid induction and long-term self-renewal of primitive neural precursors from human embryonic stem cells by small molecule inhibitors. Proc. … 108, 8299–8304. doi:10.1073/pnas.1014041108

Lim, M.-S., Lee, S.Y., Park, C.-H., 2015. FGF8 is Essential for Functionality of Induced Neural Precursor Cell-derived Dopaminergic Neurons. Int. J. stem cells 8, 228–34. doi:10.15283/ijsc.2015.8.2.228

Lin, T., Ambasudhan, R., Yuan, X., Li, W., Hilcove, S., Abujarour, R., Lin, X., Hahm, H.S., Hao, E., Hayek, A., Ding, S., 2009. A chemical platform for improved induction of human iPSCs. Nat. Methods 6, 805–8. doi:10.1038/nmeth.1393

Lin, T., Wu, S., 2015. Reprogramming with Small Molecules instead of Exogenous Transcription Factors. Stem Cells Int. 2015, 794632. doi:10.1155/2015/794632

Lippmann, E.S., Al-Ahmad, A., Palecek, S.P., Shusta, E. V, 2013. Modeling the blood–brain barrier using stem cell sources. Fluids Barriers CNS 10, 2. doi:10.1186/2045-8118-10-2

Lippmann, E.S., Azarin, S.M., Kay, J.E., Nessler, R.A., Wilson, H.K., Al-Ahmad, A., Palecek, S.P., Shusta, E. V, 2012. Derivation of blood-brain barrier endothelial cells from human pluripotent stem cells. Nat. Biotechnol. 30, 783–91. doi:10.1038/nbt.2247

Liu, G.-H., Barkho, B.Z., Ruiz, S., Diep, D., Qu, J., Yang, S.-L., Panopoulos, A.D., Suzuki, K., Kurian, L., Walsh, C., Thompson, J., Boue, S., Fung, H.L., Sancho-Martinez, I., Zhang, K., Yates, J., Izpisua Belmonte, J.C., 2011. Recapitulation of premature ageing with iPSCs from Hutchinson-Gilford progeria syndrome. Nature 472, 221–5. doi:10.1038/nature09879

Liu, H., Ye, Z., Kim, Y., Sharkis, S., Jang, Y.-Y., 2010. Generation of endoderm-derived human induced pluripotent stem cells from primary hepatocytes. Hepatology 51, 1810–9. doi:10.1002/hep.23626

Loessner, D., Meinert, C., Kaemmerer, E., Martine, L.C., Yue, K., Levett, P.A., Klein, T.J., Melchels, F.P.W., Khademhosseini, A., Hutmacher, D.W., 2016. Functionalization, preparation and use of cell-laden gelatin methacryloyl-based hydrogels as modular tissue culture platforms. Nat. Protoc. 11, 727–46. doi:10.1038/nprot.2016.037

Logan, C.Y., Nusse, R., 2004. The Wnt signaling pathway in development and disease. Annu. Rev. Cell Dev. Biol. 20, 781–810. doi:10.1146/annurev.cellbio.20.010403.113126

Loh, Y.-H., Hartung, O., Li, H., Guo, C., Sahalie, J.M., Manos, P.D., Urbach, A., Heffner, G.C., Grskovic, M., Vigneault, F., Lensch, M.W., Park, I.-H., Agarwal, S., Church, G.M., Collins, J.J., Irion, S., Daley, G.Q., 2010. Reprogramming of T cells from human peripheral blood. Cell Stem Cell 7, 15–9. doi:10.1016/j.stem.2010.06.004

Lois, C., Alvarez-Buylla, A., 1993. Proliferating subventricular zone cells in the adult mammalian forebrain can differentiate into neurons and glia. Proc. Natl. Acad. Sci. U. S. A. 90, 2074–7.

Lotharius, J., Barg, S., Wiekop, P., Lundberg, C., Raymon, H.K., Brundin, P., 2002. Effect of mutant alpha-synuclein on dopamine homeostasis in a new human mesencephalic cell line. J. Biol. Chem. 277, 38884–94. doi:10.1074/jbc.M205518200

Louvi, A., Artavanis-Tsakonas, S., 2006. Notch signalling in vertebrate neural development. Nat. Rev. Neurosci. 7, 93–102. doi:10.1038/nrn1847

Lowery, L.A., Sive, H., 2004. Strategies of vertebrate neurulation and a re-evaluation of teleost neural tube formation. Mech. Dev. 121, 1189–97. doi:10.1016/j.mod.2004.04.022

Lu, J., Liu, H., Huang, C.L., Chen, H., Du, Z., Liu, Y., Sherafat, M.A., Zhang, S.C., 2013. Generation of Integration-free and Region-Specific Neural Progenitors from Primate Fibroblasts. Cell Rep. 3, 1580–1591. doi:10.1016/j.celrep.2013.04.004

Lu, J., Zhong, X., Liu, H., Hao, L., Huang, C.T.-L., Sherafat, M.A., Jones, J., Ayala, M., Li, L., Zhang, S.-C., 2016. Generation of serotonin neurons from human pluripotent stem cells. Nat. Biotechnol. 34, 89–94. doi:10.1038/nbt.3435

Lumsden, A., Krumlauf, R., 1996. Patterning the vertebrate neuraxis. Science 274, 1109–15.

Magnuson, T., Epstein, C.J., Silver, L.M., Martin, G.R., 1982. Pluripotent embryonic stem cell lines can be derived from tw5/tw5 blastocysts. Nature 298, 750–3.

Mali, P., Yang, L., Esvelt, K.M., Aach, J., Guell, M., DiCarlo, J.E., Norville, J.E., Church, G.M., 2013. RNA-guided human genome engineering via Cas9. Science 339, 823–6. doi:10.1126/science.1232033

Marchetto, M.C.N., Carromeu, C., Acab, A., Yu, D., Yeo, G.W., Mu, Y., Chen, G., Gage, F.H., Muotri, A.R., 2010. A model for neural development and treatment of Rett syndrome using human induced pluripotent stem cells. Cell 143, 527–39. doi:10.1016/j.cell.2010.10.016

Martin, G.R., 1981. Isolation of a pluripotent cell line from early mouse embryos cultured in medium conditioned by teratocarcinoma stem cells. Proc. Natl. Acad. Sci. 78, 7634–7638. doi:10.1073/pnas.78.12.7634

Meinhardt, A., Eberle, D., Tazaki, A., Ranga, A., Niesche, M., Wilsch-Bräuninger, M., Stec, A., Schackert, G., Lutolf, M., Tanaka, E.M., 2014. 3D reconstitution of the patterned neural tube from embryonic stem cells. Stem cell reports 3, 987–99. doi:10.1016/j.stemcr.2014.09.020

Menendez, L., Kulik, M.J., Page, A.T., Park, S.S., Lauderdale, J.D., Cunningham, M.L., Dalton, S., 2013. Directed differentiation of human pluripotent cells to neural crest stem cells. Nat. Protoc. 8, 203–12. doi:10.1038/nprot.2012.156

Merling, R.K., Sweeney, C.L., Choi, U., De Ravin, S.S., Myers, T.G., Otaizo-Carrasquero, F., Pan, J., Linton, G., Chen, L., Koontz, S., Theobald, N.L., Malech, H.L., 2013. Transgene-free iPSCs generated from small volume peripheral blood nonmobilized CD34+ cells. Blood 121, e98-107. doi:10.1182/blood-2012-03-420273

Mertens, J., Marchetto, M.C., Bardy, C., Gage, F.H., 2016. Evaluating cell reprogramming, differentiation and conversion technologies in neuroscience. Nat. Rev. Neurosci. advance on. doi:10.1038/nrn.2016.46

Mertens, J., Paquola, A.C.M., Ku, M., Hatch, E., Böhnke, L., Ladjevardi, S., McGrath, S., Campbell, B., Lee, H., Herdy, J.R., Gonçalves, J.T., Toda, T., Kim, Y., Winkler, J., Yao, J., Hetzer, M.W., Gage, F.H., 2015. Directly Reprogrammed Human Neurons Retain Aging-Associated Transcriptomic Signatures and Reveal Age-Related Nucleocytoplasmic Defects. Cell Stem Cell 17, 705–18. doi:10.1016/j.stem.2015.09.001

Meyer, S., Wörsdörfer, P., Günther, K., Thier, M., Edenhofer, F., 2015. Derivation of Adult Human Fibroblasts and their Direct Conversion into Expandable Neural Progenitor Cells. J. Vis. Exp. e52831. doi:10.3791/52831

Miki, T., Yasuda, S., Kahn, M., 2011. Wnt/β-catenin signaling in embryonic stem cell self-renewal and somatic cell reprogramming. Stem Cell Rev. 7, 836–46. doi:10.1007/s12015-011-9275-1

Miller, J.C., Tan, S., Qiao, G., Barlow, K.A., Wang, J., Xia, D.F., Meng, X., Paschon, D.E., Leung, E., Hinkley, S.J., Dulay, G.P., Hua, K.L., Ankoudinova, I., Cost, G.J., Urnov, F.D., Zhang, H.S., Holmes, M.C., Zhang, L., Gregory, P.D., Rebar, E.J., 2011. A TALE nuclease architecture for efficient genome editing. Nat. Biotechnol. 29, 143–8. doi:10.1038/nbt.1755

Miller, J.D., Ganat, Y.M., Kishinevsky, S., Bowman, R.L., Liu, B., Tu, E.Y., Mandal, P.K., Vera, E., Shim, J.W., Kriks, S., Taldone, T., Fusaki, N., Tomishima, M.J., Krainc, D., Milner, T.A., Rossi, D.J., Studer, L., 2013. Human iPSC-based modeling of late-onset disease via progerin-induced aging. Cell Stem Cell 13, 691–705. doi:10.1016/j.stem.2013.11.006

Millonig, J.H., Millen, K.J., Hatten, M.E., 2000. The mouse Dreher gene Lmx1a controls formation of the roof plate in the vertebrate CNS. Nature 403, 764–9. doi:10.1038/35001573

Miura, K., Okada, Y., Aoi, T., Okada, A., Takahashi, K., Okita, K., Nakagawa, M., Koyanagi, M., Tanabe, K., Ohnuki, M., Ogawa, D., Ikeda, E., Okano, H., Yamanaka, S., 2009. Variation in the safety of induced pluripotent stem cell lines. Nat. Biotechnol. 27, 743–5. doi:10.1038/nbt.1554

Miura, T., Sugawara, T., Fukuda, A., Tamoto, R., Kawasaki, T., Umezawa, A., Akutsu, H., 2015. Generation of primitive neural stem cells from human fibroblasts using a defined set of factors. Biol. Open 4, 1595–607. doi:10.1242/bio.013151

Moon, J., Schwarz, S.C., Lee, H.-S., Kang, J.M., Lee, Y.-E., Kim, B., Sung, M.-Y., Höglinger, G., Wegner, F., Kim, J.S., Chung, H.-M., Chang, S.W., Cha, K.Y., Kim, K.-S., Schwarz, J., 2016. Preclinical Analysis of Fetal Human Mesencephalic Neural Progenitor Cell Lines: Characterization and Safety In Vitro and In Vivo. Stem Cells Transl. Med. doi:10.5966/sctm.2015-0228

Morris, R.J., Liu, Y., Marles, L., Yang, Z., Trempus, C., Li, S., Lin, J.S., Sawicki, J.A., Cotsarelis, G., 2004. Capturing and profiling adult hair follicle stem cells. Nat. Biotechnol. 22, 411–7. doi:10.1038/nbt950

Moya, N., Cutts, J., Gaasterland, T., Willert, K., Brafman, D.A., 2014. Endogenous WNT signaling regulates hPSC-derived neural progenitor cell heterogeneity and specifies their regional identity. Stem cell reports 3, 1015–28. doi:10.1016/j.stemcr.2014.10.004

Mujtaba, T., Piper, D.R., Kalyani, A., Groves, A.K., Lucero, M.T., Rao, M.S., 1999. Lineage-restricted neural precursors can be isolated from both the mouse neural tube and cultured ES cells. Dev Biol 214, 113–127. doi:10.1006/dbio.1999.9418

Nakagawa, M., Koyanagi, M., Tanabe, K., Takahashi, K., Ichisaka, T., Aoi, T., Okita, K., Mochiduki, Y., Takizawa, N., Yamanaka, S., 2008. Generation of induced pluripotent stem cells without Myc from mouse and human fibroblasts. Nat. Biotechnol. 26, 101–6. doi:10.1038/nbt1374

Nat, R., 2016. Pluripotent Stem Cells - From the Bench to the Clinic. InTech. doi:10.5772/61549

Nguyen, H.N., Byers, B., Cord, B., Shcheglovitov, A., Byrne, J., Gujar, P., Kee, K., Schüle, B., Dolmetsch, R.E., Langston, W., Palmer, T.D., Pera, R.R., 2011. LRRK2 mutant iPSC-derived DA neurons demonstrate increased susceptibility to oxidative stress. Cell Stem Cell 8, 267–80. doi:10.1016/j.stem.2011.01.013

Niehrs, C., 2004. Regionally specific induction by the Spemann-Mangold organizer. Nat. Rev. Genet. 5, 425–34. doi:10.1038/nrg1347

Nierode, G.J., Perea, B.C., McFarland, S.K., Pascoal, J.F., Clark, D.S., Schaffer, D.V., Dordick, J.S., 2016. High-Throughput Toxicity and Phenotypic Screening of 3D Human Neural Progenitor Cell Cultures on a Microarray Chip Platform. Stem Cell Reports. doi:10.1016/j.stemcr.2016.10.001

Niwa, H., 2001. Molecular mechanism to maintain stem cell renewal of ES cells. Cell Struct. Funct. 26, 137–48.

Niwa, H., Miyazaki, J., Smith, A.G., 2000. Quantitative expression of Oct-3/4 defines differentiation, dedifferentiation or self-renewal of ES cells. Nat. Genet. 24, 372–6. doi:10.1038/74199

Ogawa, M., 1993. Differentiation and proliferation of hematopoietic stem cells. Blood 81, 2844–53.

Oh, H., Bradfute, S.B., Gallardo, T.D., Nakamura, T., Gaussin, V., Mishina, Y., Pocius, J., Michael, L.H., Behringer, R.R., Garry, D.J., Entman, M.L., Schneider, M.D., 2003. Cardiac progenitor cells from adult myocardium: homing, differentiation, and fusion after infarction. Proc. Natl. Acad. Sci. U. S. A. 100, 12313–8. doi:10.1073/pnas.2132126100

Okita, K., Ichisaka, T., Yamanaka, S., 2007. Generation of germline-competent induced pluripotent stem cells. Nature 448, 313–7. doi:10.1038/nature05934

Okita, K., Matsumura, Y., Sato, Y., Okada, A., Morizane, A., Okamoto, S., Hong, H., Nakagawa, M., Tanabe, K., Tezuka, K., Shibata, T., Kunisada, T., Takahashi, M., Takahashi, J., Saji, H., Yamanaka, S., 2011. A more efficient method to generate integration-free human iPS cells. Nat. Methods 8, 409–12. doi:10.1038/nmeth.1591

Okita, K., Nakagawa, M., Hyenjong, H., Ichisaka, T., Yamanaka, S., 2008. Generation of mouse induced pluripotent stem cells without viral vectors. Science 322, 949–53. doi:10.1126/science.1164270

Okubo, T., Iwanami, A., Kohyama, J., Itakura, G., Kawabata, S., Nishiyama, Y., Sugai, K., Ozaki, M., Iida, T., Matsubayashi, K., Matsumoto, M., Nakamura, M., Okano, H., 2016. Pretreatment with a γ-Secretase Inhibitor Prevents Tumor-like Overgrowth in Human iPSC-Derived Transplants for Spinal Cord Injury. Stem Cell Reports. doi:10.1016/j.stemcr.2016.08.015

Pang, Z.P., Yang, N., Vierbuchen, T., Ostermeier, A., Fuentes, D.R., Yang, T.Q., Citri, A., Sebastiano, V., Marro, S., Südhof, T.C., Wernig, M., 2011. Induction of human neuronal cells by defined transcription factors. Nature 476, 220–223. doi:10.1038/nature10202

Park, I.-H., Arora, N., Huo, H., Maherali, N., Ahfeldt, T., Shimamura, A., Lensch, M.W., Cowan, C., Hochedlinger, K., Daley, G.Q., 2008. Disease-specific induced pluripotent stem cells. Cell 134, 877–86. doi:10.1016/j.cell.2008.07.041

Patthey, C., Edlund, T., Gunhaga, L., 2009. Wnt-regulated temporal control of BMP exposure directs the choice between neural plate border and epidermal fate. Development 136, 73–83. doi:10.1242/dev.025890

Patthey, C., Gunhaga, L., Edlund, T., 2008. Early development of the central and peripheral nervous systems is coordinated by Wnt and BMP signals. PLoS One 3, e1625. doi:10.1371/journal.pone.0001625

Peretz, Y., Eren, N., Kohl, A., Hen, G., Yaniv, K., Weisinger, K., Cinnamon, Y., Sela-Donenfeld, D., 2016. A new role of hindbrain boundaries as pools of neural stem/progenitor cells regulated by Sox2. BMC Biol. 14, 57. doi:10.1186/s12915-016-0277-y

Perrier, A.L., Tabar, V., Barberi, T., Rubio, M.E., Bruses, J., Topf, N., Harrison, N.L., Studer, L., 2004. Derivation of midbrain dopamine neurons from human embryonic stem cells. Proc. Natl. Acad. Sci. U. S. A. 101, 12543–8. doi:10.1073/pnas.0404700101

Pevny, L.H., Nicolis, S.K., 2010. Sox2 roles in neural stem cells. Int. J. Biochem. Cell Biol. 42, 421–424. doi:10.1016/j.biocel.2009.08.018

Pfisterer, U., Kirkeby, A., Torper, O., Wood, J., Nelander, J., Dufour, A., Björklund, A., Lindvall, O., Jakobsson, J., Parmar, M., 2011. Direct conversion of human fibroblasts to dopaminergic neurons. Proc. Natl. Acad. Sci. U. S. A. 108, 10343–10348. doi:10.1073/pnas.1105135108

Pollard, S.M., Conti, L., Sun, Y., Goffredo, D., Smith, A., 2006. Adherent neural stem (NS) cells from fetal and adult forebrain. Cereb. Cortex 16 Suppl 1, i112-20. doi:10.1093/cercor/bhj167

Polo, J.M., Anderssen, E., Walsh, R.M., Schwarz, B.A., Nefzger, C.M., Lim, S.M., Borkent, M., Apostolou, E., Alaei, S., Cloutier, J., Bar-Nur, O., Cheloufi, S., Stadtfeld, M., Figueroa, M.E., Robinton, D., Natesan, S., Melnick, A., Zhu, J., Ramaswamy, S., Hochedlinger, K., 2012. A molecular roadmap of reprogramming somatic cells into iPS cells. Cell 151, 1617–1632. doi:10.1016/j.cell.2012.11.039

Prè, D., Nestor, M.W., Sproul, A.A., Jacob, S., Koppensteiner, P., Chinchalongporn, V., Zimmer, M., Yamamoto, A., Noggle, S.A., Arancio, O., 2014. A time course analysis of the electrophysiological properties of neurons differentiated from human induced pluripotent stem cells (iPSCs). PLoS One 9, e103418. doi:10.1371/journal.pone.0103418

Qian, X., Shen, Q., Goderie, S.K., He, W., Capela, A., Davis, A.A., Temple, S., 2000. Timing of CNS cell generation: a programmed sequence of neuron and glial cell production from isolated murine cortical stem cells. Neuron 28, 69–80.

Qian, X., Shen, Q., Goderie, S.K., He, W., Capela, A., Davis, A.A., Temple, S., 2000. Timing of CNS Cell Generation. Neuron 28, 69–80. doi:10.1016/S0896-6273(00)00086-6

Ramalho-Santos, M., Willenbring, H., 2007. On the origin of the term “stem cell”. Cell Stem Cell 1, 35–8. doi:10.1016/j.stem.2007.05.013

Ramalho-Santos, M., Yoon, S., Matsuzaki, Y., Mulligan, R.C., Melton, D.A., 2002. “Stemness”: transcriptional profiling of embryonic and adult stem cells. Science 298, 597–600. doi:10.1126/science.1072530

Ran, F.A., Hsu, P.D., Wright, J., Agarwala, V., Scott, D.A., Zhang, F., 2013. Genome engineering using the CRISPR-Cas9 system. Nat. Protoc. 8, 2281–308. doi:10.1038/nprot.2013.143

Ranga, A., Girgin, M., Meinhardt, A., Eberle, D., Caiazzo, M., Tanaka, E.M., Lutolf, M.P., 2016. Neural tube morphogenesis in synthetic 3D microenvironments. Proc. Natl. Acad. Sci. 113, E6831–E6839. doi:10.1073/pnas.1603529113

Reinhardt, P., Glatza, M., Hemmer, K., Tsytsyura, Y., Thiel, C.S., Höing, S., Moritz, S.S., Parga, J.A., Wagner, L., Bruder, J.M., Wu, G., Schmid, B., Röpke, A., Klingauf, J.J., Schwamborn, J.C., Gasser, T., Schöler, H.R., Sterneckert, J., H??ing, S., Moritz, S.S., Parga, J.A., Wagner, L., Bruder, J.M., Wu, G., Schmid, B., R??pke, A., Klingauf, J.J., Schwamborn, J.C., Gasser, T., Sch??ler, H.R., Sterneckert, J., 2013. Derivation and expansion using only small molecules of human neural progenitors for neurodegenerative disease modeling. PLoS One 8, e59252. doi:10.1371/journal.pone.0059252

Reynolds, B.A., Weiss, S., 1992. Generation of neurons and astrocytes from isolated cells of the adult mammalian central nervous system. Science 255, 1707–10.

Rhinn, M., Dollé, P., 2012. Retinoic acid signalling during development. Development 139, 843–58. doi:10.1242/dev.065938

Rimkus, T.K., Carpenter, R.L., Qasem, S., Chan, M., Lo, H.-W., 2016. Targeting the Sonic Hedgehog Signaling Pathway: Review of Smoothened and GLI Inhibitors. Cancers (Basel). 8. doi:10.3390/cancers8020022

Ring, K.L., Tong, L.M., Balestra, M.E., Javier, R., Andrews-zwilling, Y., Li, G., Walker, D., Zhang, W.R., Kreitzer, A.C., Huang, Y., 2012. Direct reprogramming of mouse and human fibroblasts into multipotent neural stem cells with a single factor. Cell Stem Cell 11, 1–19. doi:10.1016/j.stem.2012.05.018

Rowitch, D.H., S-Jacques, B., Lee, S.M., Flax, J.D., Snyder, E.Y., McMahon, A.P., 1999. Sonic hedgehog regulates proliferation and inhibits differentiation of CNS precursor cells. J. Neurosci. 19, 8954–65.

Samanta, J., Grund, E.M., Silva, H.M., Lafaille, J.J., Fishell, G., Salzer, J.L., 2015. Inhibition of Gli1 mobilizes endogenous neural stem cells for remyelination. Nature 526, 448–52. doi:10.1038/nature14957

Sánchez-Danés, A., Richaud-Patin, Y., Carballo-Carbajal, I., Jiménez-Delgado, S., Caig, C., Mora, S., Di Guglielmo, C., Ezquerra, M., Patel, B., Giralt, A., Canals, J.M., Memo, M., Alberch, J., López-Barneo, J., Vila, M., Cuervo, A.M., Tolosa, E., Consiglio, A., Raya, A., 2012. Disease-specific phenotypes in dopamine neurons from human iPS-based models of genetic and sporadic Parkinson's disease. EMBO Mol. Med. 4, 380–95. doi:10.1002/emmm.201200215

Sasai, Y., Lu, B., Steinbeisser, H., Geissert, D., Gont, L.K., De Robertis, E.M., 1994. Xenopus chordin: a novel dorsalizing factor activated by organizer-specific homeobox genes. Cell 79, 779–90.

Schlaeger, T.M., Daheron, L., Brickler, T.R., Entwisle, S., Chan, K., Cianci, A., DeVine, A., Ettenger, A., Fitzgerald, K., Godfrey, M., Gupta, D., McPherson, J., Malwadkar, P., Gupta, M., Bell, B., Doi, A., Jung, N., Li, X., Lynes, M.S., Brookes, E., Cherry, A.B.C., Demirbas, D., Tsankov, A.M., Zon, L.I., Rubin, L.L., Feinberg, A.P., Meissner, A., Cowan, C.A., Daley, G.Q., 2015. A comparison of non-integrating reprogramming methods. Nat. Biotechnol. 33, 58–63. doi:10.1038/nbt.3070

Scholzen, T., Gerdes, J., 2000. The Ki-67 protein: from the known and the unknown. J. Cell. Physiol. 182, 311–22. doi:10.1002/(SICI)1097-4652(200003)182:3<311::AID-JCP1>3.0.CO;2-9

Seibler, P., Graziotto, J., Jeong, H., Simunovic, F., Klein, C., Krainc, D., 2011. Mitochondrial Parkin recruitment is impaired in neurons derived from mutant PINK1 induced pluripotent stem cells. J. Neurosci. 31, 5970–6. doi:10.1523/JNEUROSCI.4441-10.2011

Shen, Q., Goderie, S.K., Jin, L., Karanth, N., Sun, Y., Abramova, N., Vincent, P., Pumiglia, K., Temple, S., 2004. Endothelial cells stimulate self-renewal and expand neurogenesis of neural stem cells. Science 304, 1338–40. doi:10.1126/science.1095505

Shi, Y., Do, J.T., Desponts, C., Hahm, H.S., Schöler, H.R., Ding, S., 2008. A combined chemical and genetic approach for the generation of induced pluripotent stem cells. Cell Stem Cell 2, 525–8. doi:10.1016/j.stem.2008.05.011

Shimojo, D., Onodera, K., Doi-Torii, Y., Ishihara, Y., Hattori, C., Miwa, Y., Tanaka, S., Okada, R., Ohyama, M., Shoji, M., Nakanishi, A., Doyu, M., Okano, H., Okada, Y., 2015. Rapid, efficient, and simple motor neuron differentiation from human pluripotent stem cells. Mol. Brain 8, 79. doi:10.1186/s13041-015-0172-4

SIMINOVITCH, L., MCCULLOCH, E.A., TILL, J.E., 1963. THE DISTRIBUTION OF COLONY-FORMING CELLS AMONG SPLEEN COLONIES. J. Cell. Physiol. 62, 327–36.

Sinha, S., Chen, J.K., 2006. Purmorphamine activates the Hedgehog pathway by targeting Smoothened. Nat. Chem. Biol. 2, 29–30. doi:10.1038/nchembio753

Skaper, S.D., Kee, W.J., Facci, L., Macdonald, G., Doherty, P., Walsh, F.S., 2002. The FGFR1 Inhibitor PD 173074 Selectively and Potently Antagonizes FGF-2 Neurotrophic and Neurotropic Effects. J. Neurochem. 75, 1520–1527. doi:10.1046/j.1471-4159.2000.0751520.x

Smith, J., 1997. Neurulation: coming to closure. Trends Neurosci. 20, 510–517. doi:10.1016/S0166-2236(97)01121-1

Smith, W.C., Harland, R.M., 1992. Expression cloning of noggin, a new dorsalizing factor localized to the Spemann organizer in Xenopus embryos. Cell 70, 829–40.

Soldner, F., Hockemeyer, D., Beard, C., Gao, Q., Bell, G.W., Cook, E.G., Hargus, G., Blak, A., Cooper, O., Mitalipova, M., Isacson, O., Jaenisch, R., 2009. Parkinson's disease patient-derived induced pluripotent stem cells free of viral reprogramming factors. Cell 136, 964–77. doi:10.1016/j.cell.2009.02.013

Somers, A., Jean, J.C., Sommer, C.A., Omari, A., Ford, C.C., Mills, J.A., Ying, L., Sommer, A.G., Jean, J.M., Smith, B.W., Lafyatis, R., Demierre, M.F., Weiss, D.J., French, D.L., Gadue, P., Murphy, G.J., Mostoslavsky, G., Kotton, D.N., 2010. Generation of transgene-free lung disease-specific human induced pluripotent stem cells using a single excisable lentiviral stem cell cassette. Stem Cells 28, 1728–1740. doi:10.1002/stem.495

Sommer, C.A., Sommer, A.G., Longmire, T.A., Christodoulou, C., Thomas, D.D., Gostissa, M., Alt, F.W., Murphy, G.J., Kotton, D.N., Mostoslavsky, G., 2010. Excision of reprogramming transgenes improves the differentiation potential of iPS cells generated with a single excisable vector. Stem Cells 28, 64–74. doi:10.1002/stem.255

Sommer, C.A., Stadtfeld, M., Murphy, G.J., Hochedlinger, K., Kotton, D.N., Mostoslavsky, G., 2009. Induced pluripotent stem cell generation using a single lentiviral stem cell cassette. Stem Cells 27, 543–9. doi:10.1634/stemcells.2008-1075

Song, H., Stevens, C.F., Gage, F.H., 2002. Neural stem cells from adult hippocampus develop essential properties of functional CNS neurons. Nat. Neurosci. 5, 438–45. doi:10.1038/nn844

Spemann, H., Mangold, H., 2001. Induction of embryonic primordia by implantation of organizers from a different species. 1923. Int. J. Dev. Biol. 45, 13–38.

Spira, M.E., Hai, A., 2013. Multi-electrode array technologies for neuroscience and cardiology. Nat. Nanotechnol. 8, 83–94. doi:10.1038/nnano.2012.265

Spradling, A., Drummond-Barbosa, D., Kai, T., 2001. Stem cells find their niche. Nature 414, 98–104. doi:10.1038/35102160

Stacpoole, S.R.L., Webber, D.J., Bilican, B., Compston, A., Chandran, S., Franklin, R.J.M., 2013. Neural precursor cells cultured at physiologically relevant oxygen tensions have a survival advantage following transplantation. Stem Cells Transl. Med. 2, 464–72. doi:10.5966/sctm.2012-0144

Stadtfeld, M., Hochedlinger, K., 2010. Induced pluripotency: history, mechanisms, and applications. Genes Dev. 24, 2239–63. doi:10.1101/gad.1963910

Stadtfeld, M., Nagaya, M., Utikal, J., Weir, G., Hochedlinger, K., 2008. Induced pluripotent stem cells generated without viral integration. Science 322, 945–9. doi:10.1126/science.1162494

Staerk, J., Dawlaty, M.M., Gao, Q., Maetzel, D., Hanna, J., Sommer, C.A., Mostoslavsky, G., Jaenisch, R., 2010. Reprogramming of human peripheral blood cells to induced pluripotent stem cells. Cell Stem Cell 7, 20–4. doi:10.1016/j.stem.2010.06.002

Stappenbeck, T.S., Mills, J.C., Gordon, J.I., 2003. Molecular features of adult mouse small intestinal epithelial progenitors. Proc. Natl. Acad. Sci. U. S. A. 100, 1004–9. doi:10.1073/pnas.242735899

Steinbeck, J.A., Studer, L., 2015. Moving stem cells to the clinic: potential and limitations for brain repair. Neuron 86, 187–206. doi:10.1016/j.neuron.2015.03.002

Sterneckert, J.L., Reinhardt, P., Schöler, H.R., 2014. Investigating human disease using stem cell models. Nat. Rev. Genet. 15, 625–39. doi:10.1038/nrg3764

Studer, L., Vera, E., Cornacchia, D., 2015. Programming and Reprogramming Cellular Age in the Era of Induced Pluripotency. Cell Stem Cell 16, 591–600. doi:10.1016/j.stem.2015.05.004

Sugii, S., Kida, Y., Kawamura, T., Suzuki, J., Vassena, R., Yin, Y.-Q., Lutz, M.K., Berggren, W.T., Izpisúa Belmonte, J.C., Evans, R.M., 2010. Human and mouse adipose-derived cells support feeder-independent induction of pluripotent stem cells. Proc. Natl. Acad. Sci. U. S. A. 107, 3558–63. doi:10.1073/pnas.0910172106

Suter, D.M., Tirefort, D., Julien, S., Krause, K.-H., 2009. A Sox1 to Pax6 switch drives neuroectoderm to radial glia progression during differentiation of mouse embryonic stem cells. Stem Cells 27, 49–58. doi:10.1634/stemcells.2008-0319

Suzuki, M., McHugh, J., Tork, C., Shelley, B., Klein, S.M., Aebischer, P., Svendsen, C.N., 2007. GDNF secreting human neural progenitor cells protect dying motor neurons, but not their projection to muscle, in a rat model of familial ALS. PLoS One 2, e689. doi:10.1371/journal.pone.0000689

Svendsen, C.N., ter Borg, M.G., Armstrong, R.J.E., Rosser, A.E., Chandran, S., Ostenfeld, T., Caldwell, M.A., 1998. A new method for the rapid and long term growth of human neural precursor cells. J. Neurosci. Methods 85, 141–152. doi:10.1016/S0165-0270(98)00126-5

Szabadics, J., Varga, C., Molnár, G., Oláh, S., Barzó, P., Tamás, G., 2006. Excitatory effect of GABAergic axo-axonic cells in cortical microcircuits. Science 311, 233–5. doi:10.1126/science.1121325

Tailor, J., Kittappa, R., Leto, K., Gates, M., Borel, M., Paulsen, O., Spitzer, S., Karadottir, R.T., Rossi, F., Falk, A., Smith, A., 2013. Stem cells expanded from the human embryonic hindbrain stably retain regional specification and high neurogenic potency. J Neurosci 33, 12407–12422. doi:10.1523/JNEUROSCI.0130-13.2013

Takahashi, K., Tanabe, K., Ohnuki, M., Narita, M., Ichisaka, T., Tomoda, K., Yamanaka, S., 2007. Induction of pluripotent stem cells from adult human fibroblasts by defined factors. Cell 131, 861–72. doi:10.1016/j.cell.2007.11.019

Takahashi, K., Yamanaka, S., 2006. Induction of pluripotent stem cells from mouse embryonic and adult fibroblast cultures by defined factors. Cell 126, 663–76. doi:10.1016/j.cell.2006.07.024

Tamaki, S., Eckert, K., He, D., Sutton, R., Doshe, M., Jain, G., Tushinski, R., Reitsma, M., Harris, B., Tsukamoto, A., Gage, F., Weissman, I., Uchida, N., 2002. Engraftment of sorted/expanded human central nervous system stem cells from fetal brain. J. Neurosci. Res. 69, 976–986. doi:10.1002/jnr.10412

Tao, Y., Zhang, S.-C., 2016. Neural Subtype Specification from Human Pluripotent Stem Cells. Cell Stem Cell 19, 573–586. doi:10.1016/j.stem.2016.10.015

Temple, S., 2001. The development of neural stem cells. Nature 414, 112–7. doi:10.1038/35102174

Thier, M., Wörsdörfer, P., Lakes, Y.B., Gorris, R., Herms, S., Opitz, T., Seiferling, D., Quandel, T., Hoffmann, P., Nöthen, M.M., Brüstle, O., Edenhofer, F., 2012. Direct conversion of fibroblasts into stably expandable neural stem cells. Cell Stem Cell 10, 473–9. doi:10.1016/j.stem.2012.03.003

Thomson, J.A., 1998. Embryonic Stem Cell Lines Derived from Human Blastocysts. Science (80-.).

282, 1145–1147. doi:10.1126/science.282.5391.1145

Tiemann, U., Sgodda, M., Warlich, E., Ballmaier, M., Schöler, H.R., Schambach, A., Cantz, T., 2011. Optimal reprogramming factor stoichiometry increases colony numbers and affects molecular characteristics of murine induced pluripotent stem cells. Cytometry. A 79, 426–35. doi:10.1002/cyto.a.21072

Till, J.E., McCulloch, E.A., 1980. Hemopoietic stem cell differentiation. Biochim. Biophys. Acta 605, 431–59.

TILL, J.E., McCULLOCH, E.A., 1961. A direct measurement of the radiation sensitivity of normal mouse bone marrow cells. Radiat. Res. 14, 213–22.

Tropepe, V., Hitoshi, S., Sirard, C., Mak, T.W., Rossant, J., van der Kooy, D., 2001. Direct Neural Fate Specification from Embryonic Stem Cells. Neuron 30, 65–78. doi:10.1016/S0896-6273(01)00263-X

Tsurusaki, Y., Koshimizu, E., Ohashi, H., Phadke, S., Kou, I., Shiina, M., Suzuki, T., Okamoto, N., Imamura, S., Yamashita, M., Watanabe, S., Yoshiura, K., Kodera, H., Miyatake, S., Nakashima, M., Saitsu, H., Ogata, K., Ikegawa, S., Miyake, N., Matsumoto, N., 2014. De novo SOX11 mutations cause Coffin-Siris syndrome. Nat. Commun. 5, 4011. doi:10.1038/ncomms5011

Tumbar, T., Guasch, G., Greco, V., Blanpain, C., Lowry, W.E., Rendl, M., Fuchs, E., 2004. Defining the epithelial stem cell niche in skin. Science 303, 359–63. doi:10.1126/science.1092436

Turner, N., Grose, R., 2010. Fibroblast growth factor signalling: from development to cancer. Nat. Rev. Cancer 10, 116–29. doi:10.1038/nrc2780

Uchida, N., Buck, D.W., He, D., Reitsma, M.J., Masek, M., Phan, T. V, Tsukamoto, A.S., Gage, F.H., Weissman, I.L., 2000. Direct isolation of human central nervous system stem cells. Proc. Natl. Acad. Sci. U. S. A. 97, 14720–5. doi:10.1073/pnas.97.26.14720

Urban, S., Kobi, D., Ennen, M., Langer, D., Le Gras, S., Ye, T., Davidson, I., 2015. A Brn2-Zic1 axis specifies the neuronal fate of retinoic-acid-treated embryonic stem cells. J. Cell Sci. 128, 2303–18. doi:10.1242/jcs.168849

Vadodaria, K.C., Mertens, J., Paquola, A., Bardy, C., Li, X., Jappelli, R., Fung, L., Marchetto, M.C., Hamm, M., Gorris, M., Koch, P., Gage, F.H., 2016. Generation of functional human serotonergic neurons from fibroblasts. Mol. Psychiatry 21, 49–61. doi:10.1038/mp.2015.161

van Praag, H., Schinder, A.F., Christie, B.R., Toni, N., Palmer, T.D., Gage, F.H., 2002. Functional neurogenesis in the adult hippocampus. Nature 415, 1030–4. doi:10.1038/4151030a

Vera, E., Bosco, N., Studer, L., 2016. Generating Late-Onset Human iPSC-Based Disease Models by Inducing Neuronal Age-Related Phenotypes through Telomerase Manipulation. Cell Rep. 17, 1184–1192. doi:10.1016/j.celrep.2016.09.062

Vescovi, A.L., Parati, E.A., Gritti, A., Poulin, P., Ferrario, M., Wanke, E., Frölichsthal-Schoeller, P., Cova, L., Arcellana-Panlilio, M., Colombo, A., Galli, R., 1999. Isolation and cloning of multipotential stem cells from the embryonic human CNS and establishment of transplantable human neural stem cell lines by epigenetic stimulation. Exp. Neurol. 156, 71–83. doi:10.1006/exnr.1998.6998

Vierbuchen, T., Ostermeier, A., Pang, Z.P., Kokubu, Y., Südhof, T.C., Wernig, M., 2010. Direct conversion of fibroblasts to functional neurons by defined factors. Nature 463, 1035–41. doi:10.1038/nature08797

Vierbuchen, T., Wernig, M., 2011. Direct lineage conversions: unnatural but useful? Nat. Biotechnol. 29, 892–907. doi:10.1038/nbt.1946

Wachs, F.-P., Couillard-Despres, S., Engelhardt, M., Wilhelm, D., Ploetz, S., Vroemen, M., Kaesbauer, J., Uyanik, G., Klucken, J., Karl, C., Tebbing, J., Svendsen, C., Weidner, N., Kuhn, H.-G., Winkler, J., Aigner, L., 2003. High efficacy of clonal growth and expansion of adult neural stem cells. Lab. Invest. 83, 949–62.

Walton, N.M., Sutter, B.M., Chen, H.-X., Chang, L.-J., Roper, S.N., Scheffler, B., Steindler, D. a, 2006. Derivation and large-scale expansion of multipotent astroglial neural progenitors from adult human brain. Development 133, 3671–3681. doi:10.1242/dev.02541

Warren, L., Manos, P.D., Ahfeldt, T., Loh, Y.-H., Li, H., Lau, F., Ebina, W., Mandal, P.K., Smith, Z.D., Meissner, A., Daley, G.Q., Brack, A.S., Collins, J.J., Cowan, C., Schlaeger, T.M., Rossi, D.J., 2010. Highly efficient reprogramming to pluripotency and directed differentiation of human cells with synthetic modified mRNA. Cell Stem Cell 7, 618–30. doi:10.1016/j.stem.2010.08.012

Weissman, I.L., 2000. Stem Cells. Cell 100, 157–168. doi:10.1016/S0092-8674(00)81692-X

Wen, Z., Nguyen, H.N., Guo, Z., Lalli, M.A., Wang, X., Su, Y., Kim, N.-S., Yoon, K.-J., Shin, J., Zhang, C., Makri, G., Nauen, D., Yu, H., Guzman, E., Chiang, C.-H., Yoritomo, N., Kaibuchi, K., Zou, J., Christian, K.M., Cheng, L., Ross, C.A., Margolis, R.L., Chen, G., Kosik, K.S., Song, H., Ming, G., 2014. Synaptic dysregulation in a human iPS cell model of mental disorders. Nature 515, 414–8. doi:10.1038/nature13716

Wernig, M., Meissner, A., Cassady, J.P., Jaenisch, R., 2008. c-Myc is dispensable for direct reprogramming of mouse fibroblasts. Cell Stem Cell 2, 10–2. doi:10.1016/j.stem.2007.12.001

Wiese, S., Karus, M., Faissner, A., 2012. Astrocytes as a source for extracellular matrix molecules and cytokines. Front. Pharmacol. 3, 120. doi:10.3389/fphar.2012.00120

Wilmut, I., Schnieke, A.E., McWhir, J., Kind, A.J., Campbell, K.H., 1997. Viable offspring derived from fetal and adult mammalian cells. Nature 385, 810–3. doi:10.1038/385810a0

Woltjen, K., Michael, I.P., Mohseni, P., Desai, R., Mileikovsky, M., Hämäläinen, R., Cowling, R., Wang, W., Liu, P., Gertsenstein, M., Kaji, K., Sung, H.-K., Nagy, A., 2009. piggyBac transposition reprograms fibroblasts to induced pluripotent stem cells. Nature 458, 766–70. doi:10.1038/nature07863

Wörsdörfer, P., Thier, M., Kadari, A., Edenhofer, F., 2013. Roadmap to cellular reprogramming--manipulating transcriptional networks with DNA, RNA, proteins and small molecules. Curr. Mol. Med. 13, 868–78.

Wurst, W., Bally-Cuif, L., 2001. Neural plate patterning: upstream and downstream of the isthmic organizer. Nat. Rev. Neurosci. 2, 99–108. doi:10.1038/35053516

Xu, C., Inokuma, M.S., Denham, J., Golds, K., Kundu, P., Gold, J.D., Carpenter, M.K., 2001. Feeder-free growth of undifferentiated human embryonic stem cells. Nat. Biotechnol. 19, 971–4. doi:10.1038/nbt1001-971

Yadav, P., Selvaraj, B.T., Bender, F.L.P., Behringer, M., Moradi, M., Sivadasan, R., Dombert, B., Blum, R., Asan, E., Sauer, M., Julien, J.-P., Sendtner, M., 2016. Neurofilament depletion improves microtubule dynamics via modulation of Stat3/stathmin signaling. Acta Neuropathol. 132, 93–110. doi:10.1007/s00401-016-1564-y

Yan, C.H., Levesque, M., Claxton, S., Johnson, R.L., Ang, S.-L., 2011. Lmx1a and lmx1b function cooperatively to regulate proliferation, specification, and differentiation of midbrain dopaminergic progenitors. J. Neurosci. 31, 12413–25. doi:10.1523/JNEUROSCI.1077-11.2011

Yan, J., Xu, L., Welsh, A.M., Hatfield, G., Hazel, T., Johe, K., Koliatsos, V.E., 2007. Extensive neuronal differentiation of human neural stem cell grafts in adult rat spinal cord. PLoS Med. 4, 0318–0332. doi:10.1371/journal.pmed.0040039

Yan, Y., Shin, S., Jha, B.S., Liu, Q., Sheng, J., Li, F., Zhan, M., Davis, J., Bharti, K., Zeng, X., Rao, M., Malik, N., Vemuri, M.C., 2013. Efficient and Rapid Derivation of Primitive Neural Stem Cells and Generation of Brain Subtype Neurons From Human Pluripotent Stem Cells. Stem Cells Transl. Med. 862–870.

Yang, H., Wang, J., Wang, F., Liu, X., Chen, H., Duan, W., Qu, T., 2016. Dopaminergic Neuronal Differentiation from the Forebrain-Derived Human Neural Stem Cells Induced in Cultures by Using a Combination of BMP-7 and Pramipexole with Growth Factors. Front. Neural Circuits 10, 29. doi:10.3389/fncir.2016.00029

Yao, Z., Mich, J.K., Ku, S., Menon, V., Krostag, A.-R., Martinez, R.A., Furchtgott, L., Mulholland, H., Bort, S., Fuqua, M.A., Gregor, B.W., Hodge, R.D., Jayabalu, A., May, R.C., Melton, S., Nelson, A.M., Ngo, N.K., Shapovalova, N.V., Shehata, S.I., Smith, M.W., Tait, L.J., Thompson, C.L., Thomsen, E.R., Ye, C., Glass, I.A., Kaykas, A., Yao, S., Phillips, J.W., Grimley, J.S., Levi, B.P., Wang, Y., Ramanathan, S., 2016. A Single-Cell Roadmap of Lineage Bifurcation in Human ESC Models of Embryonic Brain Development. Cell Stem Cell. doi:10.1016/j.stem.2016.09.011

Yoo, Y.D., Huang, C.T., Zhang, X., Lavaute, T.M., Zhang, S.-C., 2011. Fibroblast growth factor regulates human neuroectoderm specification through ERK1/2-PARP-1 pathway. Stem Cells 29, 1975–82. doi:10.1002/stem.758

Yoshida, Y., Takahashi, K., Okita, K., Ichisaka, T., Yamanaka, S., 2009. Hypoxia enhances the generation of induced pluripotent stem cells. Cell Stem Cell 5, 237–41. doi:10.1016/j.stem.2009.08.001

Young, G.T., Gutteridge, A., Fox, H.D.E., Wilbrey, A.L., Cao, L., Cho, L.T., Brown, A.R., Benn, C.L., Kammonen, L.R., Friedman, J.H., Bictash, M., Whiting, P., Bilsland, J.G., Stevens, E.B., 2014. Characterizing human stem cell-derived sensory neurons at the single-cell level reveals their ion channel expression and utility in pain research. Mol. Ther. 22, 1530–43. doi:10.1038/mt.2014.86

Yu, D.X., Marchetto, M.C., Gage, F.H., 2013. Therapeutic translation of iPSCs for treating neurological disease. Cell Stem Cell 12, 678–688. doi:10.1016/j.stem.2013.05.018

Yu, J., Hu, K., Smuga-Otto, K., Tian, S., Stewart, R., Slukvin, I.I., Thomson, J.A., 2009. Human induced pluripotent stem cells free of vector and transgene sequences. Science 324, 797–801. doi:10.1126/science.1172482

Yu, J., Vodyanik, M.A., Smuga-Otto, K., Antosiewicz-Bourget, J., Frane, J.L., Tian, S., Nie, J., Jonsdottir, G.A., Ruotti, V., Stewart, R., Slukvin, I.I., Thomson, J.A., 2007a. Induced pluripotent stem cell lines derived from human somatic cells. Science 318, 1917–20. doi:10.1126/science.1151526

Yu, J., Vodyanik, M.A., Smuga-Otto, K., Antosiewicz-Bourget, J., Frane, J.L., Tian, S., Nie, J., Jonsdottir, G.A., Ruotti, V., Stewart, R., Slukvin, I.I., Thomson, J.A., 2007b. Induced pluripotent stem cell lines derived from human somatic cells. Science 318, 1917–20. doi:10.1126/science.1151526

Yusa, K., Rad, R., Takeda, J., Bradley, A., 2009. Generation of transgene-free induced pluripotent mouse stem cells by the piggyBac transposon. Nat. Methods 6, 363–9. doi:10.1038/nmeth.1323

Zannino, D.A., Sagerström, C.G., 2015. An emerging role for prdm family genes in dorsoventral patterning of the vertebrate nervous system. Neural Dev. 10, 24. doi:10.1186/s13064-015-0052-8

Zhang, M., Schöler, H.R., Greber, B., 2013. Rapid and efficient generation of neurons from human pluripotent stem cells in a multititre plate format. J. Vis. Exp. e4335. doi:10.3791/4335

Zhang, S.C., Wernig, M., Duncan, I.D., Brüstle, O., Thomson, J.A., 2001. In vitro differentiation of transplantable neural precursors from human embryonic stem cells. Nat. Biotechnol. 19, 1129–33. doi:10.1038/nbt1201-1129

Zhang, X., Huang, C.T., Chen, J., Pankratz, M.T., Xi, J., Li, J., Yang, Y., Lavaute, T.M., Li, X.-J., Ayala, M., Bondarenko, G.I., Du, Z.-W., Jin, Y., Golos, T.G., Zhang, S.-C., 2010. Pax6 is a human neuroectoderm cell fate determinant. Cell Stem Cell 7, 90–100. doi:10.1016/j.stem.2010.04.017

Zhao, X., Li, W., Lv, Z., Liu, L., Tong, M., Hai, T., Hao, J., Guo, C., Ma, Q., Wang, L., Zeng, F., Zhou, Q., 2009. iPS cells produce viable mice through tetraploid complementation. Nature 461, 86–90. doi:10.1038/nature08267

Zhou, H., Wu, S., Joo, J.Y., Zhu, S., Han, D.W., Lin, T., Trauger, S., Bien, G., Yao, S., Zhu, Y., Siuzdak, G., Schöler, H.R., Duan, L., Ding, S., 2009. Generation of induced pluripotent stem cells using recombinant proteins. Cell Stem Cell 4, 381–4. doi:10.1016/j.stem.2009.04.005

Zhou, T., Benda, C., Dunzinger, S., Huang, Y., Ho, J.C., Yang, J., Wang, Y., Zhang, Y., Zhuang, Q., Li, Y., Bao, X., Tse, H.-F., Grillari, J., Grillari-Voglauer, R., Pei, D., Esteban, M.A., 2012. Generation of human induced pluripotent stem cells from urine samples. Nat. Protoc. 7, 2080–9. doi:10.1038/nprot.2012.115

Zhou, W., Freed, C.R., 2009. Adenoviral gene delivery can reprogram human fibroblasts to induced pluripotent stem cells. Stem Cells 27, 2667–74. doi:10.1002/stem.201

Ziegler, A.N., Levison, S.W., Wood, T.L., 2015. Insulin and IGF receptor signalling in neural-stem-cell homeostasis. Nat. Rev. Endocrinol. 11, 161–70. doi:10.1038/nrendo.2014.208

Zimmermann, T., Remmers, F., Lutz, B., Leschik, J., 2016. ESC-Derived BDNF-Overexpressing Neural Progenitors Differentially Promote Recovery in Huntington's Disease Models by Enhanced Striatal Differentiation. Stem Cell Reports. doi:10.1016/j.stemcr.2016.08.018

Zweigerdt, R., Olmer, R., Singh, H., Haverich, A., Martin, U., 2011. Scalable expansion of human pluripotent stem cells in suspension culture. Nat. Protoc. 6, 689–700. doi:10.1038/nprot.2011.318

List of figures

List of tables

Curriculum Vitae

PERSONAL INFORMATION

Name	Katharina Günther
Place of Birth	Almaty, Kazakhstan
Citizenship	German

PRACTICAL EXPERIENCE

10/2013 – 12/2016	Continuation of the PhD project as a doctoral researcher at the Graduate School of Life Sciences (GSLS, DFG cluster of excellence) Institute of Anatomy und Cell Biology, University of Würzburg Stem Cells and Regenerative Medicine Group, Prof. Dr. Frank Edenhofer
09/2013	Transfer with Edenhofer Group from Bonn to Würzburg
10/2012 – 09/2013	PhD student in Molecular Biomedicine Institute of Reconstructive Neurobiology, University of Bonn Stem Cell Engineering Group, PD Dr. Frank Edenhofer
01/2012 - 04/2012	Guest researcher stay Neuroscience Research Institute, University of California, Santa Barbara, USA Molecular and Cellular Neurobiology Lab, Dr. Kenneth S. Kosik

EDUCATION

10/2006 - 12/2011	Diploma studies of Human Biology/Biomedical Science, Philipps-University of Marburg Diploma Thesis at the Department of Neurology, Marburg Neurological Therapy Research, Prof. Dr. R. Dodel Topic: Characterization of epitope specific naturally occurring autoantibodies against alpha-synuclein
06/2006	Bohnstedt-Gymnasium Luckau Abitur/A-Levels

Publications

Peer reviewed journals

Günther K*, Appelt-Menzel A*, Kwok CK, Walles H, Metzger M, Edenhofer F (2016) Rapid monolayer neural induction of induced pluripotent stem cells yields stably proliferating neural stem cells. J Stem Cell Res Ther. 6, 1-6 doi:10.4172/2157-7633.1000341

Meyer S, Wörsdörfer P, **Günther K**, Thier M, Edenhofer F (2015) Derivation of adult human fibroblasts and their direct conversion into expandable neural progenitor cells. J. Vis. Exp. e52831. doi:10.3791/52831

Appelt-Menzel A, Neuhaus W, Cubukova A, Wilhelm S, **Günther K,** Edenhofer F, Piontek J, Krause G, Stüber T, Walles H, Metzger M (2016) Establishment of a human blood-brain barrier co-culture model mimicking the neurovascular unit using induced pluripotent and multipotent stem cells. Stem Cell Reports, manuscript in revision.

Kwok CK*, Ueda Y*, Kadari A, **Günther K,** Heron A, Schnitzler A, Rook M, Edenhofer F (2016) Scalable suspension culture of billions of human induced pluripotent stem cells. Journal of Tissue Engineering and Regenerative Medicine, manuscript in revision.

* These authors contributed equally.

Abstracts for oral presentations

Derivation and stabilization of a novel early neuroepithelial precursor population from human embryonic tissue for biomedical application**.** (2015) **4th International Conference: Strategies in Tissue Engineering, June, Würzburg, Germany**

Derivation of early neuroepithelial precursors from fetal tissue to assess novel neural reprogramming pathways. (2015) **11th Meeting of the German Neuroscience Society, March, Göttingen, Germany**

Abstracts for poster presentations

Klein T, **Günther K**, Sommer C, Edenhofer F, Üçeyler N (2016) Generation of patient-derived peripheral sensory neurons using iPSCs and iNPCs obtained from patients with Fabry disease. **11th GSLS Symposium, October, Würzburg, Germany**

Kwok CK, Ueda Y, Kadari A, **Günther K,** Heron A, Schnitzler A, Rook M, Edenhofer F (2016) Scalable suspension culture of billions of human induced pluripotent stem cells. **11th GSLS Symposium, October, Würzburg, Germany**

Jansch C, Edenhofer F, Waider J, **Günther K**, Ziegler G, Lesch KP (2016) Das Zellkulturmodell humaner induzierter pluripotenter Stammzellen zur Erforschung einer neuropsychiatrischen Erkrankung. **Annual Meeting of the German Society of Biological Psychiatry, September, Würzburg, Germany**

Meyer S, Salti A**, Günther K**, Wörsdörfer P, Edenhofer F (2016) Directly converted induced neural stem cells (iNPCs) as a robust and safe source for autologous cell replacement. **14th Annual Meeting of the International Society of Stem Cell Research, June, San Francisco, USA**

Günther K, Wörsdörfer P, Meyer S, Thier M, Wischmeyer E, Edenhofer F (2016) Derivation and stabilization of novel human neural precursor cells from embryonic brain tissue for biomedical applications. **14th Annual Meeting of the International Society of Stem Cell Research, June, San Francisco, USA**

Günther K, Wörsdörfer P, Meyer S, Thier M, Edenhofer F (2016) Derivation and stabilization of novel early human neural progenitor cells from primary tissue capable of differentiation into central and peripheral lineages. **Stem Cell Models of Neural Regeneration and Disease, February, Dresden, Germany**

Kittel-Schneider S, Gersic D, Frank M, Lorenz C, Auer J, Winkler S, Lesch KP, Edenhofer F, Kadari A, **Günther K**, Klebe S, Reif A (2015) Gene Expression profile of PARK2 CNV carriers with adult ADHD. **Annual Congress of the German Association for Psychiatry, Psychotherapy and Psychosomatics, November, Berlin, Germany**

Günther K, Wörsdörfer P, Thier M, Edenhofer F (2015) Induction and stabilization of novel early neural progenitor cells from human fetal brain tissue. **13th Annual Meeting of the International Society of Stem Cell Research, June, Stockholm, Sweden**

Kittel-Schneider S, Gersic D, Frank M, Lorenz C, Auer J, Winkler S, Lesch KP, Edenhofer F, Kadari A, **Günther K**, Klebe S, Reif A (2015) Gene Expression profile of PARK2 CNV carriers with adult ADHD. **12th World Congress of Biological Psychiatry, June, Athens, Greece**

Kittel-Schneider S, Gersic D, Frank M, Lorenz C, Auer J, Winkler S, Lesch KP, Edenhofer F, Kadari A, **Günther K**, Klebe S, Reif A (2015) Gene Expression profile of PARK2 CNV carriers with adult ADHD. **5th World's Congress on ADHD, May, Glasgow, UK**

Meyer S, **Günther K**, Wörsdörfer P, Thier M, Edenhofer F (2014) Direct conversion of fibroblasts into SOX2-positive, expandable neural stem cells. **2nd International Annual Conference of the German Stem Cell Network, November, Heidelberg, Germany**

Günther K, Wörsdörfer P, Meyer S, Thier M, Edenhofer F (2014) Stabilization of an early fetal brain-derived neural stem cell population by defined small molecules. **5th International Congress on Stem Cells and Tissue Formation, July, Dresden, Germany**

Meyer S, **Günther K**, Wörsdörfer P, Edenhofer F (2014) Robust and efficient direct conversion of human fibroblasts into neural stem cells. **5th International Congress on Stem Cells and Tissue Formation, July, Dresden, Germany**

Schoeps S**, Günther K**, Wörsdörfer P, Edenhofer F (2013) Synthetic mRNAs as a tool for the manipulation of human stem cells. **7th International Meeting of the Stem Cell Network North Rhine Westphalia, March, Cologne, Germany**

Affidavit / Eidesstattliche Erklärung

I hereby confirm that my thesis entitled "Generation of early human neuroepithelial progenitors from primary cells for biomedical applications" is the result of my own work. I did not receive any help or support from commercial consultants. All sources and / or materials applied are listed and specified in the thesis.
Furthermore, I confirm that this thesis has not yet been submitted as part of another examination process neither in identical nor in similar form.

Würzburg, Signature

Hiermit erkläre ich an Eides statt, die Dissertation „Generierung früher humaner neuroepithelialer Vorläufer aus primären Zellen für biomedizinische Anwendungen" eigenständig, das heißt insbesondere selbständig und ohne Hilfe eines kommerziellen Promotionsberaters, angefertigt und keine anderen als die von mir angegebenen Quellen und Hilfsmittel verwendet zu haben.

Ich erkläre außerdem, dass die Dissertation weder in gleicher noch in ähnlicher Form bereits in einem anderen Prüfungsverfahren vorgelegen hat.

Würzburg, Unterschrift

Acknowledgements

First of all, I would like to thank **Prof. Dr. Frank Edenhofer** cordially for giving me the opportunity to carry out my doctorate thesis under his supervision. I constantly encountered constructive and encouraging advice, guidance and support in countless discussions and meetings. Thank you for sharing your passion for science and innovation and giving me a surrounding to follow my ideas and explore my opportunities.

Next, I express my gratitude towards **Prof. Dr. Albrecht Müller** and **PD Dr. Robert Blum** for willing to be part of my thesis committee and participate in annual meetings, giving useful consultations and finally the assessment of this thesis.

I would like to thank **Prof. Dr. Süleyman Ergün** for giving me the opportunity to carry out and finish my studies in the Institute of Anatomy and Cell Biology. Moreover, I am grateful for constructive and lively discussions.

I was fortunate to work in a group surrounded not only by colleagues, but by colleagues who became friends. Importantly, I have to name two PostDocs, **Dr. Philipp Wörsdörfer** and **Dr. Sandra Meyer**, who not only accompanied my time in the group from the beginning on, but shared my coffee addiction and are just awesome. Thank you, Philipp, for being constantly helpful, encouraging and positive. Your expertise and your personal attitude is very valuable to me! Thank you also for proof-reading and constructive discussions of this thesis despite your workload. Likewise, I thank Sandra for many long hours together in the lab- we were a great team! I am thankful for your scientific and mental support and your AWG-thumb, looking forward to many sailing trips and carnivals to come!

Chee Keong Kwok was my first intern, master student and became a great co-fellow PhD student and friend. Thanks for your help with the flow analysis of iPSCs, lively discussions and your efforts on proof-reading manuscripts and this thesis. I will always think back with a smile to all the fun in lab and apart from it.

Nothing in the lab would be possible without our great technicians **Heike Arthen** and **Martina Gebhardt**. For me, especially during the last year Heike was a great and reliable support with additional projects. A huge thank you to the current and former Würzburg Lab colleagues for a nice and creative working atmosphere, constructive scientific exchange and our common lunch breaks. Special thanks to the heart and the brain team: **Dr. Yuichiro Ueda**, **Naoko Nose**, **Dr. Dirk Pühringer**.

Dr. Nicole Wagner and **Prof. Dr. Esther Asan** (Institute of Anatomy and Cell Biology, Würzburg) helped me with the analysis and interpretation of TEM images. **Dr. Damiano Rovituso** assisted during the flow cytometry of eNEPs.

Further, I would like to thank **Dr. Marc Thier** (Bonn alumni, current: HI-STEM, DKFZ, Heidelberg) for his contribution to this thesis by microarray analysis and scientific discussions, especially in the first year of my thesis. Your research enthusiasm is contagious.

Nevertheless, it was the Stem Cell Engineering Group at the Reconstructive Neurobiology in

Bonn, where everything (including the panda) started for me. Although I spent only one year in Bonn, I learned so much about neural stem cell biology and really enjoyed my time there. This was made possible by **Dr. Sabrina Schoeps**, **Yenal B. Lakes**, **Dr. Johannes Jungverdorben**, **Dr. Raaj Thummer**, **Dr. Ashif Kadari**, **Thileepan Sekaran**, **Nicole Russ** and **Kathrin Vogt, the Panda** and all other members! Special thanks to Thileepan for helping me with creating the heatmap.

I would like to mention my third team- the Innsbruck Stem Cell lab which I highly appreciate and look forward for exciting projects and meetings. A special thank you to **Marta Suarez** for the PSD-95 stainings.

In the following I would like to acknowledge our collaborators from other institutes, thank you for contributing to my project!

Importantly, I would like to mention the Tissue Engineering and Regenerative Medicine Department under the leadership of **Prof. Dr. Heike Walles**. I would like to thank especially **PD Dr. Marco Metzger**, **Dr. Antje Appelt-Menzel** and **Alevtina Cubukova** for the successful collaboration on the derivation of iPSC-derived NPCs and obtaining the fetal tissue. In particular, working and discussing with Antje was always great, despite hard and stressful periods. Further, many thanks to **Dr. Tanja Stüber** (Würzburg University Clinic).

I would like to thank **Prof. Dr. K-P Lesch** for the opportunity to use the cycler at Department of Molecular Psychiatry. Thanks, **Charline Jansch** for your time and efforts!
Julia Flunkert and **Anna Maierhofer** (Department of Human Genetics, University of Würzburg) helped me with the G-band analysis.
I would like to thank **Prof. Dr. Erhard Wischmeyer** for conducting the electrophysiological recordings and thus helping with the functional analysis of differentiated neurons. Further, help with subtypes characterization of the peripheral neurons was provided by **Thomas Klein** (Department of Neurology, Würzburg).

The objectives of this project required primary tissue of various origin, I am very grateful to all participants who were willing to donate tissue. Further, I am thankful to the aforementioned collaborators and additionally the **ForIPS consortium**, **Dr. Lorenz Müller**, **Dr. Sarah Kittel-Schneider, Prof. Dr. Üceyler** for providing either cells or tissue.

I am very thankful to **Dr. Gabriele Blum-Oehler** and the **GSLS team** for being supportive, constantly informative and very friendly. Getting enrolled into the GSLS was a nice experience, not only because of the courses, but to a great part because of the interesting and open-minded people I could meet within the last years.

Next, I have to mention my close friends **Dr. Lina Matschke** und **Dr. Anne Stündl** - for the last 10 years (!!!) we were going through everything together, although half of the time not at the same location. **Daniela, Damiano, Olga, Natalia, Tobias, Markus, Yenal, Svenja, Eva** (and everybody I forgot)- thank you for being my friends and believing in me! You are the best!

I would have never come this far without the love, trust and never-ending support of my parents **Stefanie and Vadim Günther**. You are the strongest, most pragmatic and optimistic people I know, thank you for everything!